Heartwood formation and the chemical basis of natural durability in *Eucalyptus bosistoana*

A thesis

submitted in partial fulfilment of

the requirements for the degree of

Doctor of Philosophy

in Forestry

By

Gayatri Mishra

School of Forestry

University of Canterbury

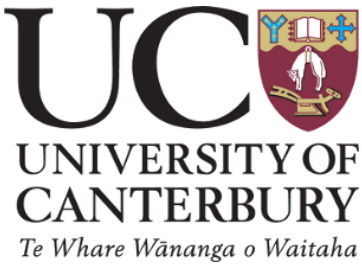

Senior supervisor:

Dr. Clemens Altaner

School of Forestry, University of Canterbury

Co-Supervisor:

Dr. Ashley Garrill

Biological Sciences, University of Canterbury

Associate Supervisor:

Dr. David Collings

School of Environmental & Life Sciences

University of Newcastle

Acknowledgements

At the outset, I express my deep sense of gratitude and appreciation to my principal supervisor, **Dr. Clemens M. Altaner**, School of Forestry, University of Canterbury for providing me an opportunity to work in this project. Without his ceaseless supervision, support, motivation and robust knowledge base this task would not have been completed. His guidance has helped me immensely in my research and writing the thesis till its logical end.

Besides, I feel extremely fortunate to work with my associate supervisor, **Dr. David Collings** and Co-supervisor, **Dr. Ashley Garrill** too.

Microscopy being a major part of my research, I feel deeply indebted to **Dr. David Collings** for introducing me into the realms of advanced microscopic skills coupled with his constant guidance. Even after his leaving the University in the meanwhile, he was considerate enough to bridge the gap through his timely communications via emails or video conversations. His unique concepts and expertise generated my strong interest in microscopy. I also thank **Dr. Ashley Garrill** for providing me with necessary lab facilities to perform bioactivity tests with fungi. His expertise has been a great source of support to my bioactivity experiments.

Proficient sectioning skills have been an important part of my research too. Hence, I gratefully acknowledge the kind assistance of technical staff, **Graeme Bull** and **Riejel Gardiner** from the School of Biological Sciences for helping me to develop sectioning skills using sledge microtome. I would also thank **Manfred Ingerfeld** profusely for assisting me in confocal microscopy. Heartfelt thanks to the technical staff, **Lachlan Kirk** and **Nigel Pink**, from the School of Forestry for their unequivocal help extended to me.

I am extremely grateful to **Meike Holzenkampfer** as she taught me to operate the gas chromatograph and her expertise in chemical analyses has been an asset in understanding the gas chromatograph with clarity.

Thanks to the authorities and staff of university library for granting me the required permission to utilise their valuable collections for my reference.

Last but not the least, I express my heartiest gratitude to my parents and sister for being supportive pillars in my current mission. **Above all, I am grateful to the almighty for paving the way in accomplishing my dream.**

Table of Contents

List of Figures

Chapter -1

Chapter -2

Chapter -3

Chapter -4

Chapter -5

Chapter -6

List of Tables

Chapter -6

Abstract

The New Zealand Dryland Forests Initiative (NZDFI), aims to establish a sustainable natural durable timber industry in New Zealand. The natural durability of heartwood is highly variable within a species and lower at the centre of a tree. Therefore, it is critical to ascertain that trees meet international standards for durability to ensure a viable industry based on plantation grown naturally durable *Eucalyptus*. A strategy to ensure that wood from future plantings meet industry requirement is to select superior genotypes in a breeding programme. Several *Eucalyptus* species have been planted by NZDFI, but the primary focus is on *E. bosistoana* as it is a class 1 durable timber.

Little is known about the heartwood formation in young trees. It is possible that the young trees do not have true heartwood, but an extended transition zone, the zone between sapwood and heartwood where parenchyma cells remain alive synthesising heartwood extractives. Therefore, the wood quality research of NZDFI needs to ensure that the young trees have formed true heartwood. Understanding heartwood formation is critical for the success of a plantation forest industry aiming to produce ground-durable timber. The objective of chapter-2 was to identify conventional and confocal microscopy methods, which allow the observation of cell organelles and the chemical composition in *E. bosistoana* parenchyma cells before and after heartwood formation. Nuclei, microtubules and peroxisomes in parenchyma cells of 2-year-old *E. bosistoana* stems were visualised by confocal microscopy combined with optimised immunolabelling protocols. Iodine/potassium iodide stained starch (amyloplasts), while amido black stained proteins in sapwood. Fluorescence emission spectra confirmed the presence of chloroplasts in xylem parenchyma of 2-year-old *E. bosistoana*. Fluorescence emission spectral (lambda) scans showed differences between parenchyma and fibre cells as well as sapwood and heartwood. The physiological changes between sapwood and heartwood visualised in parenchyma cells helped the understanding of heartwood formation in young *E. bosistoana* trees.

As part of an *E. bosistoana* breeding programme, the hypothesis of prolonged transition from sapwood to heartwood in young *E. bosistoana* trees, resulting in a wide transition zone has been tested in chapter-3. This needs to be considered when assessing trees for heartwood quantity and quality. Heartwood formation was investigated in radial profiles in cores from bark to bark of 6-year-old trees with conventional and confocal microscopy, and with a range of different staining techniques that visualised the physiological changes taking place in the parenchyma cells. Immunolabelling with antibodies against histone proteins and α-tubulin, histochemical staining using iodine/potassium iodide and fluorescence emission spectral scanning, demonstrated that in heartwood nuclei, microtubules, reserve materials (starch) and vacuoles were absent. The observations revealed that 6-

year-old *E. bosistoana* trees contained heartwood. The loss of water conductivity by tyloses and the death of the parenchyma cells occurred in close proximity resulting in a transition zone of ~1 cm.
A key feature of heartwood is the formation of extractives that impart natural durability, a sought after wood property. The durability between trees is highly variable. Apart from the quantity of heartwood extractives in the wood, the chemical composition of the extracts varies. Therefore, the objective of NZDFI is to select young *E. bosistoana* trees with the most potent extracts for next generation durability improvement.

Chapter-4 describes the development of an antifungal assay to determine the bioactivity of *E. bosistoana* heartwood extracts against a white rot (*Trametes versicolor*) and a brown rot (*Coniophora cerebella*). The most suitable procedure was to spread dimethyl sulfoxide (DMSO) solutions of extract onto solidified agar, inoculate with fungi and calculate the growth rate (cm/h) by fitting a linear regression for the diameter of fungi against time. Controls were needed to normalise the fungal growth, i.e. calculating a relative growth rate, to account for the variation in growth conditions between different runs.

Chapter-5 describes the variability in bioactivity and chemical composition of *E. bosistoana* heartwood extracts between individual trees grown on two different sites (Lawson and Craven Road). Statistical methods combining the results of the fungal assays and the quantitative gas chromatography (GC) of the extracts allowed the investigation of bioactive compounds. The bioactivity of extracts was assessed against white rot (*Trametes versicolor*) and brown rot (*Coniophora cerebella*). Ethanol extracts from *E. bosistoana* heartwood were less effective on the white rot than against the brown rot. Variability in the bioactivity of extracts against the two fungi was observed between the trees. A small site effect in the bioactivity was found for the white rot but not the brown rot. Bioactivity of the extracts against the white rot was not correlated to that against the brown rot. The absence of such a relationship indicated that the two fungi were affected by different heartwood compounds. Thirty two compounds were quantified in *E. bosistoana* ethanol extracts by GC, of which six (benzoic acid, hexadecanoic acid, 1,5-dihdroxy-12-methoxy-3,3-dimethyl-3,4-dihydro-1H-anthra[2,3-c] pyran-6,11-dione, octadecanoic acid, polyphenol and beta-sitosterol) were identified. Significant variability in eight compounds (out of the 32) was found between the two sites. Multivariate (PLSR) analysis identified compounds at retention times 10.2 and 11.5 min (hexadecanoic acid) to be most related to the bioactivity of the *E. bosistoana* heartwood extracts against white rot and brown rot.

Breeding programmes benefit from early assessment, enabling short breeding cycles. While trees only form heartwood when several years old, wounds can be induced at a young age. As wound reaction has some similarities to heartwood formation the objective of chapter-6 was to investigate if the wound reaction can be used as a proxy to assess trees early in a breeding programme for heartwood

features. 1.6-year-old individuals from 27 *E. bosistoana* families with known heartwood diameter and extractive content were wounded and the axial wound reaction was correlated to the known heartwood features. No correlation between wound reaction and heartwood features in *E. bosistoana* families was found. Wound reaction was under weak genetic control. Therefore, it seems to be not possible to assess heartwood formation early in a breeding programme by measuring the axial wound response in 1.6-year-old *E. bosistoana* trees.

Furthermore, two families with small and large wound reaction were selected to characterise physiological and chemical variations in woundwood, heartwood and sapwood by microscopy and gas chromatography. Microscopic observations revealed the absence of starch and that vessels were occluded with tyloses in woundwood and heartwood. Morphological features were not discernible by eye between the families with large and small wound reaction. Gas chromatography revealed variation in the chemical composition of woundwood, heartwood and sapwood extracts.

Chapter-1

General Introduction

1.1 New Zealand Dryland Forests Initiative's (NZDFI) *Eucalyptus* breeding programme

The plantation forests in New Zealand are dominated by radiata pine (*Pinus radiata*) and Douglas fir (*Pseudotsuga menziesii*) that account for 95% of 2 million hectares estate (Apiolaza et al., 2011). *Eucalyptus* plays a minor role in the plantation forests of New Zealand. *Eucalyptus* plantations in New Zealand cover nearly 25,000 hectares forests and accounts for 1% of timber production in New Zealand (Nicholas & Millen, 2012).

A collaborative *Eucalyptus* breeding and forestry research project was commenced by NZDFI in 2008, with a vision to establish a sustainable naturally durable timber industry in New Zealand to supply timber for a wide range of agricultural and land-based industrial applications. Currently such, naturally durable timbers are often supplied from unsustainable tropical forests (Ballekom & Millen, 2017). In order to meet the requirements of domestic and international markets, the NZDFI will need to produce high quality durable timber for use as posts, poles and utility cross-arms as well as heavy structural applications such as jetties, bridges and rail sleepers.

The forestry industry of New Zealand relies heavily on *P. radiata*. However, *P. radiata* does not produce natural durable heartwood. Thus, radiata pine products e.g. poles for vineyards are treated with inorganic water-based preservative like Copper-Chrome-Arsenate (CCA) to protect the non-durable timber against biodegradation. The global restriction on the use of this preservative (Townsend et al., 2004) opens the opportunity for NZDFI to introduce, select and cultivate some natural durable timbers. Natural durability and strength are the properties together with the ability to grow in the NZ climate, made *Eucalyptus* an obvious choice (Millen et al., 2018). NZDFI has selected three *Eucalyptus* species (*E. bosistoana, E. globoidea* and *E. quadrangulata*) fulfilling these criteria, after testing more than 20 for their suitability in NZ conditions (Millen et al., 2018). From the three selected species, the first focus is on *E. bosistoana* due to its Class 1 durable timber (Australian Standard, AS5606-2005), exceptional high stiffness and strength (Bootle, 2005) and its ability to coppice vigorously (Nicholas & Millen, 2012). A 9-year-old *E. bosistoana* plantation is shown in figure 1.1.

E. bosistoana commonly known as Coast Grey Box or Gippsland Grey Box has a small rounded crown. It is an evergreen tree with creamy-white flowers from November to February. It is a *Eucalyptus* of south eastern Australia, growing up to 60 metres tall, and reaching a stem diameter of

at least 1.5 metres. *E. bosistoana* occurs within a latitudinal range of 33-37.5°S and at altitudes between sea level and 500 m (Nicholas & Millen, 2012). *E. bosistoana* covers coastal mixed forests along the South East coast of Australia between New South Wales, west of Sydney to eastern Gippsland, and mainly thrives well on river flats (Boland et al., 2006). The tree thrives well on fertile, well-drained soils, including clay and limestone. The timber is very hard and durable (Class 1) with interlocked grain. The heartwood appears light-brown to pink and has a wide spectrum of utilization in poles, cross arms, railway sleepers, fences (Bootle, 1983) and in heavy construction (Boland et al., 2006).

Figure 1.1: 9-year-old NZDFI breeding trial of *E. bosistoana* after pruning.

1.2 Research background

A key feature of heartwood is the formation of extractives that imparts natural durability, a sought after wood property. It is well known that the natural durability of heartwood is a) highly variable within a species (e.g. in *E. globulus*) (Pereira, 1988) and b) lower at the centre of a tree (AS5604, 2005; Sherrard & Kurth, 1933). Therefore, it is critical to ascertain that trees meet international standards for durability (AS5604, 2005; EN350-1, 1994) to ensure a viable industry based on plantation grown naturally durable *Eucalyptus*. The strategy to ensure that wood from future plantings meet industry requirement is to select superior genotypes in a breeding programme.

NZDFI wood quality research involves rapid assessment of wood durability for *Eucalyptus* species (Millen et al., 2018). In the first instance young trees are screened for the amount of extractives in the heartwood by quick spectroscopic assessments (Li, 2018). However, it is necessary to ascertain that the young trees have formed true heartwood when they are assessed. Furthermore, heartwood formation commences only after ~5 years in *E. bosistoana*, resulting in considerable time delays in a breeding programme. A breeding programme and the NZDFI vision would benefit from a shorter breeding cycle, which might be possible by measuring the wounding response in younger trees, as the extractives deposited in woundwood originate from a similar metabolic pathway as in heartwood. Last, the natural durability of heartwood is not only dependent on the amount of extractives, but also their composition in the heartwood. Identifying key bioactive compounds would allow further improvement of natural durability.

1.3 Wood formation

Wood represents a major advance in plant evolution, accounting for 95% of the total tree biomass (Celedon & Bohlmann, 2017). It is a sustainable and renewable primary product that continues to be used for the production of fuel, pulp, paper and timber as well as the manufacture of secondary woody products. The formation of wood starts by mitosis in the vascular cambium followed by xylogenesis, where thin walled cambial cells develop into water conducting tubes with lignified cell walls (xylem vessels) as well as cells providing mechanical support (xylem fibres) and storage (xylem parenchyma). During primary cell wall formation the cambial cells differentiate and increase in length and width. Secondary cell wall formation results in increased wall thickness. Vascular development in woody plants includes both formation and senescence of tissue. It is a coordinated expression of numerous genes involved in cell division, cell expansion (elongation and radial arrangement), cell wall thickening (biosynthesis of cellulose, hemicelluloses, cell wall proteins and lignin), programmed cell death, and heartwood formation in some tree species (Plomion et al., 2001). Although, wood formation has been extensively studied, there still exists only a limited understanding of the process (Barnett & Jeronimidis, 2003).

The vascular cambium mainly consists of two types of cells: fusiform cells (elongated vertically) give rise to the axial cell system and ray initials (radially elongated) produce the radial cell system of wood (Evert, 2006). The cambial cells divide to form secondary phloem to the outside and secondary xylem to the inside. The non-living secondary xylem resumes its biological activity by an interconnected network of radial and axial cells linking xylem and phloem. The parenchyma cells remain alive in sapwood contributing to the transport of water, dissolved gases and organic nutrients in wood. The specialized cells (fibres, vessels and tracheids) are dead in sapwood by losing their living content after the cell lignification process (Bamber, 1964).

1.4 Wood anatomy

Three distinct zones can be distinguished in tree stems, the sapwood, heartwood and transition zone. The cells are alive in the sapwood, and function in transport (between symplast and apoplast), storage of reserves (e.g. starch, proteins and lipids) and wound response. The boundary between sapwood and heartwood is the transition zone. This is normally a narrow, often pale coloured zone surrounding the heartwood that contains living cells that are usually devoid of starch, impermeable to liquids and with moisture content lower than sapwood (Hillis, 1987; Taylor et al., 2002). The transition zone is also the region where generation of heartwood takes place. Heartwood can be defined as an internal part of the stem, often darker in appearance than surrounding sapwood, devoid of living cells, water conduction, and in which the reserve materials (e.g. starch) have been removed. Some trees species additionally deposit heartwood substances that impart biotic resistance into this part of the stem (Hillis, 1987; Taylor et al., 2002). Figure 1.3 represents a disc from 12-year-old *E. bosistoana* stem with three different zones.

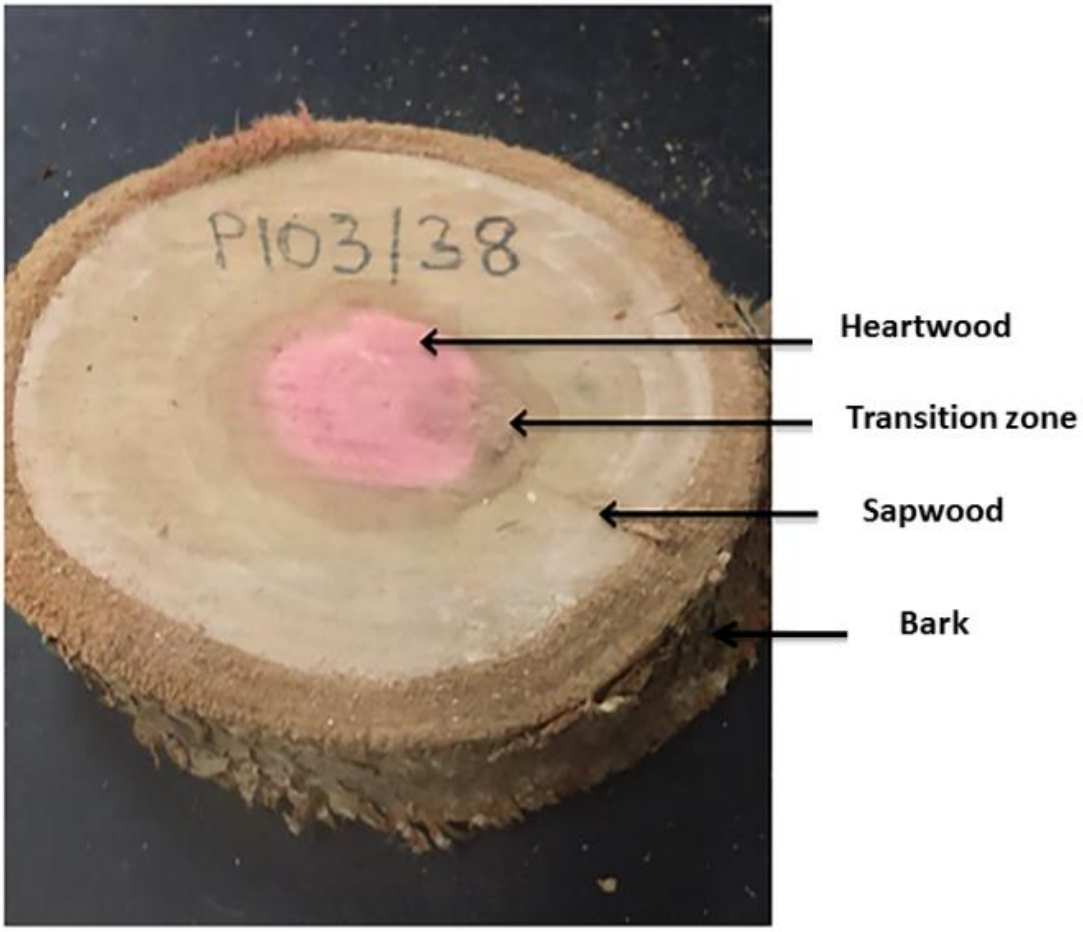

Figure 1.2: A disc from 12-year-old *E. bosistona* stem with sapwood, transition zone and heartwood. Heartwood turned pink by applying pH indicator (0.01 % methyl orange).

The axial cell system of angiosperms is comprised of water conducting vessels and optional tracheids, fibre cells which provide mechanical support and axial parenchyma cells. The radial system is mainly composed of ray parenchyma cells providing transport, metabolic activity and storage capabilities (Evert, 2006). The radial system can also contain radial tracheids (Gordon, 1912) or radial fibres (Lev-Yadun & Aloni, 1995). Heartwood sections from the three principal planes (transverse, tangential and radial) from a 12-year-old *E. bosistona* stem are shown in figure 1.4.

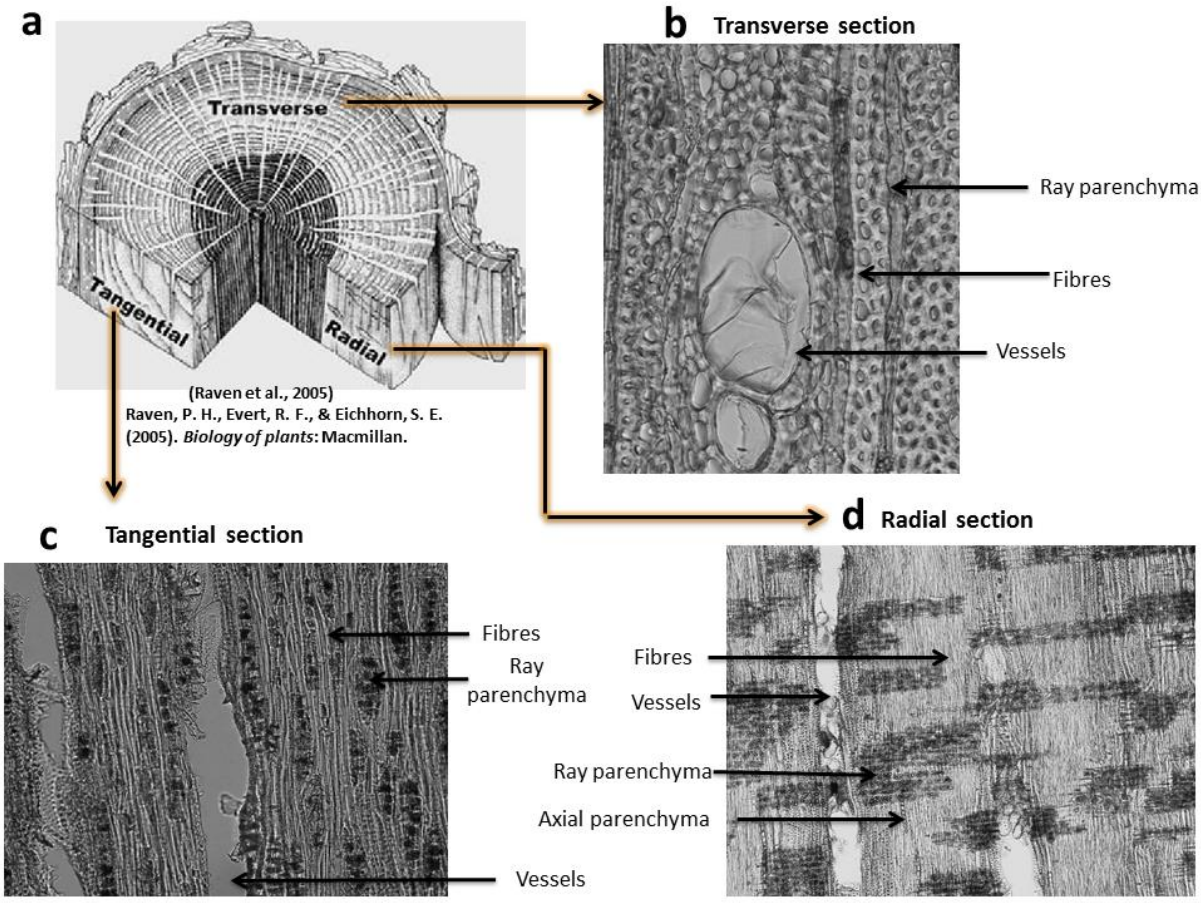

Figure 1.3: a) Anatomy of a tree stem with the three principal planes highlighted (Raven et al., 2005). Heartwood sections from the three principal planes b) transverse, c) tangential and d) radial of a 12-year-old E. bosistona stem.

1.5 Microscopy of wood

Microscopic studies of xylem cells are challenging. Difficulties are tissue sampling, sectioning and the presence of natural fluorescing compounds (e.g. lignin) (Chaffey, 1999, 2002). Obtaining the desired thin tissue sections from the three principal planes of wood is laborious. The extremely high density (>1000 kg/m^3) of *E. bosistoana* makes sectioning extremely challenging. Often only thicker sections can be cut that result in problems with getting good quality images with a whole tissue section in a single focal plane (Kitin et al., 2000). Conventional fluorescence and transmitted light

microscopy were used to visualise cell organelles and components. Out of focus light from above and below focal plane mixes and interferes with the in focus signal (Shotton, 1993; Wilson, 1990). This limits the visibility and quantification of fluorescence from plant cells, in particular when they are lignified (Hepler & Gunning, 1998; Kitin et al., 2000).
Confocal microscopy and labelling techniques like immunohistochemistry (Funada, 2003), in situ hybridization (Regan & Sundberg, 2002) or reporter gene histochemistry (Chaffey, 2002) can overcome some of the challenges. Confocal microscopy can accommodate thicker plant tissue sections in which cell components can be studied by optical sectioning without the need of mechanical sectioning (Kitin et al., 2000).

For microscopic studies of wood, the tissue is typically fixed, embedded, sectioned and stained (Alturkistani et al., 2016). Fixation aims to preserve cell structures from degradation. Fixatives cross-link proteins and hence delay degradation of cell contents (Alturkistani et al., 2016). The fixative solutions such as buffered formalin can be administered to the tissue by perfusion or immersion (Alturkistani et al., 2016). The process of embedding using plastic resin or paraffin wax hardens the tissue to aid sectioning. However, penetration of antibodies or chemicals can be inhibited by the embedding agent (Titford, 2009). If tissue sections of desired thickness can be obtained without embedding, the embedding step is optional. Then thin tissue sections are cut with a sharp blade fixed in a microtome. Sections are often mounted with glycerol on a glass slide for examination. Glycerol is a mounting medium that preserves fluorescence of tissue when stored at 4°C in the dark. The medium also reduces photobleaching of fluorescent dyes such as FITC (fluorescein isothiocyanate), cyanine, Alexa Fluor and green fluorescent protein (GFP).

1.5.1 Colour based and fluorescent stains

Stains interact selectively with tissue features thus increasing their contrast. Various colour based and fluorescent staining methods have been used to visualise different components and organelles in wood. Stains reveal the shape, size and organisation of organelles and components in the cells of a tissue section. Simultaneous staining of a tissue section by multiple stains can allow one to visualise different cell components at same time. An advantage of using chemical stains on tissue sections is that the sections can be mounted on slides and preserved for several years.

Some examples of the colour based stains which have been used to localise components and organelles in wood are potassium iodide for starch staining (Islam & Begum, 2011; Nakaba et al., 2013), Astra-blue (Vazquez-Cooz & Meyer, 2002) for cell wall staining or acetocarmine for nuclei (Fahn & Arnon, 1963; Fahn & Leshem, 1963; Islam & Begum, 2011; Nakaba et al., 2012; Nakaba et al., 2006; Nakaba et al., 2008). Toluidine blue was reported to localise pectin in bordered pit membranes in *Pinus radiata* wood West et al. (2012) and ruthenium red and hydroxylamine ferric chloride were used to localise pectin in *Picea abies* (Norway spruce) (Hornatowska, 2005). Protein

was localised in *P. abies* with mercuric bromophenol, aniline blue and amido black (Hornatowska, 2005).

Nuclei have been visualised by fluorescent DNA stains such as DAPI (4′,6-diamidino-2-phenylindole) (Spicer, 2005; Spicer & Holbrook, 2007; Zhang et al., 2015) or propidium iodide (Nakaba et al., 2011; Zhang et al., 2008). Fluorescein diacetate was used to localise the vacuoles in the cells of un-differentiated ray tracheids of *P. densiflora* (Nakaba et al., 2008). The fluorescent dye pontamine fast scarlet 4B has been used to investigate cellulose orientation in cell walls (Thomas et al., 2013).

1.5.2 Immunolabelling

The process of immunolabelling is called immunochemistry and is the biochemical process of binding antibodies to antigens. Antigens (e.g. proteins, carbohydrates, peptides) contain regions called epitopes that are capable of binding to the antibody. Antibodies can be very specific to their antigen and therefore enable the selective labelling of those structures. Immunolabelling is classified into two types based on the ability to directly or indirectly detect the antigen. In direct immunolabelling a single antibody is linked to a fluorophore (tag) (Figure 1.5a). The primary antibody binds to the epitope of the target antigen. The attached fluorophore is detected as it emits a specific wavelength (nm) of light after excitation. Indirect immunolabelling requires two antibodies. The unlabelled primary antibody binds to the antigen and a secondary antibody with an attached fluorophore, which binds to the primary antibody (Figure 1.5b). Multiple secondary antibodies with different fluorophores can attach to the single primary antibody. Advantages and disadvantages of direct and indirect immunolabelling are shown in table 1.1.

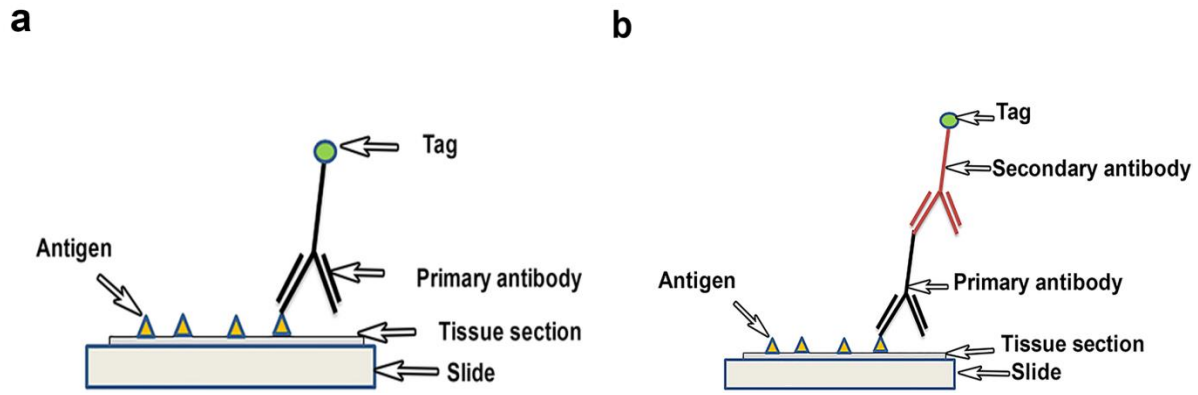

Figure 1.4: a) direct immunolabelling, where an antibody with a tag binds to the target antigen and b) indirect immunolabelling, where a primary antibody without a tag binds to the target antigen and a secondary antibody with a tag binds to the primary antibody.

Table 1.1: Advantages and disadvantages of direct and indirect immunolabelling (Abcam, 2018).

	Direct immunolabelling	**Indirect immunolabelling**
Time and complexity	Fewer steps	Additional steps and complex
Cost	Conjugated antibodies - expensive	Secondary antibodies - inexpensive
Sensitivity	Signals obtained by primary antibodies are sometimes weak	Amplified signals obtained by secondary antibody

Manifold antibodies and fluorescent tags are available for immunolabelling of wood sections. For example rat monoclonal antibodies against α–tubulin followed by incubation with FITC (Fluorescein isothiocyanate) conjugated secondary antibodies against rat IgG (immunoglobulin G) was used to localise microtubules in the parenchyma cells of *Abies sachalinensis* (Nakaba et al., 2013; Nakaba et al., 2006) or *P. densiflora* (Nakaba et al., 2008).

1.6 Natural durability

Wood is a lignocellulosic material composed of lignin, cellulose and hemicelluloses and small amounts of pectin. Wood is susceptible to biodegradation by different bio-degraders such as fungi, insects and termites, which break down plant cell wall polymers by cellulases and hemicellulases (Eaton & Hale, 1993). The ability of wood to resist biological degradation is defined as natural durability. It is generally low in the sapwood and can be high in the heartwood of some species (Hillis, 1987). The key feature of heartwood that provides natural durability is the accumulation of secondary metabolites known as extractives (Taylor et al., 2002).

Different wood degraders exist, which pose a risk of biodegradation of wood in certain environments.

1.6.1 Fungi

Fungi produce an extracellular enzymatic system, which breaks down the cell wall polymers. The monomeric degradation products are then absorbed by the fungi as a food source (Eriksson et al., 2012). Fungi require free available water for this process and therefore are a risk for wood utilisation only in wet conditions. Degradation of wood by fungi is also known as decay. Typically, two situations are distinguished when rating decay resistance of a timber: in contact with the ground (e.g. post and poles) and above the ground (e.g. decking). Standards like the NZS3602 (2003) or AS5604 (2005) classify timbers for their above-ground and in-ground performance into four durability classes: Class 1 - very durable, Class 2 - durable, Class 3 - moderately durable and Class 4 - non-durable (Page & Singh, 2014).

Wood is predominantly invaded by brown rots, white rots and soft rots, which differ in their extracellular enzymatic systems (Eriksson et al., 2012).

1.6.1.1 Brown rot

Brown rots depolymerises cellulose and hemicelluloses without removal of lignin due to the absence of lignolytic enzymes (Eriksson et al., 2012). Wood decayed by brown rots displays a crumbled, cubical and brown appearance that can be easily broken down into brown powder (Goodell, 2003). Some examples of brown rots are *Coniophora olivacea*, *C. puteana* (synonym for *C. cerebella*), *Serpula lacrymans*, *Gleophyllum abietinum*, *Antrodia xantha*, *A. vallantii*, *Postia placenta* and *Polyporus varcecundus*.

1.6.1.2 White rot

White rots are able to degrade lignin and thus making the structural polysaccharides of plant cell walls accessible to hydrolysis by cellulases and hemicelluloses. The lignolytic system of white rots is complex and consist of a cluster of oxidative enzymes, including lignin peroxidases (LiPs), manganese peroxidases (MnPs), lacases and oxidases. Some examples of white rots are *Trametes versicolor*, *Pycnoporous coccineus*, *Lopharia crassa* and *Perenniporia tephropora*.

1.6.1.3 Soft rot

Savory (1954) described a specific pattern of spongy decay by ascomycetes and deuteromycetes and termed it ‘soft rot’. Soft rot attacked wood is brown, soft in appearance and will crack when dried. The degradation of wood by soft rot involves tunnelling by fungal hyphae through the lignified cell walls (Blanchette, 1995). Soft rots share chemical characteristics with brown rots, decomposing cellulose and hemicelluloses but leaving lignin unmodified. Soft rots can sustain low oxygen levels and are therefore a more common threat to in-ground applications of wood. Some examples of soft rots include *Chaetomium globosum*, *Humicola grisea*, *Petriella setifera*, *Phialophora mutabilis* and *Trichurus spiralis* in terrestrial environments and *Halosphaeria* and *Pleospora* in marine and estuarine environments (Béguin & Aubert, 1994; Nilsson, 1973).

1.6.2 Wood degrading insects

Insects typically use wood as a habitat and not a food source (Johjima et al., 2006). Degradation is caused by mechanical chewing action. Lyctids and other borers feed on starch, which can be present in sapwood. Heartwood being devoid of starch is typically safe. However, some insects like the Asian long horn beetle (*Anoplophora glabripennis*) can be found in heartwood (Morewood et al., 2005).

Termites such as *Reticulitermes flavones* are probably the most damaging wood degrading insect in the tropics. They share an endosymbiotic relationship with microorganisms in their hindgut (Cleveland, 1923), which produce cellulose degrading enzymes (Yamaoka & Nagatani, 1978), enabling them to utilise wood cell walls as food source. Again, termite damage is caused by mechanical chewing. Some timbers have heartwood, which is resistant to termite attack.

1.7 Extractives

Wood extractives are smaller organic molecules, which can be extracted from wood. They are composed of numerous compounds of several molecule classes. Terpenes, phenols, fats and waxes as well as alkaloids have been described in wood (Rowe, 1989). Hydrophilic wood extractives typically include flavonoids, phenolic acids, tannins and stilbenes while lipophilic extractives include tryglycerides, fatty acids, diterpenoid resin acids, sterols and waxes (Oliveira et al., 2010). Different compounds and amounts are present in different tree tissues like heartwood, bark, leaves or sapwood. Heartwood extractives are primarily constituted of polyphenols, hydrolysable and condensed tannins (Duchesne et al., 1992; Hillis & Carle, 1962; Taylor et al., 2002). These compounds are responsible for the often distict colour of heartwood in some species (e.g. *Tectona grandis*, *Larix decidua*, *L. kaempferi*, *Juglans* species). Some of those compounds have bioactive properties contributing to the natural durability of the wood. As extractives are often specific to taxonomically related species they can be used as a tool for their classification.

1.7.1 Extractives variation within trees

In *Eucalyptus* extractive concentrations are higher in certain parts, e.g. heartwood, bark and branches (Hillis, 1971). Variability in composition and content of extractives exists not only between species but also between and within trees of a single species. Variability in the extractives content within individual trees is related to age of the tree's cambium, i.e. the distance from the pith. The extractive content increases from the inner to the outer heartwood (Hillis, 1987; Wilkes, 1984). As a consequence, growing heartwood trees in short rotation plantations as envisaged by NZDFI, will result in larger amounts of young heartwood, making it even more critical to ensure that it meets the technical specification of in-ground durability. This is possible as variation also exists between trees of a species and trees with good durability at a young age have been reported (Bush et al., 2011). It was shown that the variation in extractive content is partly under genetic control (Li et al., 2018) and therefore NZDFI's strategy is to select the *E. bosistoana* trees with most potent extracts. Therefore, as part of this thesis one objective was to investigate the variability in extractive composition of *E. bosistoana* heartwood between trees.

1.8 Extraction methods

Wood can be extracted with a single solvent or a combination of solvents. As wood contains numerous compounds of different molecule classes no single solvent system is able to extract all compounds. Lipophilic extractives in wood are abundant in nonpolar solvents like hexane, dichloromethane or diethyl ether and the hydrophilic fraction can be extracted with water and polar organic solvents such as acetone, ethanol, or methanol (Benouadah et al., 2018). Standard solvents used to extract wood according to ASTM D 1150 are shown in Table 1.2.

Wood extraction has been carried by hot water or stem distillation, soxhlet extraction using organic solvents or supercritical fluid (SFE) extraction using carbon dioxide at temperatures 40-100°C (Sjöström & Raimo, 1999). SFE is an alternative to conventional soxhlet extraction due to effective solute diffusion and mass transfer (Sjöström & Raimo, 1999). A recently more commonly used technique for wood extraction is automated accelerated solvent extraction (ASE). The advantage of this method is the combination of elevated temperature and pressure coupled with automation and the ability to use various solvents for extraction (Sjöström & Raimo, 1999).

Table 1.2: Extractable content in wood by different solvents (ASTMD1105-96, 2013).

Solvents	Extractable content in wood
Dichloromethane	Waxes, fats, resins, photo-sterols and non-volatile hydrocarbons
Ethanol-benzene	Dichloromethane-insoluble components, such as low-molecular-weight carbohydrates, salts, and other water-soluble substances
Hot water	Tannins, gums, sugars, starches, and colouring matter
Ethanol-methanol	Hydrophilic extractives

1.9 Extractives analysis

The development of analytical chromatographic methods like thin layer chromatography (TLC), high performance liquid chromatography (HPLC), high speed counter current chromatography (HSCCC) and gas chromatography (GC) provides numerous options for the qualitative and quantitative estimation of chemical compounds in wood (Barry et al., 2001; Benouadah et al., 2018; Davies et al., 2014; Hillis et al., 1974; Nawwar et al., 1997; Santos et al., 2011). Table 1.3 lists some compounds identified in wood and bark extracts of *Eucalyptus* species as well as the methods, which were used.

Table 1.3: Some compounds identified in wood and bark of *Eucalyptus* species and the analytical methods used.

Species	Compounds	Extract type	Analytical technique	Reference
E. grandis *E. urograndis*	Epicatechin, Quercetin-glucuronide, Ellagic acid-rhamnoside	Bark	(HPLC–ESI-MS), Tandem mass spectrometry	(Santos et al., 2012)
E. urograndis	Galloyl-*bis*-hexahydroxydiphenoyl (HHDP)-glucose, Gallic acid	Bark	(HPLC–ESI-MS), Tandem mass spectrometry	(Santos et al., 2012)
E. camaldulensis	Glycerides, Flavanols and Monosaccharides	Sapwood Heartwood	GC-MS	(Benouadah et al., 2018)

Species	Compounds	Extract type	Analytical technique	Reference
E. urograndis *E. urophylla* *E. camaldulensis*	α-Hydroxy fatty acids, β-Sitosterol, Fatty acids sterols	Bark free wood	GC-MS	(Silvério et al., 2007)

1.9.1 Gas chromatography (GC)

Gas chromatography has been used for rapid, and accurate quantification and identification of chemical compounds in wood extracts (Fernandez et al., 2001; Gutiérrez et al., 1998; Sitholé et al., 1992). A gas chromatograph is an instrument that uses a capillary through which different volatile components of a sample (e.g. extract) move in a mobile gas phase (e.g. helium) at different rates depending on their interaction with stationary phase in the capillary. The chemicals are then detected at the end of the column. The most commonly used detectors in GC are flame ionisation detectors (FID) and thermal conductivity detectors (TCD). FID is widely used to detect organic or hydrocarbon containing compounds in wood extracts (Gutiérrez et al., 1998). While these detectors allow the quantification of individual compounds, they provide no information on their chemical structure. Mass spectroscopy (MS) is able to provide information on the chemical structure of individual compounds and has been developed as a detector for GC in 1960 - 1970, now allowing identification of components in complex mixtures (Sjöström & Raimo, 1999). For example GC-MS has been used for the analysis of extractives in *E. camaldulensis* wood (Benouadah et al., 2018).

However, a requirement for GC analysis is that the wood extractives are entering the gas phase. This restricts the use of GC for larger, polymeric molecules as well as polar molecules have strong interactions (Pierce, 2004). The chemical structure of polar compounds can be modified by derivatization, reducing molecular interaction and making them more volatile. Derivatization can be achieved by different methods such as methylation, acetylation or silylation (Pierce, 2004). GC is a powerful method to directly quantify individual resin components, triglycerides and sterylesters (Sitholé et al., 1992). Wood extracts of polar solvents like ethanol require derivatization.

1.9.2 High performance liquid chromatography (HPLC)

Like GC, HPLC can be used to separate and quantify individual compounds in a wood extractive mixture. The principal difference to GC is that in HPLC a liquid instead of a gaseous phase is used to transport the compounds through a stationary phase (column) with which they interact. Interactions are manifold and give rise to a variety of different chromatographic techniques. As for GC a variety of detectors exists more or less suitable for individual compounds (Robards et al., 1994).

A requirement for HPLC is that the compounds are soluble in the mobile liquid phase. Consequently an advantage of HPLC for the analysis of wood extracts is that the extracts are already in a form which can be directly analysed. A disadvantage is a slightly lower resolution/separation of individual

compounds and that quantitative determination is not as straight forward as in GC due to the detector response being more dependent on the compound structure (Sjöström & Raimo, 1999).

Ultra-high performance liquid Chromatography (UHPLC) is a modified version of HPLC with increased column efficiency. This is mainly achieved by reducing the size of the column material to less than 2 µm (Taleuzzaman et al., 2015). The smaller particle size leads to increased back pressure of up to 100 MPa, while the HPLC operates typically at up to 40 MPa. The efficiency of UHPLC is also improved by employing higher temperatures to reduce the viscosity of mobile phase. Forty phenolics, eleven terpens and seven fatty and organic acids were characterised and identified in the extracts from heartwood, sapwood and the transition zone of *Pseudotsuga menziesii* (Ngouaby et al., 2018). Similarly, nine triterpenoids were quantified with UHPLC in root heartwood and root bark of *Ilex pubescens* (Cao et al., 2018). A comparison between HPLC and UHPLC is shown in table 1.4.

Table 1.4: Comparison between HPLC and UHPLC (Taleuzzaman et al., 2015)

Characteristics	**HPLC**	**UHPLC**
Sample injection volume	5 ml	2 ml
Particle size	3-5 µm	< 2 µm
Column temperature	30ºC	65ºC
Maximum back pressure	35-40 MPa	103.5 MPa
Column dimensions	150 x 3.2 mm	150 x 2.1 mm

1.9.3 Thin layer chromatography (TLC)

Non-volatile mixtures can also be separated by TLC. This chromatographic technique is performed on a sheet of glass, plastic, or aluminium foil coated with a thin layer of absorbent material (e.g. silica gel, aluminium oxide, or cellulose), the stationary phase (Harwood & Moody, 1989). The compounds are required to be dissolved in the mobile phase, which typically comprises a solvent mixture. The mobile phase with the analyte is then drawn up the plate via capillary action where separation occurs due to different interaction with the stationary phase. Ultraviolet light or chemical processes can be used to visualise the separated compounds. For example, anisaldehyde forms coloured adducts with many compounds and sulfuric acid will characterise organic compounds (Harwood & Moody, 1989).

TLC is inexpensive and fast as many samples can be analysed in parallel. However, quantification is difficult (Harwood & Moody, 1989) and resolution lower. Therefore, TLC has been largely replaced by GC or HPLC.

TLC has the advantage of separating the compounds non-destructively in space. Therefore, TLC plates with spatially separated compounds can be directly incubated with wood degrading fungi to test for bioactivity (Kawamura et al., 2011).

1.10 Objectives of the thesis

i) Test the hypothesis that heartwood formation in young trees differs from that in older trees, i.e. if young trees have an extended transition zone. Biological processes of heartwood formation in *E. bosistoana* trees were followed by visualising cell organelles in living parenchyma cells with microscopy (chapters 2 and 3).

ii) Identify the bioactive compounds and their variation in the heartwood of *E. bosistoana* by combining gas chromatography with fungal assays of heartwood extracts (chapters 4 and 5).

iii) Test if wound reaction in young *E. bosistoana* trees is under genetic control and correlated to heartwood features (heartwood diameter and extractive content). This would enable selection of trees for heartwood traits before heartwood formation in trees commences (chapter 6).

Figure 1.5 represents a flowchart that details the method and samples used.

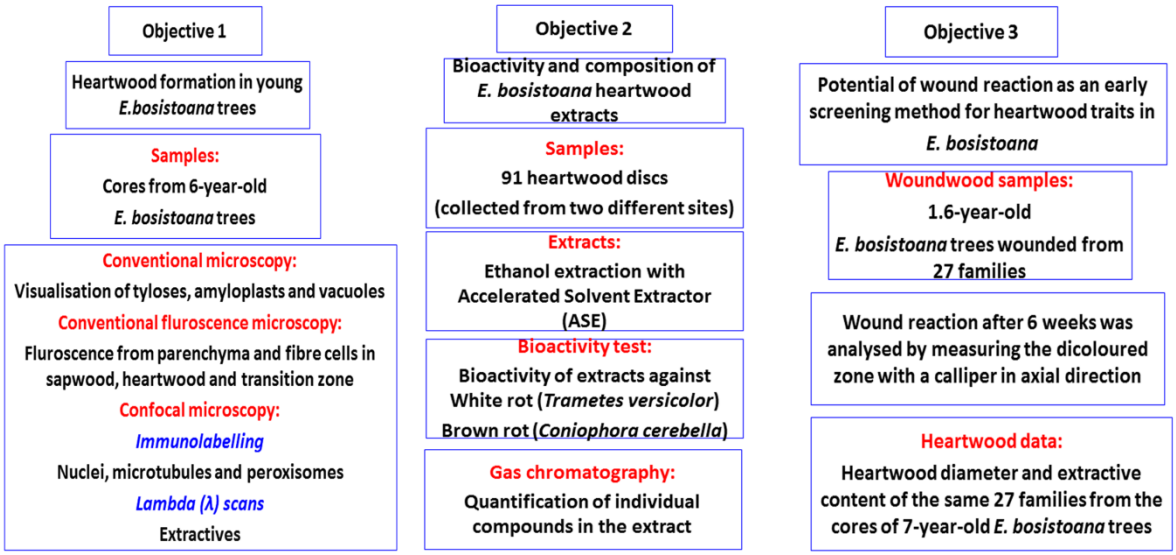

Figure 1.5: Flowchart details the methods and samples used in the objectives.

1.11 References

Abcam. (2018). *Direct vs indirect immunofluorescence.* Understand the difference between direct and indirect methods for immunofluorescence. Retieved from *https://www.abcam.com/secondary-antibodies/direct-vs-indirect-immunofluorescence*.

Apiolaza, L. A., Mcconnochie, R., Millen, P., Van Ballekom, S., & Walker, J. (2011). Introducing durable species to New Zealand drylands: genetics of early adaptation of *Eucalyptus bosistoana*. Wood Technology and Research Centre, Workshop proceedings, 137-144.

Alturkistani, H. A., Tashkandi, F. M., & Mohammedsaleh, Z. M. (2016). Histological Stains: A literature review and case study. *Global Journal of Health Science, 8*, 72–79.

AS5604. (2005). Timber—Natural durability ratings: Standards Australia Sydney.

ASTMD1105-96. (2013). Standard test method for preparation of extractive-free wood, ASTM international. West Conshohocken.

Ballekom, S. V., & Millen, P. (2017). *NZDFI: achievements, constraints and opportunities.* Paper presented at the durable *Eucalypts* on drylands: protecting and enhancing value, Marlborough Research Centre, Blenheim.

Bamber, R. (1964). Sapwood and heartwood: A review. *Forestry Abstracts, 46*, 567-580

Barnett, J., & Jeronimidis, G. (2003). *Wood quality and its biological basis*. Oxford, England: Blackwell Publishing.

Barry, K., Davies, N., & Mohammed, C. (2001). Identification of hydrolysable tannins in the reaction zone of *Eucalyptus nitens* wood by high performance liquid chromatography–electrospray ionisation mass spectrometry. *Phytochemical Analysis, 12*, 120-127.

Béguin, P., & Aubert, J. P. (1994). The biological degradation of cellulose. *FEMS Microbiology Reviews, 13*, 25-58.

Benouadah, N., Pranovich, A., Aliouche, D., Hemming, J., Smeds, A., & Willför, S. (2018). Analysis of extractives from *Pinus halepensis* and *Eucalyptus camaldulensis* as predominant trees in Algeria. *Holzforschung, 72*, 97-104.

Blanchette, R. A. (1995). Degradation of the lignocellulose complex in wood. *Canadian Journal of Botany, 73*, 999-1010.

Boland, D. J., Brooker, M. I. H., Chippendale, G., Hall, N., Hyland, B., Johnston, R. D., Kleinig, D., McDonald, M., & Turner, J. (2006). *Forest trees of Australia*. Clayton, Australia: CSIRO publishing.

Bootle, K. R. (1983). *Wood in Australia. Types, properties and uses*. Sydney, Australia: McGraw-Hill Book Company.

Bootle, K. R. (2005). Wood in Australia.Types, properties, and uses (2nd ed.): . Australia: McGraw-Hill.

Bush, D., McCarthy, K., & Meder, R. (2011). Genetic variation of natural durability traits in *Eucalyptus cladocalyx* (sugar gum). *Annals of Forest Science, 68*, 1057–1066.

Cao, D., Wang, Q., Jin, J., Qiu, M., Zhou, L., Zhou, X., Li, H., & Zhao, Z. (2018). Simultaneous qualitative and quantitative analyses of triterpenoids in *Ilex pubescens* by ultra-high-performance liquid chromatography coupled with quadrupole time-of-flight mass spectrometry. *Phytochemical Analysis, 29*, 168-179.

Celedon, J. M., & Bohlmann, J. (2017). An extended model of heartwood secondary metabolism informed by functional genomics. *Tree Physiology, 38*, 311-319.

Chaffey, N. (1999). Cambium: old challenges–new opportunities. *Trees-Structure and Function, 13*, 138-151.

Chaffey, N. (2002). Why is there so little research into the cell biology of the secondary vascular system of trees? *New Phytologist, 153*, 213-223.

Cleveland, L. R. (1923). Symbiosis between termites and their intestinal protozoa. *Proceedings of the National Academy of Sciences, 9*, 424-428.

Davies, N. T., Wu, H. F., & Altaner, C. M. (2014). The chemistry and bioactivity of various heartwood extracts from redwood (*Sequoia sempervirens*) against two species of fungi. *New Zealand Journal of Forestry Science, 44*, 17.

Duchesne, L., Hubbes, M., & Jeng, R. (1992). Biochemistry and molecular biology of defense reactions in the xylem of angiosperm trees. In R. Blanchette & A. R. Bigges (Eds.), *Defense mechanisms of woody plants against fungi* (pp. 133-146): Springer.

Eaton, R. A., & Hale, M. D. (1993). *Wood: decay, pests and protection*: Chapman and Hall Ltd.

EN350-1. (1994). Durability of wood and wood-based products – Natural durability of solid wood: Part 1: Guide to the principles of testing and classification of the natural durability of wood, European Comittee for Standardization.

Eriksson, K. E. L., Blanchette, R., & Ander, P. (2012). Microbial and enzymatic degradation of wood and wood components. Berlin: Springer Science & Business Media.

Evert, R. F. (2006). *Esau's plant anatomy: Meristems, cells, and tissues of the plant body: Their structure, function, and development* . USA, Oak Brook, IL: John Wiley & Sons.

Fahn, A., & Arnon, N. (1963). The living wood fibres of *Tamarix aphylla* and the changes occurring in them in transition from sapwood to heartwood. *New Phytologist, 62*, 99-104.

Fahn, A., & Leshem, B. (1963). Wood fibres with living protoplasts. *New Phytologist, 62*, 91-98.

Fernandez, M., Watson, P., & Breuil, C. (2001). Gas chromatography–mass spectrometry method for the simultaneous determination of wood extractive compounds in quaking aspen. *Journal of Chromatography A, 922*, 225-233.

Funada, R. (2003). Immunolocalisation and visualisation of the cytoskeleton in gymnosperms using confocal laser scanning microscopy. In N. J. Chaffey (Ed.), *Wood Formation in Trees: Cell and Molecular Biology Techniques* (pp. 163-178). London:CRC Press.

Goodell, B. (2003). Brown-rot fungal degradation of wood: our evolving view. *Wood deterioration and preservation, Advances in our changing world*. In B. Goodell, D. D. Nichola, T.P. Schultz. *ACS symposium series,845,* 378-398.

Gordon, M. (1912). Ray tracheids in *Sequoia sempervirens*. *New Phytologist, 11*, 1-6.

Gutiérrez, A., Del, R., Jose, C., González, V., Francisco, J., & Martın, F. (1998). Analysis of lipophilic extractives from wood and pitch deposits by solid-phase extraction and gas chromatography. *Journal of Chromatography A, 823*, 449-455.

Harwood, L. M., & Moody, C. J. (1989). *Instructor's Manual to Accompany Experimental Organic Chemistry: Principles and Practice*: Blackwell Scientific Publications.

Hepler, P. K., & Gunning, B. E. (1998). Confocal fluorescence microscopy of plant cells. *Protoplasma, 201*, 121-157.

Hillis, W. E., & Carle, A. (1962). The origin of the wood and bark polyphenols of eucalyptus species. *Biochemical Journal, 82*, 435.

Hillis, W. E. (1971). Distribution, properties and formation of some wood extractives. *Wood Science and Technology, 5*, 272-289.

Hillis, W. E. (1987). *Heartwood and tree exudates*. New York: Springer.

Hillis, W. E., Hart, J. H., & Yazaki, Y. (1974). Polyphenols of *Eucalyptus sideroxylo*n wood *Phytochemistry, 13*, 1591-15995.

Hornatowska, J. (2005). Visualisation of pectins and proteins by microscopy (STFI-Packforsk report no- 87). (pp. 2-21): Mechanical pulp cluster program. Eka chemicals, Holmen paper, Metsaliito Group, UPM-Kymmene.

Islam, M. A., & Begum, S. (2011). Distribution of starch, lipid and nuclei in xylem and phloem of *Tectona grandis* Linn. *Journal of Bio-Science, 19*, 29-35.

Johjima, T., Taprab, Y., Noparatnaraporn, N., Kudo, T., & Ohkuma, M. (2006). Large-scale identification of transcripts expressed in a symbiotic fungus (*Termitomyces*) during plant biomass degradation. *Applied Microbiology and Biotechnology, 73*, 195-203.

Kawamura, F., Ramle, S. F. M., Sulaiman, O., Hashim, R., & Ohara, S. (2011). Antioxidant and antifungal activities of extracts from 15 selected hardwood species of Malaysian timber. *European Journal of Wood and Wood Products, 69*, 207-212.

Kitin, P., Funada, R., Sano, Y., & Ohtani, J. (2000). Analysis by confocal microscopy of the structure of cambium in the hardwood *Kalopanax pictus*. *Annals of Botany, 86*, 1109-1117.

Lev-Yadun, S., & Aloni, R. (1995). Differentiation of the ray system in woody plants. *The Botanical Review, 61*, 45-84.

Li, Y. (2018). *Use of near infrared spectroscopy to predict wood traits in Eucalyptus species.* Doctor of Philosophy in Forestry. University of Canterbury, Christchurch, New Zealand.

Li, Y., Apiolaza, L. A., & Altaner, C. M., (2018). Genetic variation in heartwood properties and growth traits of *Eucalyptus bosistoana*. *European Journal of Forest Research, 137*, 565-572.

Millen, P., Ballekom, S. V., Altaner, C. M., Apiolaza, L., Mason, E., McConnochie, R., Morgenroth, J., & Murray, T. (2018). Durable eucalypt forests - a multi-regional opportunity for investment in New Zealand drylands. *New Zealand Journal of Forestry Science, 63*, 11–23.

Morewood, W., Hoover, K., Neiner, P., & Sellmer, J. (2005). Complete development of *Anoplophora glabripennis* (Coleoptera: *Cerambycidae*) in northern red oak trees. *The Canadian Entomologist, 137*, 376-379.

Nakaba, S., Sano, Y., Kubo, T., & Funada, R. (2006). The positional distribution of cell death of ray parenchyma in a conifer, *Abies sachalinensis*. *Plant Cell Reports, 25*, 1143-1148.

Nakaba, S., Yoshimoto, J., Kubo, T., & Funada, R. (2008). Morphological changes in the cytoskeleton, nuclei, and vacuoles during cell death of short-lived ray tracheids in the conifer *Pinus densiflora*. *Journal of Wood Science, 54*, 509-514.

Nakaba, S., Kubo, T., & Funada, R. (2011). Nuclear DNA fragmentation during cell death of short-lived ray tracheids in the conifer *Pinus densiflora*. *Journal of Plant Research, 124*, 379-384.

Nakaba, S., Begum, S., Yamagishi, Y., Jin, H., Kubo, T., & Funada, R. (2012). Differences in the timing of cell death, differentiation and function among three different types of ray parenchyma cells in the hardwood *Populus sieboldii× P. grandidentata*. *Trees, 26*, 743-750.

Nakaba, S., Sano, Y., & Funada, R. (2013). Disappearance of microtubules, nuclei and starch during cell death of ray parenchyma in *Abies sachalinensis*. *IAWA Journal, 34*, 135-146.

Nawwar, M. A. M., Marzouk, M. S., Niggea, W., & Linscheid, M. (1997). High-performance liquid chromatographic/electrospray ionization mass spectrometric screening for polyphenolic compounds of *Epilobium hirsutum*-The structure of the unique ellagitannin epilobamide-A. *Journal of Mass Spectrometry, 32*, 645-654.

Ngouaby, H., Pinault, E., Gloaguen, V., Costa, G., Sol, V., Millot, M., & Mambu, L. (2018). Profiling and seasonal variation of chemical constituents from *Pseudotsuga menziesii* wood. *Industrial Crops and Products, 117*, 34-49.

Nicholas, I., & Millen, P. (2012). *Durable eucalypt leaflet series: Eucalyptus bosistoana*. Retrieved from *http://nzdfi.org.nz/wp-content/uploads/2015/01/E-bosistoana-information-leaflet.pdf*.

Nilsson, T. (1973). Studies on wood degradation and cellulolytic activity of microfungi (pp. 104). Stockholm: Predecessors to SLU: Royal School of Forestry.

NZS3602. (2003). Timber and wood-based products for use in building (pp. 44). New Zealand.

Oliveira, L. S., Santana, A. L., Maranhão, C. A., Rita de Cássia, M., de Lima, V. L. A. G., Da Silva, S. I., Nascimento, M. S., & Bieber, L. (2010). Natural resistance of five woods to *Phanerochaete chrysosporium* degradation. *International Biodeterioration & Biodegradation, 64*, 711-715.

Page, D., & Singh, T. (2014). Durability of New Zealand grown timbers. *NZ Journal of Forestry, 58*, 27.

Pereira, H. (1988). Variability in the chemical composition of plantation *Eucalyptus* (*Eucalyptus globulus* Labill.). *Wood and Fibre Science, 20*, 82-90.

Pierce. (2004). GC derivatization *Applications Handbook & Catalog* (pp. 1-5).

Plomion, C., Leprovost, G., & Stokes, A. (2001). Wood formation in trees. *Plant Physiology, 127*, 1513-1523.

Raven, P. H., Evert, R. F., & Eichhorn, S. E. (2005). *Biology of plants*: Berlin:Macmillan.

Regan, S., & Sundberg, B. (2002). High resolution in situ hybridization in woody tissues. *Wood formation in trees, cell and molecular biology techniques* In N. J. Chaffey (Ed.), 297-317.

Robards, K., Haddad, P. R., Jackson, P. E., & Haddad, P. A. (1994). *Principles and Practice of Modern Chromatographic Methods*: Academic Press.

Rowe, J. (1989). Natural products of woody plants. I & II. *Springer: Berlin, 1243*, 373-374.

Santos, S. A. O., Carmen S. R. F., Domingues, M. R. M., Silvestre, A. J. D., & Neto, C. P. (2011). Characterization of phenolic components in polar extracts o*f Eucalyptus globulus* Labill. bark by high-performance liquid chromatography–mass spectrometry. *Journal of Agricultural and Food Chemistry, 59*, 9386–9393.

Santos, S. A. O., Villaverde, J. J., Freirea, C. S., Domingues, M. R. M., Netoa, C. P., & Silvestrea, A. J. D. (2012). Phenolic composition and antioxidant activity of *Eucalyptus grandis*, *E. urograndis* (*E. grandis* × *E. urophylla*) and *E. maidenii* bark extracts. *Industrial Crops and Products, 39*, 120-127.

Savory, J. (1954). Breakdown of timber by *Ascomycetes* and Fungi *Imperfecti*. *Annals of Applied Biology, 41*, 336-347.

Sherrard, E. C., & Kurth, E. (1933). The distribution of extractive in redwood: its relation to durability. *Industrial and Engineering Chemistry, 25*, 300-302.

Shotton, D. (1993). *Electronic light microscopy: the principles and practice of video-enhanced contrast, digital intensified fluorescence, and confocal scanning light microscopy*. New York: Wiley-Liss.

Silvério, F. O., Barbosa, L. C. A., Silvestre, A. J., Piló-Veloso, D., & Gomide, J. L. (2007). Comparative study on the chemical composition of lipophilic fractions from three wood tissues of *Eucalyptus* species by gas chromatography-mass spectrometry analysis. *Journal of Wood science, 53*, 533-540.

Sitholé, B., Sullivan, J., & Allen, L. (1992). Identification and quantitation of acetone extractives of wood and bark by ion exchange and capillary GC with a spreadsheet program. *Holzforschung, 46*, 409-416.

Sjöström, E., & Raimo, A. (1999). Extractives. In T. E. Timell (Ed.), *Analytical Methods in Wood Chemistry, Pulping, and Papermaking.* (pp. 305-315). Berlin: Springer Science & Business Media.103-120.

Spicer, R. (2005). Senescence in secondary xylem: Heartwood formation as an active developmental program. In M. N. Holbrook & M. A. Zwieniecki (Eds.), *Vascular Transport in Plants* (pp. 457-475). San Diego, Elsevier Academic Press.

Spicer, R., & Holbrook, N. (2007). Parenchyma cell respiration and survival in secondary xylem: does metabolic activity decline with cell age? *Plant, Cell & Environment, 30*, 934-943.

Taleuzzaman, M., Ali, S., Gilani, S., Imam, H. A., & Hafeez, A. (2015). Ultra Performance Liquid Chromatography (UPLC)—A Review. *Austin Journal of Analytical and Pharmaceutical Chemistry, 2*, 1-5.

Taylor, A. M., Gartner, B. L., & Morrell, J. J. (2002). Heartwood formation and natural durability- A review. *Wood and Fiber Science, 34*, 587-611.

Thomas, J., Ingerfeld, M., Nair, H., Chauhan, S. S., & Collings, D. A. (2013). Pontamine fast scarlet 4B: a new fluorescent dye for visualising cell wall organisation in radiata pine tracheids. *Wood Science and Technology, 47*, 59-75.

Titford, M. (2009). Progress in the development of microscopical techniques for diagnostic pathology. *Journal of Histotechnology, 32*, 9-19.

Townsend, T. G., Dubey, B., & Gabriele, H. (2004). Assessing potential waste disposal impact from preservative treated wood products. *Proceedings of the Environmental Impacts of Preservative-Treated Wood Conference Orlando,* Florida *169.*

Vazquez-Cooz, I., & Meyer, R. (2002). A differential staining method to identify lignified and unlignified tissues. *Biotechnic & Histochemistry, 77*, 277-282.

West, M., Vaidya. A, & Singh A. P. (2012). Correlative light and scanning electron microscopy of the same sections gives new insights into the effects of pectin lyase on bordered pit membranes in *Pinus radiata* wood. *Micron, 43,* 916-919.

Wilkes, J. (1984). The Influence of rate of growth on the density and heartwood extractives content of *Eucalypt* species. *Wood Science and Technology, 18,* 113-120.

Wilson, T. (1990). Confocal microscopy. *Academic Press: London, 426*, 1-64.

Yamaoka, I., & Nagatani, Y. (1978). Cellulose digestion system in the termite, *Reticulitermes speratus* (Kolbe). III. Ultrastructure and function of the hindgut epithelium. *Dobutsugaku zasshi*, *52*, 121-130.

Zhang, C., Barthelson, R. A., Lambert, G. M., & Galbraith, D. W. (2008). Global characterization of cell-specific gene expression through fluorescence-activated sorting of nuclei. *Plant Physiology*, *147*, 30-40.

Zhang, R., Xu, K., & Ye, K. (2015). Concentration and distribution of nuclei and plastids in xylem cells in *Cunninghamia lanceolata* and *Aquilaria sinensis*. *Bioresources*, *10*, 1304-1317.

Chapter-2

Cell organelles and fluorescence of parenchyma cells in *Eucalyptus bosistoana* sapwood and heartwood investigated by microscopy

This chapter is published:

Mishra, G., Collings, D., & Altaner, C. (2018). Cell organelles and fluorescence of parenchyma cells in *Eucalyptus bosistoana* sapwood and heartwood investigated by microscopy. *New Zealand Journal of Forestry Science*, *48*, 1-10.

2.1 Introduction

Wood formation (xylogenesis) in vascular plants is a complex biological process that includes cell division from secondary vascular cambium, cell elongation and differentiation, secondary cell wall deposition, programmed cell death and heartwood formation (Plomion et al., 2001). Wood consists of living and dead cells forming symplasmic and apoplasmic networks in trees. The apoplasmic system contains tracheids, vessels and dead fibres. The symplasmic system integrates the living parenchyma cells. These living parenchyma cells in the symplasmic system perform multiple roles in sugar transport and storage, embolism repair, defence against pathogens and secondary modification of xylem cells (Nakaba et al., 2012a).

Parenchyma refers to a tissue composed of living cells that varies widely by morphology and metabolism. Parenchyma cells are distributed throughout the plant body in different forms such as small clusters, strands or heterogeneously in tissues such as xylem and phloem (Pruyn & Spicer, 2012). In secondary vascular tissue, parenchyma cells are typically oriented radially and axially forming a three-dimensional interconnected network of living cells (Spicer, 2005, 2014).

Three distinct zones can be distinguished in the stems of older trees: sapwood; heartwood; and a transition zone. Heartwood can be defined as an internal part of the stem, often darker in appearance than surrounding sapwood, devoid of living cells, water conduction, and in which the reserve materials (e.g. starch) have been removed. Some tree species additionally deposit heartwood substances imparting biotic resistance into this part of the stem (Bamber, 1964; Nakaba et al., 2012b). Parenchyma cells remain alive for many years in the sapwood (Nakaba et al., 2011; Nakaba et al., 2008), retaining their intracellular organisation including organelles (nuclei, endomembranes, mitochondria, plastids, peroxisomes) and structural components such as the cytoskeleton (microtubules and actin microfilaments) (Fukuda, 2000; Funada, 2000; Spicer, 2005, 2014; Spicer & Holbrook, 2007). The transition zone is the boundary between sapwood and heartwood. This is normally a narrow, often pale-coloured zone surrounding the heartwood that contains living cells that

are usually devoid of starch, impermeable to liquids and with a moisture content lower than sapwood (Taylor et al., 2002). The extension and generation of heartwood takes place from the transition zone (Déjardin et al., 2010).

Heartwood formation is a genetically and metabolically controlled programmed cell death process, which leads to the formation of heartwood extractives (Magel et al., 2001). In the transition zone, an increase in metabolic activity of parenchyma cells occurs followed by a series of cumulative events (rapid synthesis of secondary metabolites called extractives, blockages of conducting elements by formation of tyloses and structural changes in pits) preceding the death of the parenchyma cells (Spicer, 2005). The extractives formed by the living parenchyma cells in the transition zone are released and deposited in the neighbouring cells, imparting durability and colour in some species. It is postulated that heartwood formation regulates the amount and function of sapwood, controlling water transport and storage of reserve materials (Spicer, 2005). Despite the ecological importance of heartwood, the biological aspects of its formation are still not well understood.

Heartwood is also of economic importance as only heartwood is coloured or naturally durable. Variations in colour and natural durability are caused by biologic differences in heartwood formation and directly impact on timber value. This is in particular true for a hardwood industry based on fast-growing, short-rotation plantations. Such sustainably managed plantations have the potential to supply the exiting demand for coloured and naturally durable timbers, which are currently often unsustainably or illegally sourced from virgin tropical forests. The New Zealand Dryland Forests Initiative (NZDFI) has identified this opportunity for New Zealand (Millen et al., 2018) and has engaged in a research programme to support the establishment of *Eucalyptus bosistoana* F.Muell., a Class 1 durable timber (Australian Standard, AS5604-2005), in New Zealand.

The purpose of the study was to a) identify microscopy techniques that are able to detect changes in chemical composition as well as cell organelles in *E. bosistoana* sapwood and heartwood and b) obtain better understanding of the changes occurring after heartwood formation.

2.2 Materials and methods

2.2.1 Wood material and fixation

Wood samples were collected in summer (December) 2014 from *E. bosistoana* trees grown at two different sites in the South Island of New Zealand. Stem sections of 2-year-old trees were collected from a research trial in Christchurch, Canterbury. 10 cm thick stem discs from 11-year-old trees were collected at breast height near Havelock, Marlborough. Heartwood and sapwood were visually distinguished in the fresh state on the samples and marked with a pencil. Radial strips (~4 cm in tangential and ~2 cm axial direction) were cut from the green samples chiselled along the grain into smaller pieces. Approximately 30 wood pieces were fixed in 1000 ml of cytoskeleton stabilisation

buffer as described in (Mishra et al., 2018). Radial sections (10-20 μm thick) were cut with a sledge microtome. Acetone treatment of tissue sections were performed at -20°C for 20 min and subsequently washed with distilled water in a beaker under gentle stirring for 15 min.

2.2.2 Histochemistry

A Nikon Eclipse 50i microscope with a Nikon digital sight DS-5 MC camera was used in transmitted light and fluorescence modes. Radial sections were stained with iodine/potassium iodide (0.1% in water) to visualise starch grains, or amido black (0.2% in 7% acetic acid) to label proteins (Islam & Begum, 2012; Nakaba et al., 2012a), or toluidine blue (0.1% in water). Sequential labelling with toluidine blue staining followed by iodine/potassium iodide was also used. Sections were mounted in glycerol.

Sections were stained with either Sudan IV (1% in 70% ethanol) (Begum et al., 2010) or Nile red (dissolved in 0.5% H_2SO_4) (Greenspan et al., 1985), to highlight lipid droplets. Protein stains such as Coomassie brilliant blue R-250 (0.25 g in 90 ml of methanol: distilled water (1:1, v/v) and 10 ml of glacial acetic acid) and Ponceau S (0.1 % (w/v) in 5% acetic acid) as well as colour-based DNA stains such as acetocarmine (1 % in acetic acid) (Islam & Begum, 2011; Nakaba et al., 2006) and methyl green pyronin (1% in acetate buffer solution comprised of glacial acetic acid and sodium acetate) (Potvin, 1979) were used on sapwood and heartwood sections. Similarly, fluorescent DNA stains such as DAPI (4′, 6-diamidino-2-phenylindole) (1 μl in 999 μl distilled water), propidium iodide (1 μl in 999 μl distilled water) and Syto-13 (1 μl in 999 μl distilled water) were found to be unreliable markers for living nuclei as these dyes bound to the cell walls and did not clearly resolve nuclei.

2.2.3 Immunofluorescence microscopy

Sections were labelled with monoclonal antibodies to visualise microtubules (mouse anti-α-tubulin, clone B512, Sigma-Aldrich, St Louis MO USA), nuclei (histone proteins or rabbit anti-histone H3, catalogue number 07-690, Merck Millipore, Billerica MA, USA) and peroxisomes (rabbit polyclonal anti-cottonseed catalase, courtesy of Dr. Richard Trelease, University of Arizona) (Kunce et al. 1988). The sections were observed with a Leica SP5 confocal microscope system operating on a DMI6000 inverted microscope with 20x NA 0.7 and 63x NA 1.3 glycerol immersion lenses (Leica, Wetzlar, Germany) after applying fluorescein and Cy5 labelled secondary antibodies. The secondary antibodies used were mixtures of either goat anti-rabbit-Cy5 (Jackson Immunoresearch, West Grove PA, USA) and sheep anti-rabbit-fluorescein (Silenus, Boronia, Vic, Australia) or goat anti-mouse-Cy5 (Jackson Immunoresearch) and sheep anti-mouse-fluorescein (Silenus). The detailed procedure was described in (Mishra et al., 2018).

For immunolocalisation of nuclei, sections were post-fixed with FAA solution (10% (v/v) formaldehyde, 5% (v/v) acetic acid and 50% (v/v) ethanol) overnight. This step, based on Nic-Can et al. (2013), reduced the background fluorescence and promoted antibody binding. Samples not post-

fixed with FAA showed minimal labelling with the antibody, and primary antibody controls were also negative.

2.2.4 Confocal microscopy

Variations in the colour of autofluorescence from wood samples, different cells and organelles were detected by recording fluorescence emission spectra using excitation wavelengths of 405 and 488 nm. Emissions were collected from 420 to 700 and 500 nm - 700 nm, respectively. Image intensities from organelles, parenchyma or from selected fibre cells were quantified using ImageJ software (FIJI installation of version 1.47v, National Institute of Health, Bethesda, MD, USA) using the 'Plot Z axis profile' function.

2.3 Results and Discussion

A range of cytological features associated with the transition of living parenchyma cells in sapwood to dead cells in heartwood using wood were investigated by microscopy in radial wood sections collected from 2-year-old and 11-year-old *E. bosistoana* trees.

2.3.1 Histochemical observations

Three different histochemical stains labelled living parenchyma. Starch, which is localised in amyloplasts, was detected as black granules with iodine/potassium iodide stain. Starch labelling was present in the radial (white arrows, Figure 2.1a) and axial (black arrows, Figure 2.1a) parenchyma cells of sapwood but was absent from heartwood (Figure 2.1d). This is consistent with previously described transitions of parenchyma cells in a variety of different angiosperm and gymnosperm species. The presence of starch was reported in sapwood and its absence from heartwood in *Larix kaempferi* (Lamb.) Carr. (Japanese larch) (Islam et al., 2012) as well as in *Tectona grandis* L.f. (Teak) (Islam & Begum, 2011). Consistent with their observations, our results suggested that starch depletion in ray cells was associated with cell death.

The second histochemical stain used was amido black, which stained proteins a bluish-black colour. This showed that parenchyma cells in sapwood retained proteins indicating that they remained alive (arrows, Figure 2.1b). The parenchyma in heartwood lacked proteins, which indicated that it had undergone cell death (Figure 2.1e). Again, these observations match literature reports. Islam & Begum (2012) investigated *Artocarpus heterophyllus* Lam. (Jackfruit) and reported the presence of more protein in younger ray parenchyma cells than in ray parenchyma of older wood. Their results suggested that dissapearance of proteins in ray cells was associated with cell death, which coincided with our observations. Similar observations were also reported by Datta and Kumar (1987) concerning the presence of starch and proteins in parenchyma cells of inner and outer sapwood of *T. grandis* and their absence in heartwood. However, it needs to be taken into account that the starch and protein content in xylem was reported to vary among seasons and species (Begum et al., 2013;

Nakaba et al., 2012a). The lowest reserves are typically present in spring after bud flush and the highest during winter dormancy (Rossi et al., 2007; Rossi et al., 2008). Round structures in heartwood (arrows, Figure 2.1d, e, f) sections were likely heartwood extractives synthesised in ray parenchyma cells that were not evident in sapwood (Figure 2.1a, b, c). This was consistent with previously reported observations of polyphenols in ray parenchyma cells of *Pinus densiflora* Siebold & Zucc. and *P. rigida* Mill. (Nakaba et al., 2008).

The third histochemical stain was toluidine blue. This stained the vacuoles and other organelles of sapwood a bluish colour indicating that they were alive (arrows, Figure 2.1c). No indications of vacuoles were observed in heartwood (Figure 2.1f). Fukuda (2000) suggested that the collapse of the vacuoles could result in the release of hydrolytic enzymes that degrade cell organelles such as nuclei (Kuriyama & Fukuda, 2002). Disruption of vacuoles followed by disappearance of nuclei was observed in ray tracheids located further inside the stem of *P. densiflora* (Nakaba et al., 2011).

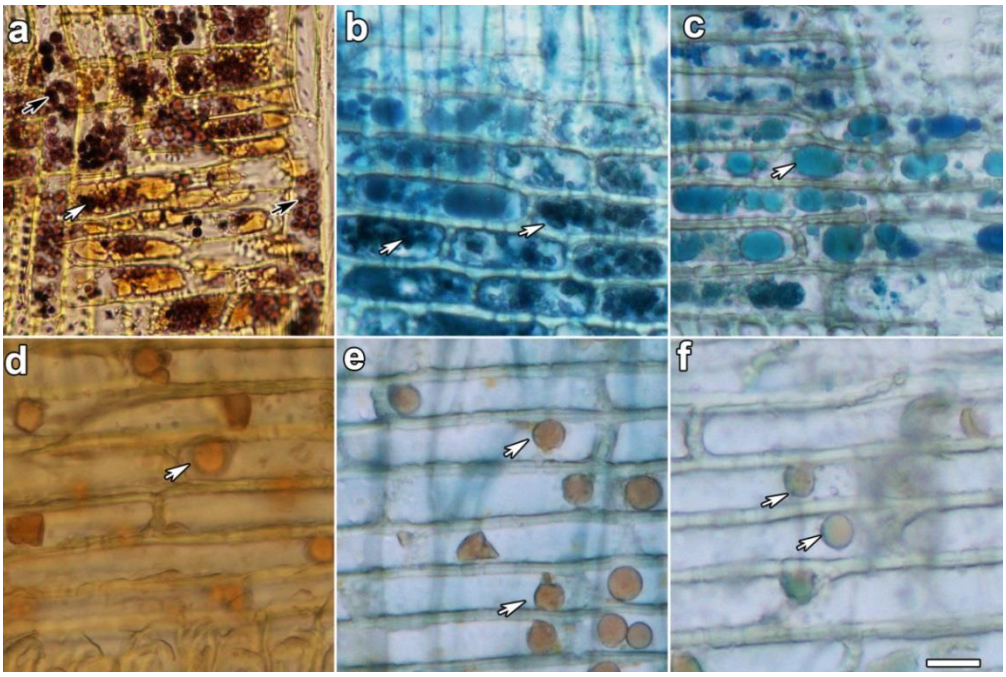

Figure 2.1: Histochemical staining of ray parenchyma in sapwood (top row) and heartwood (bottom row) from a 11-year-old *E. bosistoana* tree. Starch granules were stained black with iodine/potassium iodide in radial (white arrows) and axial (black arrows) parenchyma of sapwood but were absent in heartwood (a, d). Proteins and vacuoles (arrows) were stained bluish-black with amido black in sapwood but were absent from heartwood (b, e). Vacuoles (arrows) stained bluish with toluidine blue in parenchyma of sapwood but were absent or breaking down in heartwood (c, f). Round structures (arrows) in heartwood (d, e, f) were likely heartwood extractives synthesized in ray parenchyma cells. These round structures were not evident in sapwood. Scale bar = 20 μm for all images.

The identification of the small organelles labelled by toluidine blue remains unclear. However, sequential staining of the same section with toluidine blue (arrows, Figure 2.2a) followed by

potassium iodide (arrows, Figure 2.2b) confirmed that the toluidine blue labelled organelles were distinct from the amyloplasts.

Several other stains were investigated, but these did not provide good labelling in *E. bosistoana*. Stains for lipid droplets including Sudan IV, previously used in wood samples (Begum et al., 2010; Begum et al., 2013; Islam et al., 2012), and Nile red (Greenspan et al., 1985) failed to give good labelling. These observations suggest that unlike *T. grandis*. (Islam & Begum, 2011) and *Cryptomeria japonica* (L. f.) D.Don. (Begum et al., 2010), lipid droplets were mostly absent from the parenchyma of *E. bosistoana* samples in summer.

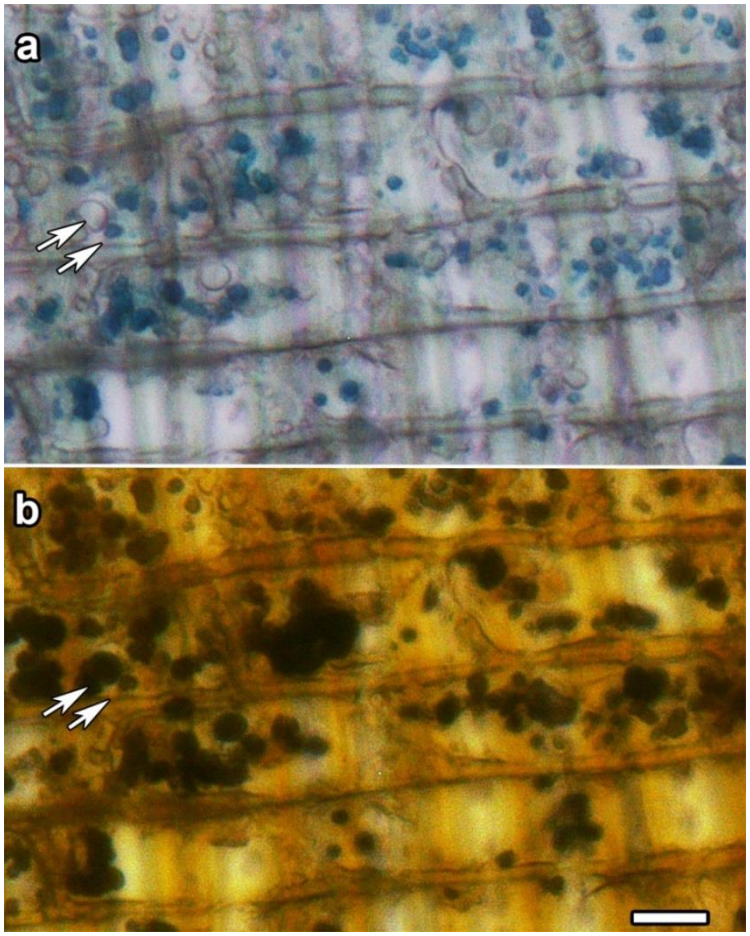

Figure 2.2: Sapwood section from a 2-year-old *E. bosistoana* tree showing ray parenchyma imaged at the same location that had been stained sequentially with: (a) toluidine blue; and (b) iodine/potassium iodide. Arrows indicate examples of organelles showing differential staining. Scale bar = 20 μm.

However, it needs to be taken into account that, similar to the starch and protein content, the lipid content in xylem has been reported to vary among seasons and species (Begum et al., 2013). Similarly, two protein stains that are more commonly associated with electrophoresis than

histochemistry, Coomassie brilliant blue R-250 and Ponceau S, failed to provide clear staining of ray parenchyma.

2.3.2 Autofluorescence

A significant problem for the analysis of *E. bosistoana* wood was the fact that the samples were autofluorescent at most wavelengths. This autofluorescence derived from at least three different sources.

The main source of autofluorescence was from the vacuoles in parenchyma cell which, in sapwood, were fluorescent at all wavelengths (arrows, Figure 2.3b, c, d), but which became degraded in heartwood (Figure 2.3f, g, h). The observations led us to use spectral imaging (lambda scanning) with excitation at 405 nm (Figure 2.3i), 488 nm (Figure 2.3j) and 561 nm (Figure 2.3k), and with the emission spectra from the sapwood vacuoles quantified from 420-700 nm, 500-700 nm and 560-700 nm respectively. The observations showed that emission spectra were shifted to longer wavelengths as excitation wavelength increased. Fluorescence peaked at 508 nm using 405 nm excitation, at 575 nm for 488 nm excitation and at about 640 nm for 561 nm excitation.

The second source of autofluorescence was from the cell walls of both the parenchyma and fibre cells. Fluorescence emission spectra of parenchyma and fibre cells of sapwood and heartwood indicated differences in chemical composition. Using 405 nm excitation, the emission spectra for fibre cells showed a peak in fluorescence at 480 nm in both sapwood and heartwood (Figure 2.4a) whereas the emission peak for the parenchyma cell walls was at a longer wavelength of almost 488 nm in sapwood and at an even longer wavelength of 500 nm in heartwood (Figure 2.4b). Using 488 nm excitation, the emission spectra for fibre cells showed a peak in fluorescence at 560 nm in both sapwood and heartwood (Figure 2.4c) whereas the emission peaks for the parenchyma cell walls were at a longer wavelength in sapwood (565 nm) and heartwood (570 nm) (Figure 2.4d). These observations showed that for 11-year-old *E. bosistoana*, the transition from sapwood to heartwood did not markedly change the fluorescence emission spectra of fibre cell walls, whereas the emission spectra for parenchyma cell walls showed consistent increase in the emission peak associated with changes in the cell wall after cell death. Variations in the location and intensity of the peaks were likely caused by the presence of extractives (Koch & Kleist, 2001; Nakaba et al., 2012a). A solvent such as acetone has been shown to remove large parts of the extractives from *E. bosistoana* heartwood (Van Lierde, 2013).

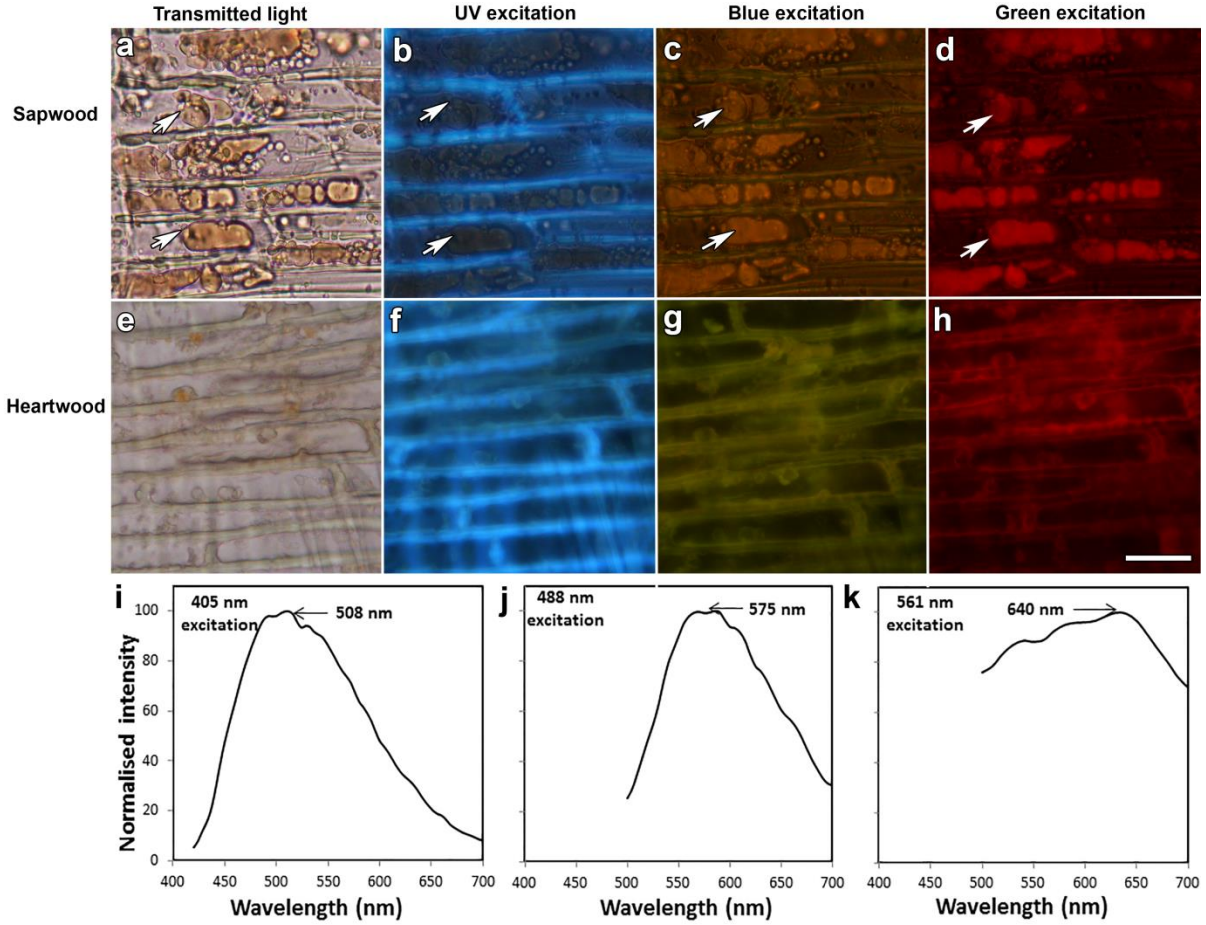

Figure 2.3: Wide-field fluorescence microscopy showed vacuole autofluorescence from ray parenchyma in sapwood (top row) and heartwood (bottom row) from a 11-year-old *E. bosistoana* tree. Images confirmed that wood samples were strongly autofluorescent at all visible wavelengths. Images were collected and processed with the same settings to demonstrate that heartwood cells were more fluorescent than sapwood using transmitted light (a, e); UV excitation (b, f); blue excitation (c, g); and green excitation (d, g). Scale bar = 30 μm. Normalised fluorescence emission spectra (lambda scans) from vacuoles in radial parenchyma cells in sapwood using: (i) 405 nm; (j) 488 nm; and (k) 561 nm excitation. As excitation wavelength increased, emission peaks were shifted to longer wavelengths.

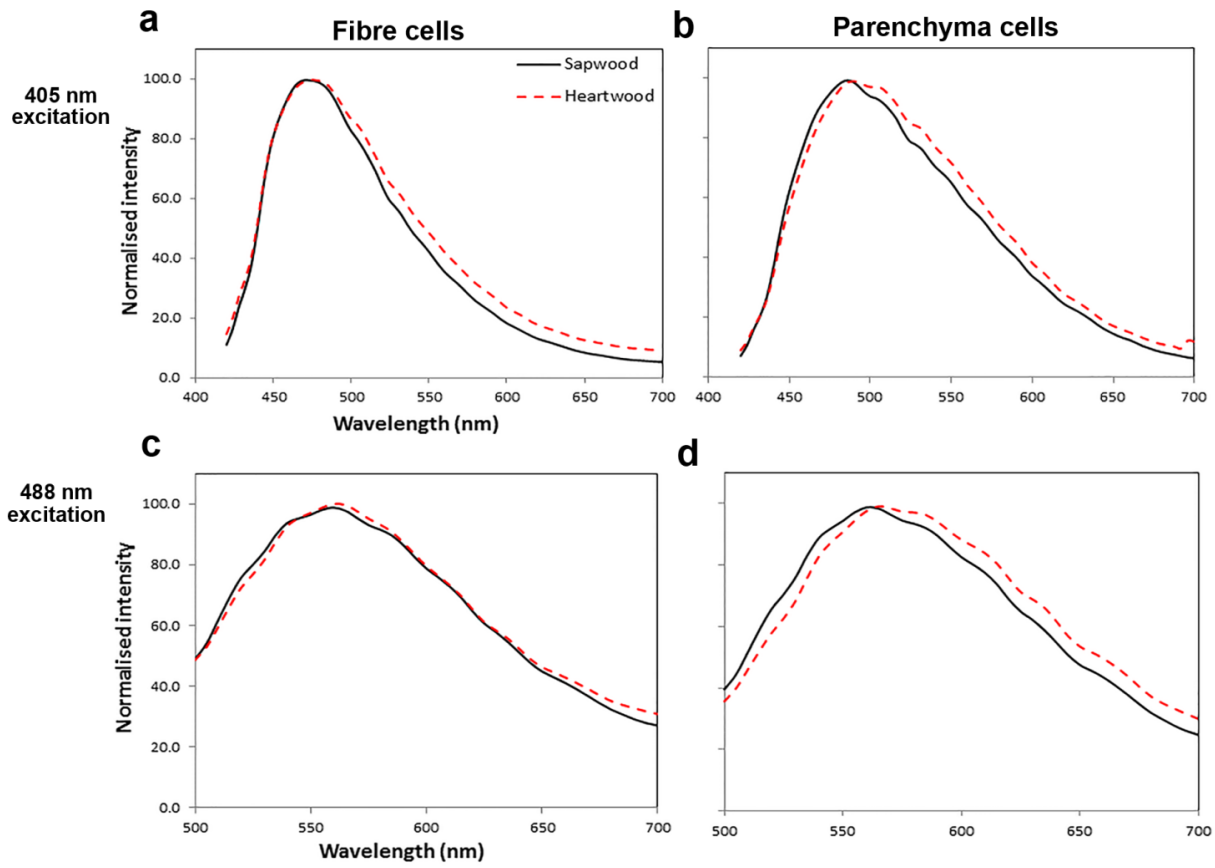

Figure 2.4: Fluorescence emission spectra from sapwood and heartwood sections using: 405 nm excitation (a, b); and 488 nm (c, d) of fibre cell walls (a, c) and parenchyma cell walls (b, d). Heartwood spectra were shifted to slightly longer wavelengths, most noticeably in the parenchyma cell walls, indicating the presence of heartwood extractives.

Spectral imaging was conducted to determine whether or not the compounds present within the cell wall might be extracted by solvents. Acetone treatments resulted in few differences between the fluorescence patterns of fibre cells (Figure 2.5a) and ray parenchyma (Figure 2.5b) in heartwood sections suggesting that the extractives dominating fluorescence of *E. bosistoana* heartwood were not significantly removed by the acetone treatment. While dried acetone extracted heartwood powder maintained a darker colour than extracted sapwood powder (unpublished) a contributing factor to the small differences in fluorescence observed here could have been that the fixation treatment of the wood during sample preparation also bound the extractive compounds to the cell walls.

Heartwood of 6-year-old *E. bosistoana* was reported to contain 1 and 15 % of ethanol soluble material (Li & Altaner, 2018). No detailed description of the chemical composition of these extracts has been published. Catechin, was observed to be a major compound in the heartwood of *E. camaldulensis* (Benouadah et al., 2018) and more generally heartwood extractives were reported to predominately be composed of phenolic compounds, e.g. tannins (Hillis, 1972, 1991; Rudman, 1964). Various tannins,

e.g. ellagitannins and condensed tannins have been described in the heartwood extracts of other *Eucalyptus* species (Hillis & Carle, 1960, 1962; Stewart et al., 1953; Taylor et al., 2002).

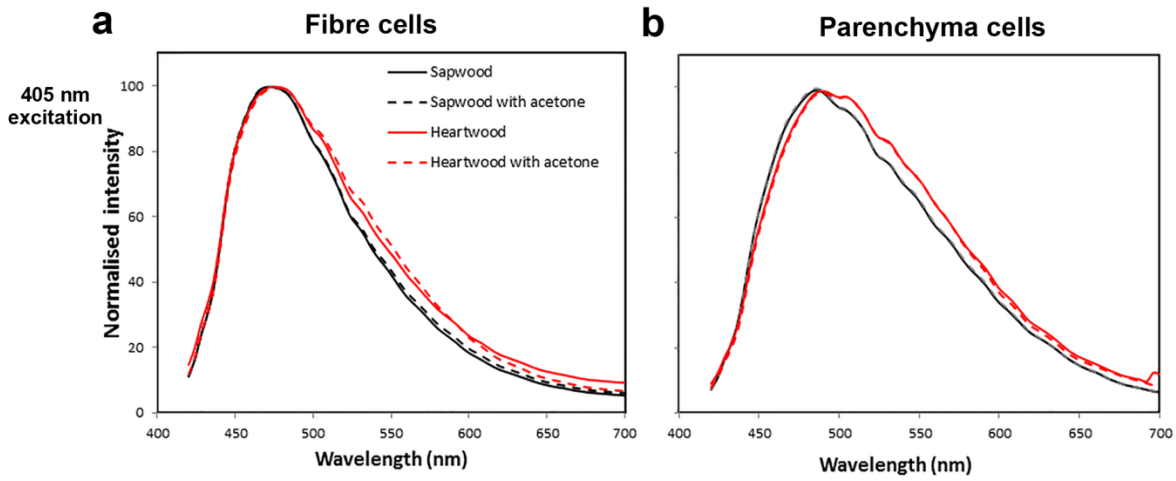

Figure 2.5: Fluorescence emission spectra from sapwood and heartwood sections with and without acetone wash using 405 nm excitation of fibre cells (a) and parenchyma cells (b). Heartwood spectra without acetone wash were shifted to slightly longer wavelengths. No difference between the fluorescence patterns of: (a) fibre cells: and (b) ray parenchyma in heartwood sections without and with acetone treatment.

The third source of autofluorescence was present only in the sapwood of the 2-year-old trees. Sections showed a scattering of small organelles with red autofluorescence (arrows, Figure 2.6a). The pigment was identified as chlorophyll, and the organelles as chloroplasts because the pigment was extracted by methanol (Figure 2.6b) and acetone washes, and as spectral analysis showed an emission peak at 680 nm (Figure 2.6c). In contrast, no indications of chlorophyll were observed in heartwood of *E. bosistoana* trees close to the pith where the cells had undergone cell death (data not shown). This was consistent with other reports showing that chloroplasts can exist within sapwood, for example, similar observations of red, chlorophyll auto-fluorescence from xylem ray cells and pith of *E. angustifolia* and *E. globulus* (Dima et al. 2006). Also, similar observations of chloroplasts present in sapwood were reported by van Cleve and co-workers based on absorption spectra maxima at 432 nm and 664 nm in methanol extracts from leaves, bark and pith of poplar (*Populus* × *canadensis*) (van Cleve et al., 1993). Furthermore, chlorophyll content were shown to depend on the age of the stem and its exposure to light (van Cleve et al., 1993; Dima et al., 2006; Larcher et al., 1988; Maxwell & Johnson, 2000; Saranpää, 1988). Published reports also provide evidence for an age-dependant decrease in stem chlorophyll content in a wide range of tree species (Pfanz et al., 2002).

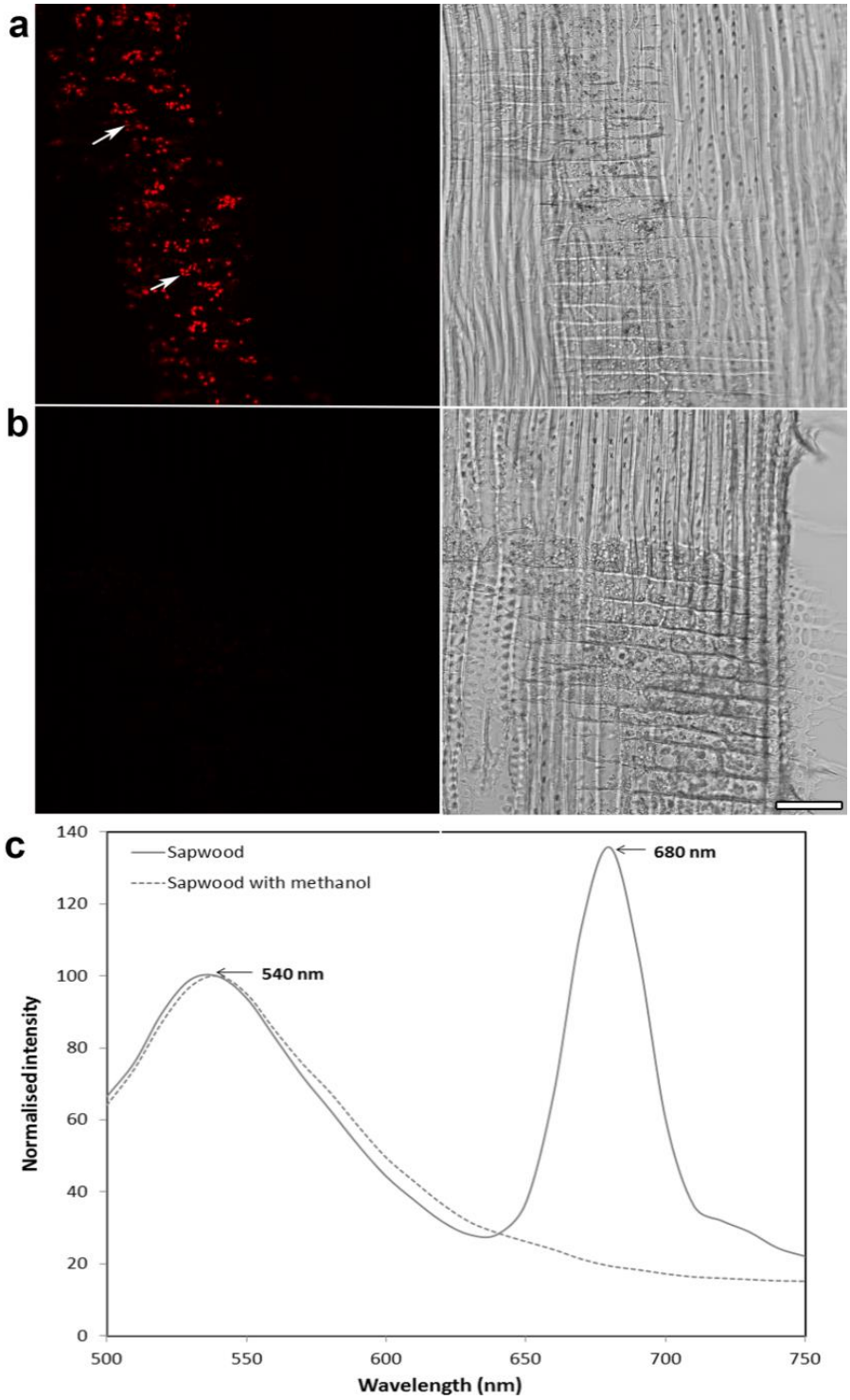

Figure 2.6: Sapwood contained chloroplasts. Concurrent confocal fluorescence (left) and transmitted light (right) images of untreated sapwood sections (a) and sections treated with methanol; and (b) from a 2-year-old *E. bosistoana* tree. Ray parenchyma cells in sections that lacked the methanol treatment contained chloroplasts that fluoresced red using 488 nm excitation (arrows in a) but these organelles were not visible following methanol washes which indicated that the chlorophyll had been washed out by the methanol (b). Scale bar = 50 μm. Fluorescence emission spectra using 488 nm excitation from sapwood ray parenchyma treated without and with methanol (c).

2.3.3 Immunolocalisation of organelles and structures

Organelles and cytoplasmic structures of living parenchyma cells in sapwood of 2-year-old *E. bosistoana* trees were visualised by immunolabelling. Fixation, extraction and labelling procedures were based on conventional immunofluorescence imaging methods (Collings and Wasteneys, 2005) that were modified to work with radial wood sections. Immunolabelling was screened visually using fluorescence from fluorescein-tagged secondary antibodies but the high autofluorescence at these wavelengths (Figure 2.3) prompted the use of a dual secondary antibody strategy, with confocal imaging conducted in the far-red with Cy5-tagged secondary antibodies.

Microtubules were visible as lines in and around the edges of both ray (white arrows, Figure 2.7a) and axial (black arrows, Figure 2.7a) parenchyma cells in sapwood and were absent from heartwood. These observations match those of Nakaba and co-workers who reported microtubules in the outer xylem parenchyma cells of *P. densiflora* Siebold & Zucc. and *Abies sachalinensis* F.Schmidt. (Nakaba et al., 2006, 2008, 2013). Similarly, peroxisomes were immunolabelled in both the radial (white arrows, Figure 2.7b) and axial (black arrows, Figure 2.7b) parenchyma of sapwood. These peroxisomes were small, round organelles that were less than 2 µm in diameter, and were abundant in the parenchyma. They too were absent from heartwood. Peroxisomes act as a source of enzymes such as polyphenol oxidases or peroxidases that contribute to the oxidation of phenolic heartwood compounds in *Juglans nigra* L. resulting in the brown colour of its heartwood (Dehon et al., 2002). Phenolic compounds are also common in heartwood extracts of *Eucalyptus* species (Da Costa & Rudman, 1958; Hart & Hillis, 1974; Hathway & Seakins, 1959; Hillis, 1956, 1991; Taylor et al., 2002).

Conventional nuclear stains failed in these *E. bosistoana* sections. Colour-based DNA stains such as acetocarmine and methyl green pyronine did not work well because they caused too much background signal. Similarly, fluorescent DNA stains such as DAPI (4′, 6-diamidino-2-phenylindole), Propidium iodide and Syto-13 were unreliable markers for living nuclei as these dyes bound to the cell walls and did not clearly resolve nuclei. Instead, nuclei were labelled with antibodies against the H3 histone protein (Nic-Can et al., 2013). The use of this antibody was complex, with samples requiring post-fixation in FAA for the histone antigen to become immunoreactive. Nuclei were observed in both ray (white arrows, Figure 2.7c) and axial (black arrows, Figure 2.7c) parenchyma cells of sapwood. The presence of nuclei indicated that parenchyma cells remained alive in the sapwood. Similar observations were reported for *Populus sieboldii* L. × *P. grandidentata* L. and *Abies sachalinensis* F. Schmidt. (Nakaba et al., 2012a, 2013).

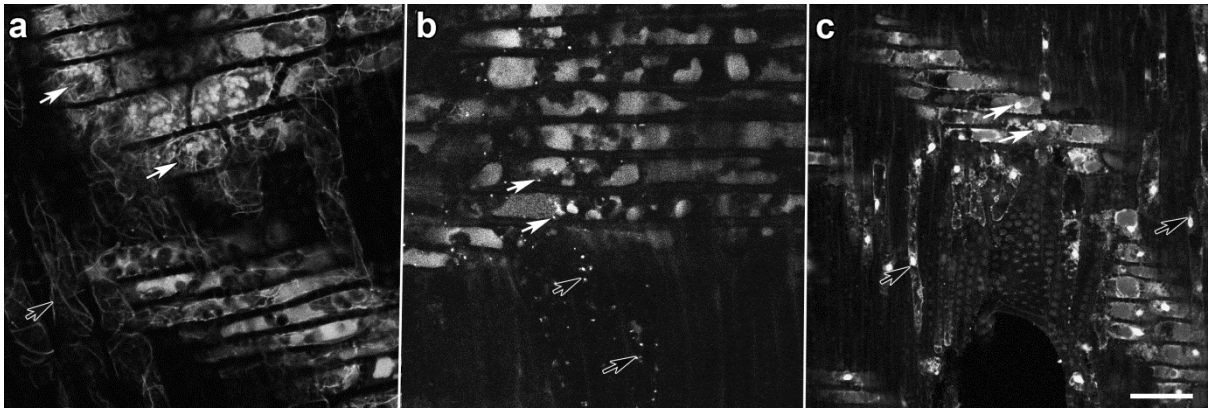

Figure 2.7: Immunolabelling allowed visualisation of organelles in living ray (white arrows) and axial (black arrows) parenchyma cells of sapwood from a 2-year-old *E. bosistoana* tree. Images are maximum projections of confocal optical sections using 633 nm excitation of Cy5 and collected between 650 and 700 nm where background autofluorescence was less severe. No labelling was seen in heartwood sections and not in the control experiments in which primary antibodies were omitted. Microtubules (arrows) labelled with mouse monoclonal anti-α-tubulin antibodies (a). Peroxisomes (arrows) labelled with rabbit polyclonal anti-catalase antibodies (b). Nuclei (arrows) labelled with rabbit polyclonal anti-histone antibodies (c). Scale bar = 50 μm.

2.4 Conclusion

Cell organelles and storage materials could be visualised in the living parenchyma cells in sapwood of 2-year-old *E. bosistoana* trees by immunolabelling and conventional histochemical staining. Extractives were localised in heartwood of 11-year-old *E. bosistoana* tree, but were absent from sapwood. It has been shown in this study that it is possible to use microscopy with appropriate staining to study physiological processes during heartwood formation. However, auto-fluorescence and unspecific staining made the use of several common staining techniques impractical. Investigating heartwood formation will aid the development of a hardwood industry based on *E. bosistoana*, which needs to ensure consistent wood properties. Early selections for heartwood in breeding programmes (Li et al., 2018) rely on the correct identification of fully developed heartwood (Mishra et al., 2018). Silviculture practices and site influences on heartwood formation have been reported and need to be understood.

2.5 References

AS5604. (2005). Timber—Natural durability ratings: Standards Australia Sydney.

Bamber, R. (1964). Sapwood and heartwood: A review. *Forestry Abstracts, 46*, 567-580

Begum, S., Nakaba, S., Oribe, Y., Kubo, T., & Funada, R. (2010). Changes in the localization and levels of starch and lipids in cambium and phloem during cambial reactivation by artificial heating of main stems of *Cryptomeria japonica* trees. *Annals of Botany, 106*, 885-895.

Begum, S., Nakaba, S., Yamagishi, Y., Oribe, Y., & Funada, R. (2013). Regulation of cambial activity in relation to environmental conditions: understanding the role of temperature in wood formation of trees. *Physiologia Plantarum, 147*, 46-54.

Benouadah, N., Pranovich, A., Aliouche, D., Hemming, J., Smeds, A., & Willför, S. (2018). Analysis of extractives from *Pinus halepensis* and *Eucalyptus camaldulensis* as predominant trees in Algeria. *Holzforschung, 72*, 97-104.

Collings, D. A., & Wasteneys, G. O. (2005). Actin microfilament and microtubule distribution patterns in the expanding root of *Arabidopsis thaliana*. *Canadian Journal of Botany, 83*, 579-590.

Da Costa, E., & Rudman, P. (1958). The causes of natural durability in timber I. The role of toxic extractives in the resistance of tallowwood (*Eucalyptus microcorys*) to decay. *Australian Journal of Biological Sciences, 11*, 45-57.

Datta, S., & Kumar, A. (1987). Histochemical studies of the transition from sapwood to heartwood in *Tectona grandis*. *IAWA Journal, 8*, 363-368.

Dehon, L., Macheix, J., & Durand, M. (2002). Involvement of peroxidases in the formation of the brown coloration of heartwood in *Juglans nigra*. *Journal of Experimental Botany, 53*, 303-311.

Déjardin, A., Laurans, F., Arnaud, D., Breton, C., Pilate, G., & Leplé, J. C. (2010). Wood formation in angiosperms. *Comptes Rendus Biologies, 333*, 325-334.

Dima, E., Manetas, Y., & Psaras, G. (2006). Chlorophyll distribution pattern in inner stem tissues: Evidence from epifluorescence microscopy and reflectance measurements in 20 woody species. *Trees, 20*, 515-521.

Fukuda, H. (2000). Programmed cell death of tracheary elements as a paradigm in plants. *Plant Molecular Biology, 44*, 245-253.

Funada, R. (2000). Control of wood structure. In P. Nick (Ed.), *Plant Microtubules* (Vol. 11, pp. 51-81). Berlin, Heidelberg: Springer.

Greenspan, P., Mayer, E. P., & Fowler, S. D. (1985). Nile red: a selective fluorescent stain for intracellular lipid droplets. *The Journal of Cell Biology, 100*, 965-973.

Hart, J. H., & Hillis, W. (1974). Inhibition of wood-rotting fungi by stilbenes and other polyphenols in *Eucalyptus sideroxylon*. *Phytopathology, 64*, 939-948.

Hathway, D., & Seakins, J. (1959). Hydroxystilbenes of *Eucalyptus wandoo*. *Biochemical Journal, 72*, 369.

Hillis, W. (1956). Leucoanthocyanins as the possible precursors of extractives in woody tissues. *Australian Journal of Biological Sciences, 9*, 263-280.

Hillis, W., & Carle, A. (1960). The formation of phenolic substances in *Eucalyptus gigantea* and *Eucalyptus sieberiana*. *Biochemical Journal, 74*, 607.

Hillis, W., & Carle, A. (1962). The origin of the wood and bark polyphenols of eucalyptus species. *Biochemical Journal, 82*, 435.

Hillis, W. (1972). Formation and properties of some wood extractives. *Phytochemistry, 11*, 1207-1218.

Hillis, W. (1991). Eucalypts: Chemistry, uses. *Appita Journal, 44*, 239-244.

Islam, M. A., & Begum, S. (2011). Distribution of starch, lipid and nuclei in xylem and phloem of *Tectona grandis* Linn. *Journal of Bio-Science, 19*, 29-35.

Islam, M., & Begum, S. (2012). Histochemical and anatomical studies of phloem and xylem cells of jackfruit (*Artocarpus heterophyllus*) tree. *International Journal of Natural Sciences, 2*, 01-07.

Islam, M., Begum, S., Nakaba, S., & Funada, R. (2012). Distribution and pattern of availability of storage starch and cell death of ray parenchyma cells of a conifer tree (*Larix kaempferi*). *Research Journal of Recent Sciences 1*, 28-37.

Koch, G., & Kleist, G. (2001). Application of scanning UV microspectrophotometry to localise lignins and phenolic extractives in plant cell walls. *Holzforschung, 55*, 563-567.

Kunce, C. M., Trelease, R. N., & Turley, R. B. (1988). Purification and biosynthesis of cottonseed (*Gossypium hirsutum* L.) catalase. *Biochemical Journal, 251*, 147-155.

Kuriyama, H., & Fukuda, H. (2002). Developmental programmed cell death in plants. *Current Opinion in Plant Biology, 5*, 568-573.

Larcher, W., Lütz, C., Nagele, M., & Bodner, M. (1988). Photosynthetic functioning and ultrastructure of chloroplasts in stem tissues of *Fagus sylvatica*. *Journal of Plant Physiology, 132*, 731-737.

Li, Y., & Altaner, C. (2018). Predicting extractives content of *Eucalyptus bosistoana* F. Muell. Heartwood from stem cores by near infrared spectroscopy. *Spectrochimica Acta Part A: Molecular and Biomolecular Spectroscopy, 198*, 78-87.

Li, Y., Apiolaza, L. A., & Altaner, C. (2018). Genetic variation in heartwood properties and growth traits of *Eucalyptus bosistoana*. *European Journal of Forest Research,* 1-8.

Magel, E. A., Hillinger, C., Wagner, T., & Höll, W. (2001). Oxidative pentose phosphate pathway and pyridine nucleotides in relation to heartwood formation in *Robinia pseudoacacia* L. *Phytochemistry, 57*, 1061-1068.

Maxwell, K., & Johnson, G. N. (2000). Chlorophyll fluorescence—a practical guide. *Journal of Experimental Botany, 51*, 659-668.

Millen, P., Ballekom, S. v., Altaner, C., Apiolaza, L., Mason, E., McConnochie, R., Morgenroth, J., & Murray, T. (2018). Durable eucalypt forests - a multi-regional opportunity for investment in New Zealand drylands. *New Zealand Journal of Forestry Science, 63*, 11–23.

Mishra, G., Collings, D.A., & Altaner, C.M. (2018). Physiological changes during heartwood formation in young (6 year-old) *Eucalyptus bosistoana*. *IAWA Journal*, 39, 1-13.

Nakaba, S., Sano, Y., Kubo, T., & Funada, R. (2006). The positional distribution of cell death of ray parenchyma in a conifer, *Abies sachalinensis*. *Plant Cell Reports, 25*, 1143-1148.

Nakaba, S., Yoshimoto, J., Kubo, T., & Funada, R. (2008). Morphological changes in the cytoskeleton, nuclei, and vacuoles during cell death of short-lived ray tracheids in the conifer *Pinus densiflora*. *Journal of Wood Science, 54*, 509-514.

Nakaba, S., Kubo, T., & Funada, R. (2011). Nuclear DNA fragmentation during cell death of short-lived ray tracheids in the conifer *Pinus densiflora*. *Journal of Plant Research, 124*, 379-384.

Nakaba, S., Begum, S., Yamagishi, Y., Jin, H., Kubo, T., & Funada, R. (2012a). Differences in the timing of cell death, differentiation and function among three different types of ray parenchyma cells in the hardwood *Populus sieboldii* × *P. grandidentata*. *Trees, 26*, 743-750.

Nakaba, S., Yamagishi, Y., Sano, Y., & Funada, R. (2012b). Temporally and spatially controlled death of parenchyma cells is involved in heartwood formation in pith regions of branches of *Robinia pseudoacacia* var. *inermis*. *Journal of Wood Science, 58*, 69-76.

Nakaba, S., Sano, Y., & Funada, R. (2013). Disappearance of microtubules, nuclei and starch during cell death of ray parenchyma in *Abies sachalinensis*. *IAWA Journal, 34*, 135-146.

Nic-Can, G., Hernández-Castellano, S., Kú-González, A., Loyola-Vargas, V. M., & De-la-Peña, C. (2013). An efficient immunodetection method for histone modifications in plants. *Plant Methods, 9*, 47.

Pfanz, H., Aschan, G., Langenfeld-Heyser, R., Wittmann, C., & Loose, M. (2002). Ecology and ecophysiology of tree stems: Corticular and wood photosynthesis. *Naturwissenschaften, 89*, 147-162.

Plomion, C., Leprovost, G., & Stokes, A. (2001). Wood formation in trees. *Plant Physiology, 127*, 1513-1523.

Potvin, C. (1979). A simple, modified Methyl Green-Pyronin Y stain for DNA and RNA in formalin-fixed tissues. *Laboratory Medicine, 10*, 772-774.

Pruyn, M. L., & Spicer, R. (2012). Parenchyma. *eLS*, 1-8.

Rossi, S., Deslauriers, A., Anfodillo, T., & Carraro, V. (2007). Evidence of threshold temperatures for xylogenesis in conifers at high altitudes. *Oecologia, 152*, 1-12.

Rossi, S., Deslauriers, A., Anfodillo, T., & Carrer, M. (2008). Age-dependent xylogenesis in timberline conifers. *New Phytologist, 177*, 199-208.

Saranpaa, P. (1988). Plastids and glycolipids in the stemwood of *Pinus sylvestris* L. *Trees, 2*, 180-187.

Spicer, R. (2005). Senescence in secondary xylem: Heartwood formation as an active developmental program. In M. N. Holbrook & M. A. Zwieniecki (Eds.), *Vascular Transport in Plants* (pp. 457-475). San Diego, SD: Elsevier Academic Press.

Spicer, R. (2014). Symplasmic networks in secondary vascular tissues: Parenchyma distribution and activity supporting long-distance transport. *Journal of Experimental Botany, 65*, 1829-1848.

Spicer, R., & Holbrook, N. (2007). Parenchyma cell respiration and survival in secondary xylem: does metabolic activity decline with cell age? *Plant, Cell & Environment, 30*, 934-943.

Stewart, C., mos, G., & Harvey, L. J. (1953). Chemical studies on *Eucalyptus regnans* F. Muell. *Australian Journal of Biological Sciences 6*, 21 – 47.

Taylor, A. M., Gartner, B. L., & Morrell, J. J. (2002). Heartwood formation and natural durability- A review. *Wood and Fiber Science, 34*, 587-611.

van Cleve, B., Forreiter, C., Sauter, J. J., & Apel, K. (1993). Pith cells of poplar contain photosynthetically active chloroplasts. *Planta, 189*, 70-73.

Van Lierde, J. (2013). *What causes natural durability in Eucalyptus bosistoana timber? a dissertation submitted in partial fulfilment of the requirements for the degree of Bachelor of Forestry Science with Honours.* B For Sci (Hon), University of Canterbury, Christchurch, New Zealand.

Chapter-3

Physiological changes during heartwood formation in young (6-year-old) *Eucalyptus bosistoana*

This chapter is published online on the advance platform of IAWA's publisher Brill:

Mishra, G., Collings, D.A., & Altaner, C.M. (2018). Physiological changes during heartwood formation in young (6-year-old) *Eucalyptus bosistoana*. *International Journal of Wood Anatomists*, 39, 1-13.

3.1 Introduction

Heartwood, defined as the inner layers of a tree, which have ceased to contain living cells and in which the reserve materials (e.g. starch) have been removed or converted into heartwood substances (IAWA, 1964), often determines the economic and aesthetic value of wood due to its colour and natural durability. Heartwood is formed in the inner layers of the sapwood, known as transition zone or intermediate wood, which have transitional characteristics between sapwood and heartwood in colour. Understanding heartwood formation is important due to its economic significance.

During heartwood formation, the parenchyma cells undergo complex metabolic and physiological changes in the transition zone. Heartwood formation is a combined phenomenon of both endogenous genetic expression and extraneous environmental factors. Genetic signals can trigger the production of polyphenols and other organic molecules in the transition zone followed by a chain of events climaxing in the formation of heartwood (Plomion et al., 2001). In some species, prior to or during the transition to heartwood, vessels are blocked by tyloses, protruding structures that grow through the pits from neighbouring parenchyma (Chattaway, 1949; Foster, 1967). In some species, the parenchyma cells synthesise secondary metabolites during the transition from sapwood to heartwood. The extractives, formed by the living parenchyma cells in the transition zone, are released and deposited in the neighbouring cells. This accumulation of secondary metabolites referred to as heartwood extractives frequently improves natural durability and gives colour (Taylor et al., 2002; Wardrop & Cronshaw, 1962; Wiedenhoeft & Miller, 2005). In *Eucalypts*, these extractives are predominately comprised of tannins (Conde et al., 1995; Hillis, 1972, 1991; Rudman, 1964).

During the conversion of sapwood to heartwood, the parenchyma cells undergo programmed cell death (PCD). The cellular events in PCD include chromatin condensation and vacuole proliferation in dying parenchyma cells (Atale et al., 2014). The vitality of parenchyma cells can be recorded by cytological changes of organelles (nuclei, cytoskeleton, vacuoles) and disappearance of reserve

materials such as starch (Bamber, 1976; Bamber & Fukazawa, 1985; Fukuda, 2000; Funada, 2000; Islam et al., 2012; Islam & Begum, 2011; Nakaba et al., 2013; Nakaba et al., 2008a). The loss of water conductivity in sapwood and the transition into heartwood (PCD of parenchyma) can be independent processes (Ziegler, 1968). For example in *Quercus phellos* tyloses was found to precede PCD of parenchyma by ~10 years. However, in other species both physiological changes coincide.

Published reports concerning heartwood formation are typically based on the heartwood of old trees. Durability as well as extractive content of heartwood increases from pith to bark in older trees (Sherrard & Kurth, 1933). This is recognised in relevant standards such as AS5604: Timber – naturally durability ratings. Supply of heartwood species is shifting from virgin old-growth forests to fast-growing, short-rotation plantations (Moya et al., 2014). These trees are young when harvested and little information is available for heartwood formation in young trees. The radial differences in heartwood durability and extractive content have been attributed to the degradation of extractives over time (Resch & Arganbright, 1968) as well as the availability of more resources for the synthesis of extractive in bigger trees (Wilkes, 1984). It might, however, be possible that heartwood formation in young trees differs from that in old trees with the parenchyma cells, which synthesise the heartwood extractives, remaining active for a longer period. This would result in a wider transition zone, which is not heartwood and in which parenchyma cells remain alive (Figure 3.1). The implication from such a result would be that the extractive content at the centre of the stem (and consequently wood quality), could increase as young trees become older. This hypothesis would be consistent with published data for some tree species. For example, when old and young *Sequoia sempervirens* trees were tested for natural durability, non-resistant heartwood samples were only found in the young trees (Clark & Scheffer, 1983; Jones et al., 2011). Extractive content in *Tectona grandis* heartwood close to the pith also appears to be higher in older trees compared to younger trees (Lukmandaru & Takahashi, 2009). However, Hills (1987) reported the transition zone to be 1.5 cm wide in 15-year-old *T. grandis* trees of 15 cm diameter.

Eucalyptus bosistoana is a medium to large tree growing to 60 m in height with a trunk diameter of up to 1.5 m. It grows naturally in mixed forests on fertile soils and river flats along the south eastern Australian coast from eastern Gippsland (Victoria) to Sydney (NSW). Its dense timber is ranked as class 1 durable, lasting more than 25 years in-ground, (Bootle 2005). Although not anymore widely used as a timber in Australia due to the lack of a forest resource, the species has attracted attention in New Zealand because of its good wood properties and ability to tolerate the cooler climatic conditions. Work is underway to establish a durable hardwood industry in New Zealand based on sustainably grown plantation *Eucalypts*, which can supply the demand for preservative free durable timber (Altaner et al., 2017). A prerequisite is to ensure abundant amounts of quality timber, i.e. naturally durable heartwood. Assessments need to be based on heartwood rather than the intermediate transition wood and therefore the timing of heartwood formation and tyloses need to be known.

In this study, radial cores from bark to bark of 6-year-old *E. bosistoana* trees were observed for cytological changes, using conventional and confocal microscopy with a range of different staining techniques. This allowed to determine a) the radial width of the transition zone in young *E. bosistoana* trees and b) the timing of the loss of water conductivity in sapwood.

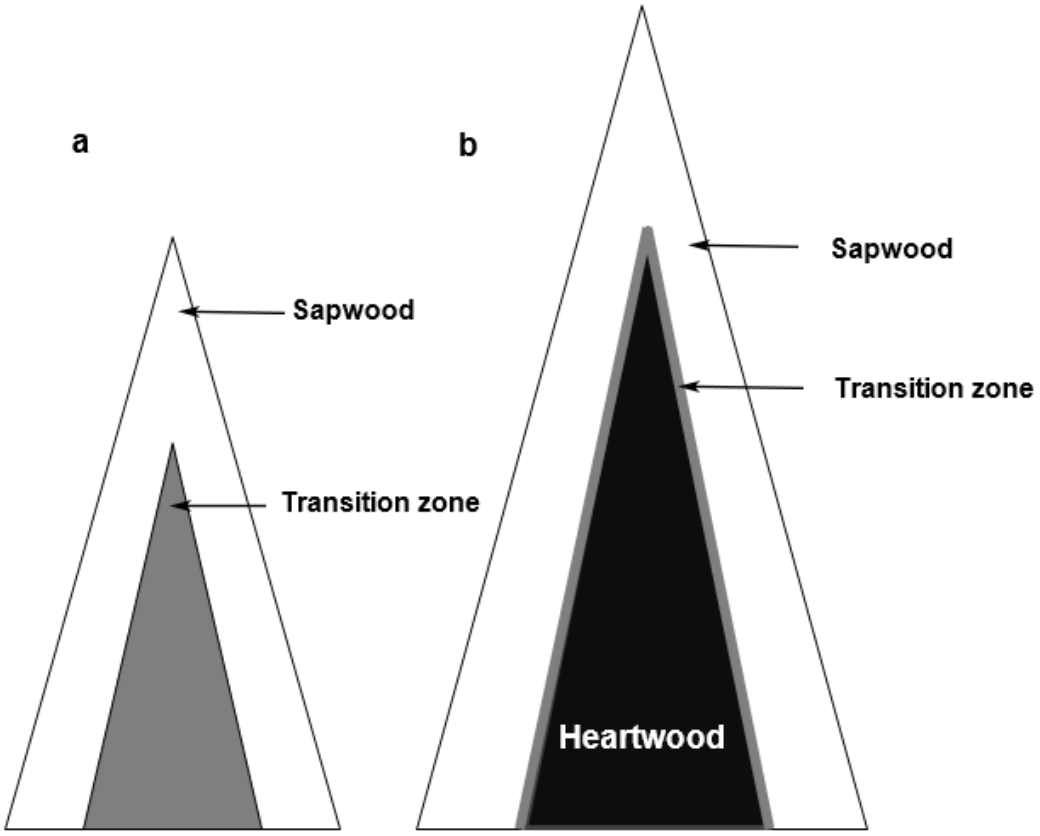

Figure 3.1: The hypothesis of prolonged transition from sapwood to heartwood in young trees suggests that young trees (a) have a wider transition zone where parenchyma cells remain alive synthesising heartwood extractives, and do not have heartwood. However, older trees (b) have a narrow transition zone with heartwood where parenchyma cells are dead.

3.2 Materials and methods

3.2.1 Wood material and fixation

Cores were obtained using a corer (14 mm diameter) at breast height from four, medium sized 6-year-old *E. bosistoana* trees grown in North Canterbury, New Zealand in spring (November) 2015. The trees were ~10 to 15 m in height and ~8 cm in diameter. Immediately after coring, the wood samples were fixed in the field in 50 ml Falcon tubes in a buffer comprising cytoskeleton buffer stock solution (PME, 50 mM Pipes pH 7.2, 2 mM EGTA, 2 mM $MgSO_4$) supplemented with Triton X-100

(0.1%), dimethylsulfoxide (DMSO) (1%), formaldehyde (3.7%) and glutaraldehyde (1%) under vacuum using a portable vacuum pump. During the initial 15 minutes of fixation, the vacuum was drawn and released several times. Samples were stored in the tubes with fixative in a refrigerator until used. The fixed wood cores were washed extensively with water. Cores were split into 1 cm pieces from which radial sections (10 - 20 μm) were prepared with a sledge microtome. A core across a 6-year-old *E. bosistoana* stem is shown in Figure 3.2.

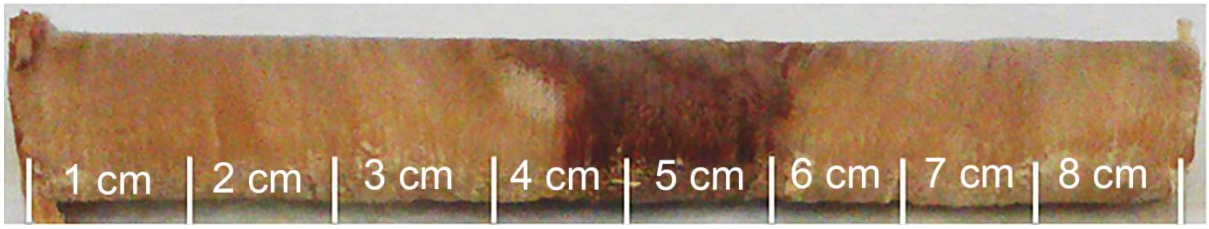

Figure 3.2: Core across a 6-year-old *E. bosistoana* stem.

3.2.2 Wide-field fluorescence microscopy

A Nikon eclipse 50i fluorescence microscope equipped with a Nikon digital sight DS-5 MC camera was used in transmitted light and fluorescence modes. Radial sections, either unstained or stained with iodine/potassium iodide (0.1% in water) to visualise starch grains, were mounted in glycerol. Fluorescence images were taken with UV excitation (360 - 400 nm) and a 420 nm long-pass emission filter.

3.2.3 Immunolabelling nuclei and microtubules

Radial sections were post-fixed with FAA solution (10% (v/v) formaldehyde, 10% (v/v) acetic acid, 50% (v/v) ethanol and 30% (v/v) distilled water) overnight before immunolabelling of nuclei. The post-fixation, based on Nic-Can et al. (2013), reduced the background fluroscence, and modified the histone to promote antibody binding. Samples not post-fixed with FAA showed minimal binding of the antibody. Washed sections were extracted with 1% Triton X-100 solution in phosphate buffered saline (PBS; 131 mM NaCl, 5.1 mM Na_2HPO_4, 1.56 mM KH_2PO_4,pH 7.2) for 1 h. Tissues were further washed with PBS followed by an acetone treatment for 20 min at -20°C and sodium borohydride (0.1% in PBS) for 10 min to reduce background fluorescence. Before incubation, sections were then washed extensively with PBS and blocked by incubation buffer (1.0% BSA in PBS with 0.1% Tween-20) for 20 min. Sections were then incubated for 1 h at room temperature with primary antibodies (either rabbit anti-histone H3, catalogue number 07-690, Merck Millipore, Billerica MA, USA, diluted 1/200 in incubation buffer, or mouse anti-α-tubulin, clone B512, Sigma-Aldrich, St Louis MO, USA, diluted 1/1000), washed 3 times with PBS and then incubated for 1 h at room temperature in secondary antibodies. These were concurrent mixes of either anti-rabbit

antibodies (goat anti-rabbit-Cy5, Jackson Immunoresearch, West Grove PA, USA, diluted 1:200 and sheep anti-rabbit-fluorescein, Silenus, Boronia, Vic, Australia diluted 1/100) or anti-mouse antibodies (goat anti-mouse-Cy5, Jackson Immunoresearch, diluted 1:200 and sheep anti-mouse-fluorescein, Silenus, diluted 1/100). This dual labelling allowed direct visualisation of nuclei and microtubules by eye using fluorescein fluorescence and images to be recorded using 633 nm excitation of Cy5. Sections were washed with PBS and mounted in glycerol. Controls, run in the absence of primary antibodies, showed no labelling of nuclei and microtubules.

3.2.4 Confocal laser scanning (confocal) microscopy

A Leica SP5 confocal microscope system operating on a DMI6000 inverted microscope, equipped with 20x NA 0.7 and 63x NA 1.3 glycerol immersion objective lenses (Leica, Wetzlar, Germany), was used for imaging.

High resolution Z stack images (1,024 pixels square) were recorded with 4-fold line averaging and a 1.00 μm step size. Along with concurrent transmitted light images, fluorescence images were collected from 500 - 550 nm and 650 - 700 nm using excitation at 488 nm and 633 nm.

To detect variations in the colour of fluorescence emission spectra from radial sections, image series were recorded using 405 nm excitation from 420 - 700 nm (λ scan). Images were recorded with a 10 nm wide window and with a 5 nm step size at a resolution of 512 pixels square using 4-fold line averaging. All image series were captured with the same imaging conditions. Image intensities were quantified from image stacks in ImageJ (FIJI installation of version 1.47v, National Institute of Health, Bethesda, MD, USA) after selecting regions of parenchyma or fibre cells with the 'Plot Z axis profile' function.

3.2.5 Image processing

Images were modified using standard brightness and contrast settings in Photoshop (version CS4, Adobe Systems, San Jose, CA, USA) and ImageJ.

3.3 Results and discussion

Bark-to-bark cores through the central pith were sampled from four 6-year-old *E. bosistoana* trees. Rapid fixation of these cores on site allowed for the investigation of the radial distribution of a range of cytological features associated with parenchyma cells, their programmed cell death and the transformation of sapwood into heartwood. All cores showed similar physiological changes through the radial profiles, which are summarised in Table 3.1.

3.3.1 Visualisation of starch

Starch, which is localised in amyloplasts, was detected as black granules with iodine/potassium iodide stain (Figure 3.3). Radial sections from the transition zone showed a decrease in starch from bark to

pith (arrows, Figure 3.4a), indicating the mobilisation of starch. Islam et al. (2012) reported presence of starch in sapwood and its absence from heartwood in *Larix kaempferi*. Their results suggested that starch depletion in ray cells was associated with cell death, which coincides with our observations.

Table 3.1: Physiological changes in parenchyma cells through a single, representative 6-year-old *E. bosistoana* stem ~80 mm in diameter.

Tissue feature	**Position (cm)**							
Tissue type	**1**	**2**	**3**	**4**	**5**	**6**	**7**	**8**
Starch	yes	yes	some	no	no	no	some	yes
Vacuoles	yes	yes	some	no	no	no	some	yes
Nuclei	yes	yes	yes	no	no	no	yes	yes
Microtubules	yes	yes	yes	no	no	no	yes	yes
Tyloses	no	no	yes	yes	yes	yes	yes	no
Extractives	no	no	no	yes	yes	yes	no	no
Tissue type	sapwood	sapwood	transition zone	heartwood	heartwood	heartwood	transition zone	sapwood

The parenchyma in heartwood (Figure 3.3, 4 - 6 cm) lacked detectable starch. This was consistent with what was commonly reported for heartwood. Starch in radial and axial parenchyma cells disappeared simultaneously. This differed to the observations reported by Nakaba et al. (2012b) in *Robinia pseudoacacia*, which suggested mobilisation of starch in axial parenchyma cells prior to ray parenchyma cells. However, it needs to be taken into account that the starch content in xylem was reported to vary between seasons and species (Begum et al., 2013).

3.3.2 Vacuoles

Vacuoles were confined to the ray parenchyma cells in the outer part of *E. bosistoana* and absent in the centre of the stem (Figure 3.5, 4 - 6 cm). Degradation of vacuoles was observed in the transition zone (arrows, Figure 3.5, 3 & 7 cm) close to the pith. The observation suggested that degradation and disappearance of cell contents (nuclei, microtubules) begun with the collapse of vacuoles. Fukuda (2000) suggested that the collapse of the vacuoles could result in the release of hydrolytic enzymes that degrade cell organelles such as nuclei (Kuriyama and Fukuda 2002). Disruption of vacuoles

followed by disappearance of nuclei was observed in ray parenchyma located further inside the stem of *Pinus densiflora* (Nakaba et al., 2011).

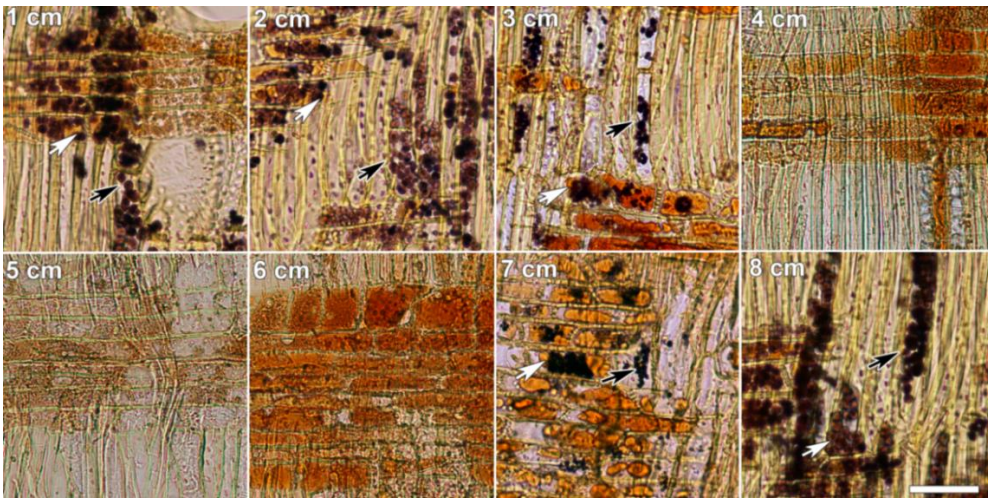

Figure 3.3: Bright-field micrographs of radial sections from 6-year-old *E. bosistoana* stained with iodine/potassium iodide showed starch-containing amyloplasts stained black. Amyloplasts were present in the radial (white arrows) and axial (black arrows) parenchyma cells of sapwood (1, 2 & 8 cm), were present in reduced numbers in the transition zone (3 & 7 cm), and were absent from heartwood (4 - 6 cm). Scale bar = 50 µm for all images.

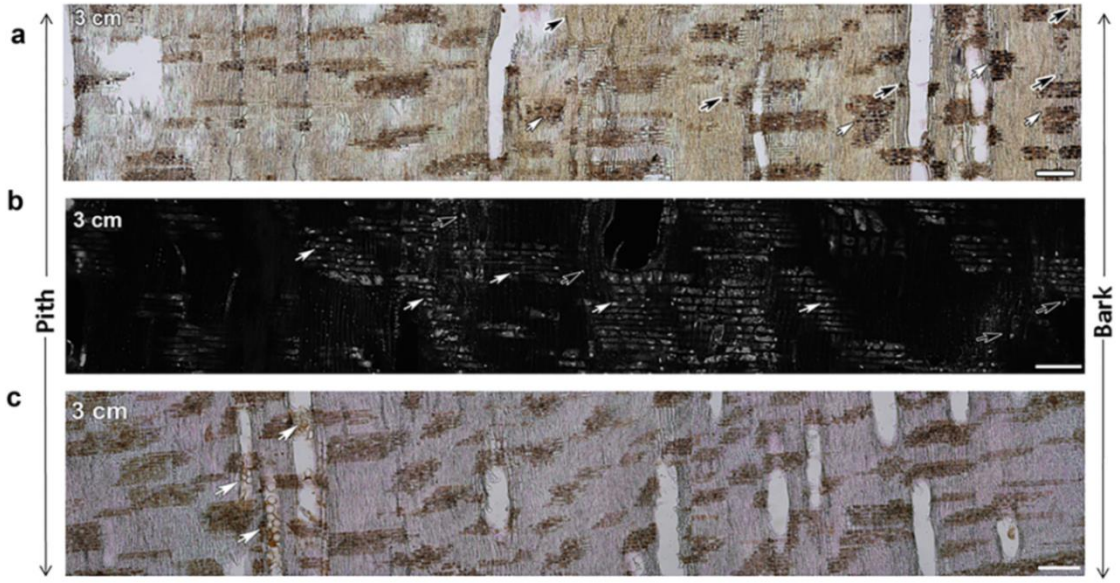

Figure 3.4: Radial sections of 6-year-old *E. bosistoana* in the transition zone. (a) staining for starch with iodine/potassium iodide. Amyloplast labelling in the radial (white arrows) and axial (black arrows with white outline) parenchyma cells was reduced towards the pith. (b) Maximum projections of confocal optical sections of immunolabelled nuclei. More nuclei were present in the radial (white arrows) and axial (arrows with white outline) parenchyma cells towards the bark than towards the pith. (c) Unstained sections showing tyloses (arrows) which were absent nearer the bark and appeared towards the pith. Scale bar = 200 µm.

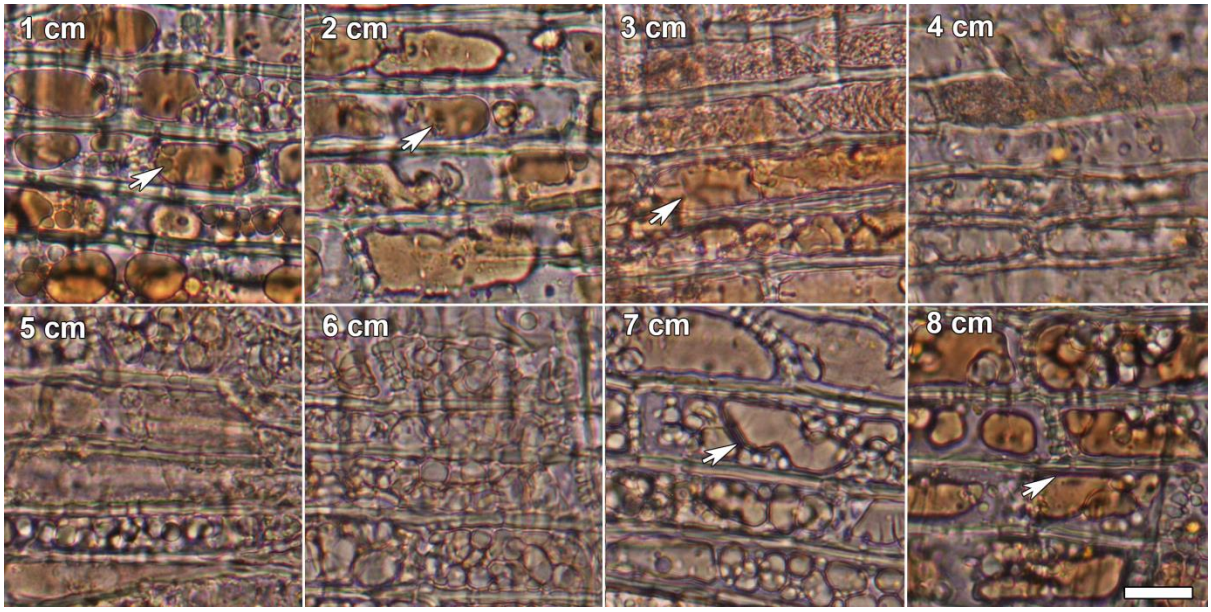

Figure 3.5: Bright-field micrographs of radial sections from 6-year-old *E. bosistoana* showing variations in vacuoles (arrows) in ray parenchyma cells. Vacuoles (arrows) were observed in the parenchyma cells of sapwood (1, 2 & 8 cm) and gradual disintegration of vacuoles were observed in the transition zone (3 & 7 cm) but were absent from heartwood (4 - 6 cm). Scale bar = 20 µm for all images.

3.3.3 Nuclei

High background fluorescence from parenchyma and fibre cells made colour-based DNA stains such as acetocarmine and methyl green pyronine unsuitable for the wood sections. Similarly, fluorescent DNA stains such as DAPI, Syto-13 and propidium iodide were unreliable markers for living nuclei as these dyes bound to the wood sample itself and did not clearly resolve nuclei. Instead, we labelled nuclei with antibodies against the H3 histone protein (Nic-Can et al., 2013). Even the use of this antibody is complex, with samples requiring post-fixation in FAA for the histone antigen to become immunoreactive. The disappearance of nuclei was monitored in each section of the core as an indication of cell death of parenchyma cells. Nuclei were observed in the outer parts of the stem in sapwood (arrows, Figure 3.6) and the transition zone (arrows, Figure 3.6), and in both ray and axial parenchyma cells. The presence of nuclei indicated that parenchyma cells remained alive in the sapwood. Radial sections from the transition zone showed a decrease in nuclei from bark to pith (Figure 3.4b), which coincided with mobilisation of starch and disintegration of vacuoles. No nuclei were found in the centre of the stem (Figure 3.6, 4 - 6cm) indicating that the parenchyma cells in the heartwood were dead. Both ray and axial parenchyma cells underwent PCD at the same time. Similar observations were reported for *Populus sieboldii* x *P. grandidentata* (Nakaba et al., 2012a).

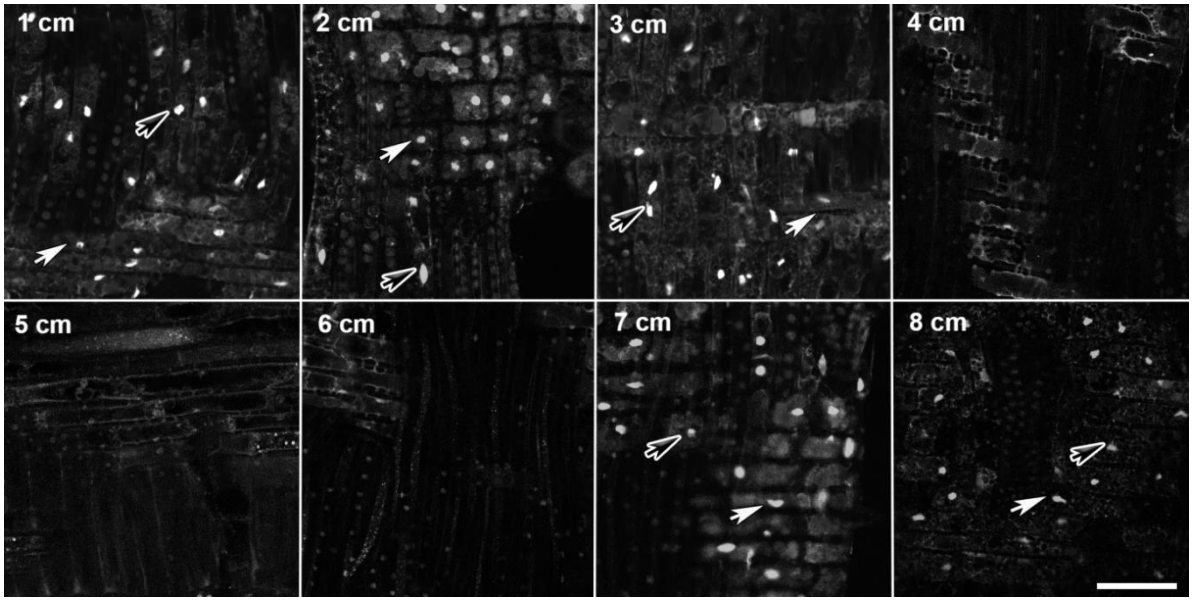

Figure 3.6: Maximum projections of confocal optical sections of radial sections of 6-year-old *E. bosistoana* labelled with histone antibodies. Nuclei were observed in both radial (white arrows) and axial (arrows with white outline) parenchyma cells of both sapwood (1, 2 & 8 cm) and the transition zone (3 & 7 cm) but were absent from heartwood (4 - 6 cm). Scale bar = 50 µm.

3.3.4 Microtubules

Microtubules were visible as circular bands in and around the edges of both ray and axial parenchyma cells in sapwood and the transition zone, indicating living cells (arrows, Figure 3.7). No indication of microtubules was found in the centre of the stem, which was consistent with dead parenchyma cells in heartwood. The disintegration and disappearance of microtubules coincided with the disappearance of starch, vacuoles and nuclei in heartwood. Similar observations were reported during cell death of ray parenchyma in *Pinus densiflora* (Nakaba et al., 2008b).

3.3.5 Tyloses

Vessels were open in sapwood (Figure 3.8, 1, 2 & 8 cm), whereas, vessels were blocked by tyloses in heartwood sections (Figure 3.8, 4 - 6 cm). This was consistent with conductive sapwood fulfilling the function of water transport in a tree. Initial formation of tyloses was observed in the transition zone concurrent with the mobilisation of starch but before the death of the parenchyma cells (Figure 3.4c). Similar observations were reported in other *Eucalypts* such as *E. oblique* and *E. miniata* (Foster, 1964, 1967).

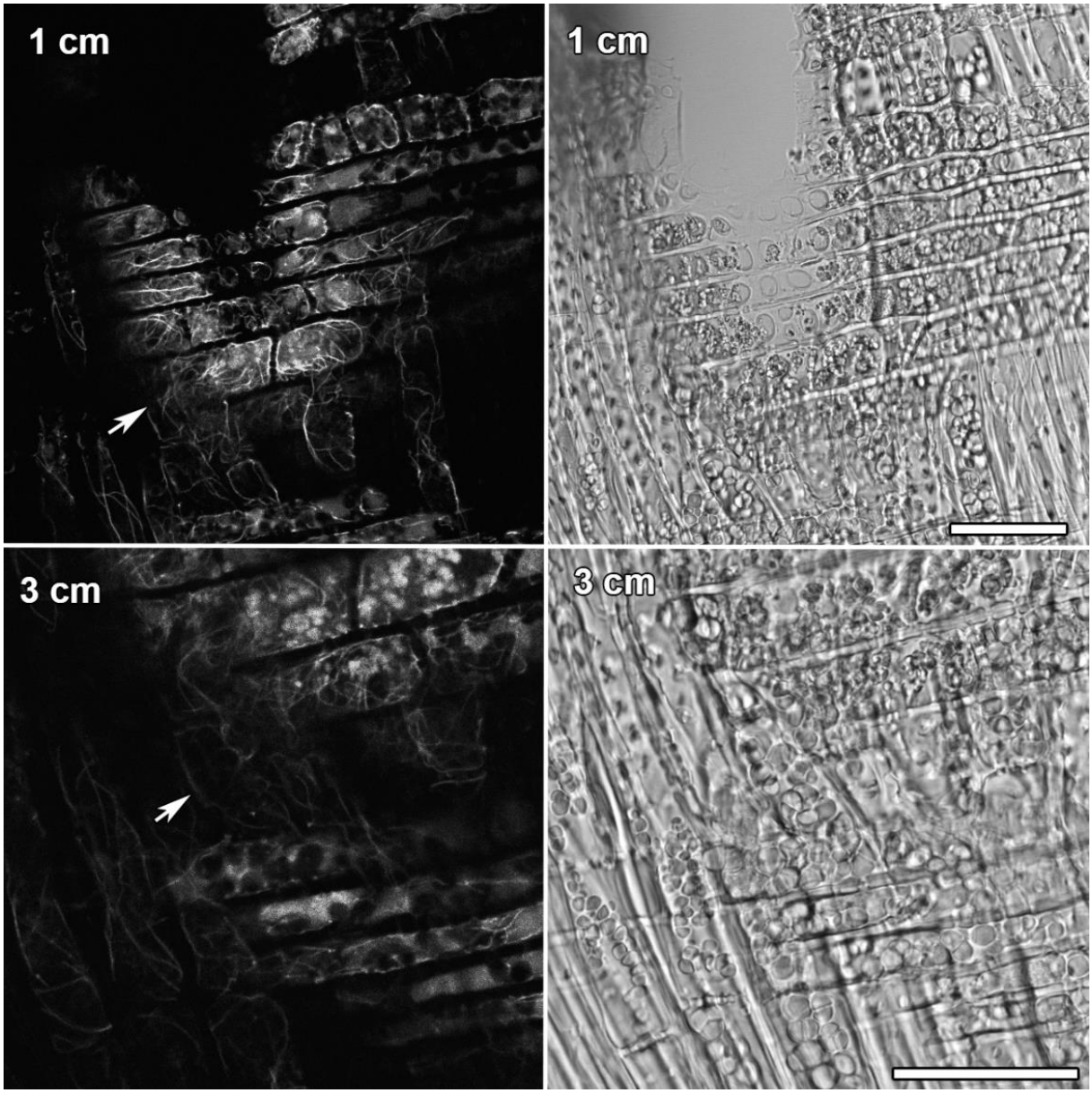

Figure 3.7: Transmitted light images of radial sections of 6-year-old *E. bosistoana* labelled with antibodies against α-tubulin. Microtubules (arrows) were observed in the parenchyma cells of both sapwood (1, 2 & 8 cm) and the transition zone (3 & 7 cm). Scale bar = 50 µm.

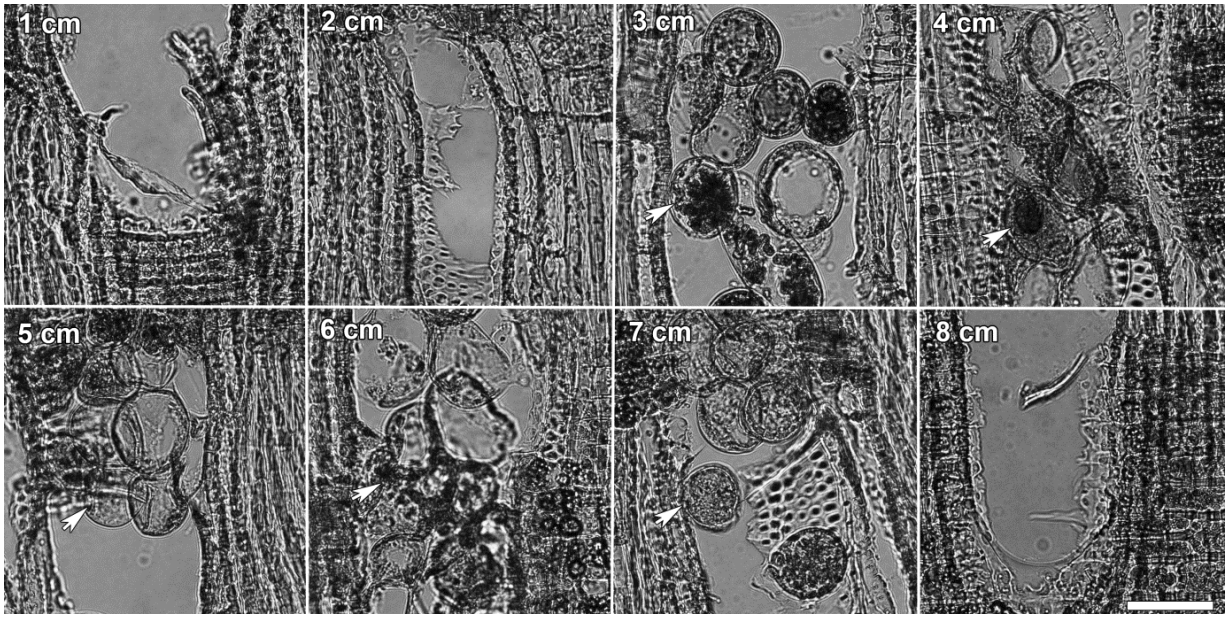

Figure 3.8: Radial sections of 6-year-old *E. bosistoana* showing variations in tyloses formation (arrows) in vessels. Tyloses were absent in the vessels of sapwood (1, 2 & 8 cm) but were present in the transition zone (3 & 7 cm) and heartwood (4 - 6 cm). Scale bar = 50 µm.

3.3.6 Variation in autofluorescence

Wide-field fluorescence microscopy of sapwood, transition zone and heartwood sections using UV excitation (360 - 400 nm) revealed subtle differences in the colour of the fluorescence from parenchyma and fibre cell walls in heartwood (Figure 3.9a, b). Heartwood sections were fluorescing brighter compared to sapwood and transition zone sections. The fluorescence from these sections was further quantified with spectral (λ) scans with a confocal microscope using UV excitation at 405 nm. Fluorescence emission spectra of parenchyma and fibre cell walls of sapwood, the transition zone and heartwood indicated differences in chemical composition (Figure 3.9c, d). When comparing heartwood with sapwood, the fluorescence emission spectra of heartwood occurred at longer wavelengths with maximum emission at 488 nm. However, the fluorescence emission of sapwood and the transition zone sections showed similar spectra with maximum emission at 476 nm. Variations in intensity of peaks were likely caused by the presence of extractives (Koch & Kleist, 2001). *E. bosistoana* contains pale-brown coloured heartwood with a pinkish tint (Bootle, 2005). This is consistent with the small spectral differences between the different wood tissues and a redshift of the heartwood spectra.

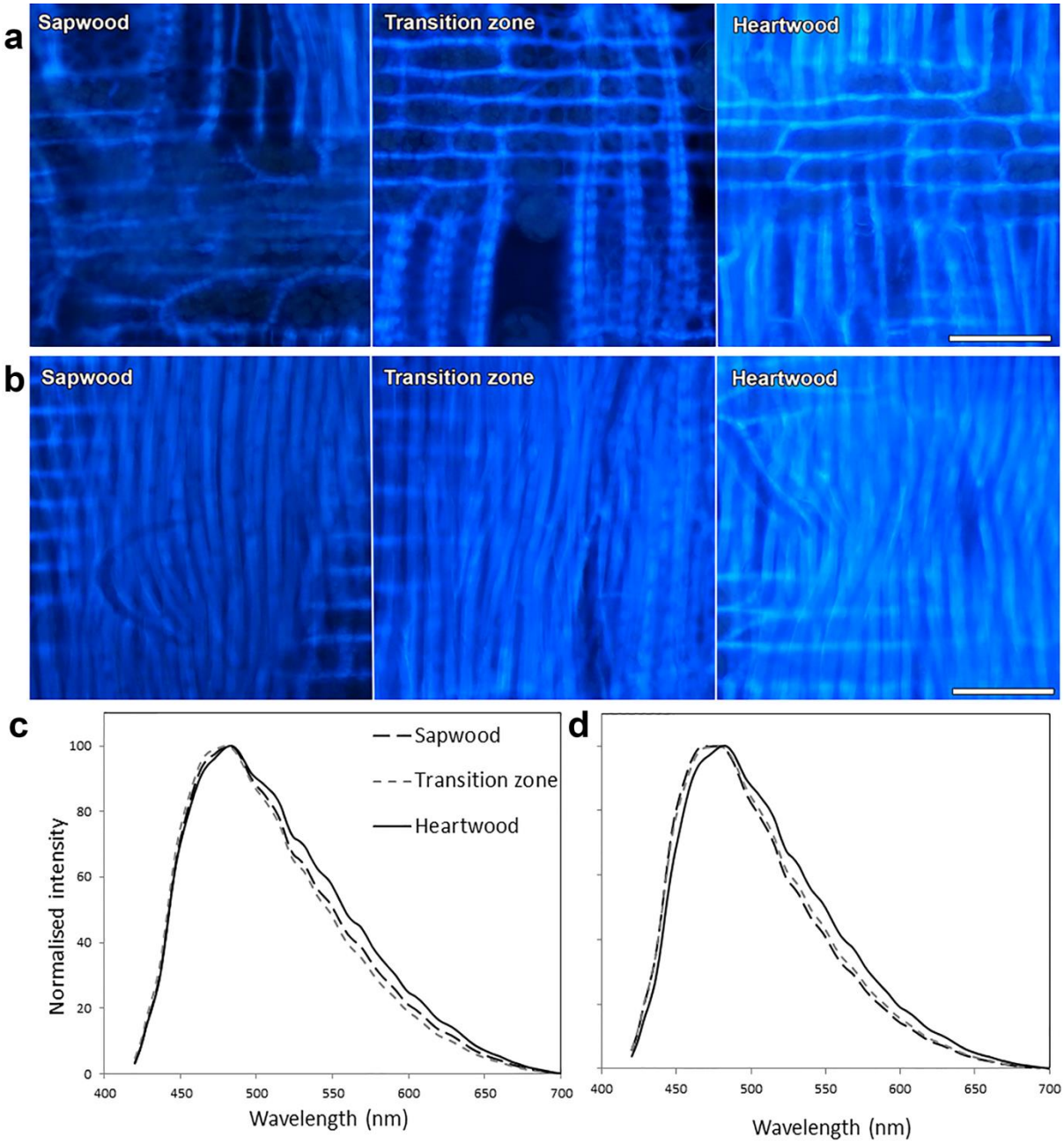

Figure 3.9: Differences in autofluorescence from cell walls. a, b: Conventional, wide-field fluorescence microscopy (UV excitation, 360 - 400 nm, long-pass 420 nm) showing intensity of fluorescence of parenchyma (a) and fibre cell walls (b) in radial tissue sections of sapwood, the transition zone and heartwood of 6-year-old *E. bosistoana*. Heartwood cell walls were more fluorescent than cell walls in sapwood and the transition zone. Scale bar = 50 µm. c, d: Fluorescence emission spectra (λ scans) of parenchyma (c) and fibre cell walls (d) from radial tissue sections of sapwood, the transition zone and heartwood of 6-year-old *E. bosistoana* using 405 nm excitation. Sapwood and the transition zone wood gave similar spectra, while the heartwood spectra were shifted to slightly longer wavelengths.

3.4 Conclusion

Table 3.1 shows physiological changes in parenchyma cells through a single 6-year-old *E. bosistoana* stem.The observed physiological changes were consistent with the formation of heartwood (i.e. no living parenchyma cells) at the centre of young (6-year-old) *E. bosistoana* trees.

The transition zone in which sapwood is transformed into heartwood, was found to be ~1 cm in radial width, with the loss of conductivity, removal of reserve carbohydrates (starch) and the deposition of extractives all occurring in close proximity.

3.5 References

Altaner, C. M., Murray, T. J., & Morgenroth, J. (2017). *Durable Eucalypts on Drylands: Protecting and Enhancing Value: Workshop Proceedings 2017*: New Zealand School of Forestry, University of Canterbury.

AS5604. (2005). Timber—Natural durability ratings: Standards Australia Sydney.

Atale, N., Gupta, S., Yadav, U., & Rani, V. (2014). Cell-death assessment by fluorescent and nonfluorescent cytosolic and nuclear staining techniques. *Journal of Microscopy, 255*, 7-19.

Bamber, R. (1976). Heartwood, its function and formation. *Wood Science and Technology, 10*, 1-8.

Bamber, R., & Fukazawa, K. (1985). Sapwood and heartwood: A review. *Forestry Abstracts, 46*, 567-580.

Begum, S., Nakaba, S., Yamagishi, Y., Oribe, Y., & Funada, R. (2013). Regulation of cambial activity in relation to environmental conditions: understanding the role of temperature in wood formation of trees. *Physiologia Plantarum, 147*, 46-54.

Bootle, K. R. (2005). *Wood in Australia Types, Properties, and Uses* (2nd ed.): McGraw-Hill Australia.

Chattaway, M. M. (1949). The development of tyloses and eecretion of gum in heartwood formation. *Australian Journal of Biological Sciences, 2*, 227-240.

Clark, J. W., & Scheffer, T. C. (1983). Natural decay resistance of the heartwood of coast redwood *Sequoia sempervirens* (D. Don) Endl. *Forest Products Journal, 33*, 15-20.

Conde, E., Cadahía, E., García-Vallejo, M., & de Simón, M. F. (1995). Polyphenolic composition of wood extracts from *Eucalyptus camaldulensis*, *E. globulus* and *E. rudis*. *Holzforschung, 49*, 411-417.

Foster, R. (1964). Fine structure of tyloses. *Nature, 204*, 494.

Foster, R. (1967). Fine structure of tyloses in three species of the Myrtaceae. *Australian Journal of Botany, 15*, 25-34.

Fukuda, H. (2000). Programmed cell death of tracheary elements as a paradigm in plants. *Plant Molecular Biology, 44*, 245-253.

Funada, R. (2000). Control of wood structure. In P. Nick (Ed.), *Plant Microtubules* (Vol. 11, pp. 51-81). Berlin, Heidelberg: Springer.

Hillis, W. (1972). Formation and properties of some wood extractives. *Phytochemistry, 11*, 1207-1218.

Hillis, W. E. (1987). *Heartwood and tree exudates*. New York: Springer.

Hillis, W. (1991). Eucalypts: Chemistry, uses. *Appita Journal, 44*, 239-244.

International Association of Wood Anatomists. (1964). Multilingual glossary of terms used in wood anatomy. *Verlagsbuchanstalt Konkordia, Winterthur, Switzerland*, 186.

Islam, M., Begum, S., Nakaba, S., & Funada, R. (2012). Distribution and pattern of availability of storage starch and cell death of ray parenchyma cells of a conifer tree (*Larix kaempferi*). *Research Journal of Recent Sciences 1*, 28-37.

Islam, M. A., & Begum, S. (2011). Distribution of starch, lipid and nuclei in xylem and phloem of *Tectona grandis* Linn. *Journal of Bio-Science, 19*, 29-35.

Jones, T., Meder, R., Low, C., O'Callahan, D., Chittenden, C., Ebdon, N., Thumm, A., & Riddell, M. (2011). Natural durability of the heartwood of coast redwood [*Sequoia sempervirens* (D. Don) Endl.] and its prediction using near infrared spectroscopy. *Journal of Near Infrared Spectroscopy, 19*, 381-389.

Koch, G., & Kleist, G. (2001). Application of scanning UV microspectrophotometry to localise lignins and phenolic extractives in plant cell walls. *Holzforschung, 55*, 563-567.

Kuriyama, H., & Fukuda, H. (2002). Developmental programmed cell death in plants. *Current Opinion in Plant Biology, 5*, 568-573.

Lukmandaru, G., & Takahashi, K. (2009). Radial distribution of quinones in plantation teak (*Tectona grandis* Lf). *Annals of Forest Science, 66*, 605-605.

Moya, R., Bond, B., & Quesada, H. (2014). A review of heartwood properties of *Tectona grandis* trees from fast-growth plantations. *Wood Science and Technology, 48*, 411-433.

Nakaba, S., Begum, S., Yamagishi, Y., Jin, H., Kubo, T., & Funada, R. (2012a). Differences in the timing of cell death, differentiation and function among three different types of ray parenchyma cells in the hardwood *Populus sieboldii* × *P. grandidentata*. *Trees, 26*, 743-750.

Nakaba, S., Yamagishi, Y., Sano, Y., & Funada, R. (2012b). Temporally and spatially controlled death of parenchyma cells is involved in heartwood formation in pith regions of branches of *Robinia pseudoacacia* var. *inermis*. *Journal of Wood Science, 58*, 69-76.

Nakaba, S., Kubo, T., & Funada, R. (2008a). Differences in patterns of cell death between ray parenchyma cells and ray tracheids in the conifers *Pinus densiflora* and *Pinus rigida*. *Trees, 22*, 623.

Nakaba, S., Yoshimoto, J., Kubo, T., & Funada, R. (2008b). Morphological changes in the cytoskeleton, nuclei, and vacuoles during cell death of short-lived ray tracheids in the conifer *Pinus densiflora*. *Journal of Wood Science, 54*, 509-514.

Nakaba, S., Kubo, T., & Funada, R. (2011). Nuclear DNA fragmentation during cell death of short-lived ray tracheids in the conifer *Pinus densiflora*. *Journal of Plant Research, 124*, 379-384.

Nakaba, S., Sano, Y., & Funada, R. (2013). Disappearance of microtubules, nuclei and starch during cell death of ray parenchyma in *Abies sachalinensis*. *IAWA Journal, 34*, 135-146.

Nic-Can, G., Hernández-Castellano, S., Kú-González, A., Loyola-Vargas, V. M., & De-la-Peña, C. (2013). An efficient immunodetection method for histone modifications in plants. *Plant Methods, 9*, 47.

Plomion, C., Leprovost, G., & Stokes, A. (2001). Wood formation in trees. *Plant Physiology, 127*, 1513-1523.

Resch, H., & Arganbright, D. G. (1968). Variation of specific gravity, extractive content, and tracheid length in redwood trees. *Forest Science, 14*, 148-155.

Rudman, P. (1964). Durability in the genus *Eucalyptus*. *Australian Forestry, 28*, 242-257.

Sherrard, E. C., & Kurth, E. F. (1933). Distribution of extractive in redwood - Its relation to durability. *Industrial and Engineering Chemistry, 25*, 300-302.

Taylor, A. M., Gartner, B. L., & Morrell, J. J. (2002). Heartwood formation and natural durability- A review. *Wood and Fiber Science, 34*, 587-611.

Wardrop, A., & Cronshaw, T. (1962). Formation of phenolic substances in the ray parenchyma of angiosperms. *Nature, 193*, 90-92.

Wiedenhoeft, A. C., & Miller, R. B. (2005). Structure and Function of Wood. In R. M. Rowell (Ed.), *Handbook of Wood Chemistry and Wood Composites* (2nd ed., pp. 9-33). New York, NY: Taylor and Francis Group.

Wilkes, J. (1984). The influence of rate of growth on the density and heartwood extractives content of eucalypt species. *Wood Science and Technology, 18*, 113-120.

Ziegler, H. (1968). Biological aspects of heartwood formation. *Holz als Roh- und Werkstoff, 2*, 61-68.

Chapter-4

Development of a bioactivity assay for ethanol extracts from *Eucalyptus bosistoana* heartwood

Objective

The objective of this study was the development of an assay to test the antifungal activity of heartwood extractives. The assay was subsequently used on a range of heartwood samples representing a range of the genetic variation in the *E. bosistoana* breeding population to assess the bioactivity of their extract.

4.1 Introduction

Durability of wood is attributed to secondary metabolites known as extractives (Hawley et al., 1924; Taylor et al., 2002). Their abundance is variable within a species (Haupt et al., 2003; Hillis, 1987; Li & Altaner, 2018; Rowe, 1989) and the extractive content has been linked to a timber's resistance to fungal decay (Mohareb et al., 2010; Taylor et al., 2002). However, extractives are composed of numerous bioactive compounds including flavonoids, phenols, phenolic glycosides, saponins and glucosinolates (Quiroga et al., 2001; Rowe, 1989), which in turn vary in their relative quantites within a species. Therefore, both, extractive content and the composition of the extractives contribute to the natural durability of a piece of wood.

In order to assess the bioactivity of an extract (here fungicidal activity) and further identify the most effective components among the numerous compounds, the influence of extractive content needs to be removed. In other words two pieces of wood can have the same extractive content but of different relative composition and therefore be of different natural durability.

The most active compounds in the naturally durable *E. bosistoana*, which inhibited fungal growth have been found to be in the ethanol extracts (Van Lierde, 2013). Therefore, this work focused on the ethanol extracts of *E. bosistoana*.

Numerous methods have been reported to test the bioactivity of plant extracts. Standard susceptibility methods are broth or agar dilution tests and disk diffusion assays (Balouiri et al., 2016). These assays have been used to analyse the antifungal and antimicrobial activity in countless medicinal plant extracts (Bafi-Yeboa et al., 2005; Chandrasekaran & Venkatesalu, 2004; Quiroga et al., 2001). The usage of different non-standardized approaches, inoculum preparation techniques, inoculum sizes, growth media, incubation conditions and endpoint determinations make the comparison between studies difficult (Balouiri et al., 2016). Dilution methods are the most commonly used techniques for

the determination of minimal inhibitory or fungicidal concentration (MIC, MFC) values. Either broth or agar dilution methods may be used for quantitative in vitro measurements of the antifungal or antimicrobial activity in extracts. Other methods that have been developed to determine antifungal or antimicrobial activity of extracts are the time-kill test (time-kill curve), an ATP bioluminescence assay, flow cytofluorometric and thin-layer chromatography (TLC)-bioautography, which includes several bioautographic techniques like agar diffusion, direct bioautography or the agar-overlay assay (Balouiri et al., 2016). These methods can also provide information on the nature of the inhibitory effect (bactericidal or bacteriostatic; time-dependent or concentration-dependent) or the cell damage inflicted to the test microorganism (Balouiri et al., 2016).

The agar dilution method involves the incorporation of different concentrations of extracts into agar medium followed by the application of a fungal or bacterial inoculum to the surface of the agar plate (Wiegand et al., 2008). This method can be used to determine the minimal inhibitory or fungicidal concentration (MIC, MFC) after a defined time of incubation. Most reports on the bioactivity of heartwood extracts against wood decaying fungi employed this method, which are summarised in Table 4.1.

Table 4.1: Summary of reports using the agar dilution method to investigate the bioactivity of wood extracts against wood decaying fungi.

Tree species	**Extract type**	**Fungi**	**Reference**
Dipteryx odorata	Heartwood extracts	*Postia placenta*	(Wanschura et al., 2016)
Acacia mangium and *A. auriculiformis*	Heartwood extracts	*Phellinus noxius, P. badius*	(Mihara et al., 2005)
Pinus banksiana and *P. resinosa*	Pine bark cones (Stilbenes)	*Trametes versicolor, Phanerochaete chrysosporium, Neolentinus lepideus, Gloeophyllum trabeum , Postia placenta*	(Celimene et al., 1999)
Michelia formosana	Heartwood extracts	*Lenzites betulina, T. versicolor, Laetiporus sulphureus, G. trabeum, Fomitopsis pinicola*	(Wu et al., 2012)

Tree species	Extract type	Fungi	Reference
Calocedrus macrolepis	Heartwood extracts	*L. betulina*, *T. versicolor*, *Schizophyllum commune*, *L. sulphureus*, *G. trabeum*, *F. pinicola*	(Yen et al., 2008)
Juniperus virginiana	Heartwood extracts	*T. versicolor*, *G. trabeum*	(Mun & Prewitt, 2011)
Sequoia sempervirens	Heartwood extracts	*T. versicolor*, *G. trabeum*	(Davies et al., 2014)
Tectona grandis	Heartwood extracts	*T.versicolor*, *F. palustris*, *Rhizopus oryzae*, *Cladosporium cladosporioides*, *Chaetomium globosum*	(Lukmandaru, 2017)
Aquilaria crassna	Heartwood extracts	*Fusarium solani*	(Novriyanti et al., 2010).
Taiwania cryptomerioides	Heartwood extracts	*P. noxius*	(Chen et al., 2017)

The broth dilution procedure involves adding extracts at various concentrations to a liquid growth medium and inoculate with a microbial organism (Balouiri et al., 2016). After incubation the turbidity represents the growth of the test organism (Balouiri et al., 2016; Wiegand et al., 2008). Broth dilution assays require fungal spores for analysis. Therefore, these methods are difficult to apply to basidiomycetes, the main wood decaying fungi, as they do not form spores until developed into mycelia (Wanschura et al., 2016). However, they were successfully used to identify a naphthoquinone derivative from teak (*T. grandis*) heartwood extracts with fungicidal activity against *T. versicolor* (Niamké et al., 2012) and used to investigate the fungicidal activity of *Cinnamomum camphora* heartwood extracts against *G. trabeum* and *T. versicolor* (Li et al., 2014).

In disk diffusion assays agar plates are inoculated with a standardized inoculum of the test microorganism. Then, filter paper disks, which have been immersed in the extract solution, are placed on the agar surface. Extracts diffuse into the agar and inhibit the growth of the test microorganism. The gap of the inhibition zone around the filter paper disks is measured (Balouiri et al., 2016). This method is not appropriate to determine MIC or MIF, because it is not possible to quantify the amount of extract that diffuses into the agar medium (Balouiri et al., 2016). A further difficulty to determine

the bioactivity against fungi is that the hyphae can easily overgrow the disk (Wanschura et al., 2016). The method has beed applied to assess antimicrobial activities in crude extracts of *E. globulus* stump wood and bark (Luís et al., 2014).

A bioassay was developed by Kawamura et al. (2011) in which potato dextrose agar medium was dispensed with homogenised hyphae and poured into Petri dishes onto which paper disks, which had been immersed in extract solutions, were placed. This method is a modified version of the disk diffusion assay. Antifungal activity in the heartwood extracts from the *Cinnamomum porrectum*, *Mangifera indica* and *Endospermum malaccense* was assessed with this method (Kawamura et al., 2011).

The TLC method was used to screen wood extracts. First compounds in crude extracts were separated on a cellulose TLC plate, which was subsequently inoculated with the test fungi. This method allowed the isolation of bioactive compounds from root extracts of *Vernonanthura tweedieana* (Portillo et al., 2005) or stem extracts of *Rhodiola rosea* (Ming et al., 2005). Kawamura et al. (2004) used this method to isolate four constituents which showed antifungal activity against *T. versicolor* from the ethyl acetate soluble *Gmelina arborea* heartwood extracts.

Bioassays were also performed with the essential oils and leaf extracts from *Eucalypts*. For example agar dilution and disk diffusion assays were used to determine the antibacterial and antifungal activities in the essential oils from *E. camendulensis* (Mouna & Segni, 2014), *E. bicostata, E. cinerea, E. maidenii, E. odorata* and *E. sideroxylon* (Elaissi et al., 2012), *E. tereticornis* (Maurya et al., 2016), *E. citriodora* (Javed et al., 2012) or the *Eucalyptus* hybrid *E. camaldulensis* × *E. tereticornis* (Varshney et al., 2012). A broth dilution assay was used to test antifungal activity of *E. maculata* leaves extracts (Takahashi et al., 2004).

Antifungal and antimicrobial activities of methanolic extracts from leaves, stems and flowers of *E. torquata and E. sideroxylon* were assessed by a modified disk diffusion assay (Ashour, 2008). Wells were drilled in the agar medium, which was previously inoculated with fungal or bacterial cultures. These wells were filled with extract and inhibition zones were recorded after incubation.

The approach taken in this work was to add a known, constant amount of bioactive substance (i.e. powdered wood or ethanol extract) to agar in a Petri dish and then measure the growth rate of wood decaying fungi. The resulting difference in growth rate between extracts should be due to the relative amounts of the individual components in the extract, not the amount of extract.

4.2 Materials

4.2.1 Wood

Heartwood and sapwood were sampled by drilling into the cross section of a disc from a 30-year-old *Eucalyptus bosistoana* tree. The collected drill dust was milled in a Wiley mill to pass a 20 mesh

screen. The samples were oven dried at 60°C (an assumed commercial timber drying temperature) to stable the moisture content (MC) of ~2%.

4.2.2 Extracts

Heartwood powder was extracted using an Accelerated Solvent Extractor (Dionex ASE 350, Thermo Scientific) equipped with 33 ml cells. In each run approximately 8 g milled heartwood was extracted with ethanol of HPLC grade as a solvent. The extraction conditions were two cycles at 70°C for 15 min (static time) followed by rinsing with 100% of the cell volume, resulting in approximately 70 ml of extract. The extract solutions were transferred to pre-dried labelled aluminium foil trays of known mass and placed in the fume hood overnight to evaporate the ethanol. The extracts were further dried using a vacuum oven at 60°C to remove moisture. The dried extract was stored in Eppendorf tubes.

4.2.3 Fungi and media

The white rot *Trametes versicolor* and brown rot *Coniophora cerebella* were obtained from the School of Biological Sciences, University of Canterbury. *T. versicolor* and *C. cerebella* (facultative synonym for *C. puteana*) are listed in European standards EN 113 (1996), EN 350–1 (1994) and by the Australian Wood Preservation Committee (2007) for accessing the durability of wood. The fungi were grown on potato dextrose agar media (Oxoid) containing 4.0 g/L potato extract, 20.0 g/L dextrose and 15.0 g/L agar.

4.3 Results and discussion

4.3.1 Method 1: Heartwood powder mixed with agar

Although difficult to control the extractive content in the experiment, adding wood powder directly to agar has the advantage of not requiring the preparation of wood extracts, which is a) resource intensive and b) has the potential to alter the chemical nature of the extracts.

The media as well as *E. bosistoana* heartwood and sapwood powder were sterilized in an autoclave at 121°C for 12 min. Wood powders were added in concentrations of 0% (control), 1% $_{w/v}$, 10% $_{w/v}$ and 30% $_{w/v}$ to 50 ml hot media, respectively. Then 10 ml of the suspensions were poured into Petri dishes (7 cm diameter). The dishes were inoculated with *T. versicolor* (0.5 mm diameter transplant) in sterile condition in a laminar flow cabinet and stored at 24°C in a temperature-controlled room. The radius of the fungus in each plate was measured every 24 h up to 6 days. The growth rates (cm/h) were calculated by fitting a linear regression for the diameter against time for each dish.

No consistent and pronounced effect on growth rate of wood type or wood concentration was observed (Table 4.2). This was likely caused by media surrounding the wood particles offering the fungi a healthy living environment. Furthermore, it was difficult to achieve a homogeneous

suspension of the wood particles in the media and the mixing procedure was a source for frequently observed contamination of the plates (Figure 4.1a, b).

The results suggested that the powdered wood needs to be extracted with solvents to determine antifungal activity in vitro. The extractives remained confined to the wood particles allowing growth of the fungi in the media. Furthermore, it was difficult to maintain aseptic conditions while transferring the suspension of wood powder, resulting in contamination of the plates.

Table 4.2: Growth rate (cm/h) of *T. versicolor* on agar mixed with *E. bosistoana* wood powder (n = 1).

Heartwood			**Sapwood**			**Control (agar only)**
1%	***10%***	***30%***	***1%***	***10%***	***30%***	0.077
0.066	0.044	0.055	0.056	0.065	0.075	

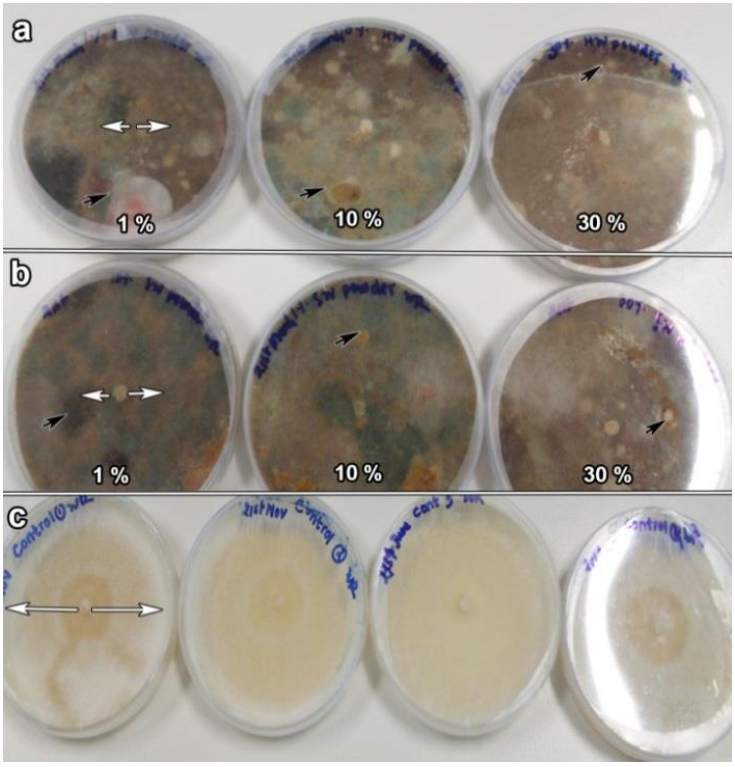

Figure 4.1: Growth (white arrows) of *T. versicolor* on agar mixed with different amounts of (a) heartwood and (b) sapwood powder as well as (c) the controls (agar only) after 168 h. Contamination (black arrows) were observed in the Petri dishes with wood powder.

4.3.2 Method 2: Extractives added to the agar

4.3.2.1 *T. versicolor*

To improve mixing of the bioactive compounds with the agar, and therefore create a homogenous living environment for the fungi, a solution of extract was applied to solidified media in Petri dishes.

In detail, 250 mg of dried *E. bosistoana* heartwood extract was added to 1 ml of dimethyl sulfoxide (DMSO). The mixture was placed in a shaker overnight. 10 ml media was poured into Petri dishes (7 cm diameter) and left to cool and solidify. 10 µl, 25 µl, 50 µl and 100 µl of the extract solution (i.e. 2.5 mg, 6.25 mg, 12.5 mg, 25 mg of extract, respectively) were transferred into the Petri dishes. Controls were prepared with 0 µl, 10 µl, 25 µl, 50 µl and 100 µl DMSO. The extracts and DMSO were spread on the surface of the media using disposable spreaders (Thermo Fischer). The plates were then inoculated with *T. versicolor* in sterile condition in a laminar flow cabinet and stored at 24°C to monitor the growth of the fungi for 7 days at 24 h intervals. The radius of the fungi in each Petri dish was measured using a pair of digital callipers until the fungi covered the dish. The growth rates (cm/h) were calculated as described above. Observations (Table 4.3) suggested that:

a) DMSO of up to 100 µl added to 10 ml of agar did not interfere with the growth of *T. versicolor*.
b) The growth of fungi was not significantly inhibited by the used amount of extracts as the growth rate of the fungus exposed to *E. bosistoana* heartwood extracts did not conclusively differ from those without extracts. However, a slightly slower growth was observed with 100 µl extracts.
c) No contamination was observed, indicating that maintaining sterile conditions was easier when applying an extract solution compared to adding wood powder (Figure 4.2).

Table 4.3: Growth rate (cm/h) of *T. versicolor* on 10 ml agar dosed with *E. bosistoana* heartwood extract and DMSO (n = 1).

Extract				**DMSO + Agar**				**Control (agar only)**
10 µl (2.5 mg)	***25 µl (6.25 mg)***	***50 µl (12.5 mg)***	***100 µl (25 mg)***	***10 µl***	***25 µl***	***50 µl***	***100 µl***	
0.018	0.017	0.015	0.014	0.017	0.017	0.016	0.016	0.016

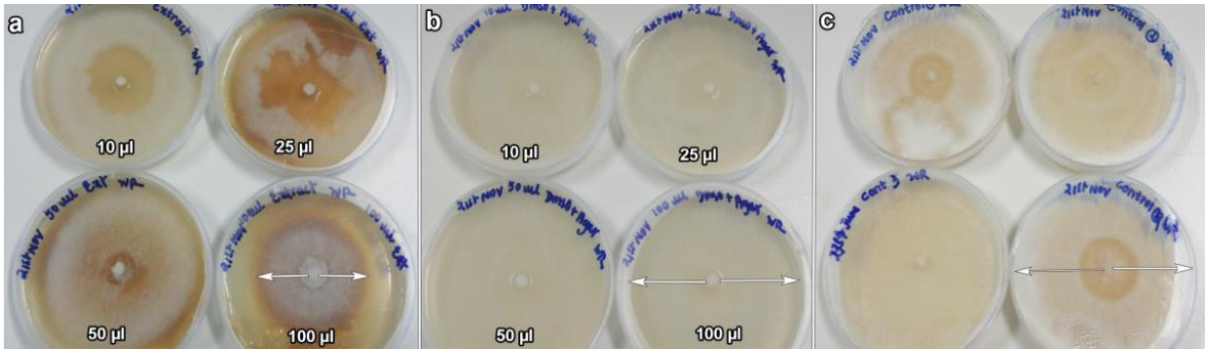

Figure 4.2: Growth (white arrows) of *T. versicolor* on agar (a) with *E. bosistoana* heartwood, (b) DMSO and (c) only agar after 168 h.

Consequently, higher amounts of *E. bosistoana* heartwood extracts were tested. This was achieved by adding larger amounts of the extract solution (100 µl, 500 µl, 1000 µl and 1500 µl) and DMSO to the agar. Observations (Table 4.4) suggested that:

a) 500 µl DMSO and above affected the growth of the white rot *T. versicolor*.
b) The growth of *T. versicolor* was completely inhibited with 1500 µl extract solution added to the Petri dish.
c) Heartwood extractives slowed the growth of the fungus at each of the tested concentrations.

Table 4.4: Growth rate (cm/h) of *T. versicolor* on 10 ml agar dosed with *E. bosistoana* heartwood extract and DMSO (n = 1).

Extract				**DMSO + Agar**				**Control (only agar)**
100 µl (25 mg)	***500 µl (125 mg)***	***1000 µl (250 mg)***	***1500 µl (375 mg)***	***100 µl***	***500 µl***	***1000 µl***	***1500 µl***	
0.017	0.009	0.004	no growth	0.024	0.015	0.010	no growth	0.029

100 µl DMSO solution containing 25 mg of extract was chosen to assess the bioactivity of extracts against the white rot *T. versicolor*.

The results suggested that heartwood extracts at different tested concentrations inhibited the growth of fungi. This mimicked earlier studies, which used DMSO solutions of heartwood extractives of *Chamaecyparis obtusa*, *P. rigida* and *D. odorata* to determine their antifungal activity (Morikawa et al., 2012; Salem et al., 2016; Wanschura et al., 2016). While an inhibitory effect of higher DMSO concentrations on the growth rate of dermatophytes e.g. *Candida albicans* is known (Randhawa 2008), low concentrations of DMSO do not affect the growth of fungi, as studies on fungal activity of *D. odorata* heartwood extracts showed (Wanschura et al., 2016). However, the effect of DMSO would

not be the same for all wood degrading fungi due to variation in their susceptibility. Therefore the maximum DMSO concertation needs to be tested individually for each fungus.

4.3.2.2 *C. cerebella*

To develop an assay for assessing the bioactivity of extracts against the brown rot *C. cerebella* the same procedures as described in 4.3.2.1 were followed.

C. cerebella were growing slower and more sensitive to the *E. bosistoana* heartwood extract (Table 4.5). The growth of the brown rot was completely inhibited at the used extract dosages. Like for the white rot DMSO inhibited the growth of *C. cerebella* above 100 µl and stopped growth when adding 1500 µl DMSO. Again no contamination was observed (Figure 4.3).

Table 4.5: Growth rate (cm/h) of *C. cerebella* on 10 ml agar dosed with *E. bosistoana* heartwood extract and DMSO (n = 1).

Extract				**DMSO + Agar**				**Control (only agar)**
100 µl (25 mg)	***500 µl (125 mg)***	***1000 µl (250 mg)***	***1500 µl (375 mg)***	***100 µl***	***500 µl***	***1000 µl***	***1500 µl***	
no growth	no growth	no growth	no growth	0.007	0.006	0.005	no growth	0.007

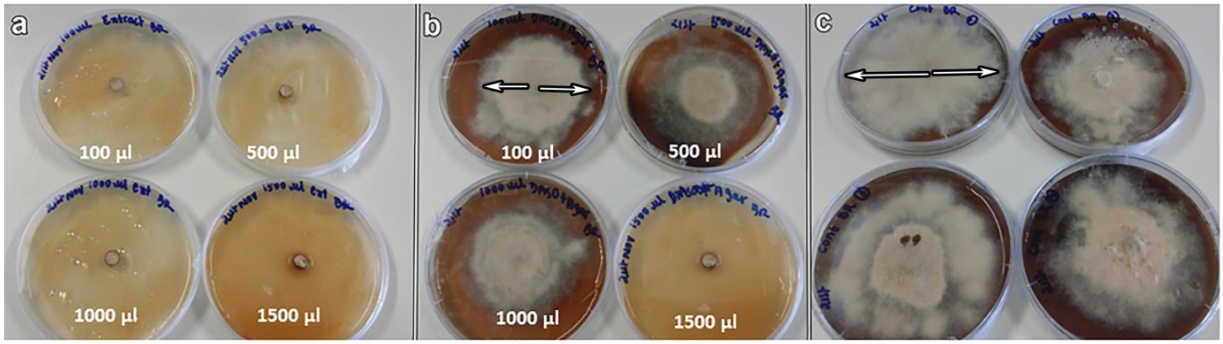

Figure 4.3: Growth (white arrows) of *C. cerebella* on agar (a) with *E. bosistoana* heartwood, (b) DMSO and (c) only agar after 432 h.

The dosage was optimised by diluting 300 µl of the above described *E. bosistoana* heartwood extract solution with 500 µl DMSO, resulting in a concentration of 93.75 mg/ml. 50 µl (i.e. 4.7 mg extract) and 100 µl (i.e. 9.4 mg extract) of this solution as well as corresponding amounts of DMSO were transferred to Petri dishes and inoculated with *C. cerebella* as described above.

Consistent with the experiment above, the growth of *C. cerebella* was not affected by the amount of added DMSO (Table 4.6, Figure 4.4). The growth of the fungus was inhibited with 50 µl extract (~ 4.7 µg).

50 µl extract solution containing 4.7 µg *E. bosistoana* heartwood extract in DMSO were deemed suitable to assess the bioactivity against *C. cerebella*.

C. cerebella was more sensitive to *E. bosistoana* heartwood extracts than *T. versicolor*. This confirmed reports, which suggested that *C. puteana* (facultative synonym of *C. cerebella)* was found to be more sensitive than *T. versicolor* to phenols, phenol ethers, and aromatic aldehydes (Voda et al., 2003). Phenolic and aromatic compounds have been reported in eucalyptus heartwood extracts (Hillis, 1987). The brown rot decay resistance was compared between *C. puteana* and *Poria placenta* in different larch heartwood species (*L. decidua*, *L. kaempferi*, *L. eurolepis*) (Gierlinger et al., 2004). The results suggested *C. puteana* was more sensitive to the chemical composition of larch heartwood extracts.

Table 4.6: Growth rate (cm/h) of *C. cerebella* on agar dosed with *E. bosistoana* heartwood extract and DMSO (n = 1).

Extract		**DMSO + Agar**		**Control (only agar)**
50 µl (4.7 mg)	***100 µl (9.4 mg)***	***50 µl***	***100 µl***	
0.002	0.003	0.005	0.006	0.007

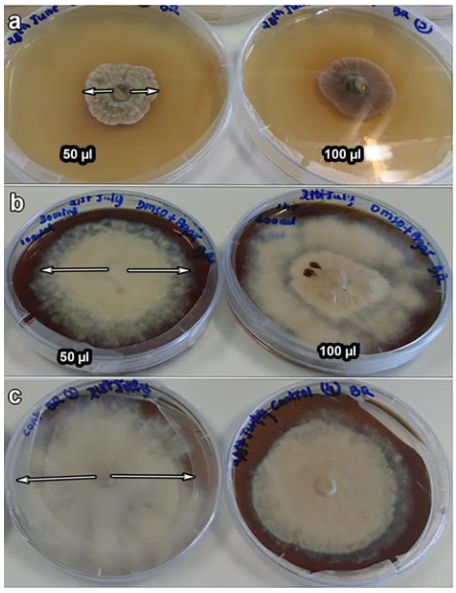

Figure 4.4: Growth (white arrows) of *C. cerebella* on agar (a) with *E. bosistoana* heartwood, (b) DMSO and (c) only agar after 432 h.

4.3.2.3 Diffusion of DMSO into agar

DMSO was found to affect the growth of the test fungi (Table 4.3, 4.4). After applying the DMSO extract solutions to the agar surface the DMSO starts to diffuse into agar, reducing the surface

concentration. To avoid excessively high DMSO concentrations at the time of inoculation, different time intervals between extract application and inoculation were investigated. 100 µl and 500 µl DMSO was transferred to the Petri dishes as described above and left for 15 min, 30 min, and 1 h to diffuse into the media. The plates were inoculated with *T. versicolor* and assessed as described above.

Again, while 100 µl DMSO did not affect the growth of the fungi, the higher concentration did (Table 4.7). Allowing at least 15 min for DMSO to diffuse into the agar was sufficient to obtain growth rates similar to that on pure agar. Again, no contamination was observed (Figure 4.5). The results suggested that DMSO can be used to solubilize heartwood extracts.

Table 4.7: Effect of diffusion time on growth rate (cm/hr) of *T. versicolor* exposed to 100 µl and 500 µl DMSO on 10 ml agar (n=1).

100 µl DMSO			**500 µl DMSO**			**Control (only agar)**
DMSO exposure time						
15 mins	***30 mins***	***1 hr***	***15 mins***	***30 mins***	***1 hr***	
0.013	0.013	0.013	0.009	0.010	0.009	0.015

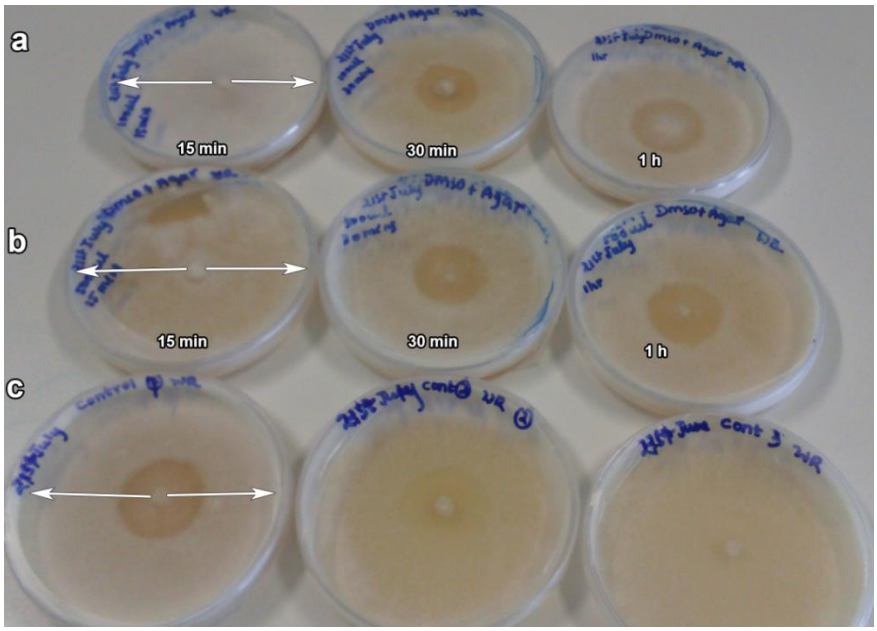

Figure 4.5: Growth (white arrows) of *T. versicolor* exposed to (a) 100 µl and (b) 500 µl DMSO at different intervals and (c) only agar after 168 h.

4.3.3 Repeatability of the bioactivity test

To investigate the repeatability of the above described method, five solutions of the same *E. bosistoana* heartwood extract were prepared by adding 0.05 g dried extract to 0.2 ml DMSO. These were assessed for their bioactivity against white rot. 100 µl of the extract solutions were transferred to Petri dishes. For brown rot tests, five solutions of 0.018 g dried extract added to 0.2 ml DMSO were prepared. 50 µl of these extract solutions were transferred to Petri dishes. The subsequent procedure was as described above.

The diameter of the fungi increased linearly with time (Figure 4.6, 4.7). However, the fungi needed a certain lag time to establish, where no growth was observed. Restricting the calculation of the growth rate to the linear growth phase improved the correlation coefficients from 0.87-0.95 to > 0.95 for white rot (Figure 4.6) and 0.90-0.95 to > 0.95 for brown rot (Figure 4.7). Once the fungi came close the walls of the Petri dishes the growth rate slowed again (data not shown).

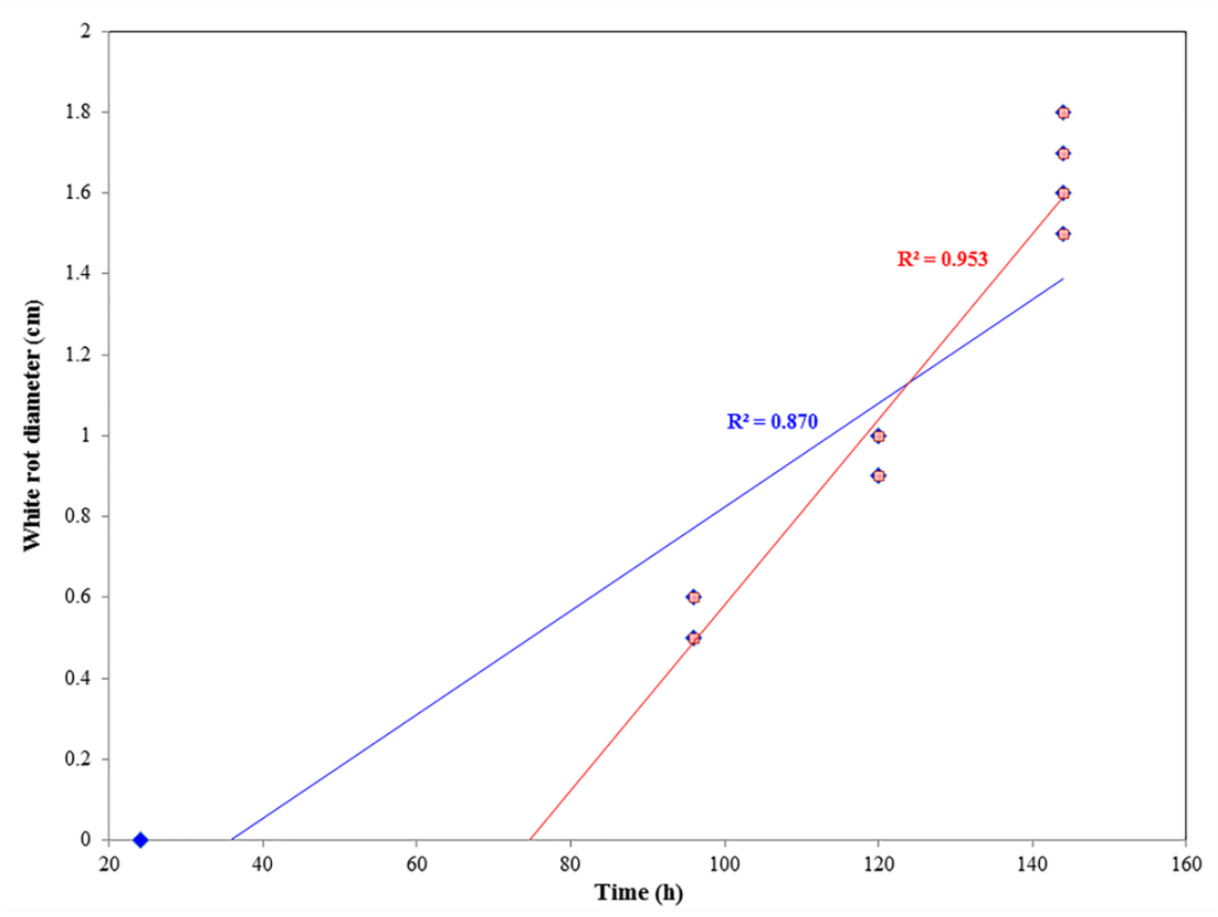

Figure 4.6: Fitting linear growth rates to white rot grown in Petri dishes with heartwood extracts for 144 h; n = 5. Excluding a lag phase in which the fungi established (red) increased the linear fit compared to conserving all data (blue).

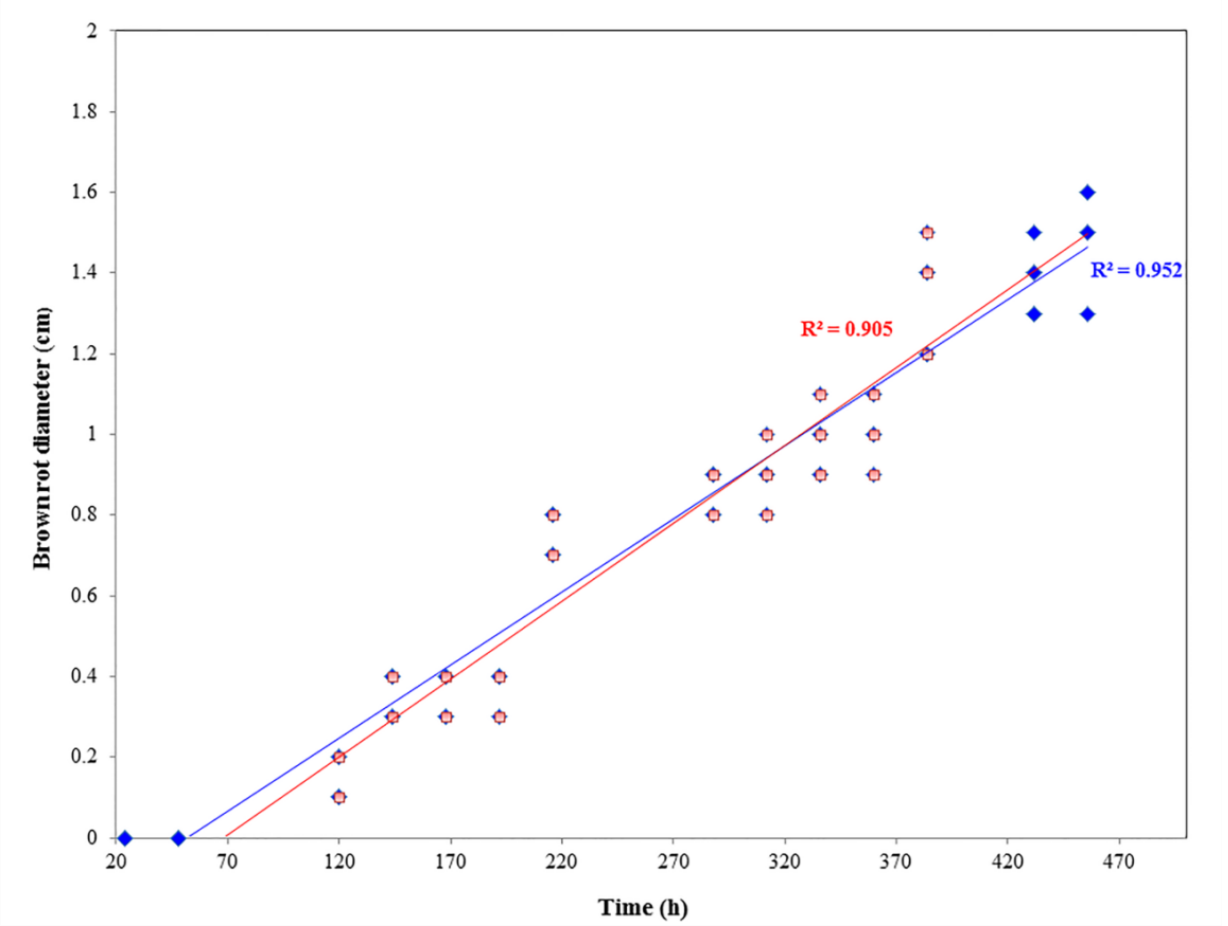

Figure 4.7: Fitting linear growth rates to brown rot grown in Petri dishes with heartwood extracts for 456 h; n = 5. Excluding a lag phase in which the fungi established (red) increased the linear fit compared to conserving all data (blue).

The coefficient of variation (CV) was similar for the two fungi (Table 4.8, 4.9). The repeatability of the growth of the fungi on the controls was better (CV 3.2 to 5.4%) than for the plates with extracts (CV 11.1 and 9.6%). This suggested that while the fungi expressed consistent growth the preparation of the extract solutions or their application to the agar introduced some variability. Pauli and Schilcher (2010) reported that in bioassay several factors (fungi mycelium size, pH of growth medium, incubation, time and temperature) may interfere in the results of repeatability. The repeatability of the test was generally good but to get a more precise bioactivity measure the heartwood extracts should be measured as replicates. This would also account for potentially contamination, which had not occurred in these preliminary tests.

Bioassays are known for their high variability. For example, the Clinical Laboratory Standards Institute (CLSI) and the European Committee on Antimicrobial Susceptibility Testing (EUCAST) specified discrepancies between Minimum Inhibitory Concentration MIC results of no more than ± 2 two fold dilutions between the runs and antifungal assays (Chryssanthou & Cuenca, 2006).

Table 4.8: Mean growth rate (cm/h), standard deviation (SDEV) and coefficient of variation (CV) of *T. versicolor* on 10 ml agar dosed with *E. bosistoana* heartwood extract and DMSO (n = 5).

Extract			**DMSO + Agar**			**Control (only agar)**		
Mean	***SDEV***	***CV (%)***	***Mean***	***SDEV***	***CV (%)***	***Mean***	***SDEV***	***CV (%)***
0.0229	0.0026	11.1	0.0363	0.0011	3.2	0.0346	0.0011	3.3

Table 4.9: Mean growth rate (cm/h), SDEV and CV of *C. cerebella* on 10 ml agar dosed with *E. bosistoana* heartwood extract and DMSO (n = 5).

Extract			**DMSO + Agar**			**Control (only agar)**		
Mean	***SDEV***	***CV (%)***	***Mean***	***SDEV***	***CV (%)***	***Mean***	***SDEV***	***CV (%)***
0.0039	0.0004	9.6	0.0072	0.0003	3.6	0.0068	0.0004	5.4

The differences in growth rate of the white rot fungus between the tests on the same medium (Table 4.3, 4.4, 4.8) indicted that the growth was also affected by variables not controlled in the test set up. This can include variations in the room temperature or the vitality of the fungus inoculum (Hawker, 1950). These differences can be accounted for by normalising for the control growth rate, i.e. calculating the relative growth rate, which expresses by how much fungal growth was inhibited by the treatment. This a common parties for such tests (Balouiri et al., 2016).

Relative growth rate (%) = Ds / Dc × 100 ---------- **Equation 1**

Where, Ds is the diameter of growth in the plate containing the tested antifungal agent and Dc is the diameter of growth in the control plate.

4.4 Conclusion

A method of testing the bioactivity of *E. bosistoana* heartwood extracts against *T. versicolor* and *C. cerebella* was developed. 100 µl for white rot and 50 µl for brown rot of extract DMSO solution (250 mg/ml for white rot and 93.75 mg/ml for brown rot) were transferred to 7 cm Petri dishes filled with 10 ml hardened agar. The extracts were spread on the surface of agar media using disposable spreaders. The dishes were inoculated with 0.5 mm mycelium after 15 minutes in sterile condition in laminar hood and stored at 24°C. The diameter of the fungus in the agar plates was measured daily until it filled the Petri dish. Controls were run with (100 µl for white rot and 50 µl for brown rot) and without (agar only) DMSO. Tests were done as replicates of five. The growth rates (cm/h) were calculated by fitting a linear regression for the diameter against time for each dish, considering only

the linear growth of the fungi. Good sterility i.e. no contamination was observed and the test had a CV of less than 11.1% within a batch. Variation in growth rate between different runs needed to be accounted for by normalising the fungal growth rate by that in the controls, i.e. calculating a relative growth rate.

4.5 References

Ashour, H. M. (2008). Antibacterial, antifungal, and anticancer activities of volatile oils and extracts from stems, leaves, and flowers of *Eucalyptus sideroxylon* and *Eucalyptus torquata*. *Cancer Biology & Therapy, 7*, 399-403.

Bafi-Yeboa, N., Arnason, J., Baker, J., & Smith, M. (2005). Antifungal constituents of Northern prickly ash, *Zanthoxylum americanum* Mill. *Phytomedicine, 12*, 370-377.

Balouiri, M., Sadiki, M., & Ibnsouda, S. K. (2016). Methods for in vitro evaluating antimicrobial activity: A review. *Journal of Pharmaceutical Analysis, 6*, 71-79.

Celimene, C. C., Micales, J. A., Ferge, L., & Young, R. A. (1999). Efficacy of pinosylvins against white-rot and brown-rot fungi. *Holzforschung, 53*, 491-497.

Chandrasekaran, M., & Venkatesalu, V. (2004). Antibacterial and antifungal activity of *Syzygium jambolanum* seeds. *Journal of Ethnopharmacology, 91*, 105-108.

Chen, Y. H., Lin, C. Y., Yen, P. L., Yeh, T. F., Cheng, S. S., & Chang, S. T. (2017). Antifungal agents from heartwood extract of *Taiwania cryptomerioides* against brown root rot fungus *Phellinus noxius*. *Wood Science and Technology, 51*, 639-651.

Chryssanthou, E., & Cuenca, E. M. (2006). Comparison of the EUCAST-AFST broth dilution method with the CLSI reference broth dilution method (M38-A) for susceptibility testing of posaconazole and voriconazole against *Aspergillus* spp. *Clinical Microbiology and Infection, 12*, 901-904.

Davies, N. T., Wu, H. F., & Altaner, C. M. (2014). The chemistry and bioactivity of various heartwood extracts from redwood (*Sequoia sempervirens*) against two species of fungi. *New Zealand Journal of Forestry Science, 44*, 17.

Elaissi, A., Rouis, Z., Salem, N. A. B., Mabrouk, S., ben Salem, Y., Salah, K. B. H., Aouni, M., Farhat, F., Chemli, R., & Harzallah, S. F. (2012). Chemical composition of 8 *Eucalyptus* species essential oils and the evaluation of their antibacterial, antifungal and antiviral activities. *BMC Complementary and Alternative Medicine, 12*, 81.

Gierlinger, N., Jacques, D., Schwanninger, M., Wimmer, R., & P, L. E. (2004). Heartwood extractives and lignin content of different larch species (*Larix* sp.) and relationships to brown rot decay resistance. *Trees Structure and Function, 18*, 230-236.

Haupt, M., Leithoff, H., Meier, D., Puls, J., Richter, H., & Faix, O. (2003). Heartwood extractives and natural durability of plantation-grown teakwood (*Tectona grandis* L.)—a case study. *European Journal of Wood and Wood Products, 61*, 473-474.

Hawker, L. E. (1950). *Pysiology of fungi*. England: London press.

Hawley, L., Fleck, L., & Richards, C. A. (1924). The relation between durability and chemical composition in wood. *Industrial & Engineering Chemistry, 16*, 699-700.

Javed, S., Shoaib, A., Mahmood, Z., Mushtaq, S., & Iftikhar, S. (2012). Analysis of phytochemical constituents of *Eucalyptus citriodora* L. responsible for antifungal activity against post-harvest fungi. *Natural Product Research, 26*, 1732-1736.

Kawamura, F., Ohara, S., & Nishida, A. (2004). Antifungal activity of constituents from the heartwood of *Gmelina arborea*: Part 1. Sensitive antifungal assay against basidiomycetes. *Holzforschung, 58*, 189-192.

Kawamura, F., Ramle, S. F. M., Sulaiman, O., Hashim, R., & Ohara, S. (2011). Antioxidant and antifungal activities of extracts from 15 selected hardwood species of Malaysian timber. *European Journal of Wood and Wood Products, 69*, 207-212.

Li, Q., Wang, X. X., Lin, J. G., Liu, J., Jiang, M. S., & Chu, L. X. (2014). Chemical composition and antifungal activity of extracts from the xylem of *Cinnamomum camphora*. *BioResources, 9*, 2560-2571.

Li, Y., & Altaner, C. (2018). Predicting extractives content of *Eucalyptus bosistoana* F. Muell. heartwood from stem cores by near infrared spectroscopy. *Spectrochimica Acta Part A: Molecular and Biomolecular Spectroscopy, 198*, 78-87.

Luís, Â., Neiva, D., Pereira, H., Gominho, J., Domingues, F., & Duarte, A. P. (2014). Stumps of *Eucalyptus globulus* as a source of antioxidant and antimicrobial polyphenols. *Molecules, 19*, 16428-16446.

Lukmandaru, G. (2017). Antifungal activities of certain components of teak wood extractives. *Jurnal Ilmu dan Teknologi Kayu Tropis, 11*, 11-18.

Maurya, A., Verma, S. C., Jayanthy, A., Shankar, M., & Sharma, R. K. (2016). A concise review on phytochemistry and pharmacological properties of *Eucalyptus tereticornis* Smith. *Asian Journal of Research in Chemistry, 9*, 457-461.

Mihara, R., Barry, K. M., Mohammed, C. L., & Mitsunaga, T. (2005). Comparison of antifungal and antioxidant activities of *Acacia mangium* and *A. auriculiformis* heartwood extracts. *Journal of Chemical Ecology, 31*, 789-804.

Ming, D. S., Hillhouse, B. J., Guns, E. S., Eberding, A., Xie, S., Vimalanathan, S., & Towers, G. (2005). Bioactive compounds from *Rhodiola rosea* (Crassulaceae). *Phytotherapy Research, 19*, 740-743.

Mohareb, A., Sirmah, P., Desharnais, L., Dumarçay, S., Pétrissans, M., & Gérardin, P. (2010). Effect of extractives on conferred and natural durability of Cupressus lusitanica heartwood. *Annals of Forest Science, 67*, 504-504.

Morikawa, T., Ashitani, T., Sekine, N., Kusumoto, N., & Takahashi, K. (2012). Bioactivities of extracts from *Chamaecyparis obtusa* branch heartwood. *Journal of Wood Science, 58*, 544-549.

Mouna, M., & Segni, L. (2014). Biological activity of essential oil of *Eucalyptus camendulensis* on some fungi and bacteria. *International Journal of Engeneering Research and Applications, 4*, 71-73.

Mun, S. P., & Prewitt, L. (2011). Antifungal activity of organic extracts from *Juniperus virginiana* heartwood against wood decay fungi. *Forest Products Journal, 61*, 443-449.

Niamké, F. B., Amusant, N., Stien, D., Chaix, G., Lozano, Y., Kadio, A. A., Lemenager, N., Goh, D., Adima, A. A., & Kati-Coulibaly, S. (2012). 4′, 5′-Dihydroxy-epiisocatalponol, a new naphthoquinone from *Tectona grandis* L. f. heartwood, and fungicidal activity. *International Biodeterioration & Biodegradation, 74*, 93-98.

Novriyanti, E., Santosa, E., Syafii, W., Turjaman, M., & Sitepu, I. R. (2010). Anti fungal activity of wood extract of *Aquilaria crassna* against agarwood-inducing fungi, *Fusarium solani*. *Indonesian Journal of Forestry Research, 7*, 155-165.

Pauli, A., & Schilcher, H. (2010). 12 In vitro antimicrobial activities of essential oils monographed in the european Pharmacopoeia 6th Edition. In K. H. C. In: Baser & G. Buchbauer (Eds.), *Handbook of Essential Oils: Science, Technology and Applications.* (pp. 353). Boca Raton: CRC Press.

Portillo, A., Vila, R., Freixa, B., Ferro, E., Parella, T., Casanova, J., & Cañigueral, S. (2005). Antifungal sesquiterpene from the root of *Vernonanthura tweedieana*. *Journal of Ethnopharmacology, 97*, 49-52.

Quiroga, E. N., Sampietro, A. R., & Vattuone, M. A. (2001). Screening antifungal activities of selected medicinal plants. *Journal of Ethnopharmacology, 74*, 89-96.

Rahalison, L., Hamburger, M., Hosttetman, K., Monod, M., & Frank, E. (1991). A bioautography agar overlay method for the detection of antifungal compound from higher plants. *Journal of Phytochemical Analysis, 2*, 199-203.

Randhawa, M. A. (2008). Dimethyl Sulfoxide (DMSO) Inhibits the germination of *Candida albicans* and the arthrospores of *Trichophyton mentagrophytes*. *Nippon Ishinkin Gakkai Zasshi, 49*, 125-128.

Rowe, J. (1989). Introduction and historical background. Natural products of woody plants. I. *Springer: Berlin, 1-13*.

Salem, M. Z., Zidan, Y. E., Hadidi, N. M., Mansour, M. M., & Elgat, W. A. A. (2016). Evaluation of usage three natural extracts applied to three commercial wood species against five common molds. *International Biodeterioration & Biodegradation, 110*, 206-226.

Takahashi, T., Kokubo, R., & Sakaino, M. (2004). Antimicrobial activities of *Eucalyptus* leaf extracts and flavonoids from *Eucalyptus maculata*. *Letters in Applied Microbiology, 39*, 60-64.

Taylor, A. M., Gartner, B. L., & Morrell, J. J. (2002). Heartwood formation and natural durability- A review. *Wood and Fiber Science, 34*, 587-611.

Van Lierde, J. (2013). *What causes natural durability in Eucalyptus bosistoana timber? a dissertation submitted in partial fulfilment of the requirements for the degree of Bachelor of Forestry Science with Honours.* B For Sci (Hon), University of Canterbury, Christchurch, New Zealand.

Varshney, V. K., Pandey, A., Onial, P. K., & Dayal, R. (2012). Antifungal activity of phytochemicals from *Eucalyptus* hybrid leaves against some plant pathogenic and wood decay fungi. *Archives of Phytopathology and Plant Protection, 45*, 2347-2354.

Voda, K., Boha, B., Vrtačnika, M., & Pohlevenb, F. (2003). Effect of the antifungal activity of oxygenated aromatic essential oil compounds on the white rot *Trametes versicolor* and the brown rot *Coniophora puteana*. *International Biodeterioration & Biodegradation, 51*, 51-59.

Wanschura, R., Holzhauser, E. W., & Richter, K. (2016). *Screening of bioactive extracts for selected tropical hardwood species and identification of key substances.* In: Proceedings of 14th European Workshop on Lignocellulosics and Pulp, 433-436.

Wiegand, I., Hilpert, K., & Hancock, R. E. (2008). Agar and broth dilution methods to determine the minimal inhibitory concentration (MIC) of antimicrobial substances. *Nature Protocols, 3*, 163.

Wu, C. C., Wu, C. L., Huang, S. L., & Chang, H. T. (2012). Antifungal activity of liriodenine from *Michelia formosana* heartwood against wood-rotting fungi. *Wood Science and Technology, 46*, 737-747.

Yen, T. B., Chang, H. T., Hsieh, C. C., & Chang, S. T. (2008). Antifungal properties of ethanolic extract and its active compounds from *Calocedrus macrolepis* var. *formosana* (Florin) heartwood. *Bioresource Technology, 99*, 4871-4877.

Yusiasih, R., Yoshimura, T., Umezawa, T., & Imamura, Y. (2003). Screening method for wood extractives: direct cellulose thin-layer chromatography plate. *Journal of Wood Science, 49*, 377-380.

Chapter-5

Bioactivity of ethanol extracts from *Eucalyptus bosistoana* heartwood

5.1 Introduction

Heartwood extractives are composed of hundreds of secondary metabolites including terpenes, flavonoids, phenylpropanoids, amines and alkaloids that impart durability and biotic resistance to heartwood (Duchesne et al., 1992). In *Eucalypts*, heartwood extractives are predominately comprised of polyphenols such as tannins, the esters of gallic and ellagic acids or cinnamic acid derivatives (Conde et al., 1995; Hillis, 1971, 1991; Rudman, 1964). The quantity and composition of these extractives varies between species, between individual trees of a species and within a tree (Hillis, 1987; Taylor et al., 2002). The natural durability of timber does not necessarily correspond to the amount of extractives i.e. extractive concentrations, but also depends on the composition of extractives (Taylor et al., 2002). Therefore, heartwood durability research in a breeding programme needs to consider the most potent extracts and their chemical composition for the next generation durability improvement. The variability in extractive content and composition, which exists between trees of a species, is influenced by environmental and genetic factors. Variation in extractive content in *E. globulus* heartwood was observed between trees and sites (Morais & Pereira, 2012). Mosedale et al. (1996a) reported variation in the concentration of ellagitannins in the heartwood of oak species (*Quercus robur* and *Q. petraea*) between forests and found that the ellagitannins content is under strong genetic control (Mosedale et al., 1996b). Significant variation in the heartwood compounds (β-thujaplicin, ratio between γ- and β-thujaplicin and methyl thujate) was detected within and between western red cedar (*Thuja plicata*) within and between regions (Daniels & Russell, 2007).

Variation in the composition of heartwood flavonoids in regional populations of sweet cherry (*Prunus avium*) was reported under genetic and environmental control while age of the trees had no effect on the distribution of flavonoid aglycones (Vinciguerra et al., 2003). This line with reports by Fries et al. (2000), who suggested, the phenotype of extractive compounds can be influenced by environmental conditions such as soil fertility. Site soil composition was reported to influence the amount of lipophilic extractives in *E. dunnii* and *E. grandis* (Kilulya et al., 2014). Also variation in decay resistance among individual trees of a single species has been reported to be extensive due to genetic and environmental factors (Yu et al., 2003).

Eucalyptus species were classified into four groups, based on the extractive composition (Hillis, 1991). Condensed tannins are characteristic in the heartwood of a group with pink to red brown heartwood (e.g. *E. camaldulensis*, *E. grandis*, *E. marginata*), while hydrolysable tannins are characteristic for a group with pale-light coloured outer heartwood (e.g. *E. delegatensis*). A third group with brown heartwood (e.g. *E. wandoo*) features stilbenes, ellagitannins and ellagic acids and a fourth group with heartwood that has a greasy feel (e.g. *E. maculata*, *E. microcorys*) contain eucalenol and steroids in addition to ellagic acid and ellagitannins.

The quantification of individual extractive components is difficult because the numerous compounds have different physical and chemical properties. However, selective identification and quantification of some compounds are feasible by chromatographic methods such as Gas Chromatography (GC) and High Performance Liquid Chromatography (HPLC) combined with mass spectrometry (MS). Literature shows that the GC is now the most common technique for the characterisation of wood extractives (Fernandez et al., 2001; Gutiérrez et al., 1998; Sitholé et al., 1992). For GC analysis heartwood extractives often need to be derivatized by methylation, silylation or acetylation to allow analysis (Davies et al., 2014; Fernandez et al., 2001). Compounds identified in the heartwood extracts of *Eucalyptus* species by various chromatographic techniques are summarised in Table 5.1.

Table 5.1: Compounds identified in the heartwood extracts of *Eucalyptus* species by different chromatographic techniques.

Species	Compounds	Analytical technique	Reference
E. marginata	Catechin, Proanthocyanidins, Ellagitannins, Stilbenes	Paper and liquid chromatography	(Hillis & Carle, 1962)
E. wandoo	Resveratrol (3,5, trihydroxystilbene), 3 β-D-glucoside	Paper chromatography	(Hathway, 1962)
E. sideroxylon	Resveratrol (3,5, trihydroxystilbene), Ellagic acid, Gallic acid, Catechin, Ellagitannins	Two dimensional paper chromatography	(Hillis & KoichiroIsoi, 1965)
	Resveratrol (resveratrol-β-glucoside), 3,3′-di- and 3,3′,4-tri-*o*-methylellagic acids and their glucosides	Paper chromatography with NMR spectroscopy	(Hillis et al., 1974)
E. sieberiana	Catechin	Paper chromatography with	(Hillls & Carle, 1959)
E. grandis *E. dunnii*	Octanoic acid, Decanoic acid, Octanedioic acid, 1-dodecanol, Dodecanoic acid, Nonanedioic acid, Tridecanoic acid, 12-methyltridecanoic acid, Tetradecanoic acid	Gas chromatography-mass spectrometry (GC-MS)	(Kilulya et al., 2014)

Species	Compounds	Analytical technique	Reference
E. camaldulensis	Polyphenol (Catechin), Resin acids, Fatty acids, Glycerides, Triterpenes, Steryl esters, Sterols and fatty alcohols, Stilbenes, Flavanols, Monosaccharides and cyclic polyols	GC-MS	(Benouadah et al., 2018)
E. wandoo	Reveratrol glucoside Aglucone	Paper chromatography	(Hathway & Seakins, 1959)
E. astrigens	Stilbenes	Paper and liquid chromatography	Hillis and Carle (1962)
E. citriodora	Trans-calamenene, muurolol	Thin layer chromatography	(Lee & Chang, 2000)
E. delegatensis	Ellagitannins, Ellagic acid	Paper chromatography	(Hillls & Carle, 1959; Seikel & Hillis, 1970)

Van Lierde (2013) determined the bioactivity ethanol, ethyl acetate and water extracts of *E. bosistoana* heartwood and found that ethanol extracts have highest fungicidal activity against *Trametes versicolor* and *Gloeophyllum trabeum*. In order to assess the bioactivity of an ethanol extract and further quantify the most effective component among the numerous compounds by gas chromatography, the influence of extractive content needs to be removed. In other words two pieces of wood can have the same extractive content but of different relative composition (or vice versa) and therefore different natural durability.

The objectives of this study were to i) quantify the variability in bioactivity of *E. bosistoana* heartwood extracts, ii) quantify the variability of the composition of *E. bosistoana* heartwood extracts and iii) identify key chemical compounds affecting the growth of wood decaying organisms. In this study the bioactivity of 91 *E. bosistoana* extracts from two different sites was investigated. A constant amount of extract was added to agar in a Petri dish and then the growth rate of wood decaying fungi on extracts was compared to the growth rate on pure agar. The resulting difference in growth rate between extracts was due to the relative amounts of the individual components in the extract, not the amount of extract. Variation in extractive components was quantified by gas chromatography for all 91 trees and subsequently correlated to the relative growth rates.

5.2 Materials and methods

5.2.1 Material

91 Heartwood disks were obtained from 7-year-old *E. bosistoana* breeding trials planted in 2009. These trees were grown at two different sites, Lawson and Craven Road (41°26´S, 173°56´E and 41°43´S, 173°02´E) in Marlborough, New Zealand. Two wood rot fungi, the white rot *Trametes*

versicolor and the brown rot *Coniophora cerebella*, obtained from the School of Biological Sciences, University of Canterbury were used for the fungal assays.

Heartwood powder was prepared and extracted with ethanol as described in chapter 4. The mass of each oven-dried extract was measured and the extractive content was calculated on a dry mass basis.

5.2.2 Fungal assays

The method described in chapter 4 was used to test the bioactivity of the *E. bosistoana* heartwood ethanol extracts. In brief, 10 ml of autoclaved (121°C, 12 min) potato dextrose agar (Oxoid - containing 4.0 g/L potato extract, 20.0 g/L dextrose and 15.0 g/L agar) was poured into 7 cm Petri dishes. 100 µl (250 mg/ml) or 50 µl (93.75 mg/ml) of dimethyl sulfoxide (DMSO) extract solution were spread onto the surface of the solidified agar with a disposable spreader for white rot and for brown rot tests, respectively. Controls were run with pure agar and 100 µl or 50 µl DMSO, respectively. Five replicates for each fungi and extract were conducted resulting in 1160 dishes. The assays were conducted in 25 batches over a period of 20 weeks due to lack of space and time taken for growth rate measurements of the large number of dishes. The relative growth rate was calculated as defined in equation 1 (chapter 4) using the agar controls only.

5.2.3 Gas chromatography (GC)

For each sample, 10 mg of dried heartwood extract were mixed with 90 µl pyridine in Eppendorf (1.5 ml) tubes to which 10 µl internal standard solution (5 mg betulin (Sigma Aldrich) dissolved in 1 ml of pyridine) was added. A 15 µl aliquot of this solution was trimethylsilylated at room temperature using 50 µl of N,O-bis(trimethylsilyl)-trifluoroacetamide (BSTFA, Supelco Analytical) in a septum-sealed vial for 20 min according to the supplier's recommendations. The trimethylsilyl derivatives were analysed with a gas chromatograph (Agilent 7820A), fitted with a fused-silica capillary column (Agilent DB-5 - 30 m x 0.320 mm x 0.25 µm) using helium as the carrier gas and FID detection at 300°C. The initial oven temperature was set to 116°C, ramped up to 280°C at 7°C/min and held for 20 min. Each sample was analysed twice after a blank and a pyridine run.

Individual compounds were identified by comparing the *E. bosistoana* heartwood extracts with an *E. globoidea* heartwood extract. Some compounds were previously identified in *E. globoidea* heartwood extracts by GS-MS (Schroettke, 2018). These *E. globoidea* extracts were previously run on the same GC system but in the meantime shortening of the column resulted in a shift of the retention times of up to 0.7 min (i.e. the internal standard betulin at ~27.9 min).

5.2.4 Data extraction from chromatograms and data analysis

Peaks of the chromatograms were integrated using integration tool in the Chem Station software (Agilent, Rev.c.01.07) and refined manually for the largest 33 peaks including the internal standard. Peak areas and retention times were extracted as .csv files and the retention times for 91 samples were

aligned manually in Excel. Peak area of 32 retention times were normalised by the peak area of the internal standard before duplicate runs were averaged. Data analysis was performed using R programming language (Team, 2013) including ANOVA and T-tests. The ggplot2 (version 2.2.1) package (Wickham, 2009) was used to plot graphs. An alpha of 0.05 is used as the cut off for significance in this chapter.

Multivariate analysis (Partial Least Squares Regression) between the quantified heartwood compounds and the relative growth rates of white rot (*T. versicolor*) and brown rot (*C. cerebella*) was performed using the plsdepot (version-0.1.17) package in R (Sanchez, 2012). This analysis was performed to identify the most important compounds showing bioactivity of the *E. bosistoana* heartwood extracts on the growth of white rot (*T. versicolor*) and brown rot (*C. cerebella*).

5.3 Results and discussion

Data for extractive content and relative growth rates of white rot (*T. versicolor*) and brown rot (*C. cerebella*) in heartwood extracts of 91 samples are shown in the Table 5.2. The largest variation was found for extractive content, with the samples from the Craven Road site having a lower extractive content. Brown rot was more susceptible to the *E. bosistoana* heartwood extracts and the effect was also more variable than for white rot.

Table 5.2: Summary statistics of extractive content in *E. bosistoana* heartwood from 7-year-old trees and the effect of ethanol extracts on the relative growth rates of the white rot *Trametes versicolor* and the brown rot *Coniophora cerebella* for 2 sites. CV: Coefficient of variation, n: number of samples.

	Lawson (n = 33)			**Craven Road (n = 58)**		
	Relative growth rate (%) (white rot)	**Relative growth rate (%) (brown rot)**	**Extractive content (%)**	**Relative growth rate (%) (white rot)**	**Relative growth rate (%) (brown rot)**	**Extractive content (%)**
Min	70.47	36.31	4.34	69.03	33.73	1.32
Max	94.83	95.59	14.78	94.66	80.36	7.85
CV (%)	7.5	26.6	24.1	7.2	16.6	37.4

5.3.1 Bioactivity of extracts

An F-test (ANOVA) of the growth rates for the controls between the batches showed significant differences for both fungi (Table 5.3). This confirmed the need to normalise the growth rate of fungi exposed to extracts by the growth rate of the controls (only agar) without extract in order to make the data comparable between the batches. The subsequent analysis was based on the relative growth rate,

which expressed how much slower (or faster) the fungus grew when exposed to the extract compared to the control conditions.

Table 5.3: F-test (ANOVA) of the growth rate of the controls in different batches (white rot (*T. versicolor*): 15 batches with 5 replicates for each control type; brown rot (*C. cerebella*): 10 batches with 5 replicates for each control type).

Fungi	**F value**		**P value**	
	only agar	***DMSO + agar***	***only agar***	***DMSO + agar***
White rot	108.71	212.89	<2.2 e-16	<2.2 e-16
Brown rot	53.04	116.13	<2.2 e-16	<2.2 e-16

There was no evidence of different growth rates in the two type of controls for both, white rot ($t = 0.24$, $p = 0.814$) and brown rot ($t = 0.15$, $p = 0.878$) (Table 5.4). This confirmed that the used quantities of DMSO had no effect on the test, and the changes in growth rate were caused by the heartwood extracts.

Table 5.4: T-test showing no difference in the growth rates of the white rot (*T. versicolor*) and brown rot (*C. cerebella*) between the controls, i.e. with and without DMSO (white rot: 15 batches with 5 replicates for each control type; brown rot: 10 batches with 5 replicates for each control type).

Fungi	**T-test**	**p value**
White rot	0.24	0.814
Brown rot	0.15	0.878

The relative growth rate of white rot ($t = 42.65$, $p < 2.2$ e-16) and brown rot ($t = 27.13$, $p < 2.2$ e-16) was significantly lower when exposed to ethanol extracts of *E. bosistoana* heartwood compared to the controls (Table 5.5). The brown rot was more sensitive to the *E. bosistoana* extracts than the white rot as the growth was more retarded by smaller amounts of extract (Figure 5.1).

Table 5.5: T-test showing lower relative growth rates of white rot (*T. versicolor*) and brown rot (*C. cerebella*) when exposed to ethanol extracts of *E. bosistoana* heartwood compared to the controls.

Fungi	**T-test**	**p value**	**Mean in group (sample estimate)**	
			Both controls	***Extracts***
White rot	42.65	p < 2.2 e-16	100.14 %	82.96%
Brown rot	27.13	p < 2.2 e-16	100.38%	60.47%

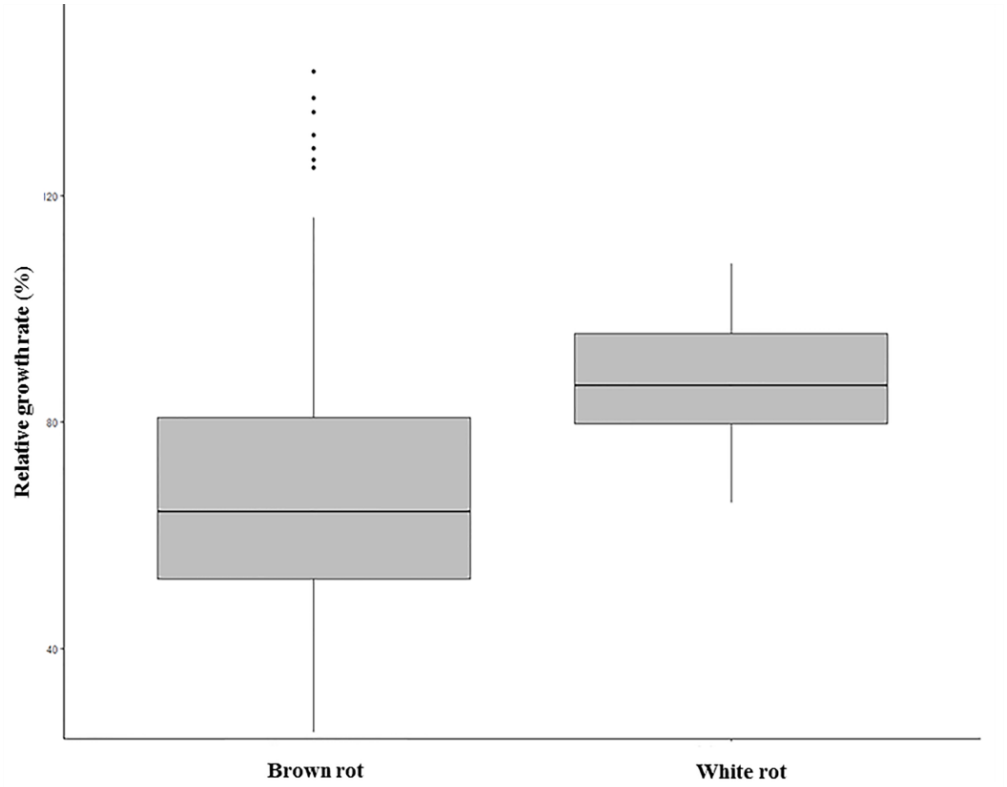

Figure 5.1: Box-and-whisker plot of relative growth rates of brown rot (*C. cerebella*) and white rot (*T. versicolor*) when exposed to ethanol extracts of *E. bosistoana* heartwood. The white rot was less affected.

No relationship between the growth rates of white rot and brown rot in extracts was observed for either of the two sites. A t-test showed that the slope was not different than 0, ($t = 0.09$, $p = 0.932$) (Table 5.6). This was consistent with the small coefficient of determination ($R^2 = 0.01$) (Figure 5.2). Similar observations were reported by Davies et al. (2014) for *Sequoia sempervirens* (redwood) and Ohtani et al. (2009) for *Cryptomeria japonica* (sugi) heartwood extracts. The observation suggested that the growth rates of the fungi were inhibited by different compounds of the extracts. Kirker et al. (2013) reported that individual components in extractives confer durability rather than bulk presence of extractive. For example in vitro tests suggested that thujaplicin, a natural fungicide in the heartwood extracts of *Thuja plicata* (western red cedar), was found to be toxic to brown rot but not so effective against white rot (Roff & Atkinson, 1954). Similarly naphthoquinone, a compound in the heartwood of *Tectona grandis* (teak) was found to have a stronger negative effect on the brown rots *Polyporus palustris* and *Gloeophyllum trabeum* than the white rots *T. hirsuta*, *T. versicolor* and *Pycnoporous sanguineus* (Thulasidas & Bhat, 2007). Therefore, as stated by Taylor et al. (2006) or Morris and Stirling (2012), it is not possible to focus on a single heartwood compound to understand the resistance of the wood against multiple biodegrading organisms.

In *Eucalypts*, extractives are predominately comprised of tannins (Conde et al., 1995; Hillis, 1972, 1991; Rudman, 1964). Ellagitannins in the heartwood extractives from *Quercus alba* (white oak) were

reported to be less inhibitory to *T. versicolor* (white rot) than *Poria manticola* (brown rot) (Hart & Hillis, 1972). It was suggested that this variation was caused by the difference in the protein-tannin binding capacity of different tannin protein mixtures, which is influenced by molecular size and chemical structure (Rudman, 1963).

Table 5.6: T-test and coefficient of determination between the growth rates of white rot (*T. versicolor*) and brown rot (*C. cerebella*) when exposed to ethanol extracts of *E. bosistoana* heartwood.

T-test	p value	Coefficient of determination (R^2)
0.09	0.932	0.01

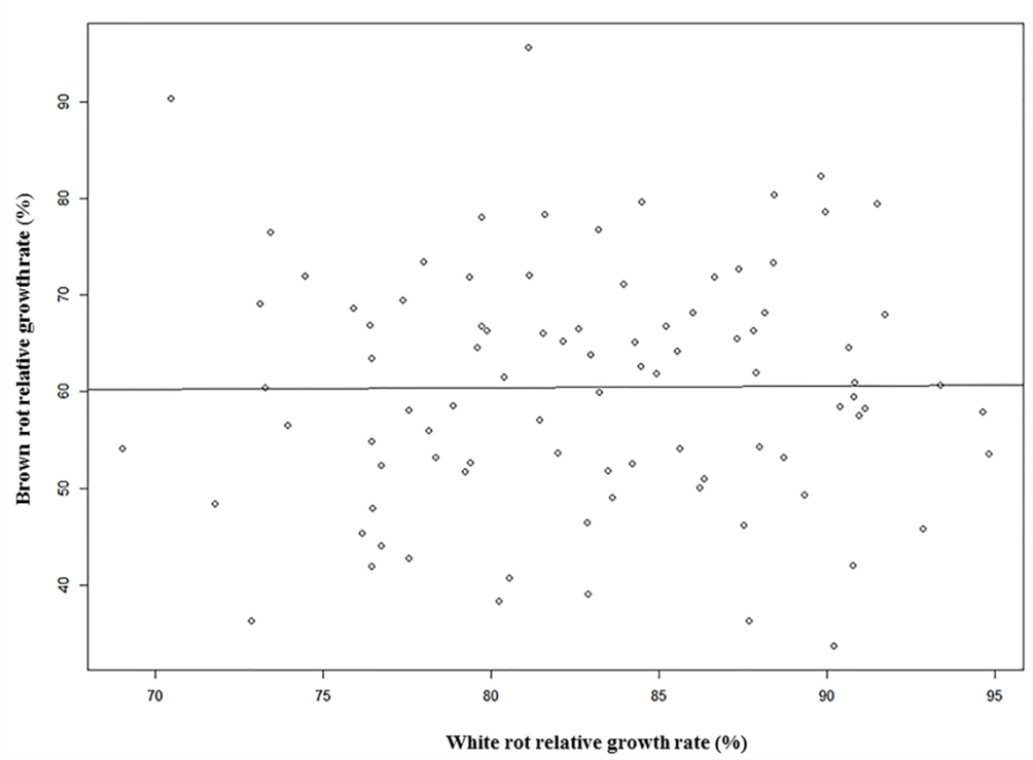

Figure 5.2: Relationship between the growth rates of white rot (*T. versicolor*) and brown rot (*C. cerebella*) when exposed to ethanol extracts of *E. bosistoana* heartwood. $R^2 = 0.01$.

No correlation was observed between the extractive content in the wood, which was variable, and the relative growth rates of the fungi exposed to a fixed quantity of extract (Table 5.7, Figure 5.3). However, when taking sites factors into account the extractive content had a negative influence on the bioactivity towards the white rot for the Lawson, but not the Craven Road site (Table 5.8, Figure 5.4a). This suggested that the trees with elevated extractive content at the Lawson site deposited more compounds into the heartwood, which were not bioactive against *T. versicolor*. For the brown rot *C. cerebella* no evidence of a relationship between growth rate and extractive content in the wood was

found in either of the two sites (Table 5.8, Figure 5.4b). This suggested that extractive content was not associated with a change in extractive composition increasing or decreasing the amount of fungicidal compounds for these fungi.

Table 5.7: Coefficient of determination between the extractive content in heartwood of 7-year-old *E. bosistoana* and relative growth rates of white rot (*T. versicolor*) and brown rot (*C. cerebella*).

white rot	Brown rot
0.010	0.004

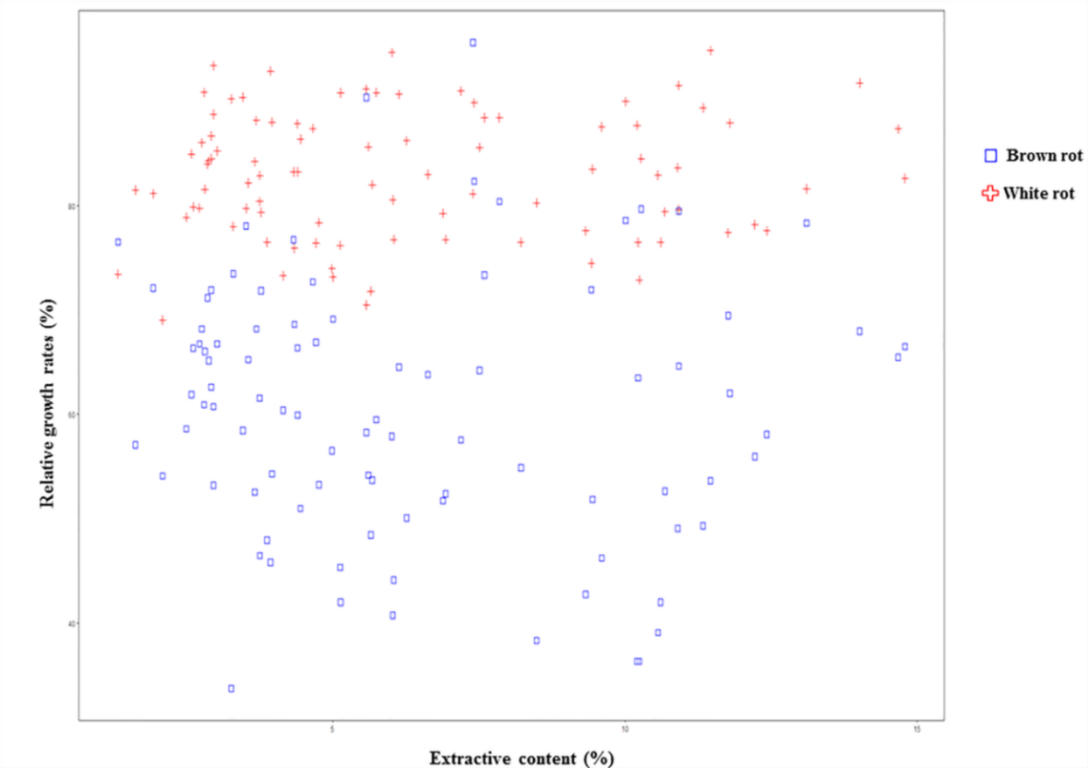

Figure 5.3: Relationships between the relative growth rates of white rot (*T. versicolor*) (R^2 = 0.010) and brown rot (*C. cerebella*) (R^2 = 0.004) with extractive content in *E. bosistoana*.

Table 5.8: Relationship between growth rates of white rot (*T. versicolor*) brown rot (*C. cerebella*) with extractive content in Lawson and Craven Road.

Sites	White rot			Brown rot		
	Slope	T-test	P value	Slope	T-test	P value
Lawson	1.01	2.45	0.020	-0.42	-0.35	0.723
Craven Road	0.77	1.54	0.128	-0.87	-1.04	0.303

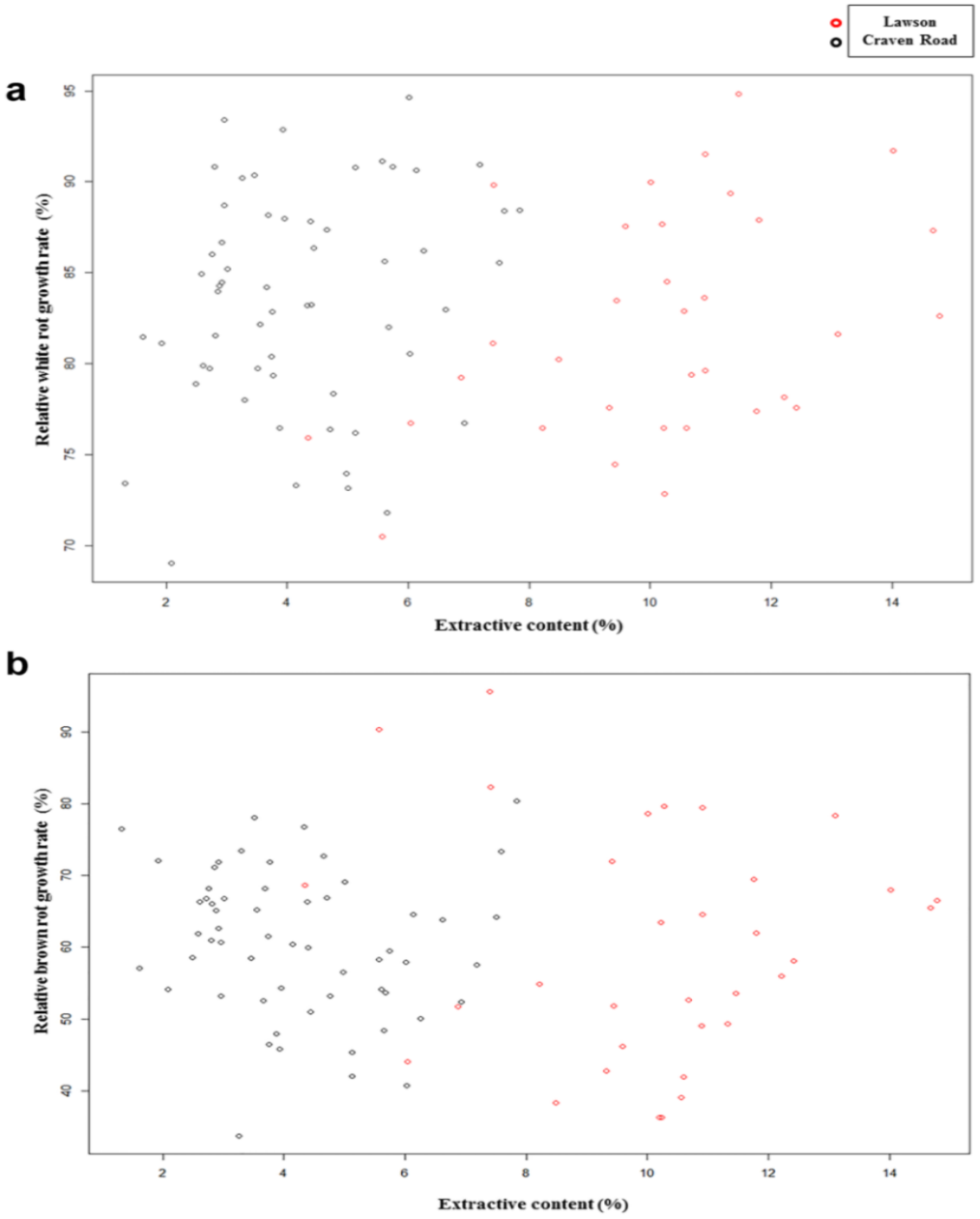

Figure 5.4: Relationship between the heartwood extractive content of 7-year-old *E. bosistoana* and the relative growth rate of a) white rot (*T. versicolor*) and b) brown rot (*C. cerebella*). Red: Lawson; black Craven Road.

5.3.2 Variation in bioactivity between trees

Variation in the relative growth rates of white rot (Figure 5.5a) and brown rot (Figure 5.5b) were observed between trees (see also Appendix 1). Tukey tests were conducted to compare the relative growth rates of white rot (Figure 5.6a) and brown rot (Figure 5.6b) exposed to the sample extracts. The results showed that there were significant differences between the trees and consequently suggested an influence of genetic factors on the composition of heartwood extracts of *E. bosistoana*.

Erdtman et al. (1951) reported a regional influence on the amount of pinosylvin in *Pinus sylvestris* in Sweden. Later high heritability of the heartwood extractives pinosylvin, resin acids, fatty acids and sterols were found for this species (Fries et al., 2000). Gansel & Squillace (1976) reported strong genetic control of the terpene composition in *P. ellotti* with negligible plantation effects. Genetic variability in the quantity of 10 out of 42 terpenes was reported for *P. nigra* and based on the terpene composition *P. nigra* populations were divided into two geographical groups (Bojovic et al., 2005). Genetic analysis of β-pinene concentration in individual trees demonstrated monogenic heredity (Zavarin et al., 1990a, 1990b). Tree-to-tree phenotypic variation and high heritabilities were also reported for the bioactive heartwood compounds plicatic acid, thujaplicatin methyl ether, β-thujaplicin, γ-thujaplicin, β-thujaplicinol, thujic acid, and methyl thujate, in the ethanol extract of *Thuja plicata* (Daniels & Russell, 2007).

Puech et al. (1999) summarised natural variation in the concentration of heartwood tannins in oaks. High variation within and between trees and populations was observed. However, the relative importance of different factors such as species, forest origin (or provenance) that influenced the variation in the concentration of ellagitannins remained unclear. A study suggested that the variation in the concentration of heartwood ellagitannins was a heritable property and not influenced by the growth rate of the trees. This agreed with the observation that ellagitannins and volatile compounds were highly variable among individuals in heartwood of *Q. pyrenaica* (Fernández et al., 2006). Guilley et al. (2004) reported positive correlations between the amount of the ellagitannins roburine, grandinin, vescalagin and castalagin and decay resistance in *Q. petraea*.

Extractive content is known to increase radially from pith to the sapwood-heartwood boundary, including *Eucalyptus* species (Wilkes, 1984). This radial pattern of within tree extractive content cannot be considered for variation in decay resistance between *E. bosistoana* trees in this experiment as all trees were of the same age and sampled at the same location (i.e. stem base).

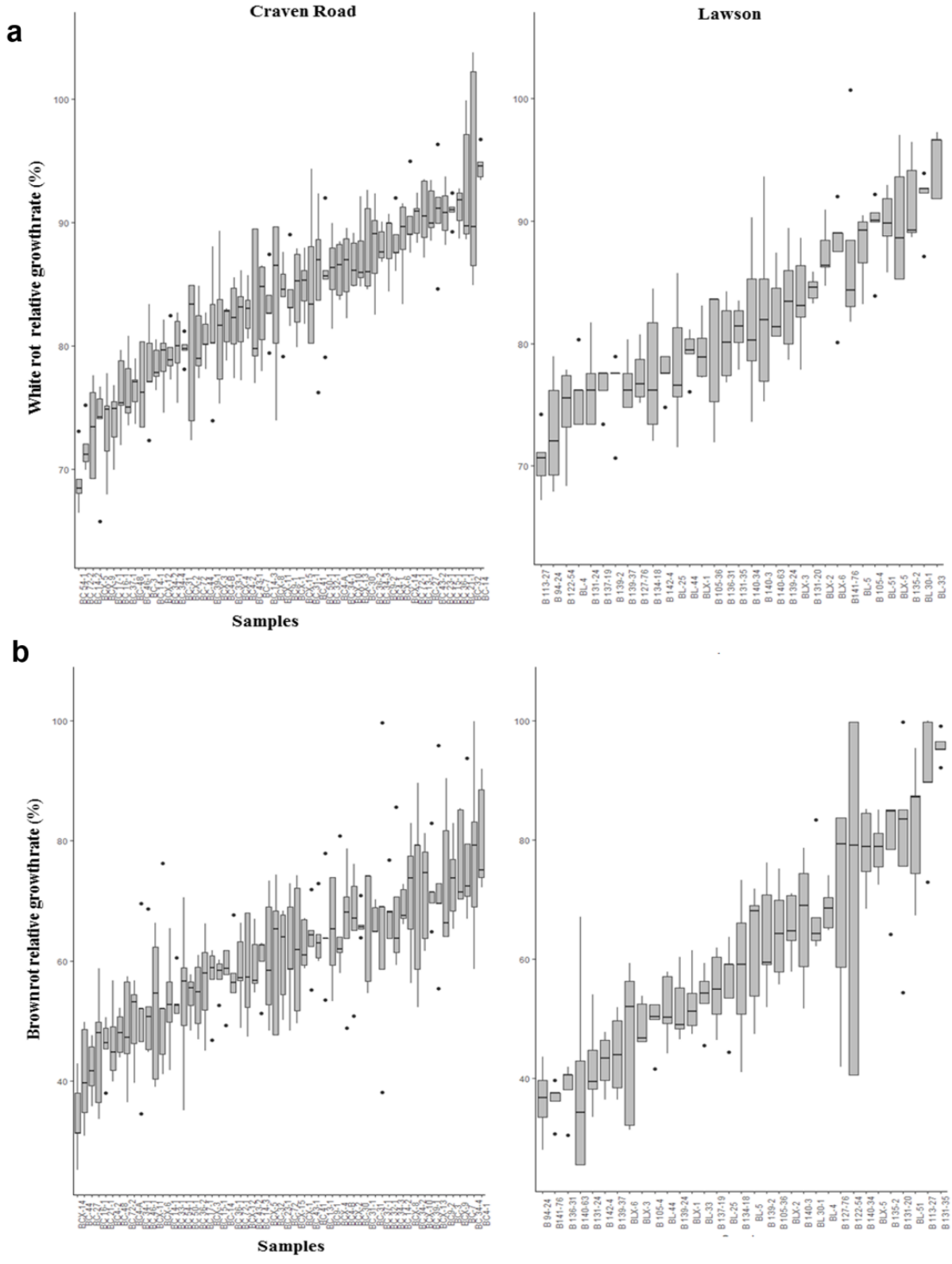

Figure 5.5: Box-and-whisker plots representing variation in relative growth rates of a) white rot (*T. versicolor*) and b) brown rot (*C. cerebella*) between the trees and sites.

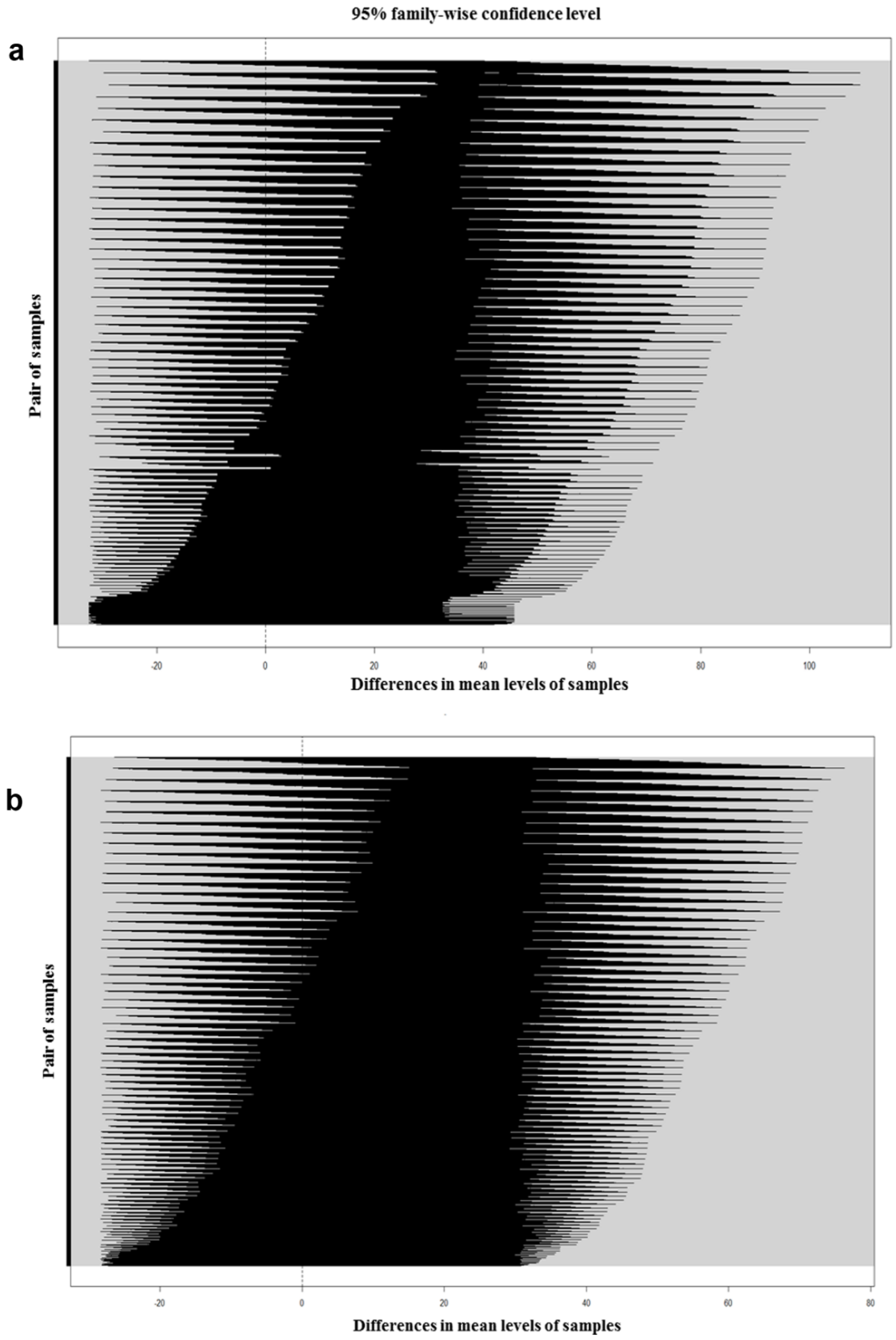

Figure 5.6: Tukey test shows all 4095 pairwise 95% confidence intervals in mean differences between 91 samples from a) white rot (*T. versicolor*) and b) brown rot (*C. cerebella*). There are 1190 significantly different pairs of samples for a) white rot (*T. versicolor*) and 536 for brown rot (*C. cerebella*).

No statistical significant difference in relative growth rates was observed between the two sites for the brown rot (Table 5.9). Although statistically significant (p = 0.028), the difference in the relative growth rates between both sites for the white rot was small, with 82.01% and 83.50% for Lawson and Craven Road, respectively (Table 5.9). Reports on differences in durability between sites were typically associated with a higher extractive content in wood, for which was normalised in this experiment. For example Harju et al. (2003) found that *P. sylvestris* from a site with more durable wood contained also higher amounts of heartwood extractives (total acetone-soluble extractives, resin acids, pinosylvin and the total phenolics quantified as tannin acid equivalents). This lines with observations on *T. grandis*, for which variability in natural durability, total extractive content as well as the amounts of individual compounds was reported between trees, plantations and geographical zones (Kokutse et al., 2006; Thulasidas & Bhat, 2007; Windeisen et al., 2003). Morais & Pereira (2012) reported an influence of site on the extractive content in *E. globulus*.

Table 5.9: Site effect on the relative growth rates of white rot (*T. versicolor*) and brown rot (*C. cerebella*) exposed to *E. bosistoana* heartwood extract.

Fungi	**T-test**	**p value**	**Mean in group (sample estimate)**	
			Lawson	Craven Road
White rot	2.21	0.028	82.01%	83.50%
Brown rot	0.27	0.791	60.19%	60.62%

5.3.3 Identification of compounds in ethanol extracts of *E. bosistoana* heartwood

The chemical composition in the ethanol extracts was analysed by GC. A typical chromatogram of silylated *E. bosistoana* heartwood extracts is shown in Figure 5.7 and in higher resolution in Appendix 2. Numerous compounds were well separated. The chromatogram was overlaid with that of a silylated *E. globoidea* heartwood ethanol extract. The heartwood extracts of the two species were similar and differed mainly in the relative amounts of the individual compounds. The *E. globoidea* heartwood extract was previously analysed by GC-MS, what allowed the identification of some compounds (Schroettke, 2018). By comparing the *E. bosistoana* and *E. globoidea* extracts six compounds were identified (Table 5.10). The unspecified ‘polyphenol’ peak at 25.1 min might be catechin, which was observed in heartwood of *E. camaldulensis* (Benouadah et al., 2018). The authors also reported the presence of monosaccharides including fructose, glucose and another unidentified hexose in the hydrophilic heartwood extract.

Similarities in the chemical composition of heartwood extracts of *Eucalyptus* species have been described (Hillis, 1991). While compounds such as stilbenes have been suggested as taxonomic marker for closely related *Eucalyptus* species, the heartwood compound, 3',4-tri-o-methylellagic acid-4'-glucoside was considered a marker for the close relationship between the *Eucalyptus* groups iron barks (e.g. *E. paniculata* and *E. sideroxylon*) and boxes (e.g. *E. bosistoana*) (Brooker, 2000; Hillis et al., 1974). The compound is related to hydrolysable tannin, which has been described characteristic for eucalypts with pale-light coloured heartwood such as *E. bosistoana* (Bootle, 2005; Hillis, 1991).

Limited information is available about the identification of *Eucalyptus* species based on the chemical composition in heartwood. Chemotaxonomy studies were mainly based on leaf extracts (Hillis, 1966, 1967), however, it was possible to draw conclusions on the polyphenols in *Eucalyptus* wood from the leaf extracts.

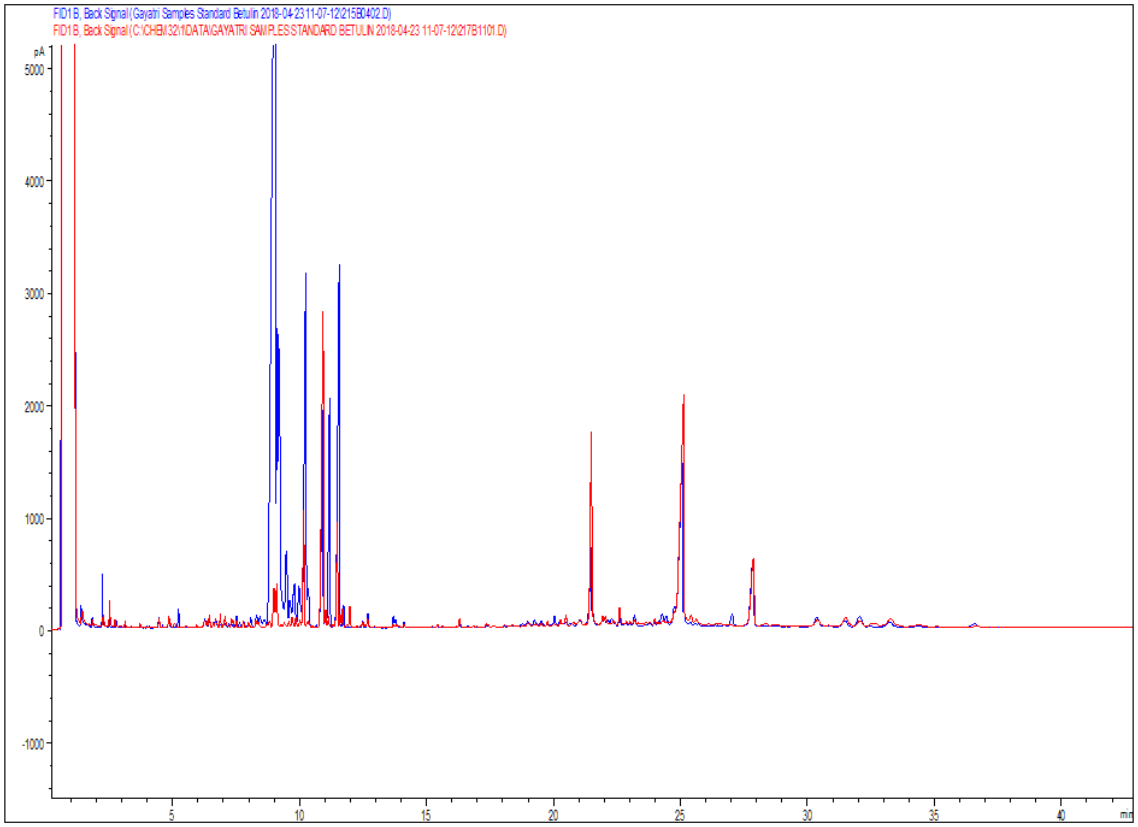

Figure 5.7: Gas chromatograms of silylated ethanol extracts from heartwood of *E. bosistoana* (blue) and *E. globoidea* (red) between 0 and 40 min retention time.

Table 5.10: Compounds identified by comparing the chromatograms of *E. bosistoana* heartwood extracts with *E. globoidea* (Schroettke, 2018).

Retention times (min)	Chemical compounds
10.9	benzoic acid
11.5	hexadecanoic acid
12.5	1,5-dihdroxy-12-methoxy-3,3-dimethyl-3,4-dihydro-1H-anthra[2,3-c]pyran-6,11-dione
14.1	Octadecanoic acid, TMS ester
25.1	polyphenol
25.2	beta-sitosterol

5.3.4 Chemical composition of extracts

5.3.4.1 Identification of bioactive compounds

Analysis was performed to correlate the normalised peak areas of the retention times with the relative growth rates of brown rot and white rot. None of the considered compounds showed a significant correlation to the bioactivity tests (Table 5.11).

Table 5.11**:** Coefficients of determination (R^2) between the relative amounts of *E. bosistoana* heartwood compounds and the relative growth rates of brown rot (*C. cerebella*) and white rot (*T. versicolor*).

Retention times (min)	R^2 Brown rot	R^2 White rot
4.5	0.005	0.012
6.2	0.013	0.001
6.4	0.008	0.007
6.7	0.006	0.001
8.4	0.014	0.001
9.0	0.003	0.009
9.1	0.002	0.001
9.2	0.003	0.002
9.7	0.004	0.001
9.9	0.003	0.006
10.2	0.011	0.062
10.9 **(Benzoic acid, 3,4,5-tris[TMS(oxy)]- ,TMS ester)**	0.016	0.004
11.1	0.001	0.017
11.2	0.003	0.004
11.5 **(Hexadecanoic acid, TMS ester)**	0.011	0.021
11.7	0.001	0.012
12.7	0.024	0.002
19.5	0.004	0.001
21.4	0.005	0.001
21.5	0.006	0.001
22.3	0.006	0.009

22.8	0.002	0.013
23.3	0.001	0.015
24.8	0.002	0.007
24.9	0.003	0.006
25.1 **(Polyphenol)**	0.012	0.041
25.2 **(Beta-sitosterol TMS ether)**	0.013	0.031
25.4	0.006	0.003
31.5	0.009	0.004
32.7	0.002	0.026
33.3	0.007	0.003
34.7	0.006	0.014

Multivariate analysis identified two groups of compounds (Figure 5.8). Compounds 10.2 and 11.5 (Hexadecanoic acid) were most important for predicting the bioactivity of the *E. bosistoana* heartwood extracts towards white rot (*T. versicolor*) (Figure 5.8a) and brown rot (*C. cerebella*) (Figure 5.8b). The same compounds were affecting the growth of the brown rot (*C. cerebella*), but the other 30 components differed in the first principal component for the brown rot. The other 30 compounds were grouped together and differed in the second principle component for white rot and in the first principal component for brown rot.

However, for both fungi, only a small part of the variation in bioactivity was explained by two principal components (Appendix 3, 4). The total variance in relative growth rate explained by the first two principle components was 13.1% (9.2% and 3.9%, respectively) for white rot (*T. versicolor*) and 15.8% (8.9% and 6.9%, respectively) for brown rot (*C. cerebella*). This suggested that other compounds, not captured in the GC analysis contributed to the bioactivity against the two tested fungi. GC relies on compounds entering the gas phase, which is difficult for larger and more hydrophilic molecules. Derivatisation, like acetylation or silylation, can aid the transition of hydrophilic compounds into the gas phase; however, the size of a molecule makes this more difficult. Therefore, the GC analysis of the hydrophilic ethanol extracts form *E. bosistoana* heartwood was likely not to capture larger compounds. HPLC was suggested as an alternative method to quantify larger molecular mass compounds in wood extracts (Smeds et al., 2018).

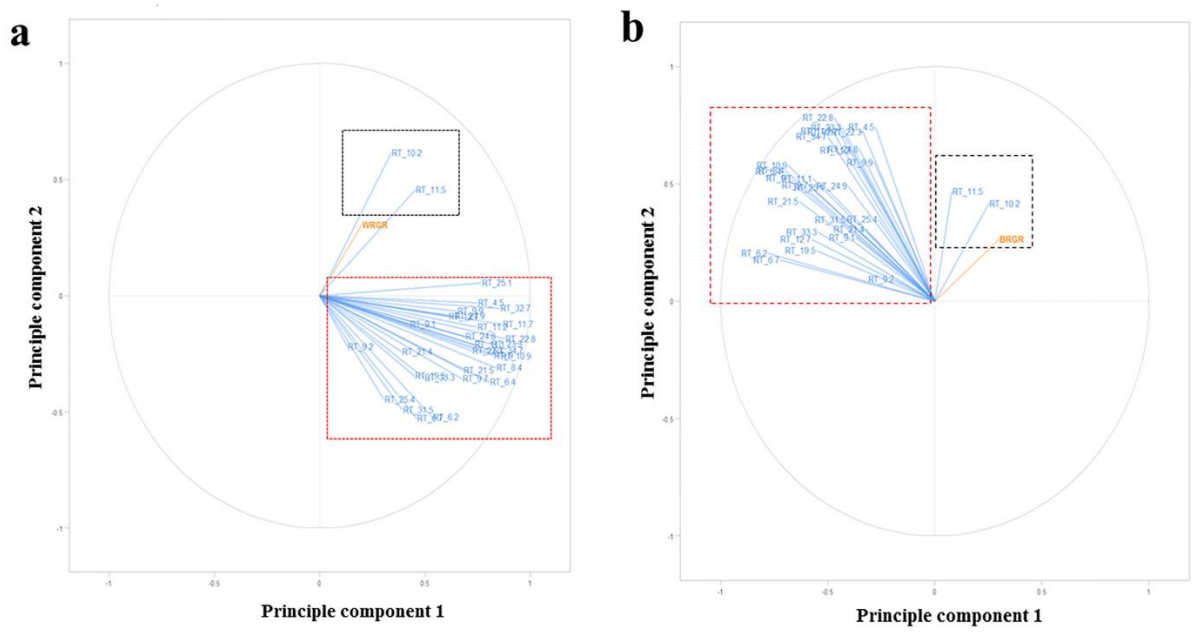

Figure 5.8: Influence of heartwood compounds in *E. bosistoana* heartwood on the growth of the a) white rot (*T. versicolor*) and b) brown rot (*C. cerebella*) analysed by partial least squares regression analysis (PLSR). Compounds that are near each other are highly correlated in the first two principal components. Compounds at 10.2 and 11.5 (Hexadecanoic acid) min in the black box aligned with the relative growth rate (orange line) and were considered different to the other 30 compounds grouped together in red box.

5.3.4.2 Site influence on the chemical composition

Figure 5.9 shows the variation in relative proportions of 32 *E. bosistoana* compounds between the two sites. Differences in the chemical composition between the sites were analysed with a T-test for the peak areas after normalisation by internal standard, for each of the quantified compounds. P values suggested significant variation for eight compounds between the sites (Table 5.12). One of the compounds could be identified as "polyphenol" and is potentially catechin.

The identified site influences are in agreement with the statement by Hillis (1987) that extractive composition is dependent on species, and varies within a species with the morphological part of the tree (roots, knots, bark, stem), age, season and location. Variation in heartwood extractives between species and locations (sites) are relevant to this study.

Investigation of the influence of geographical origin and species on extractives in oaks (*Q. alba*, *Q. robur* and *Q. petraea*) suggested variations in the content of whiskey lactone and ellagitannins differentiated species, whereas the content of eugenol, 2-phenylethanol, vanillin, and syringaldehyde were the most important features for distinguishing the geographical origin within species (Prida & Puech, 2006). Similar observations were reported by Guchu et al. (2006) who demonstrated variation in the content of volatile compounds (cis- and trans- methyl-γ-octalactones, furfural, 5-methylfurfural,

guaiacol, eugenol and vanillin) between *Q. robur* and *Q. petraea*. The content of volatile compounds in *Q. petraea* was higher than in *Q. robur* and variation between geographical provenances was less than between species. Kilulya et al. (2014), evaluated the effect of site, species and tree sizes on the amount of lipophilic heartwood extractives from *E. dunnii* and *E. grandis*. GC–MS analysis showed that saturated fatty acids dominated in lipophilic extracts of *E. dunnii* from one site, whereas unsaturated fatty acids dominated in samples from another two sites. Correlation of the amount of lipophilic extractives with tree species/clones and soil type was revealed by principal component analysis (PCA), with trees grown on sites with high clay and organic matter content containing higher amounts of lipophilic extractives. However, in all the sampled sites *E. dunnii* was found to contain a higher amount of lipophilic extractives than *E. grandis*.

Table 5.12: *E. bosistoana* heartwood compounds with a significant difference between the Lawson and Craven Road sites.

Retention times (min)	**p-values (Bonferroni corrected)**
9.9	5.70e-13
11.2	4.20e-07
11.7	4.28e-05
22.3	0.0004
22.8	0.0004
23.3	0.0011
25.1 **(polyphenol)**	6.15e-07
33.3	0.0002

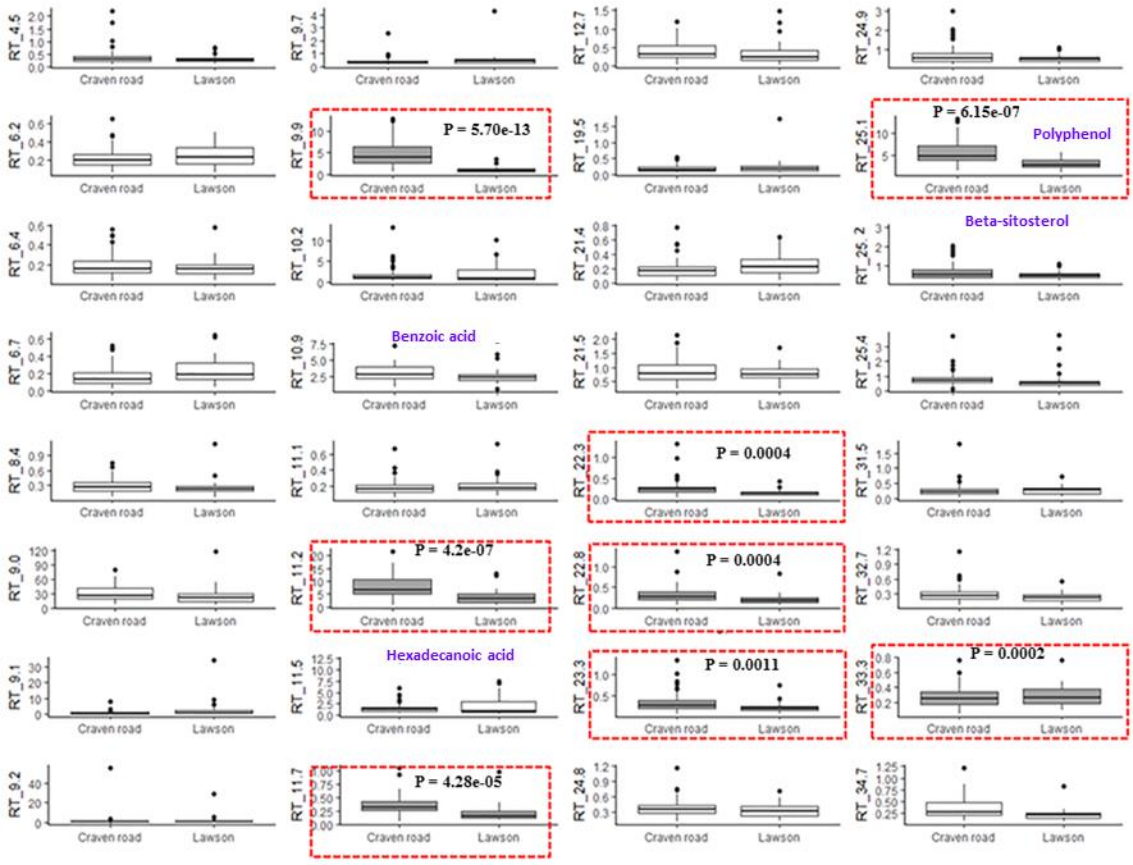

Figure 5.9: Box-and-whisker plots representing amount of heartwood compounds in *E. bosistoana* between Lawson and Craven Road. Eight compounds showing significant variation between the sites are highlighted by a box. RT: retention time in min; X-axis units: Peak area in relation to internal standard.

5.4 Conclusion

Ethanol extracts from *E. bosistoana* heartwood were less effective on the white rot (*T. versicolor*) with a relative growth rate of 82.96% than the brown rot (*C. cerebella*) (60.47%)**.** No relationship was found between the growth rates of white rot and brown rot in extracts (t = 0.09, p = 0.932) indicating that different compounds in the extracts inhibited the growth of the two fungi.

No correlation was observed between the extractive content in the wood and the bioactivity of the extracts against the brown rot (R^2 = 0.004). Extractive content in the wood had a negative influence on the bioactivity towards the white rot for the Lawson, but not the Craven Road site. This suggested that the trees with elevated extractive content at the Lawson site deposited more compounds into the heartwood, which were not bioactive against white rot.

Significant variability was found in the bioactivity of *E. bosistoana* heartwood extracts against white rot (stdev = 6.1 %, min = 69.03%, max = 94.83%) and brown rot (stdev = 12.5%, min =33.73%, max

= 95.59%) between the trees. The difference in the relative growth rates of white rot between the sites was small and only significant for white rot. Therefore, the site influence on the bioactivity of the heartwood extracts was small.

Thirty two compounds were quantified by GC in *E. bosistoana* ethanol extracts of which six were identified. Variation was present in composition of the extracts between trees and sites. Multivariate (PLSR) analysis identified compounds eluting at 10.2 and 11.5 min (Hexadecanoic acid) to be most related to the bioactivity of the *E. bosistoana* heartwood extracts against the tested white rot and brown rot. Significant variation in eight compounds (9.9, 11.2, 11.7, 22.3, 22.8, 23.3, 25.1, 33.3), out of 32 compounds was found between the sites. However, these did not have a large effect on the bioactivity of the heartwood extracts towards the two tested fungi.

5.5 References

Benouadah, N., Pranovich, A., Aliouche, D., Hemming, J., Smeds, A., & Willför, S. (2018). Analysis of extractives from *Pinus halepensis* and *Eucalyptus camaldulensis* as predominant trees in Algeria. *Holzforschung, 72*, 97-104.

Bojovic, S., Jurc, M., Drazic, D., Pavlovic, P., Mitrovic, M., Djurdjevic, L., Dodd, R. S., Afzal-Rafii, Z., & Barbero, M. (2005). Origin identification of *Pinus nigra* populations in southwestern Europe using terpene composition variations. *Trees, 19*, 531-538.

Brooker, M. I. H. (2000). A new classification of the genus *Eucalyptus* L'Her.(Myrtaceae). *Australian Systematic Botany, 13*, 79-148.

Bootle, K. R. (2005). *Wood in Australia Types, Properties, and Uses (2nd ed.):* . Australia: McGraw-Hill.

Conde, E., Cadahía, E., García, V. M., & de Simón, M. F. (1995). Polyphenolic composition of wood extracts from *Eucalyptus camaldulensis*, *E. globulus* and *E. rudis*: Walter de Gruyter, Berlin/New York.

Daniels, C. R., & Russell, J. H. (2007). Analysis of western red cedar (*Thuja plicata* Donn) heartwood components by HPLC as a possible screening tool for trees with enhanced natural durability *Journal of Chromatographic Science, 45*, 281–285.

Davies, N. T., Wu, H. F., & Altaner, C. M. (2014). The chemistry and bioactivity of various heartwood extracts from redwood (*Sequoia sempervirens*) against two species of fungi. *New Zealand Journal of Forestry Science, 44*, 17.

Erdtman, H., Frank, A., & Lindstedt, G. (1951). Constituents of pine heartwood. XXVII. The content of pinosylvin phenols in Swedish pines. *Svensk papperstidning, 8*, 275-279.

Fernández, B.S., Sanz, M., Cadahia, E., Poveda, P., & Broto, M . (2006). Chemical characterization of oak heartwood from spanish forests of *Quercus pyrenaica* (Wild.). Ellagitannins, low molecular weight phenolic, and volatile compounds. *Journal of Agricultural and Food Chemistry, 54*, 8314-8321.

Fernandez, M., Watson, P., & Breuil, C. (2001). Gas chromatography–mass spectrometry method for the simultaneous determination of wood extractive compounds in quaking aspen. *Journal of Chromatography A, 922*, 225-233.

Fries, A., Ericsson, T., & Gref, R. (2000). High heritability of wood extractives in *Pinus sylvestris* progeny tests. *Canadian Journal of Forestry Research, 30*, 1707–1713.

Gansel, C. R., & Squillace, A. (1976). Geographic variation of monoterpenes in cortical oleoresin of slash pine. *Silvae Genetica*, 150-154.

Guchu, E., Conseulo, M., Marato, I. J. D., Lamireo, P. V., & Coello, M. S. P. (2006). Influence of the species and geographical location on volatile composition of spanish oak wood (*Quercus petraea* Liebl. and *Quercus robur* L.). *Journal of Agricultural and Food Chemistry, 54*, 3062−3066.

Guilley, E., Charpentier, P., Ayadi, G. N., Snakkers, G., & Charrier, N. (2004). Decay resistance against *Coriolus versicolo*r in sessile oak (*Quercus petraea* Liebl.): analysis of the between-tree variability and correlations with extractives, tree growth and other basic wood properties. *Wood Science and Technology, 38*, 539–554.

Gutiérrez, A., Rıo, J. C., González, F. J., & Martın, F. (1998). Analysis of lipophilic extractives from wood and pitch deposits by solid-phase extraction and gas chromatography. *Journal of Chromatography A, 823*, 449-455.

Harju, A. M., Venäläinen, M., Anttonen, S., Viitanen, H., Kainulainen, P., Saranpää, P., & Vapaavuori, E. (2003). Chemical factors affecting the brown-rot decay resistance of Scots pine heartwood. *Trees, 17*, 263–268.

Hart, J. H., & Hillis, W. (1972). Inhibition of wood-rotting fungi by ellagitannins in the heartwood of *Quercus alba*. *Phytopathology, 62*, 620-626.

Hathway, D., & Seakins, J. (1959). Hydroxystilbenes of *Eucalyptus wandoo*. *Biochemical Journal, 72*, 369.

Hathway, D. (1962). The use of hydroxystilbene compounds as taxonomic tracers in the genus *Eucalyptus*. *Biochemical Journal, 83*, 80.

Hillis, W., & KoichiroIsoi. (1965). Variation in the chemical composition of *Eucalyptus sideroxylon*. *Phytochemistry, 4*, 541-550.

Hillis, W. (1966). Variation in polyphenol composition within species of *Eucalyptus* L'Herit. *Phytochemistry, 5*, 541-556.

Hillis, W. (1967). Polyphenols in the leaves of *Eucalyptus*: A chemotaxonomic survey—I.: Introduction and a study of the series globulares. *Phytochemistry, 5*, 1075-1090.

Hillis, W. (1971). Distribution, properties and formation of some wood extractives. *Wood Science and Technology, 5*, 272-289.

Hillis, W. (1972). Formation and properties of some wood extractives. *Phytochemistry, 11*, 1207-1218.

Hillis, W. (1987). *Heartwood and tree exudates*. New York: Springer.

Hillis, W. (1991). *Eucalypts*: Chemistry, uses. *Appita Journal, 44*, 239-244.

Hillis, W., & Carle, A. (1962). The origin of the wood and bark polyphenols of *Eucalyptus* species. *Biochemical Journal, 82*, 435.

Hillis, W., Hart, J. H., & Yazaki, Y. (1974). Polyphenols of *Eucalyptus sideroxylo*n wood. *Phytochemistry, 13*, 1591-1595.

Hillis, W., & Yazaki, Y. (1973). Wood polyphenols of *Eucalyptus polyanthemos*. *Phytochemistry, 12*, 2969-2977.

Hillls W., & Carle. (1959). The Formation of phenolic substances in *Eucalyptus gigantea* and *Eucalyptus sieberiana*. *Biochemical Journal, 74*, 607-615.

Kilulya, K. F., Msagati, T. A., Mamba, B. B., Ngila, J. C., & Bush, T. (2014). Effect of site, species and tree size on the quantitative variation of lipophilic extractives in *Eucalyptus* woods used for pulping in South Africa. *Industrial Crops and Products, 56*, 166-174.

Kirker, G., Blodgett, A., Arango, R., Lebow, P., & Clausen, C. (2013). The role of extractives in naturally durable wood species. *International Biodeterioration & Biodegradation, 82*, 53-58.

Kokutse, A. D., Stokes, A., Baillères, H., Kokou, K., & Baudasse, C. (2006). Decay resistance of Togolese teak (*Tectona grandis* Lf) heartwood and relationship with colour. *Trees, 20*, 219-223.

Lee, C. K., & Chang, M. H. (2000). The chemical constituents from the heartwood of *Eucalyptus citriodora*. *Journal of Chinese Chemical Society, 45*, 555-560.

Morais, M. C., & Pereira, H. (2012). Variation of extractives content in heartwood and sapwood of *Eucalyptus globulus* trees. *Wood Science and Technology, 46*, 709-719.

Morris, P. I., & Stirling, R. (2012). Western red cedar extractives associated with durability in ground contact. *Wood Science and Technology, 46*, 991-1002.

Mosedale, J., Charrier, B., Crouch, N., Janin, G., & Savill, P. (1996a). Variation in the composition and content of ellagitannins in the heartwood of European oaks *(Quercus robur and Q petraea).* A comparison of two French forests and variation with heartwood age. Paper presented at the Annales des sciences forestières.

Mosedale, J., Charrier, B., & Janin, G. (1996b). Genetic control of wood colour, density and heartwood ellagitannin concentration in European oak (*Quercus petraea* and *Q. robur*). *Forestry: An International Journal of Forest Research, 69*, 111-124.

Ohtani, Y., Noguchi, T., & Ichiura, H. (2009). Relationship between sugi [*Cryptomeria japonica*] butt-rot disease and norlignans in the heartwood. *Journal of the Japan Wood Research Society 55*, 92–100.

Prida, A., & Puech, J. L. (2006). Influence of geographical origin and botanical species on the content of extractives in american, french, and east european oak woods. *Journal of Agricultural and Food Chemistry, 54*, 8115−8126.

Puech, Feuillat, F., & Mosedale, J. R. (1999). The tannins of oak heartwood: structure, properties, and their influence on wine flavor. *American Journal of Enology and Viticulture, 50*, 469-478.

Roff, J., & Atkinson, J. (1954). Toxicity tests of a water-soluble phenolic fraction (thujaplicin-free) of western red cedar. *Canadian Journal of Botany, 32*, 308-309.

Rudman, P. (1963). The causes of natural durability in timber-Part XI. Some tests on the fungi toxicity of wood extractives and related compounds. *Holzforschung, 17*, 54-57.

Rudman, P. (1964). Durability in the genus *Eucalyptus*. *Australian Forestry, 28*, 242-257.

Sanchez, G. (2012). Partial Least Squares (PLS) data analysis methods (version-0.1.17).

Schroettke, N. (2018). Natural variability in the extract composition of *Eucalyptus globoidea.* Master's thesis for obtaining the academic degree, Master of Science in Forestry. Center for Forestry, Institute of Chemical Wood Technology. University of Hamburg, Germany.

Seikel, M. K., & Hillis, W. (1970). Hydrolysable tannins of *Eucalyptus delegatensis* wood. *Phytochemistry, 9*, 1115-1128.

Sitholé, B., Sullivan, J., & Allen, L. (1992). Identification and quantitation of acetone extractives of wood and bark by ion exchange and capillary GC with a spreadsheet program. *Holzforschung, 46*, 409-416.

Smeds, A. I., Eklund, P. C., & Willför, S. M. (2018). Characterization of high-molar-mass fractions in a Scots pine (*Pinus sylvestris* L.) knotwood ethanol extract. *Holzforschung, 72*, 201-213.

Taylor, A. M., Gartner, B. L., & Morrell, J. J. (2002). Heartwood formation and natural durability- A review. *Wood and Fiber Science, 34*, 587-611.

Taylor, A. M., Gartner, B. L., Morrell, J. J., & Tsunoda, K. (2006). Effects of heartwood extractive fractions of *Thuja plicata* and *Chamaecyparis nootkatensis* on wood degradation by termites or fungi. *Journal of Wood Science, 52*, 147-153.

Team, R. C. (2013). *R: A language and environment for statistical computing.* Vienna, Austria.

Thulasidas, P., & Bhat, K. (2007). Chemical extractive compounds determining the brown-rot decay resistance of teak wood. *Holz als Roh-und Werkstoff, 65*, 121-124.

Van Lierde, J. (2013). *What causes natural durability in Eucalyptus bosistoana timber? a dissertation submitted in partial fulfilment of the requirements for the degree of Bachelor of Forestry Science with Honours.* Bachelor of Forestry Science (Hon), University of Canterbury, Christchurch, New Zealand.

Vinciguerra, V., Luna, M., Bistoni, A., & Zollo, F. (2003). Variation in the composition of the heartwood flavonoids of *Prunus avium* by on-column capillary gas chromatography. *Phytochemical Analysis, 14*, 371-377.

Wickham, H. (2009). ggplot2: Elegant Graphics for Data Analysis Springer-Verlag New York.

Wilkes, J. (1984). The influence of rate of growth on the density and heartwood extractive content of *Eucalypt* species. *Wood Science and Technology, 18*, 113-120.

Windeisen, E., Klassen, A., & Wegener, G. (2003). On the chemical characterisation of plantation teakwood from Panama. *Holz als Roh- und Werkstoff, 61*, 416–418.

Yazaki, & Hillis. (1976). Polyphenols of *Eucalyptus globulus* , *Eucalyptus regnans* and *Eucalyptus deglupta*. *Phytochemistry, 15*, 1180-1182.

Yu, Q., Yang, D. Q., Zhang, S., Beaulieu, J., & Duchesne, I. (2003). Genetic variation in decay resistance and its correlation to wood density and growth in white spruce. *Canadian Journal of Forest Research, 33*, 2177-2183.

Zavarin, E., Snajberk, K., & Cool, L. (1990a). Chemical differentiation in relation to the morphology of the single-needle pinyons. *Biochemical Systematics and Ecology, 18*, 125-137.

Zavarin, E., Snajberk, K., & Cool, L. (1990b). Monoterpene variability of *Pinus monticola* wood. *Biochemical Systematics and Ecology, 18*, 117-124.

5.6 Appendixes

Appendix 1: Extractive content (ethanol) of the *E. bosistoana* wood samples and the mean relative growth rates for white rot (*T. versicolor*) and brown rot (*C. cerebella*) when exposed to the extract as well as their standard deviation (SDEV) (n=5).

Samples	Sites	Extractive content (%)	Mean relative white rot growth rate (%)	SDEV relative white rot growth rate (%)	Mean relative brown rot growth rate (%)	SDEV relative brown rot growth rate (%)
B 105-36	Lawson	10.918	79.599	5.621	64.591	8.096
B 105-4	Lawson	11.334	89.346	3.165	49.292	4.427
B 113-27	Lawson	5.574	70.467	2.596	90.371	11.018
B 122-54	Lawson	9.424	74.466	3.883	71.939	29.843
B 127-76	Lawson	11.762	77.375	2.308	69.464	18.535
B 131-20	Lawson	10.274	84.496	1.026	79.642	16.610
B 131-24	Lawson	10.607	76.454	3.449	41.973	7.833
B 131-35	Lawson	7.396	81.113	2.226	95.598	2.496
B 134-18	Lawson	12.424	77.562	5.364	58.053	12.632
B 135-2	Lawson	10.918	91.506	3.532	79.454	9.025
B 136-31	Lawson	8.485	80.244	3.225	38.331	4.603
B 137-19	Lawson	8.216	76.454	1.806	54.881	6.494
B 139-2	Lawson	10.22	76.454	3.307	63.482	9.775
B 139-24	Lawson	9.444	83.485	4.384	51.852	5.734
B 139-37	Lawson	6.043	76.731	2.318	44.101	6.758
B 140-3	Lawson	14.789	82.609	7.346	66.474	11.156
B 140-34	Lawson	13.102	81.605	6.411	78.314	7.017
B 140-63	Lawson	10.562	82.898	2.971	39.064	17.225
B 142-4	Lawson	9.325	77.562	1.696	42.747	4.699
B 94-24	Lawson	10.244	72.853	4.656	36.312	5.940
B141-76	Lawson	10.204	87.681	7.711	36.316	3.378
BC 13-1	Craven road	6.131	90.651	2.799	64.519	8.733
BC 14	Craven road	6.009	94.660	1.317	57.873	5.133
BC 14-1	Craven road	4.762	78.358	1.689	53.240	8.690
BC 14-2	Craven road	5.002	73.130	3.843	69.117	3.059
BC 14-3	Craven road	4.399	83.234	2.897	59.919	5.019
BC 15-1	Craven road	17.190	90.956	1.128	57.550	3.010
BC 16-1	Craven road	5.125	76.177	3.115	45.324	10.279
BC 17-1	Craven road	4.984	73.938	2.718	56.495	8.288
BC 21-1	Craven road	3.932	92.873	5.225	45.813	4.828
BC 23-1	Craven road	2.797	90.830	2.206	60.924	8.198
BC 27	Craven road	5.133	90.792	2.087	41.992	4.781
BC 3	Craven road	3.293	77.987	4.100	73.468	6.949
BC 30	Craven road	4.392	87.823	3.774	66.350	2.652
BC 31	Craven road	2.719	79.735	1.107	66.741	2.598
BC 31-1	Craven road	3.018	85.220	6.028	66.741	10.211
BC 32	Craven road	2.956	93.396	8.936	60.712	12.290
BC 32-1	Craven road	2.758	86.011	3.279	68.161	5.338
BC 33-1	Craven road	5.675	81.990	3.332	53.699	3.916
BC 34-1	Craven road	4.444	86.341	3.037	50.955	12.643
BC 34-2	Craven road	3.773	79.354	1.965	71.848	15.690
BC 34-3	Craven road	3.69	88.153	1.410	68.161	10.692
BC 34-4	Craven road	3.514	79.715	2.935	78.038	15.531

Samples	Sites	Extractive content (%)	Relative white rot growth rate (%)	SDEV	Relative brown rot growth rate (%)	SDEV
BC 36-1	Craven road	5.570	91.153	1.706	58.261	5.405
BC 36-2	Craven road	3.959	87.993	3.848	54.268	5.971
BC 37-1	Craven road	4.71	76.395	2.989	66.896	22.281
BC 39-1	Craven road	1.926	81.132	5.167	72.073	6.635
BC 41	Craven road	7.506	85.554	6.091	64.187	5.232
BC 43-1	Craven road	6.625	82.976	6.018	63.787	6.001
BC 43-2	Craven road	5.743	90.818	4.220	59.491	5.190
BC 44	Craven road	6.026	80.536	1.779	40.741	8.356
BC 46-1	Craven road	6.93	76.731	3.476	52.366	9.733
BC 48	Craven road	3.873	76.464	2.003	47.941	3.603
BC 50-1	Craven road	5.606	85.625	4.575	54.146	3.733
BC 54-1	Craven road	2.084	69.030	2.459	54.102	13.069
BC 7	Craven road	4.327	83.214	3.839	76.725	10.547
BC 72	Craven road	3.746	80.393	3.127	61.531	9.676
BC 72-1	Craven road	3.457	90.384	1.619	58.450	6.756
BC 72-2	Craven road	5.647	71.785	2.066	48.420	8.777
BC4-1	Craven road	7.85	88.427	2.250	80.363	9.151
BC4-2	Craven road	3.75	82.865	1.999	46.452	6.695
BC4-A	Craven road	6.259	86.212	2.247	50.047	6.992
BC4-B	Craven road	2.809	81.548	1.916	66.013	11.056
BC9-1	Craven road	2.877	84.273	2.854	65.150	9.046
BC9-2	Craven road	7.593	88.407	2.648	73.333	12.059
BCX-1	Craven road	2.917	84.477	3.486	62.602	4.073
BCX-10	Craven road	2.917	86.658	1.995	71.895	8.761
BCX-11	Craven road	3.662	84.203	3.168	52.521	12.458
BCX-12	Craven road	2.492	78.873	2.846	58.588	9.270
BCX-13	Craven road	4.656	87.374	2.998	72.671	14.651
BCX-14	Craven road	3.261	90.208	2.854	33.733	6.854
BCX-15	Craven road	2.58	84.940	2.355	61.894	11.297
BCX-2	Craven road	2.61	79.874	6.230	66.322	9.713
BCX-3	Craven road	1.622	81.460	5.529	57.072	6.010
BCX-4	Craven road	3.553	82.151	3.464	65.235	8.992
BCX-5	Craven road	4.149	73.284	4.357	60.385	10.599
BCX-6	Craven road	2.957	88.723	3.347	53.177	13.737
BCX-8	Craven road	2.854	83.962	6.817	71.151	10.504
BCX-9	Craven road	1.323	73.422	3.812	76.510	8.002
BL 25	Lawson	12.219	78.158	5.481	55.929	7.425
BL 30-1	Lawson	14.014	91.724	2.657	67.968	8.799
BL 33	Lawson	11.46	94.834	2.740	53.618	5.169
BL 4	Lawson	4.34	75.900	2.838	68.601	3.833
BL 44	Lawson	6.881	79.242	1.940	51.703	5.768
BL 5	Lawson	11.794	87.885	3.006	62.001	10.704
BL 51	Lawson	7.418	89.826	2.780	82.320	11.278
BLX-1	Lawson	10.681	79.384	2.466	52.638	5.557
BLX-2	Lawson	14.673	87.327	2.419	65.460	5.470
BLX-3	Lawson	10.901	83.616	4.124	49.065	3.771
BLX-5	Lawson	10.010	89.967	5.208	78.571	4.871
BLX-6	Lawson	9.599	87.537	4.451	46.197	13.475

Appendix 2: Gas chromatograms of silylated ethanol extracts from heartwood of *E. bosistoana* (blue) and *E. globoidea* (red) with retention times.

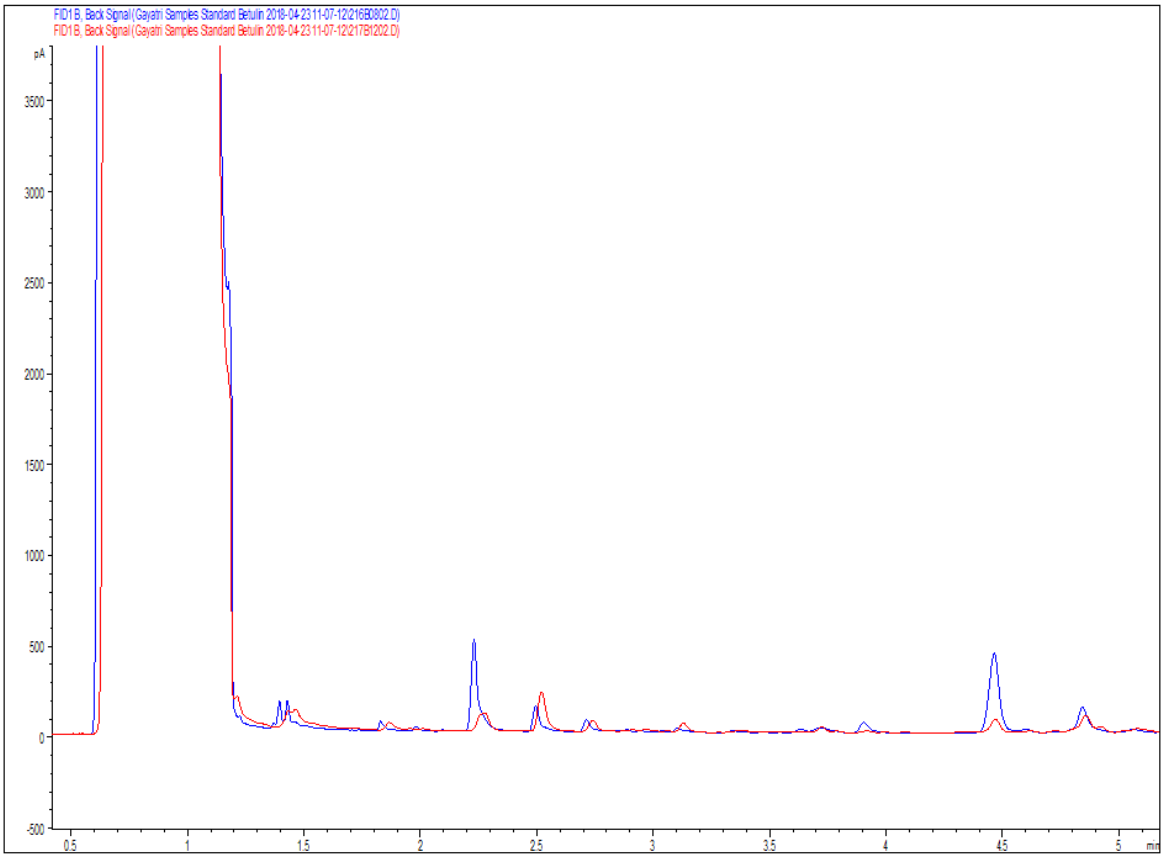

Figure 1: Gas chromatograms of silylated ethanol extracts from heartwood of *E. bosistoana* (blue) and *E. globoidea* (red) between 0.5 and 4.5 min retention time.

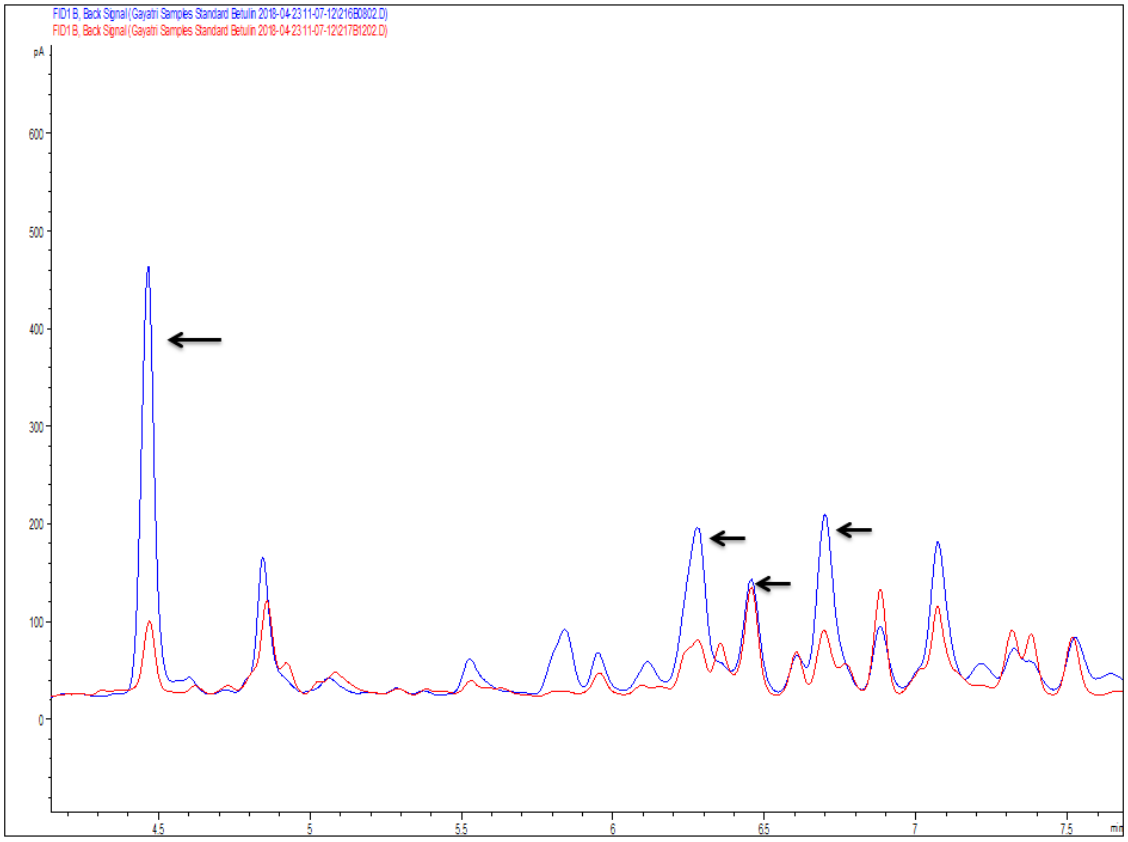

Figure 2: Gas chromatograms of silylated ethanol extracts from heartwood of *E. bosistoana* (blue) and *E. globoidea* (red) between 4.5 and 7.5 min retention time. Black arrows indicating peaks at retention times 4.5, 6.2, 6.4 and 6.7 were selected for further analysis.

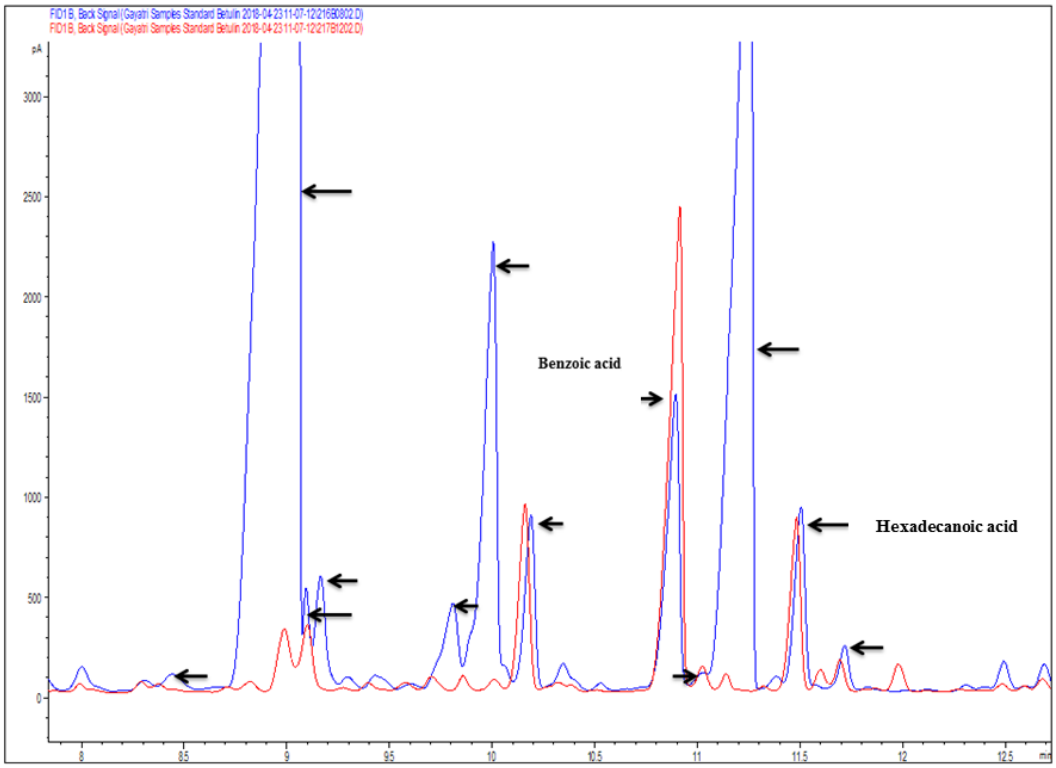

Figure 3: Gas chromatograms of silylated ethanol extracts from heartwood of *E. bosistoana* (blue) and *E. globoidea* (red) between 8 and 12.5 min retention time. Indicated peaks (arrows) at the retention times 8.4, 9.0, 9.1, 9.2, 9.7, 9.9, 10.2, 10.9, 11.1, 11.2, 11.5 and 11.7 were selected for further analysis. Compound identified at the retention times 10.9 and 11.5 min by comparing the chromatograms of *E. bosistoana* heartwood extracts with *E. globoidea* (Schroettke, 2018).

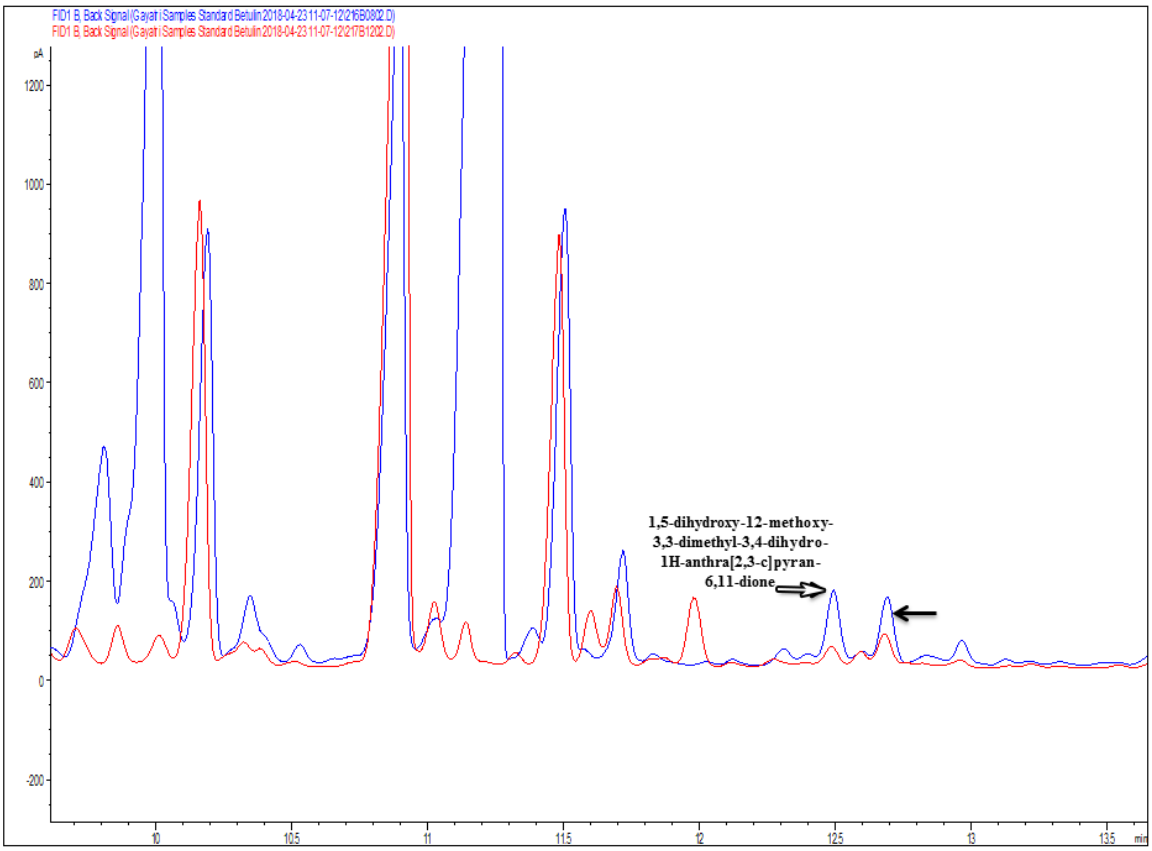

Figure 4: Gas chromatograms of silylated ethanol extracts from heartwood of *E. bosistoana* (blue) and *E. globoidea* (red) between 10 and 13.5 min retention time. Indicated peak (arrow) at the retention times 12.7 min was selected for further analysis. Compound identified at the retention time 12.5 min (arrow) by comparing chromatograms of *E. bosistoana* heartwood extracts with *E. globoidea* (Schroettke, 2018).

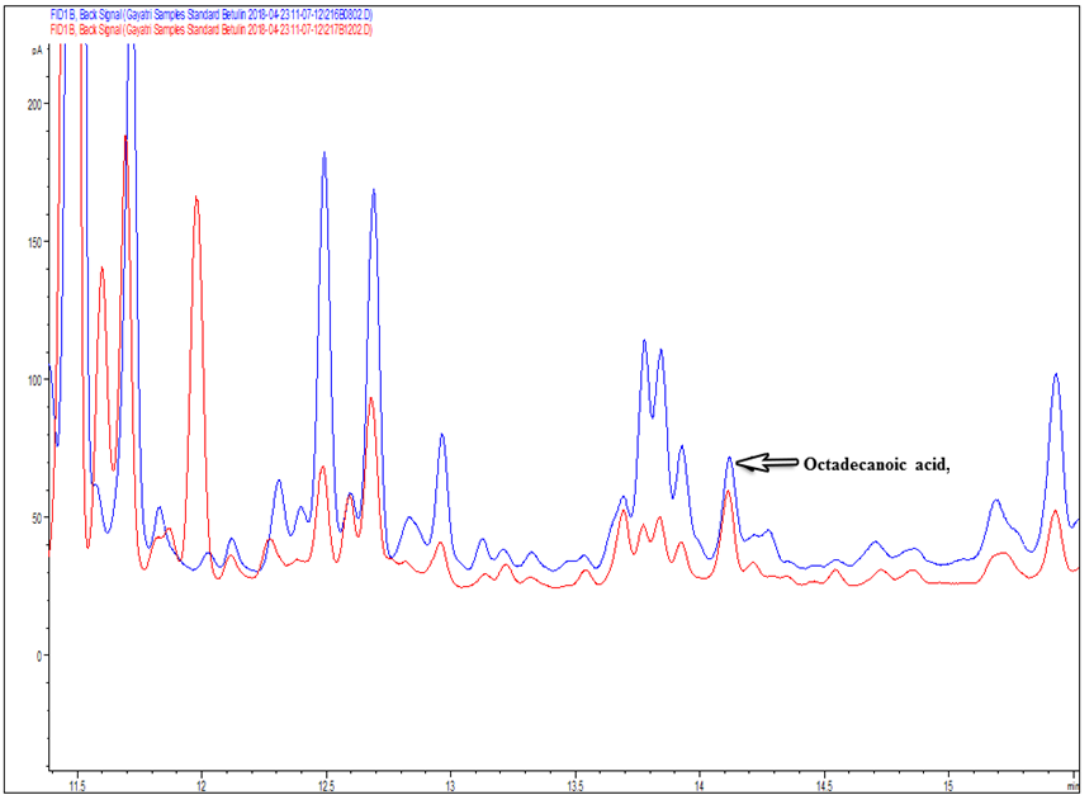

Figure 5: Gas chromatograms of silylated ethanol extracts from heartwood of *E. bosistoana* (blue) and *E. globoidea* (red) between 11.5 and 16 min retention time. Compound identified at the retention time 14.1 min (arrow) by comparing chromatograms of *E. bosistoana* heartwood extracts with *E. globoidea* (Schroettke, 2018).

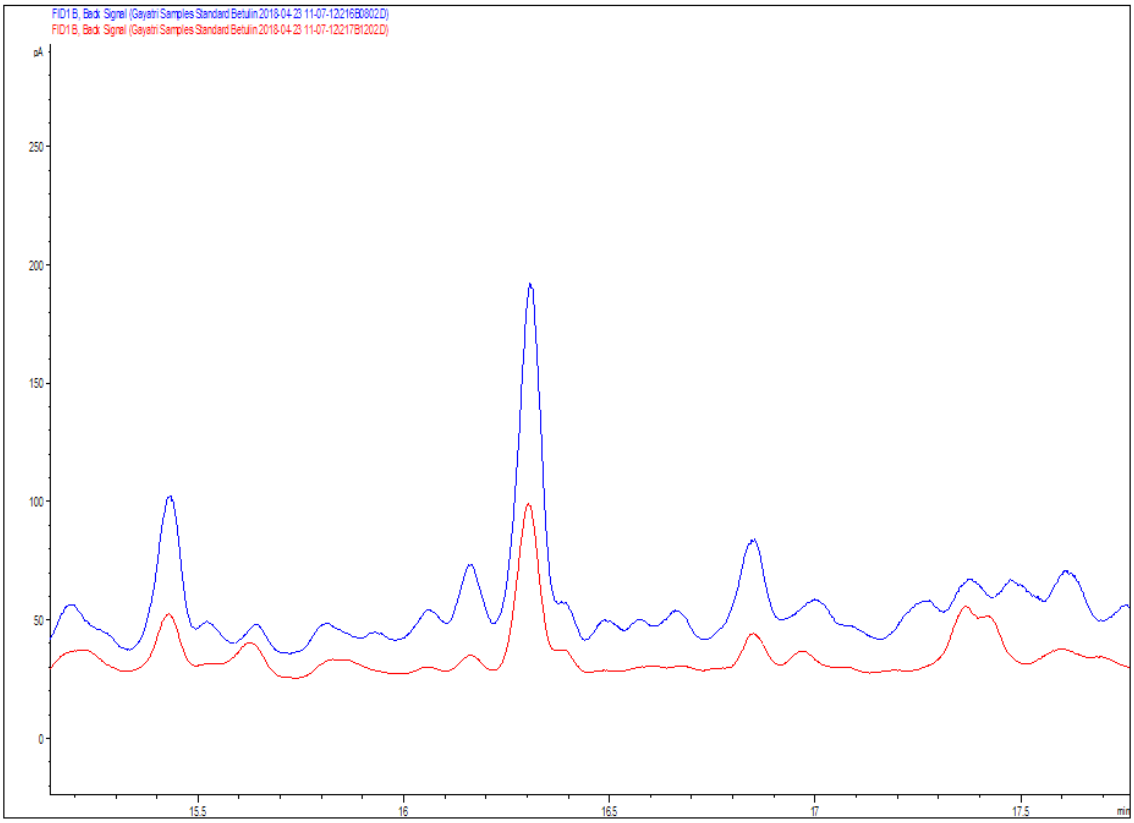

Figure 6: Gas chromatograms of silylated ethanol extracts from heartwood of *E. bosistoana* (blue) and *E. globoidea* (red) between 15.5 and 17.5 min retention time.

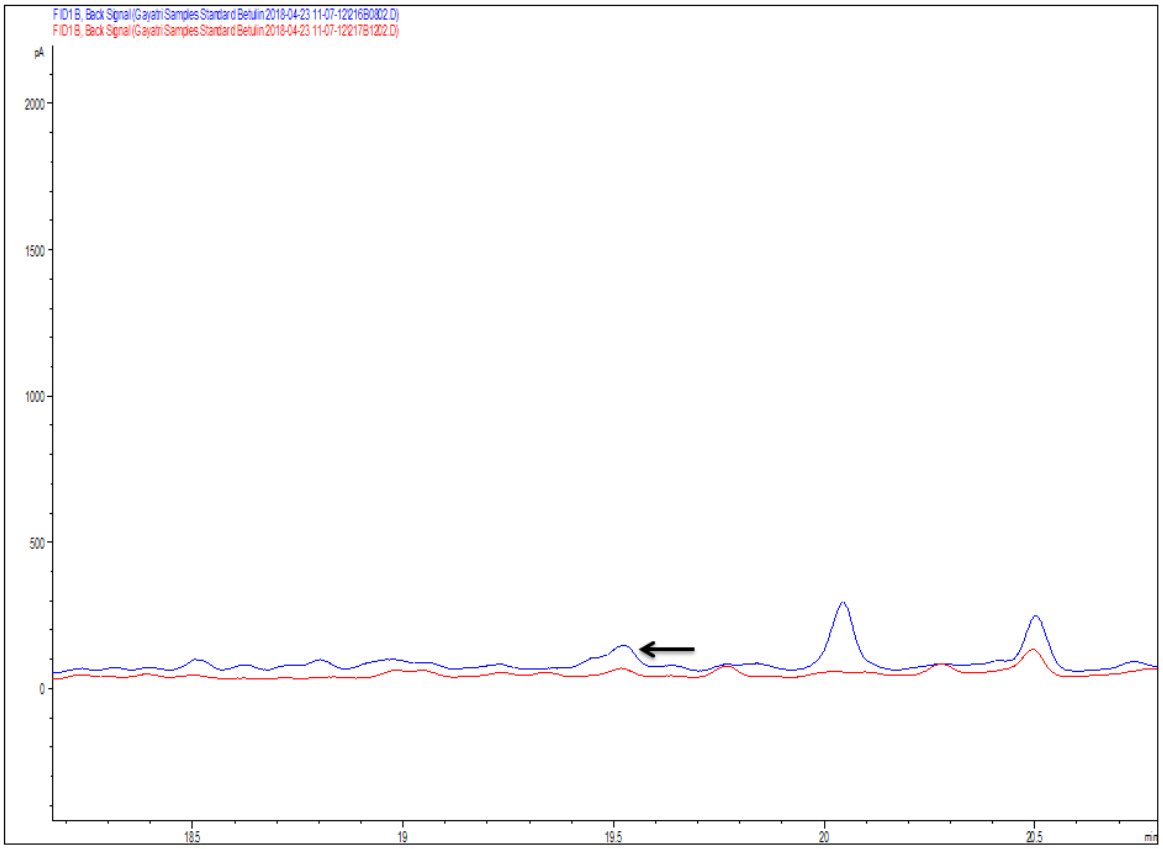

Figure 7: Gas chromatograms of silylated ethanol extracts from heartwood of *E. bosistoana* (blue) and *E. globoidea* (red) between 18.5 and 20.5 min retention time. Indicated peak (arrow) at the retention time 19.5 min was selected for further analysis.

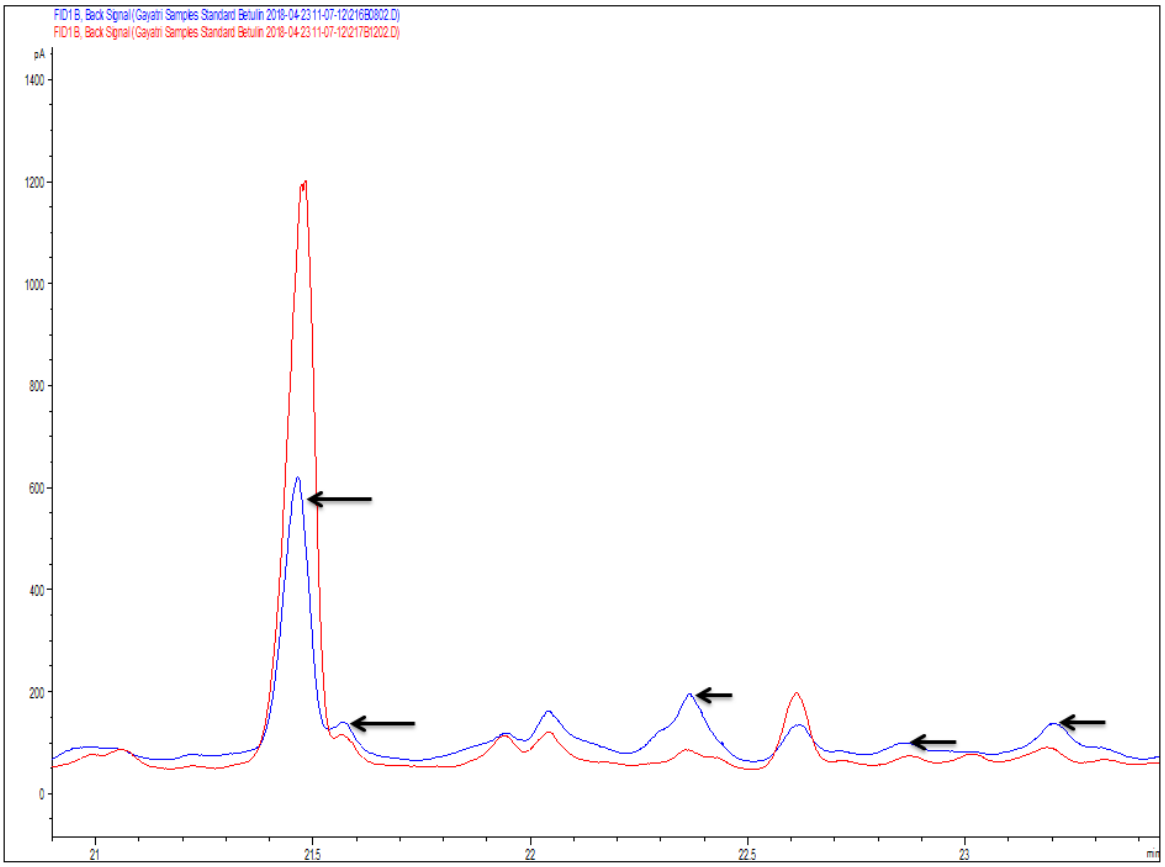

Figure 8: Gas chromatograms of silylated ethanol extracts from heartwood of *E. bosistoana* (blue) and *E. globoidea* (red) between 21 and 23.5 min retention time. Indicated peaks (arrow) at the retention times 21.4, 21.5, 22.3, 22.8 and 23.3 min were selected for further analysis.

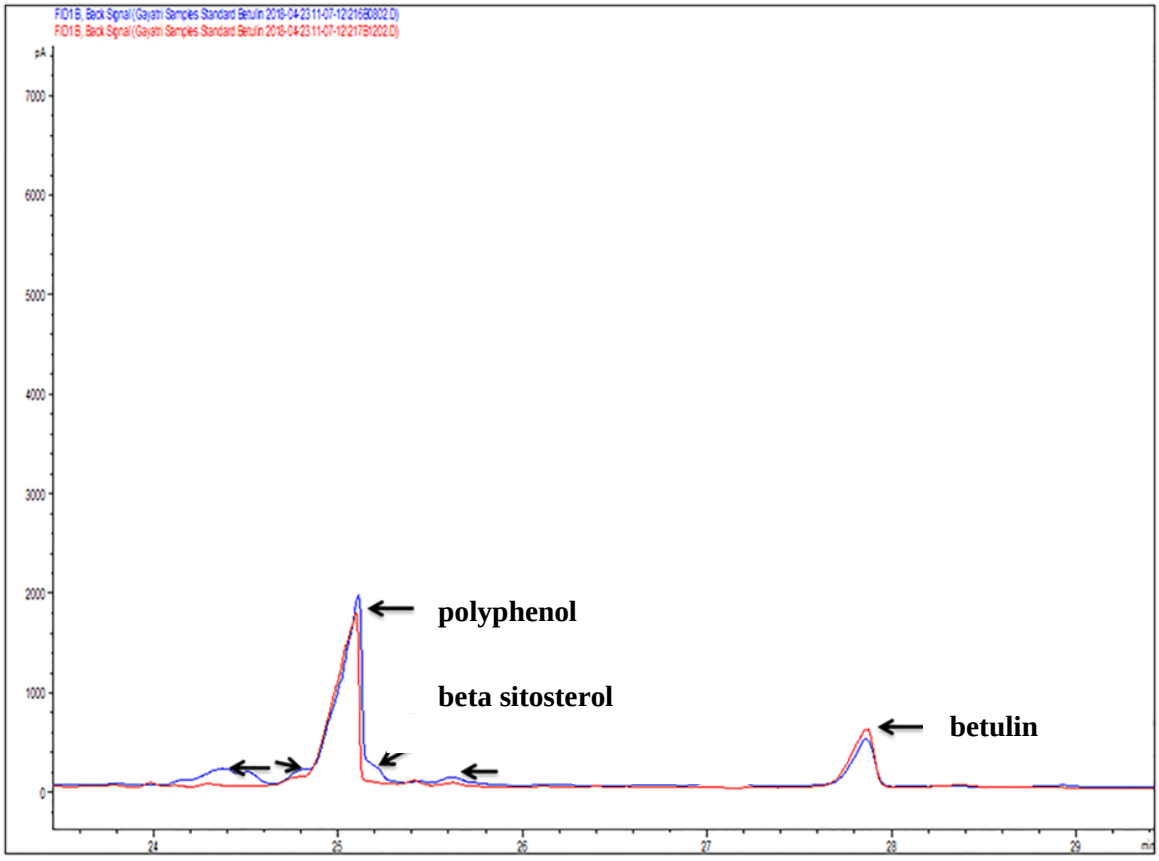

Figure 9: Gas chromatograms of silylated ethanol extracts from heartwood of *E. bosistoana* (blue) and *E. globoidea* (red) between 24 and 29 min retention time. Indicated peaks (arrow) at the retention times 24.8, 24.9, 25.1, 25.2 and 25.4 min were selected for further analysis. Compound identified at the retention times 25.1 and 25.2 min (arrow) by comparing chromatograms of *E. bosistoana* heartwood extracts with *E. globoidea* (Schroettke, 2018). Standard (betulin) at 27.9 min (arrow).

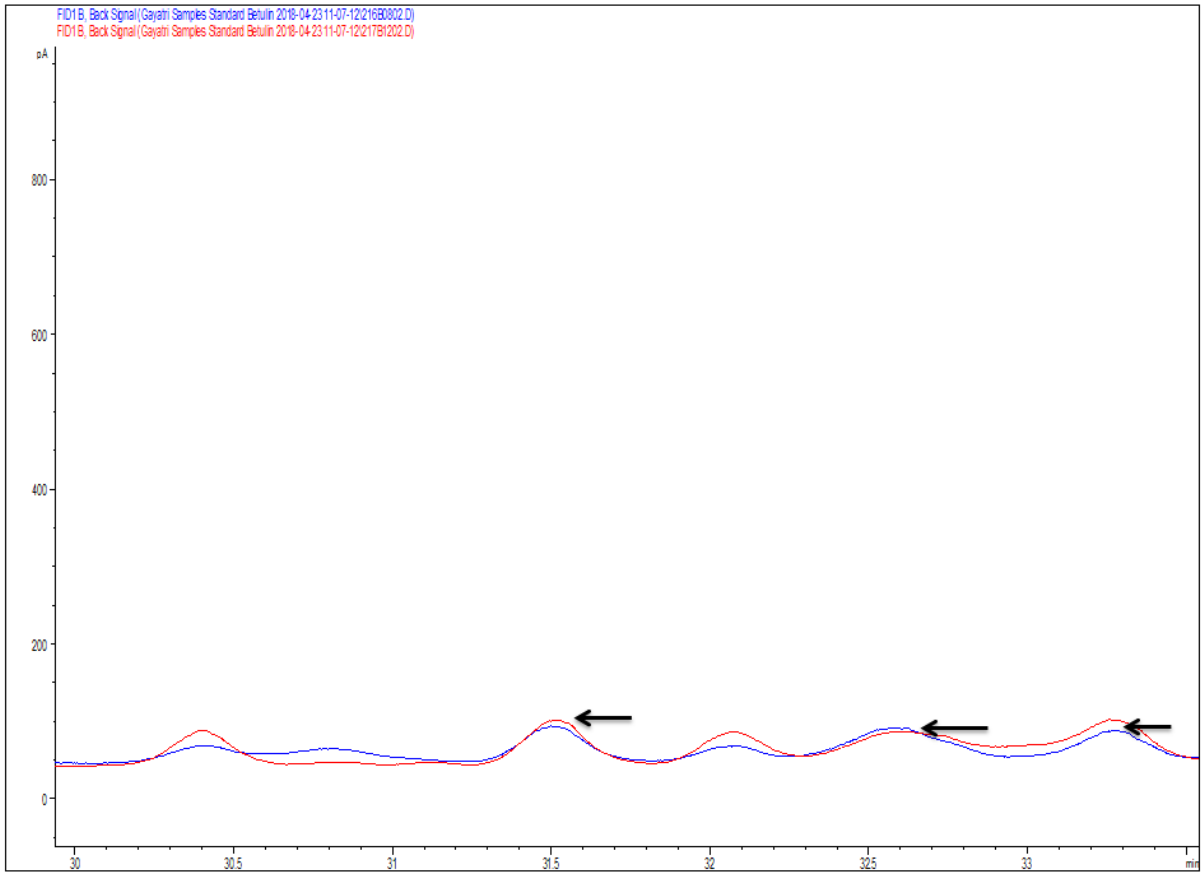

Figure 10: Gas chromatograms of silylated ethanol extracts from heartwood of *E. bosistoana* (blue) and *E. globoidea* (red) between 30 and 33 min retention time. Indicated peaks (arrow) at the retention times 31.5, 32.7 and 33.3 min were selected for further analysis.

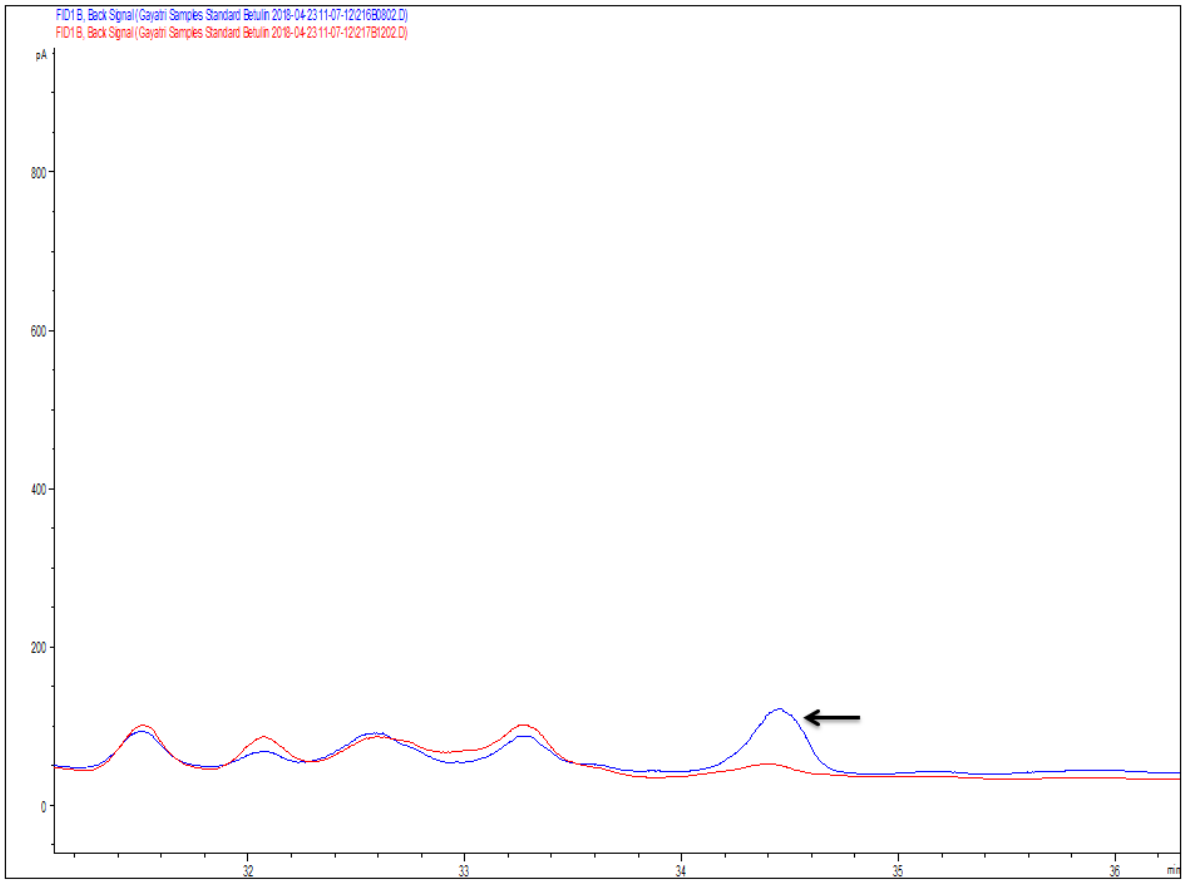

Figure 11: Gas chromatograms of silylated ethanol extracts from heartwood of *E. bosistoana* (blue) and *E. globoidea* (red) between 32 and 36 min retention time. Indicated peak (arrow) at the retention times 34.7 min was selected for further analysis.

Appendix 3: Loadings of the 1st and 2nd principal components for partial least squares regression (P LSR) model of the growth of the white rot *T. versicolor* by the 31 quantified compounds in *E. bosisto ana* heartwood ethanol extracts.

Retention times (min)	Pc 1	Pc 2
4.5	0.268	-0.020
6.2	0.192	-0.335
6.4	0.289	-0.238
6.7	0.165	-0.338
8.4	0.299	-0.198
9.0	0.295	-0.165
9.1	0.153	-0.079
9.2	0.047	-0.141
9.7	0.242	-0.229
9.9	0.233	-0.042
10.2	0.122	0.392
10.9	0.307	-0.167
11.1	0.262	-0.135
11.2	0.268	-0.086
11.5	0.162	0.290
11.7	0.311	-0.079
12.7	0.218	-0.057
19.5	0.161	-0.221
21.4	0.139	-0.154
21.5	0.244	-0.205
22.3	0.259	-0.151
22.8	0.315	-0.119
23.3	0.292	-0.133
24.8	0.247	-0.113
24.9	0.229	-0.056
25.1	0.275	0.035
25.2	0.235	0.025
25.4	0.110	-0.286
31.5	0.141	-0.315
32.7	0.306	-0.034
33.3	0.178	-0.226
34.7	0.293	-0.152

plsmod2$R2	
t1	0.039
t2	0.092
Sum (plsmod2$R2)	0.131

The results of Appendix 3 shows that the two PLS components have a r-square of 0.133 by adding values of t1 and t2 in predicting white rot (*T. versicolor*) relative growth rate (WRGR). Results can be further simplified by the total variance in relative growth rate explained by the first two principle components was 13.1% (9.2% and 3.9%, respectively) for white rot (*T. versicolor*).

Appendix 4: Loadings of the 1st and 2nd principal components for partial least squares regression (P LSR) model of the growth of the brown rot (*C. cerebella*) by the 31 quantified compounds in *E. bosist oana* heartwood ethanol extracts

Retention times (min)	Pc 1	Pc 2
4.5	-0.205	0.269
6.2	-0.574	0.074
6.4	-0.524	0.200
6.7	-0.531	0.064
8.4	-0.516	0.202
9.0	-0.511	0.191
9.1	-0.272	0.098
9.2	-0.136	0.033
9.7	-0.433	0.179
9.9	-0.209	0.215
10.2	0.185	0.151
10.9	-0.505	0.210
11.1	-0.419	0.190
11.2	-0.287	0.234
11.5	0.058	0.170
11.7	-0.352	0.264
12.7	-0.423	0.096
19.5	-0.407	0.078
21.4	-0.240	0.111
21.5	-0.466	0.154
22.3	-0.248	0.262
22.8	-0.346	0.284
23.3	-0.318	0.269
24.8	-0.261	0.236
24.9	-0.299	0.178
25.1	-0.375	0.176
25.2	-0.374	0.167
25.4	-0.194	0.126
31.5	-0.304	0.126
32.7	-0.330	0.262
33.3	-0.402	0.106
34.7	-0.369	0.255

plsmod3$R3	
t1	0.089
t2	0.069
Sum (plsmod3$R3)	0.158

The results of Appendix 4 shows that the two PLS components have a r-square of 0.158 by adding values of t1 and t2 in predicting brown rot (*C. cerebella*) relative growth rate (BRGR). Results can be further simplified by the total variance in relative growth rate explained by the first two principle components was 15.8% (8.9% and 6.9%, respectively) for brown rot (*C. cerebella*).

Chapter-6

Woundwood and heartwood features in *Eucalyptus bosistoana*

6.1 Introduction

Trees can be screened in a breeding programme at age (1 - 2 years) for wood properties such as growth stress, collapse, density or stiffness. Early selection reduces trial costs, shortens breeding cycles and ensures timely deployment of improved material. Early selection for heartwood is challenging because heartwood formation in *Eucalypts* starts at age ~5 years. Early selection for heartwood would be possible if a strong correlation of heartwood to another tree feature is found (Harju et al., 2009; Yu et al., 2003). Woundwood originates from a similar metabolic pathway as heartwood, with both tissues featuring reduced permeability and water content as well as deposited extractives (Hillis, 1987; Shigo & Hillis, 1973; Taylor et al., 2002). The objective of this study was to correlate wound reaction with heartwood features in *E. bosistoana* families using statistical, microscopic and chemical analysis. A strong correlation would allow screening *Eucalypts* for heartwood at age 1 - 2, i.e. before heartwood is formed.

Xylem responds to injury by tissue regeneration. Trees have a defence mechanism which is triggered by injury or infection. The concept of a tree's response to wounding was described as "compartmentalisation", which is also known under the acronym CODIT "compartmentalisation of decay in trees" (Shigo, 1984). Compartmentalisation may be considered as a conceptual model related to the process of boundary formation in trees, which prevents the spread of infection in tree stems. This model describes four different types of static barriers called "walls" that resist the spread of infection. Wall 1 resists vertical (axial) spread, wall 2 resists inward (radial) spread, and wall 3 resists lateral (tangential) spread. Among these defence walls, wall 1 (axial) is the weakest, whereas, wall 2 (radial) is moderately strong. When the injuries approach deeper sheaths of xylem, the resisting power of wall 2 decreases. Wall 3 (lateral) is the strongest wall of compartmentalisation. Wall 4 differs from the other boundaries, because it is newly produced by living cells after wounding, while walls 1 to 3 are established ahead of wounding during wood formation (Nakaba et al., 2017). Wall 4 contains an anatomically modified tissue layer near the wound known as barrier zone, which can be observed in form of discolouration and is referred to as "woundwood" in this study. Several terms are used for this dynamic mechanism in trees such as pathological heartwood (Busgen et al., 1929; Chattaway, 1952), protection wood (Jorgensen, 1961), discoloured wood (Shigo & Hillis, 1973) or reaction zone (Shain, 1967).

Two types of tissue, i.e. the newly formed and the existing modified tissue can be distinguished in the response to wounding. First the formation of new callus tissue with which trees closes the wound. Parenchyma cells in phloem and sapwood xylem are associated with the production of callus. Secondly xylem tissue existing prior to wounding and undergoing anatomical and histochemical changes due to injury (Eyles et al., 2003). This second type of tissue is the focus of this study and referred to as "woundwood". In many species such as *Acer* and *Betula* (Bauch et al., 1980), *Fagus sylvatica* (European beech) (Torelli et al., 1994) and *Liriodendron tulipifera* (Yellow-poplar) (Lowerts et al., 2007), physiological and metabolic changes in parenchyma cells are visible in form of deposition of secondary metabolites (extractives), metabolisation of reserve material (e.g. starch) or formation of protruding structures called tyloses. The extent of discolouration depends on the size of the wound. Discolouration may be a few centimetres in length for smaller wounds such as drill holes, but could extend to several decimetres or more with severe damage to trees (Liese & Dujesiefken, 1990).

Parenchyma cells are also involved in heartwood formation. Physiological changes observed during heartwood formation are similar to the changes after wounding. During heartwood formation, parenchyma cells metabolise reserve materials and typically synthesize secondary metabolites as well as develop blockages in the conducting cells, which in hardwoods often involves formation of tyloses. The parenchyma cells then undergo programmed cell death. The accumulation of secondary metabolites called heartwood extractives imparts natural durability and colour to xylem.

While woundwood and heartwood formation have similarities including the presence of secondary metabolites (extractives) and reduced permeability, there are also differences. Woundwood is triggered by external events, whereas heartwood is initiated by internal factors (Spicer, 2005). The chemical composition of extractives found in woundwood was reported to differ both qualitatively and quantitatively from those of heartwood (Hillis, 1987). Little information is available on woundwood formation in *Eucalyptus* species. Barry et al. (2001) identified wide range of hydrolysable tannins in both healthy sapwood and in reaction zone extracts of *E. nitens* by HPLC with ESI-MS (electrospray ionisation-mass spectroscopy). The compounds in the extracts included gallotannins (tri-O-galloyl-β-D-glucose, tetra-O-galloyl-β-D-glucose, penta-O-galloyl-β-D-glucose), and ellagitannins (pedunculagin, tellimagrandin I, casuarinin, casuarictin, tellimagrandin I). Pedunculagin was more abundant in the reaction zone than in sapwood. Eyles et al. (2003) reported a range of secondary metabolites such as polyphenols (proanthocyanidins, flavonol, flavanone glycosides, hydrolysable tannins such as pedunculagin, stilbene glycosides, terpenes) in the woundwood of *E. globulus* and *E. nitens*.

The correlation between heartwood features of *Pinus sylvestris* (Scots pine) trees and the wound reaction of the offspring of these trees has been investigated (Harju et al., 2009). A heritability of 0.31

between the concentration of the heartwood compound pinosylvin in the woundwood of the offspring and that in the heartwood of the mother trees was reported. Li et al. (2018) reported heritabilities of 0.66 - 0.71 for heartwood diameter and 0.16 - 0.25 for extractive content in 7-year-old *E. bosistoana* trees.

This work details the correlation of wound reaction of 27 *E. bosistoana* families with heartwood diameter and extractive content. Variation in starch, tyloses and extractives between woundwood, heartwood and sapwood in two families, one with large and one with small wound reaction, were analysed in more detail by microscopy and gas chromatography (GC).

6.2 Materials and methods

6.2.1 Woundwood data

In 2015, *E. bosistoana* breeding trial was established at a tree nursery in Woodville, New Zealand. Trees were planted in family blocks of eight individuals, with blocks replicated at least 3 times (Altaner, 2017; Davies & Altaner, 2017). This trial included 27 families (seed of one tree), which were present in breeding trials planted in 2009 and previously assessed for heartwood (Li, 2018). The surviving individuals with a stem diameter >3 cm in 3 blocks i.e. 8 - 22 individuals per family (Appendix 1) were wounded by drilling a 5 mm hole through the stem at ~50 cm height with a battery powered drill (Figure 6.1). The 1.6-year-old trees were wounded on the 29th September 2016. Wounds on the trees were marked with spray paint to assist harvest after 6 weeks of wounding, on the 10th November 2016. The wounded section of the stem was recovered and the wound was exposed by splitting the stem through the pith perpendicular to the drilled hole. The two halves of each sample were oven dried at 60°C and the wound reaction was assessed with and without staining using a pH indicator (0.01 % methyl orange in water) (Figure 6.2). Like heartwood, the discoloured zone (woundwood) changed pink in colour by application of indicator solution, which indicated presence of acidic extractives similar to heartwood (Li et al., 2018). Hillis (1987) reported a pH value of 2.6 in the heartwood of *E. diversicolor*. The discoloured zone was measured with a calliper in the axial direction excluding the drilled holes. Variation in the colour of the indicator reaction on woundwood was observed between the samples. This indicated differences in the chemical composition of extracts between samples. Only the measurement of the wound reaction in one stem half was considered in the following analysis as the measurements on the 2 halves were identical.

Two families with small (family 2) and large (family 24) wound reactions were selected to investigate physiological and chemical variations in woundwood, heartwood and sapwood by microscopy and GC. 21 trees were available for family 2 and 22 for family 24.

Data for other tree and wood properties of the 27 *E. bosistoana* families at age 1.6-years-old were available from the trial planted in 2015. This included growth strain, acoustic velocity, density,

stiffness, volumetric shrinkage, tree height and diameter. For a detailed description of the experimental procedures see Davies and Altaner (2017).

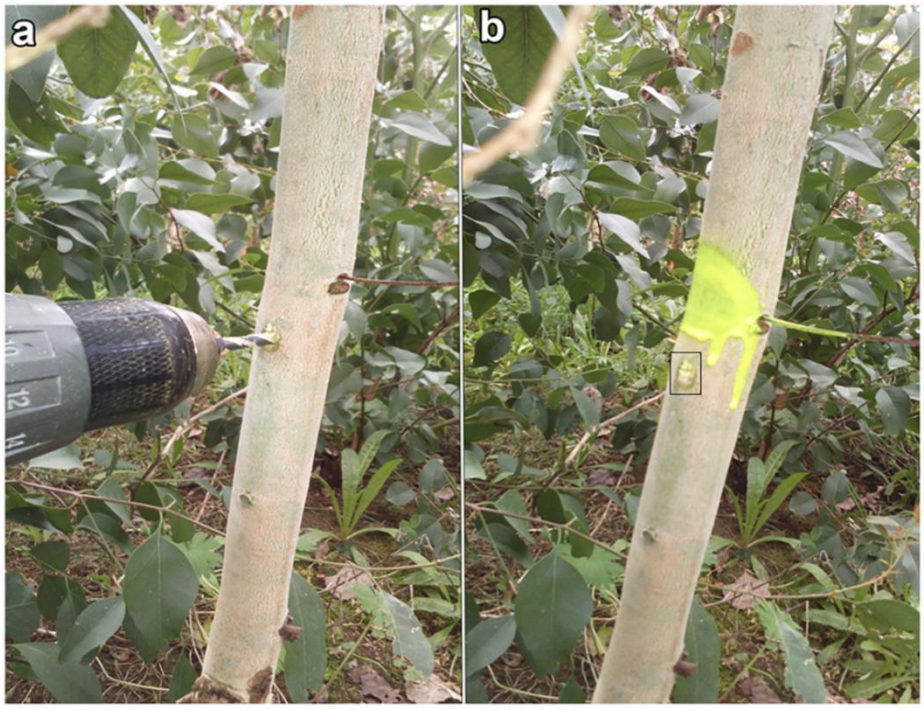

Figure 6.1: Wounding of 1.6-year-old *E. bosistoana* by drilling a hole through the stem at ~50 cm height with a battery powered drill (a). Wound marked with a box on the tree (b).

6.2.2 Heartwood data

Data on heartwood diameter and extractive content were available for 7-year-old *E. bosistoana* from breeding trials planted in 2009 (Li & Altaner, 2018). These were established at two sites (Craven Road, Lawson) and assessed in 2016 by taking a ~14 mm diameter core from the base of the stem. The sapwood and heartwood diameter were measured on the green cores after highlighting the heartwood with a pH indicator (methyl orange). The ethanol soluble extractive content was predicted from NIR spectra taken from the cross-section of dried cores (Li, 2018). A detailed description on genetic heritability between heartwood diameter and extractive content between the *E. bosistoana* families was reported by (Li et al., 2018).

Ten cores for family 2 (small wound reaction) and eight cores for family 24 (large wound reaction) were available for microscopy and GC analysis. Table 6.1 outlines the number of samples used for the different experiments.

Table 6.1: Woundwood and heartwood samples used for woundwood analyses.

Number of samples	Family 2		Family 24	
	Woundwood samples	Heartwood cores	Woundwood samples	Heartwood cores
Total	22	10	21	8
Microscopy	4	4	4	4
GC	18	6	17	4

6.2.3 Sample preparation for microscopy

Four samples/trees from each family were used for the sample preparation. Sections, 2 - 3 cm containing the wounded tissue, were cut from the 1.6-year-old wounded stems with a band saw and chiselled into pieces ~0.5 cm in tangential and 0.5 - 1 cm in the radial direction. Heartwood from four cores (14 mm diameter) from the 7-year-old-trees were split into 1 cm (radial) pieces. The wood pieces were immersed in hot water for 48 h to reduce the hardness of the wood. Longitudinal sections (10 - 20 µm thick) were prepared using a sledge microtome and mounted in glycerol for microscopy.

6.2.4 Microscopy

Radial sections, either unstained or stained with iodine/potassium iodide (0.1% in water) to visualise starch grains, were mounted in glycerol. Subsequent steps were the same as described in chapter 3 (3.2.2) including image processing (3.2.5).

6.2.5 Spectral analysis

A Leica SP5 confocal microscope system operating on a DMI6000 inverted microscope and equipped with 20x NA 0.7 and 63x NA 1.3 glycerol immersion lenses (Leica, Germany) was used for imaging. To detect variations in the autofluorescence of the wood samples on the cellular level, fluorescence emission spectra were recorded using an excitation wavelengths of 405 nm, with emission collected from 420 to 700 nm. Images were recorded at 512 pixels square resolution with a 10 nm wide window and with a 5 nm step size. Image intensities were quantified as described in chapter 3 (3.2.4).

While heartwood samples came from cores of 7-year-old trees of the 2009 *E. bosistoana* breeding trial, woundwood and healthy sapwood near woundwood originated from 1.6-year-old trees if the 2015 *E. bosistoana*. For each of the four trees of the families chosen for small and large wound reaction two sections were prepared. Therefore in total eight spectra were collected for each wood and cell type, which were finally averaged.

6.2.6 Extraction

Heartwood was isolated from six cores of 7-year-year-old trees of family 2 (small wound reaction) and four cores of family 24 (large wound reaction). Discoloured tissue (i.e. woundwood) was isolated by drilling into the stem halves of the 1.6-year-old trees with a 0.5 mm drill. Healthy sapwood near woundwood was obtained accordingly. 18 trees for family 2 and 17 samples for family 24 were used.

Heartwood pieces from the cores and sawdust collected from woundwood and heathy sapwood were pooled for each family, milled to pass a 20 mesh screen and oven dried at 60°C. The wood powder samples were stored in paper bags inside a desiccator over silica gel prior use.

Samples were extracted using an Accelerated Solvent Extractor (Dionex ASE 350, Thermo Scientific) equipped with 33 ml cells. Subsequent steps were the same as described in chapter 4 (4.2.2). Extractive content of heartwood was calculated on a dry mass basis.

6.2.7 Gas chromatography (GC)

Subsequent steps were the same as described in chapter 5 (5.2.3). Peaks of the chromatograms were manually integrated in the Chem Station software (Agilent, Rev.c.01.07) and 37 peaks were chosen including the internal standard. Subsequent steps were same as described in chapter 5 (5.2.4). GC data was analysed in the R programming language (Team, 2013) including ANOVA and T-test. The ggplot2 (version 2.2.1) package (Wickham, 2009) was used to plot graphs. The package 'ggfortify' auto plot (version- 0.4.5) (Horikosh et al., 2018) was used to perform principle component analysis. An alpha of 0.05 is used as the cut off for significance in this chapter.

6.2.8 Statistical analysis

A mixed multivariate 'animal' model was used to estimate the heritability of the wound reaction of the population. The model consisted of fixed (replicates, staking and edge effects) and random plot effects to describe environmental influences. Numerous site and operational effects were checked for significance within this framework, and found to be negligible. The pls package (version 2.5 - 0) (Mevik et al., 2015) using the plsr algorithm with leave-one-out cross-validation to develop calibration models and the ggplot2 package (version 2.2.1) (Wickham, 2009) was used to plot graphs.

6.3 Results and discussion

6.3.1 Wound reaction

The wound reactions, observed in form of discolourations, were more prominent in the axial than the radial direction (Figure 6.2). This coincided with the CODIT model Shigo (1984) that states that the axial wall is much weaker than the radial barrier. Discolourations were reported after mechanical wounding in the stems of various species and age, such as 20-year-old *Fagus sylvatica* (European beech) (Schmitt & Liese, 1993), 20-year-old *E. regnans* (White & Kile, 1993), 14-year-old *E. maculata*, 9-year-old *E. globulus* and *E. nitens* (Eyles et al., 2003), 60-year-old *Cryptomeria japonica* (Japanese cedar) (Nakaba et al., 2017) or 45-year-old *Tilia americana* (Basswood) (Schmitt & Koch, 2009). While the brown discolourations around the edges of the wound coincided with the observations reported here, it was difficult to compare the size and shape of the discolourations as they were reported to vary between species, tree age and wound size. Nakaba et al. (2017) reported that the autoflurorescence from ray parenchyma cells became stronger with time due to deposition of

phenolic compounds, from 1 - 8 weeks after wounding in *C. japonica*. This lines up with the observations of Yamada (1998), suggesting xylem parenchyma synthesize phenolic compounds in response to wounding in *C. japonica*.

The wounded tissue of the stem recovered by splitting showed variation in the extent of wound reaction between trees (Table 6.2). Large within family variation in the wound reaction was observed (Figure 6.3). Apart from low genetic control of the trait, uncertainty in the assessment caused by low contrast between sapwood and woundwood could have contributed to the large variation. Furthermore, the wounded stem section sometimes contained knots, potentially adding noise to the wound reaction data.

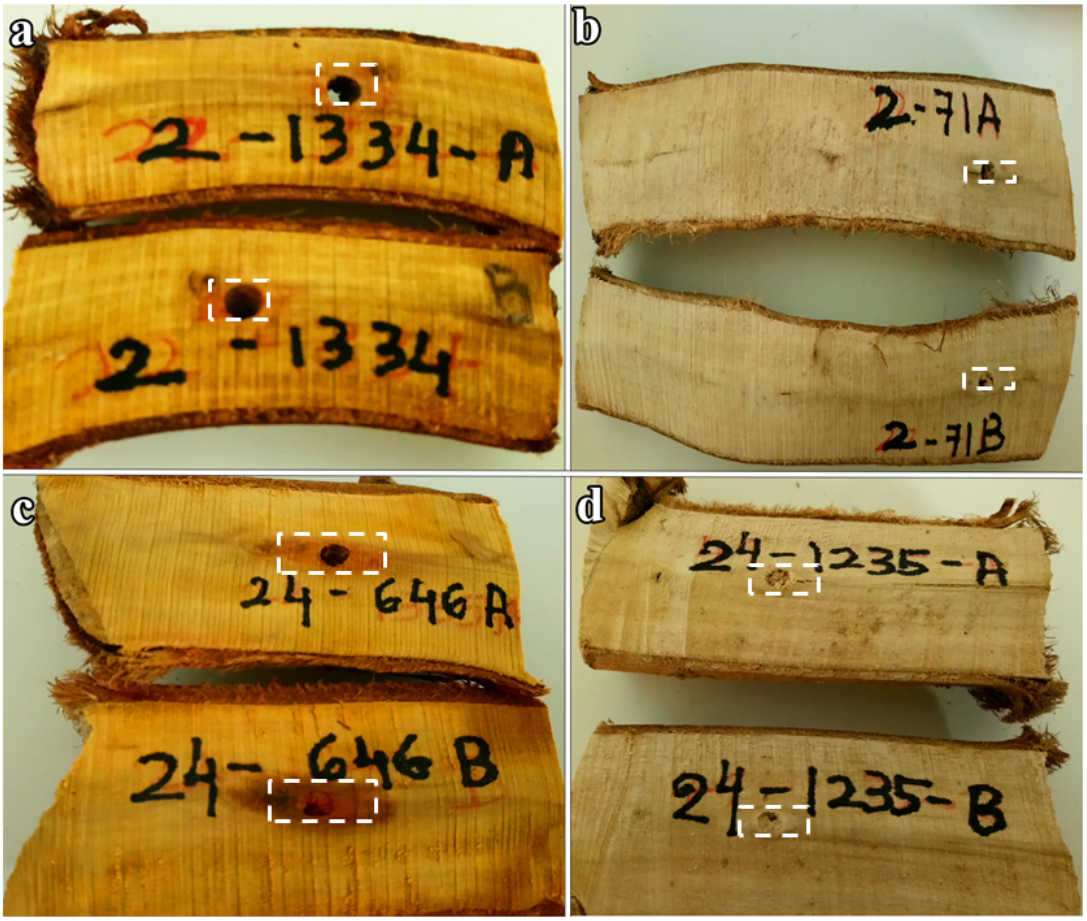

Figure 6.2: Representative wound reaction in dried samples of 1.6-year-old *E. bosistoana* families 6 weeks after wounding. Family 2 with small wound reaction (top row) and family 24 with large wound reaction (bottom row). Discolouration (marked with a box) was accessed with (a, c) and without (b, d) pH indicator (methyl orange).

Table 6.2: Summary statistics for wound reaction in 27 *E. bosistoana* families at age 1.6-year-old from Woodville. Extractive content and diameter of heartwood for 27 *E. bosistoana* families aged 7-year-old from the Lawson and Craven Road sites. CV: Coefficient of variation, n: number of samples.

	Wound reaction (mm) **(n = 470)**	**Extractive content (%)** **(n = 528)**	**Heartwood diameter (mm)** **(n = 528)**
Min	0.1	0.04	3
Max	3.5	13.34	82
CV (%)	49	44	59

6.3.2 Heritability of wound reaction

Figure 6.3 shows the 27 *E. bosistoana* families ranked for wound response 6 weeks after wounding. The heritability of the wound reaction was estimated from the data. The heritability of the wound reaction was 0.26 with a 95% credibility interval of 0.00 to 0.53. The genetic control was similar to that of growth-strain, but lower than those of other physical wood properties for trees from a different trial (Davies et al., 2015). In agreement with this result, compartmentalisation in seven half-sibling tree pairs of *Juglans nigra* was reported to be genetically controlled (Armstrong et al., 1981).

Heritability (h^2) of 0.26 would allow for genetic selection. However, selection for wound reaction is not desirable in itself as the amount of wound reaction is of no commercial benefit. Nevertheless, if the wound reaction is correlated to a trait of commercial interest it can be used as a proxy for genetic selection. This can be useful if the wound reaction is more efficient (cost, time) to analyse than the target trait.

Harju et al. (2009) investigated mechanical wounding in *P. sylvestris* seedlings as an early testing method for heartwood durability. They estimated a heritability of 0.31 for the concentrations of the heartwood compound pinosylvin in the heartwood of the mother trees from its concentration in the woundwood of the offspring. Apart from the chemical composition, the decay resistance has also been shown to be under genetic control, e.g. moderate to high heritability was reported for *E. cladocalyx* provenances (Bush et al., 2011) or moderate heritabilities of decay resistance against brown rots (h^2 = 0.21) and white rots (h^2 = 0.27) for *Picea glauca* (Yu et al., 2003).

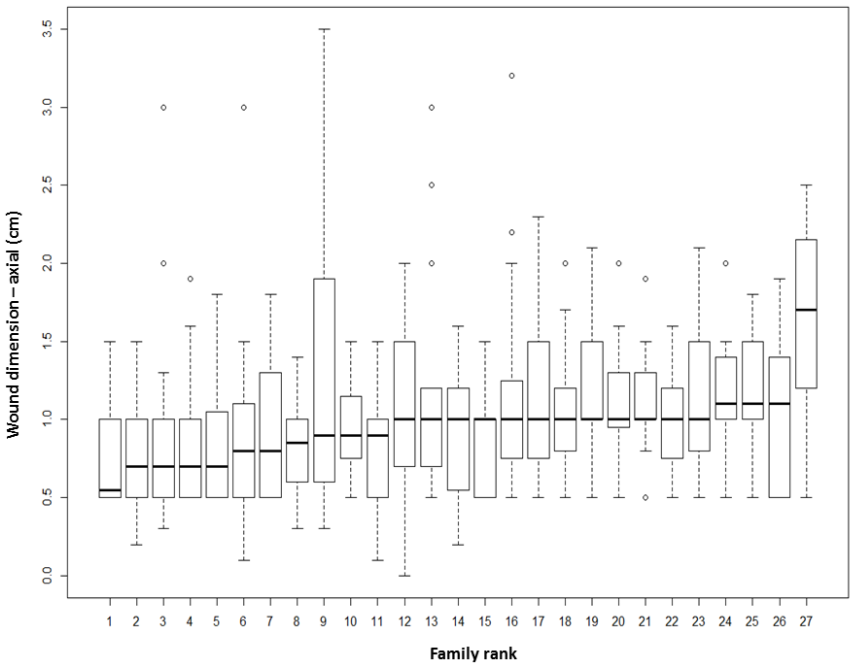

Figure 6.3: 27 *E. bosistoana* families ranked for the axial size of their wound response 6 weeks after wounding at age 1.6-year-old.

6.3.3 Correlation of wound reaction to heartwood features

Heartwood features were not assessed on the same trees, which were wounded. However, heartwood data was available for the same families from another trial (Li & Altaner, 2018). Therefore, correlation between heartwood and wound reaction traits was possible on a family basis. The amount of heartwood as well as the extractive content within the heartwood differed between the sites. Differences were observed for the population means as well as the individual family means. No strong correlations were found between the axial dimensions of the wound reaction and heartwood diameter or extractive content for the individual sites or the pooled data (Table 6.3). The weak correlations between wound reaction and heartwood diameter for Lawson East and the pooled data as well as the extractive content at Lawson North were not significant considering the large confidence intervals.

Table 6.3: Correlations between family means of length of axial wound reaction (mm) and heartwood diameter (mm) as well as extractive content (%). 95% credibility intervals are given in parentheses.

Site	Heartwood diameter	Extractive content
Lawson North	-0.18 (-0.57, 0.27)	-0.11 (-0.52, 0.34)
Lawson East	-0.30 (-0.61, 0.95)	0.12 (-0.28, 0.48)
Craven Road	-0.15 (-0.50, 0.25)	-0.07 (-0.44, 0.32)
All	-0.28 (-0.60, 0.11)	0.00 (-0.38, 0.38)

Genetic and environmental factors influenced the ranking of families based on wound reaction and heartwood properties. In this study, environmental factors might have had a stronger impact because the trials were situated in different topographic and climatic conditions. Larger environmental effects are likely to weaken the correlations between wound reaction and heartwood properties of families. Li et al. (2018) reported stable and moderately stable rankings of *E. bosistoana* families for heartwood diameter and extractive content, respectively. Several reports suggest the season of wounding, growth rate of trees, interval of wound exposure and wound size affect the wound reaction in trees. Armstrong et al. (1981) reported greater discolouration in the stems of *J. nigra* (Black walnut) wounded in fall than in spring. Mireku and Wilkes (1989) concluded season, climatic conditions and species influenced the development of discolouration in *E. maculata*, while the seasonal pattern was found inconclusive in *E. delegatensis* (Gadgil & Bawden, 1981) and other deciduous hardwoods (Shigo, 1976).

Therefore, it might still be possible to screen *E. bosistoana* early (at age ~1.6-year-old) for natural durability but with a different assessment of the wound reaction. If the study is to be repeated it should be considered to place trials on the same site with uniform environmental conditions and exposing the trees for a longer interval after wounding.

6.3.4 Phenotypic and genetic correlation between wound reactions to other wood properties

Wood properties of 27 *E. bosistoana* families from Woodville Davies and Altaner (2017) were correlated with the wound reactions from same families (Table 6.4). Coefficients of determination showed no phenotypic correlation between wound reactions with wood properties in 27 families (Table 6.4). Likewise, no strong genetic correlation between the axial length of the wound reaction and other properties or tree size was observed. This implied that the wound reaction cannot be used as a proxy measure for those traits. In particular the independence of the wound reaction from tree size is noteworthy as larger trees with large and small wound reaction can be found. This might indicate that the available physiological resources for a tree are not a restricting factor for wound response, at least at young age.

Table 6.4: Genetic and phenotypic correlations between length of axial wound reaction and other wood and tree properties in *E. bosistoana* at age ~2. 95% credibility intervals are given in parentheses.

Traits	Genetic correlation to wound reaction	Phenotypic correlation to wound reaction
Growth-strain	-0.02 (-0.64, 0.60)	0.0001
Acoustic velocity	0.15 (-0.25, 0.55)	0.0009
Density	0.27 (-0.17, 0.70)	0.0003
Stiffness	0.22 (-0.20, 0.64)	0.0014
Volumetric shrinkage	0.26 (-0.25, 0.76)	0.000001
Tree height	0.04 (-0.65, 0.73)	0.0026
Diameter	0.08 (-0.68, 0.84)	0.0158

6.3.5 Variation in starch and tyloses

Starch, which is localised in amyloplasts was detected as black granules with potassium iodide stain. Starch labelling was present in the radial parenchyma cells of healthy sapwood (black arrows, Figure 6.4b, d). This matched observations described in chapter 3 where starch was found in sapwood of 6-year-old *E. bosistoana* trees (Figure 3.3). As with heartwood (Figure 3.3, 4 - 6 cm) amyloplasts were absent from woundwood (Figure 6.4a, c). The loss of starch was observed as a first detectable cytological response in the injured parenchyma cells of *Quercus bicolor* (Swamp white oak) (Wardell & Hart, 1970). Similar observations were reported in the woundwood of *C. japonica* (Nakaba et al., 2017). Longitudinal sections from wounded sapwood xylem showed the presence of starch away from the wound (black arrows, Figure 6.5), similar to formation heartwood (Figure 3.3, 4 - 6 cm).

Vessels were open in healthy sapwood away from the wound (Figure 6.4b, d) whereas they were blocked with tyloses in woundwood (arrows, Figure 6.4a, c). This was similar to heartwood formation (arrows, Figure 3.8, 4-6 cm). Vessels were either blocked by tyloses or open indicating that the wound response was finalised (white arrows, Figure 6.5). This was different to heartwood formation in the transition zone, where vessels in the early stages of tyloses were found towards the cambium (arrows, Figure 3.8, 3 & 7 cm). Schmitt and Liese (1993) reported vessels blocked by tyloses in mechanically wounded *F. sylvatica*, which is consistent with the present study.

Physiological variations in amyloplasts and tylose formation were indistingushable between the families with small (Figure 6.4a, b, Figure 6.5 a) and large (Figure 6.4c, d, Figure 6.5b) wound reaction.

Figure 6.4: Starch-containing amyloplasts stained black with iodine/potassium iodide in longitudinal sections of 1.6-year-old wounded *E. bosistoana* xylem. Top row (a, b): family 2 with small wound reaction; bottom row (c, d): family 24 with large wound reaction. Amyloplasts were absent in woundwood (a, c), but were present in healthy sapwood away from the wound (b, d, black arrows). Tyloses were present in the vessels of woundwood (a, c, white arrows) but were absent in the healthy sapwood away from the wound (b, d). Scale bars = 50 μm.

Figure 6.5: Longitudinal sections from of 1.6-year-old wounded *E. bosistoana* xylem stained for starch with potassium iodide. Amyloplast labelling in radial (black arrows) parenchyma cells was

reduced towards the woundwood. Tyloses (white arrows) were present in the vessels of woundwood, but absent in the vessels in healthy sapwood away from the wound. a) Family 2 with small wound reaction and b) family 24 with large wound reaction. Scale bars = 300 μm.

6.3.6 Variation in extractives using confocal microscopy

Fluorescence emission spectra of parenchyma and fibre cells of woundwood and healthy sapwood from 1.6-year-old stems of *E. bosistoana* as well as heartwood from 7-year-old *E. bosistoana* trees cores were quantified with spectral (λ) scans using a confocal microscope at 405 nm excitation. Fluorescence emission spectra of parenchyma and fibre cells of heartwood, woundwood, and healthy sapwood indicated differences in chemical composition (Figure 6.6). The emission spectra for woundwood were more similar to those of healthy sapwood than those of heartwood. Emission spectra maxima for heartwood were at longer wavelengths reflecting the light-brown 'pinkish' colour of the heartwood (Bootle, 2005). The slight redshift of the emission spectra of from healthy sapwood (472 - 480 nm) to woundwood (476 - 484 nm) agreed with the macroscopic observation of a slightly discoloured wound reaction zone (Figure 6.2). For both, woundwood and healthy sapwood the emission spectra of the fibres were redder than the parenchyma cells. This was reversed in the heartwood, with the parenchyma cells having fluorescence emission maxima at higher wavenumbers, indicating that the heartwood extracts are predominately located in parenchyma cells, what was also found in samples described in chapter 3 (Figure 3.9c, d). Emission spectra for family 24 were consistently shifted to longer wavenumbers indicating a difference in colour between the 2 families. As differences in emission spectra were likely caused by the presence of extractives in heartwood (Koch & Kleist, 2001) and woundwood (Faizal et al., 2017; Harju et al., 2009; Nakaba et al., 2017), the difference between the families could be interpreted as a difference in chemical composition. These in turn could influence timber traits like natural durability. The colour differences in themselves are of interest for appearance grade timber, where a consistent colour is valued (Lambert, 2002).

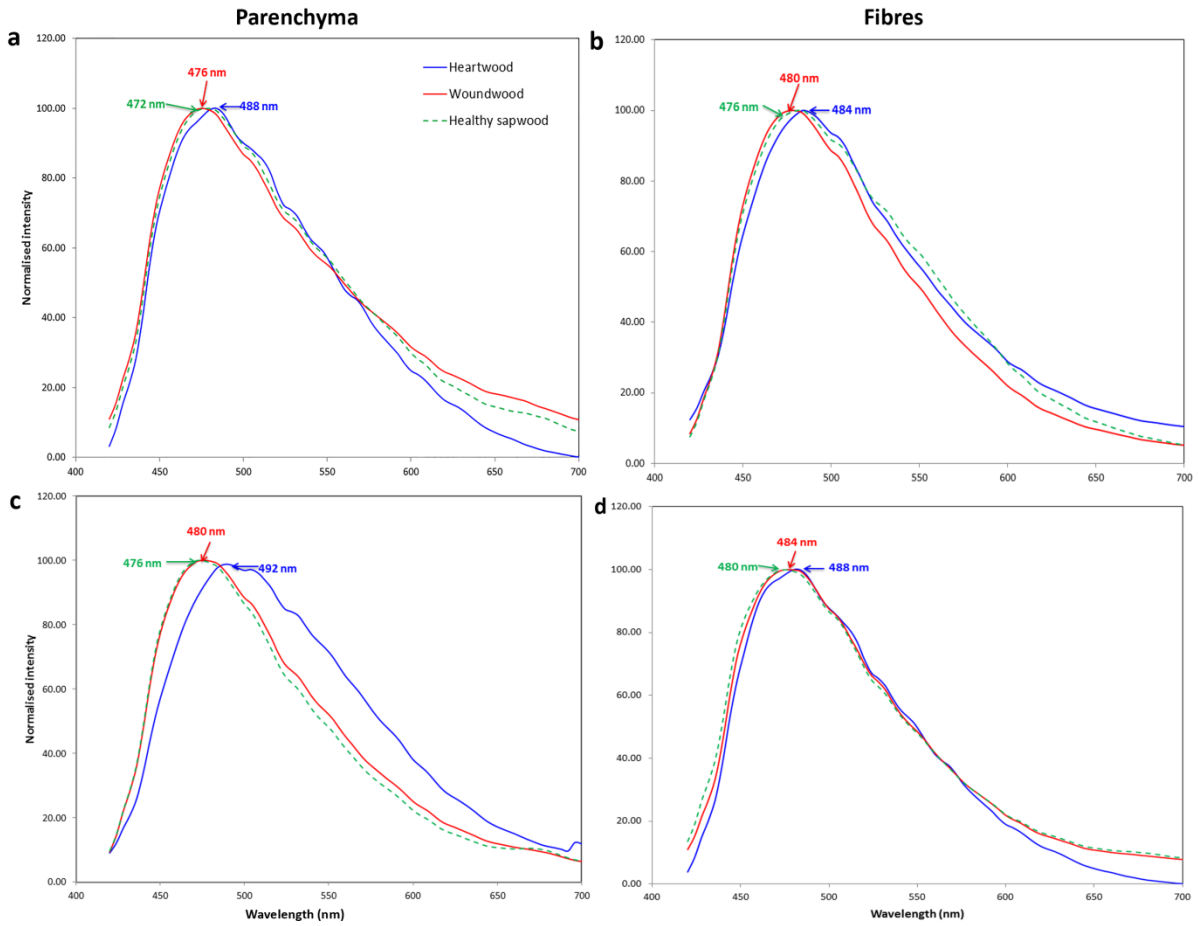

Figure 6.6: Fluorescence emission spectra (λ scans) of parenchyma cells (a, c) and fibre cells (c, d) from heartwood (blue), woundwood (red) and healthy sapwood (green) tissue sections using 405 nm excitation. Family 2 with small wound reaction (a, b) and family 24 with large wound reaction (c, d). Each spectrum is the average of 8 spectra (2 sections of 4 trees each).

6.3.7 GC analysis of woundwood extractives

The chemical compositions of the ethanol extracts of woundwood, heartwood and sapwood were analysed by GC. A typical chromatogram of silylated *E. bosistoana* woundwood, heartwood and sapwood is shown in Figure 6.7 and appendix 2. The chromatograms showed differences in chemical composition of the ethanol extracts between the three wood tissues. Six compounds (benzoic acid, hexadecanoic acid, 1,5-dihdroxy-12-methoxy-3,3-dimethyl-3,4-dihydro-1H-anthra[2,3-c]pyran-6,11-dione, octadecanoic acid, a polyphenol and beta-sitosterol) were identified by comparing the *E. bosistoana* and *E. globoidea* heartwood extracts, which had been previously analysed by GC-MS (chapter 5, Table 5.10) (Schroettke, 2018). In analogy six compounds (tentatively identified as benzoic acid, tentatively identified as hexadecanoic acid, 1,5-dihdroxy-12-methoxy-3,3-dimethyl-3,4-dihydro-1H-anthra[2,3-c]pyran-6,11-dione, octadecanoic acid, polyphenol, and tentatively identified as beta-sitosterol) were identified from sapwood extracts (Table 6.5, Appendix 3). This compares to

reports of hydrophilic *E. camaldulensis* sapwood extracts, for which monosaccharides such as fructose, glucose, another unidentified hexose and polyols such as pinitol and quinic acid were reported to be the main compounds (Benouadah et al., 2018).

Table 6.5: Compounds identified by comparing the chromatograms of silylated *E. bosistoana* sapwood extracts with GC-MS data from *E. globoidea* sapwood (Schroettke, 2018).

Retention times (min)	Chemical compound
10.9	Tentatively identified as benzoic acid
11.5	Tentatively identified as hexadecanoic acid
12.5	1,5-dihdroxy-12-methoxy-3,3-dimethyl-3,4-dihydro-1H-anthra[2,3-c]pyran-6,11-dione
14.1	Octadecanoic acid
25.1	polyphenol
25.2	Tentatively identified as beta-sitosterol

It is interesting to note that the peak at 25.1 min identified as 'polyphenol' in heartwood (Schroettke, 2018) appeared to composed of at least 4 poorly separated compounds, which were better resolved due to more equal concentrations in *E. bosistoana* sapwood and woundwood. The overlapping compound eluating slightly after the polyphenol were identified as beta-sitosterol in sapwood. Beta-sitosterol is a commonly reported sapwood component and was also identified by GC-MS in the sapwood of wounded *F. salvytica* (Vek et al., 2014).

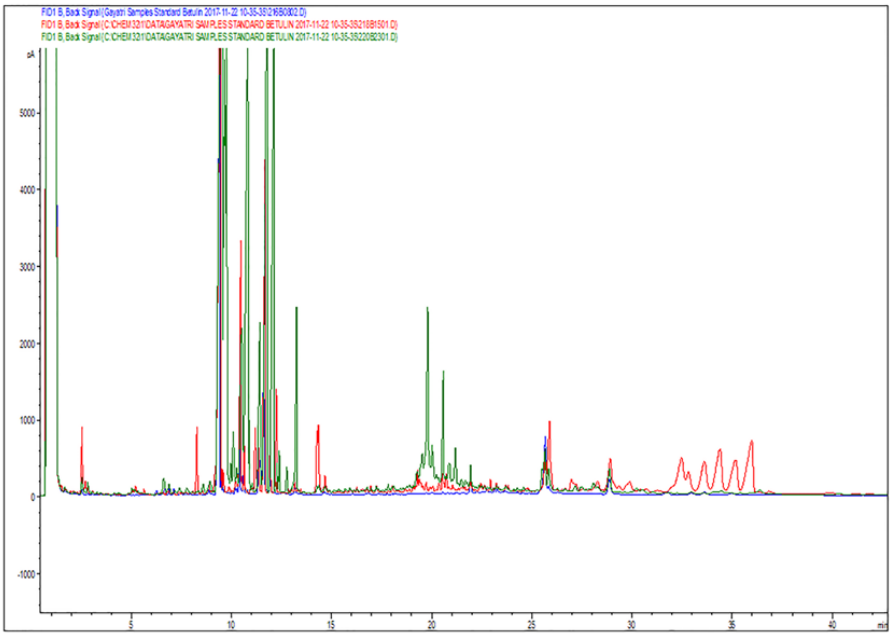

Figure 6.7: Gas chromatograms of silylated ethanol extracts from heartwood (blue), woundwood (red) and sapwood (green) of *E. bosistoana* between 0 and 40 min retention time.

Eyles et al. (2003) reported a diverse range of polyphenolic compounds such as proanthocyanidins, flavonol, flavanone glycosides, stilbene glycosides and hydrolysable tannins such as pedunculagin in the woundwood of *E. globulus* and *E. nitens*. The authors speculated that these compounds impart pathogenic resistance against wood degraders such as white and brown rots. Similarly, the compounds in *E. bosistoana* could act in a synergistic way. However, such compounds were not identified in the woundwood ethanol extracts of *E. bosistoana* by GC-MS analysis after silylation. *E. globulus* and *E. nitens* woundwood extracts have also been analysed by high performance liquid chromatography (HPLC) (Eyles et al., 2003), which offers the advantage of a) being able to identify underivatised compounds and b) not requiring the compounds to enter the gas-phase. It is likely that the databases used to identify the compounds by GC-MS contained only a limited number of silylated compounds Schroettke (2018) and that a large proportion of the ethanol soluble compounds from the *E. bosistoana* wood were too large or hydrophilic to suit GC analysis.

As only a fraction of the extractive compounds was identified in this study, the chemical composition of the extracts was analysed by a principle component analysis of the major 36 compounds. Woundwood extracts were more similar to heartwood extracts than sapwood extracts, as both principle components separated sapwood from woundwood extracts but only principle component 1 separated heartwood from woundwood extracts (Figure 6.8). Woundwood formation was also shown to include the biosynthesis of secondary metabolites by parenchyma cells in *C. japonica* and *P. taeda* (Loblolly pine) (Nakaba et al., 2017; Shain, 1967). This agreed with our observations.

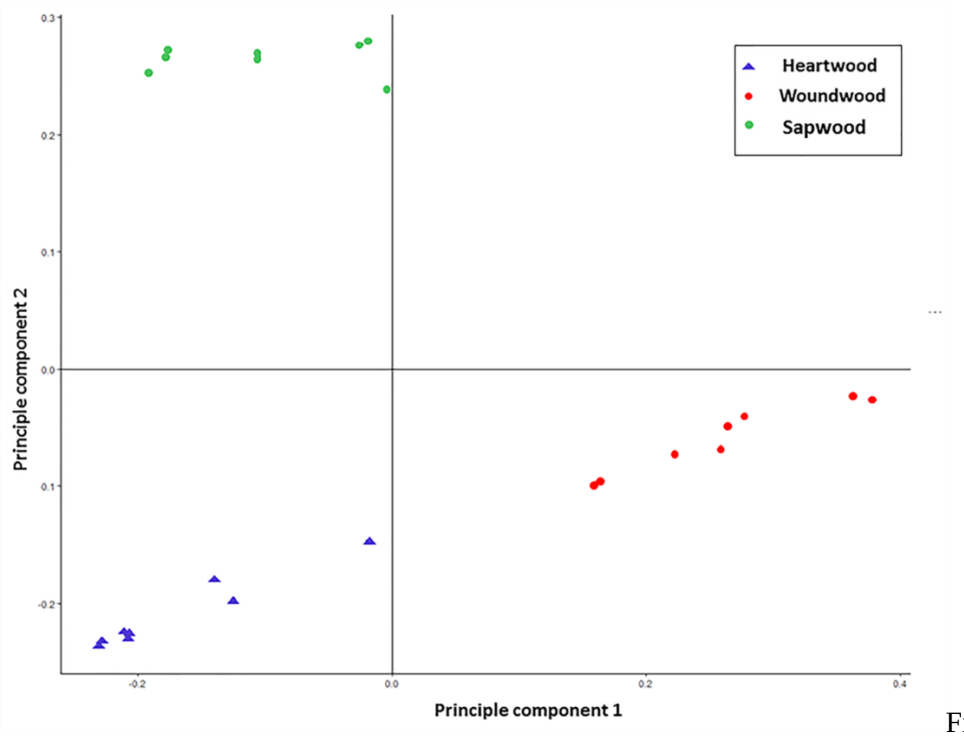

Figure 6.8: Principal component analysis of the composition of ethanol extracts of *E. bosistoana* heartwood, woundwood and healthy sapwood near woundwood using 36 major compounds.

The loadings of principle components give insight into the nature of the differences between the extracts. Principal component 1, which separated woundwood from sapwood and heartwood was dominated by the compound at the retention time 9.0 min followed by those at 11.2, 25.1 ('polyphenol'), 9.2 and 10.2 min (Figure 6.9). As the loadings were negative, ethanol extracts of woundwood contained less of these compounds.

Similarly, Figure 6.10 represents the loadings of the second principle component, which differentiated sapwood from woundwood and heartwood. The loadings of the compounds at the retention times 9.1, 9.2, 10.2, 11.5 ('tentatively identified as hexadecanoic acid') min were positive and therefore, sapwood contained higher amounts of these than heartwood and woundwood. The loadings of the compounds at the retention times 9.0, 9.9, 11.2 and 25.1 ('polyphenol') min were negative suggesting lower concentrations in sapwood than heartwood and woundwood.

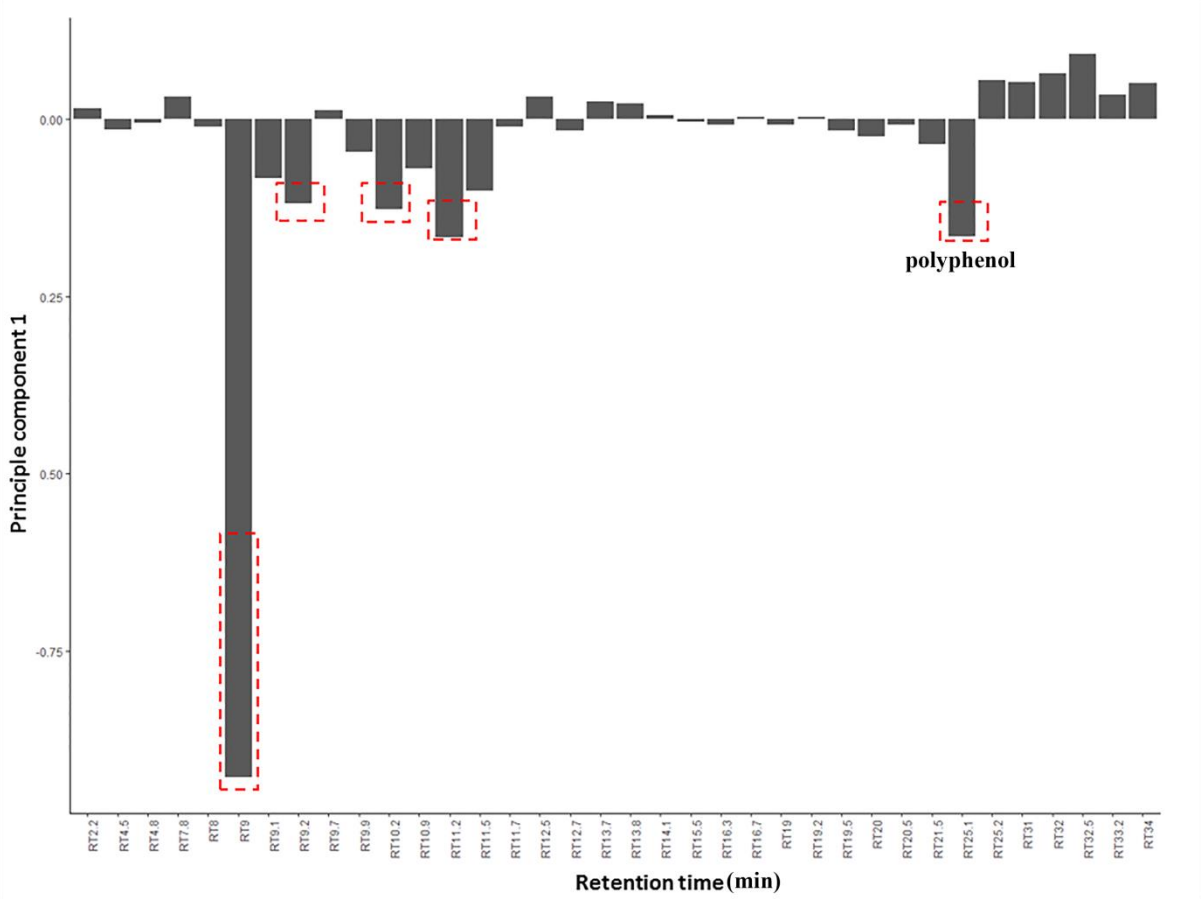

Figure 6.9: The loadings of principle component 1 separating the chemical composition of woundwood, sapwood and heartwood ethanol extract. Important compounds are highlighted in red boxes.

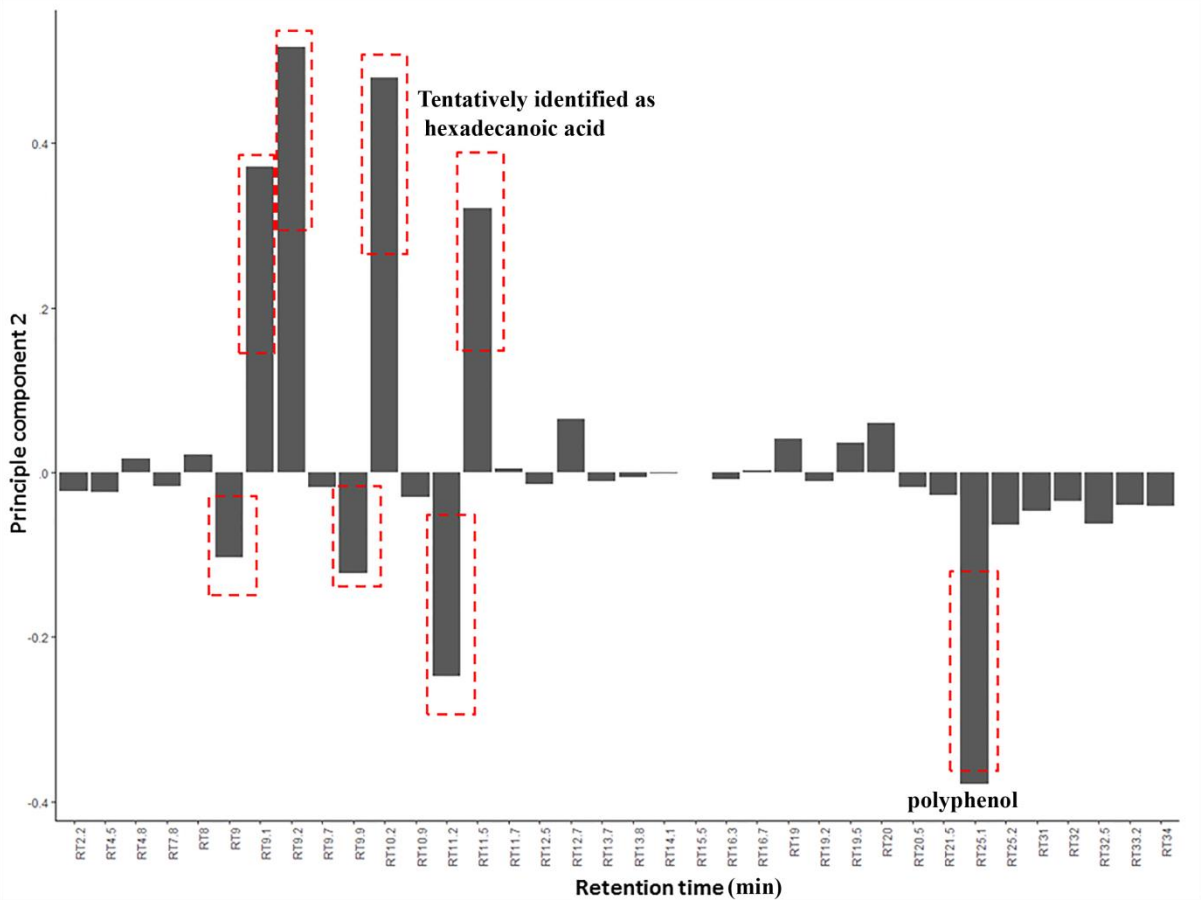

Figure 6.10: The loadings of principle component 2 separating the chemical composition of woundwood, sapwood and heartwood ethanol extract. Important compounds are highlighted in red boxes.

Figure 6.11 shows variation in compounds between heartwood, woundwood and sapwood. Compounds at the retention times 31.0, 32.5, 33.2 and 34.0 min were present in heartwood and woundwood, but not in sapwood.

Statistical analysis (ANOVA) showed significant variation in all the 36 compounds between ethanol extracts of heartwood, woundwood and sapwood near woundwood (Appendix 4). However, t-test revealed that some compounds occurred in the same concentration in two of the three extract types. Woundwood contained the same amounts of compounds eluting after 9.9, 11.2 and 20.5 min as sapwood (Appendix 5) and the same amount of the compound eluating at 19.2 min as heartwood (Appendix 6). This was in general consitent with observation by Vek et al. (2014), who reported differences in the extractive composition of woundwood and heartwood of *F. sylvatica*. Hydrophilic extracts of *F. sylvatica* woundwood were reported to consist of soluble sugars and phenolic compounds, e.g. catechin, which was different from extractives composition in heartwood.

Similarly t-tests showed that *E. bosistoana* heartwood and sapwood differed in most of the quantified compounds, except for those with retention times of 9.7, 11.7, 12.5 (1,5-dihdroxy-12-methoxy-3,3-

dimethyl-3,4-dihydro-1H-anthra[2,3-c]pyran-6,11-dione) and 14.1 (octadecanoic acid) min (Appendix 7).

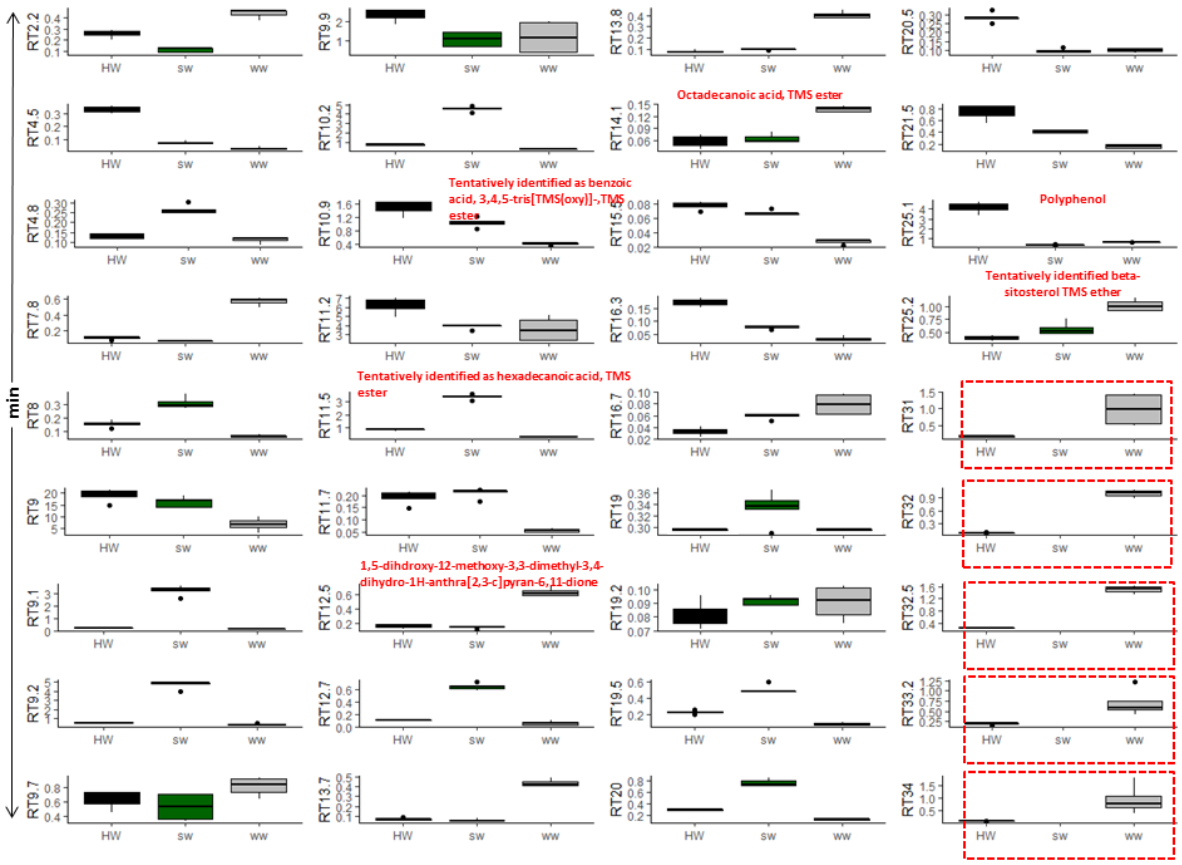

Figure 6.11: Box-and-whisker plots showing variation in amount of heartwood (HW, black), sapwood (SW, green) and woundwood (WW, grey) compounds in *E. bosistoana*. Compounds at the retention times 31.0, 32.0, 32.5, 33.2 and 34.0 min highlighted by a red box were absent from sapwood.

The variation in heartwood, woundwood and sapwood compounds in *E. bosistoana* ethanol extracts from two families chosen for large (family 24) and small (family 2) wound reaction are shown as box-plots in Figures 6.12 - 6.14. The significance of the difference in the abundance of each compound in the extracts of the two families was assessed by t-tests (Appendixes 8). Several compounds showed significant variability between both families, indicating genetic control over the chemical composition of wood extracts. However, of the compounds, which have been shown inhibit fungal growth (Chapter 5), only hexadecaonic acid contents differed significantly ($P = < 0.001$) in the woundwood between the two families. No statistical significant differences in contentations ofhexadeconic acid contents in sapwood and heartwood or the compound eluating at 10.2 min were found. It has to be kept in mind that the other heartwood compounds, not extracted with ethanol or quantified by GC, can be under genetic control and contribute to the variability in durabilty of *E. bosistoana* families.

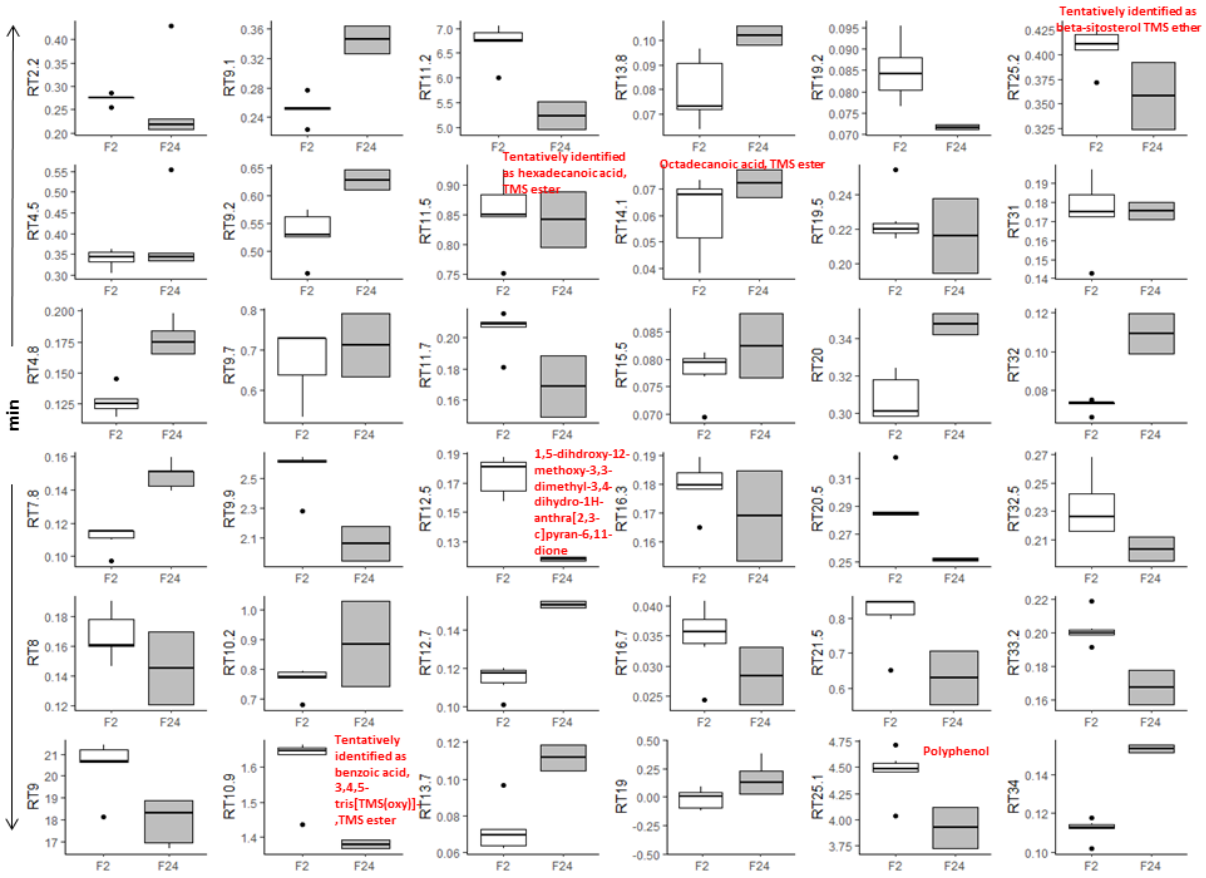

Figure 6.12: Box-and-whisker plots representing variation in the amount of heartwood compounds between two different *E. bosistoana* families (F2 – small and F24 – large wound reaction).

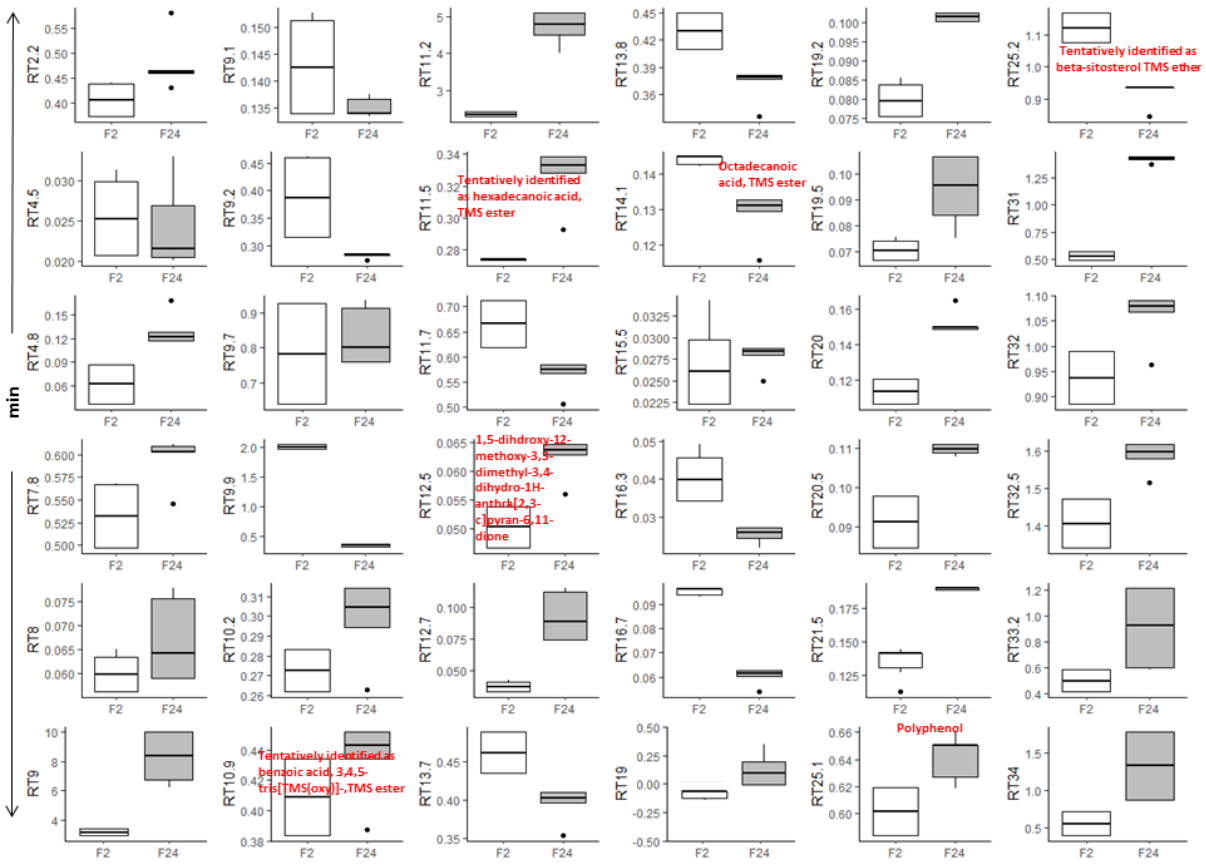

Figure 6.13: Box-and-whisker plots representing variation in amount of woundwood compounds in *E. bosistoana* between two different families (F2–family with small wound reaction and F24-family with large wound reaction).

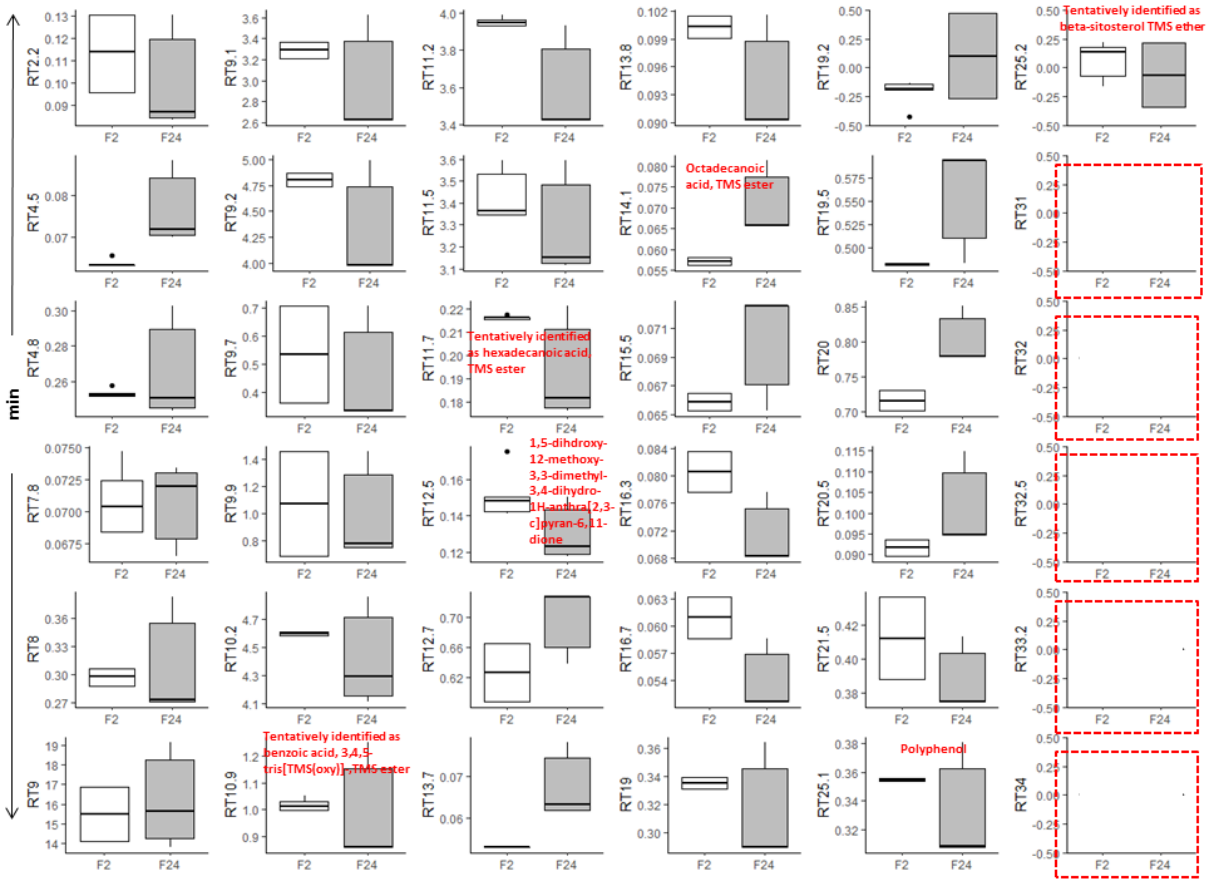

Figure 6.14: Box-and-whisker plots representing variation in amount of sapwood compounds in *E. bosistoana* between two different families (F2–family with small wound reaction and F24-family with large wound reaction). Compounds at the retention times 31.0, 32.0, 32.5, 33.2 and 34.0 min highlighted by a red box were not present in sapwood.

6.4 Conclusion

The extension of the axial wound response of ~1.6-year-old *E. bosistoana* was found to be under weak genetic control, with a heritability (h^2) of 0.26 with a 95% credibility interval of 0.00 to 0.53. However, no correlation between the axial wound response in the ~1.6-year-old trees and heartwood features in 7-year-old trees was found. Therefore, it is not possible to assess heartwood formation early in an *E. bosistoana* breeding programme by measuring the axial wound response in ~1.6-year-old trees.

Microscopic observations showed the woundwood and heartwood of *E. bosistoana* showed parenchyma cells devoid of the storage material starch and vessels blocked with tyloses. Red shift of autofluorescence emission spectra indicted presence of extractives heartwood, in particular located in the parenchyma cells. Woundwood spectra were more similar to sapwood spectra and no preferred accumulation of extractives was found in the parenchyma cells. The peak of fluorescence for all

tissues and cell types was at longer wavelengths for a family chosen for large wound reaction compared to one chosen for small wound reaction.

GC analysis showed variation in the composition of woundwood, heartwood and sapwood ethanol extracts of *E. bosistoana*. Woundwood extracts differed from sapwood more than from heartwood, suggesting some similarities between woundwood and heartwood and consequently indicating similar metabolic pathways. Further, the data indicated genetic control of the extractive composition as statistical significant differences in the abundance of compounds were found between two *E. bosistoana* families. Genetic control over the extractive chemistry is likely to reflect wood properties like natural durability or colour. These are important traits in the breeding programme of *E. bosistoana*.

Finally, ethanol heartwood extracts of *E. bosistoana* contained large quantities of larger, hydrophilic compounds, for which the chosen analytical method of GC after silylation was not ideal. It is likely that these compounds can be better identified by liquid chromatography.

6.5 References

Altaner, C. (2017). SFF grant 407602 - Milestone M-3461: Woodville harvest (Summer 2016/17). New Zealand: School of Forestry, University of canterbury.

Armstrong, J., Shigo, A., Funk, D., McGinnes, E., & Smith, D. (1981). A macroscopic and microscopic study of compartmentalization and wound closure after mechanical wounding of black walnut trees. *Wood and Fiber Science, 13*, 275-291.

Barry, K., Davies, N., & Mohammed, C. (2001). Identification of hydrolysable tannins in the reaction zone of *Eucalyptus nitens* wood by high performance liquid chromatography–electrospray ionisation mass spectrometry. *Phytochemical Analysis, 12*, 120-127.

Bauch, J., Shigo, A., & Starck, M. (1980). Wound effects in the xylem of *Acer* and *Betula* species. *Holzforschung, 34*, 153-160.

Benouadah, N., Pranovich, A., Aliouche, D., Hemming, J., Smeds, A., & Willför, S. (2018). Analysis of extractives from *Pinus halepensis* and *Eucalyptus camaldulensis* as predominant trees in Algeria. *Holzforschung, 72*, 97-104.

Bootle, K. R. (2005). Wood in Australia.Types, properties, and uses (2nd ed.): Australia: McGraw-Hill.

Busgen, M., Munch, E., & Thomson, T. (1929). *The structure and life of forest trees*. London, England: Chapman & Hall.

Bush, D., McCarthy, K., & Meder, R. (2011). Genetic variation of natural durability traits in *Eucalyptus cladocalyx* (sugar gum). *Annals of Forest Science, 68*, 1057–1066.

Chattaway, M. M. (1952). The sapwood-heartwood transition. *Australian Forestry, 16*, 25-34.

Davies, N., & Altaner, C. (2017). SFF grant 407602 - Milestone M-3462: Wood properties (Summer 2016/17). New Zealand: School of Forestry, University of Canterbury.

Davies, N. T., Sharma, M., Altaner, C. M., & Apiolaza, L. A. (2015). *Screening eucalypts for growth-strain.* Paper presented at the "8th Plant Biomechanics International Conference, Nagoya.

Eyles, A., Davies, N. W., & Mohammed, C. (2003). Wound wood formation in *Eucalyptus globulus* and *Eucalyptus nitens*: anatomy and chemistry. *Canadian Journal of Forest Research, 33*, 2331-2339.

Faizal, A., Esyanti, R. R., Aulianisa, E. N., Santoso, E., & Turjaman, M. (2017). Formation of agarwood from *Aquilaria malaccensis* in response to inoculation of local strains of *Fusarium solani*. *Trees, 31*, 189-197.

Gadgil, P., & Bawden, A. (1981). Infection of wounds in *Eucalyptus delegatensis*. *New Zealand Journal of Forestry Science, 11*, 262-270.

Harju, A. M., Venäläinen, M., Laakso, T., & Saranpää, P. (2009). Wounding response in xylem of Scots pine seedlings shows wide genetic variation and connection with the constitutive defence of heartwood. *Tree physiology, 29*, 19-25.

Hillis, W. E. (1987). *Heartwood and tree exudates*. New York: Springer.

Horikosh, M., Tang, Y., Dickey, A., Grenié, M., Thompson, R., Selzer, L., Strbenac, D., & Voronin, K. (2018). Package for data visualization tools for statistical analysis results (version-0.4.5).

Jorgensen, E. (1961). The formation of pinosylvin and its monomethyl ether in the sapwood of *Pinus resinosa*. *Canadian Journal of Botany, 39*, 1765-1772.

Koch, G., & Kleist, G. (2001). Application of scanning UV microspectrophotometry to localise lignins and phenolic extractives in plant cell walls. *Holzforschung, 55*, 563-567.

Lambert, J. (2002). *Blackwood features in demand: A victorian case study*. Paper presented at the Blackwood Management: Learning from New Zealand. Proceedings of an international workshop, Rotorua, New Zealand.

Li, Y. (2018). *Use of near infrared spectroscopy to predict wood traits in Eucalyptus species.* Doctor of Philosophy in Forestry. University of Canterbury, Christchurch, New Zealand.

Li, Y., & Altaner, C. (2018). Predicting extractives content of *Eucalyptus bosistoana* F. Muell. Heartwood from stem cores by near infrared spectroscopy. *Spectrochimica Acta Part A: Molecular and Biomolecular Spectroscopy, 198*, 78-87.

Li, Y., Apiolaza, L. A., & Altaner, C. (2018). Genetic variation in heartwood properties and growth traits of *Eucalyptus bosistoana*. *European Journal of Forest Research*, 1-8.

Liese, W., & Dujesiefken, D. (1990). Principles of compartmentalisation in trees. *11*, 129-130.

Lowerts, G., Wheeler, E., & Kellison, R. C. (2007). Characteristics of wound-associated wood of yellow-poplar (*Liriodendron tulipifera* L.). *Wood and Fiber Science, 18*, 537-552.

Mevik, B., Wehrens, R., & Hovde, L. (2015). Partial least squares and principal component regression. R package version. 2.5-0.

Mireku, E., & Wilkes, J. (1989). Seasonal variation in the ability of the sapwood of *Eucalyptus maculata* to compartmentalize discolouration and decay. *Forest Ecology and Management, 28*, 131-140.

Nakaba, S., Morimoto, H., Arakawa, I., Yamagishi, Y., Nakada, R., & Funada, R. (2017). Responses of ray parenchyma cells to wounding differ between earlywood and latewood in the sapwood of *Cryptomeria japonica*. *Trees, 31*, 27-39.

Schmitt, U., & Koch, G. (2009). Characterisation of wound reaction compounds in the xylem of *Tilia americana* L. by electron microscopy and cellular uv. *New Zealand Journal of Forestry Science, 39*, 233-241.

Schmitt, U., & Liese, W. (1993). Response of xylem parenchyma by suberization in some hardwoods after mechanical injury. *Trees, 8*, 23-30.

Schroettke, N. (2018). Natural variability in the extract composition of *Eucalyptus globoidea.* Master's thesis for obtaining the academic degree, Master of science in forestry. Center for forestry, Institute of hemical Wood Technology. University of Hamburg, Germany.

Shain, L. (1967). Resistance of sapwood in stems of loblolly pine to infection by *Fomes annosus*. *Phytopathology, 57*, 1034-1045.

Shigo, A. (1976). microorganisms isolated from wounds inflicted on red maple paper birch American beech and red oak in winter, summer, and autumn. *Phytopathology*. *11*, 197-222.

Shigo, A. L. (1984). Compartmentalization - a conceptual framework for understanding how trees grow and defend themselves. *Annual Review of Phytopathology, 22*, 189-214.

Shigo, A. L., & Hillis, W. E. (1973). Heartwood, discolored wood, and microorganisms in living trees. *Annual Review of Phytopathology, 11*, 197-222.

Spicer, R. (2005). Senescence in secondary xylem: Heartwood formation as an active developmental program. In M. N. Holbrook & M. A. Zwieniecki (Eds.), *Vascular Transport in Plants* (pp. 457-475). San Diego, SD: Elsevier Academic Press.

Taylor, A. M., Gartner, B. L., & Morrell, J. J. (2002). Heartwood formation and natural durability- A review. *Wood and Fiber Science, 34*, 587-611.

Team, R. C. (2013). *R: A language and environment for statistical computing*. Vienna, Austria.

Torelli, N., Križaj, B., & Oven, P. (1994). *Barrier zone (CODIT) and wound-associated wood in beech (Fagus sylvatica L.)*, 279-284.

Vek, V., Oven, P., Ters, T., Poljanšek, I., & Hinterstoisser, B. (2014). Extractives of mechanically wounded wood and knots in beech. *Holzforschung, 68*, 529-539.

Wardell, J., & Hart, J. (1970). Early responses of sapwood of *Quercus bicolor* to mechanical injury. *Canadian Journal of Botany, 48*, 683-686.

White, D., & Kile, G. (1993). Discolouration and decay from artificial wounds in 20-year-old *Eucalyptus regnans*. *Forest Pathology, 23*, 431-440.

Wickham, H. (2009). ggplot2: Elegant Graphics for Data Analysis Springer-Verlag New York.

Yamada, T. (1998). Contribution of active defense responses in the limitation of fungal spread in the sapwood of living sugi (*Cryptomeria japonica*) tree. *Journal of Forest Research, 3*, 103-109.

Yu, Q., Yang, D.-Q., Zhang, S., Beaulieu, J., & Duchesne, I. (2003). Genetic variation in decay resistance and its correlation to wood density and growth in white spruce. *Canadian Journal of Forest Research, 33*, 2177-2183.

6.6 Appendixes

Appendix 1: Wound reactions, extractive content and diameter of heartwood data aggregated for each family

Family	Number of samples	Mean Wound reaction (cm)	SDEV	CV (%)	Mean Heartwood extractives content (%) (cores)	SDEV	CV (%)	Mean Heartwood diameter (mm) (cores)	SDEV	CV (%)
1	18	1.02	0.48	47	5.15	2.42	47	14.14	17.97	127
2	22	0.91	0.60	66	4.31	2.43	57	22.06	18.74	85
3	22	0.85	0.28	34	3.97	2.13	54	17.81	21.21	119
4	14	0.75	0.37	49	3.11	1.80	58	29.85	29.82	100
5	17	1.21	0.74	61	5.13	3.80	74	10.50	14.01	133
7	21	0.77	0.36	47	4.08	2.15	53	12.23	13.39	109
14	20	1.23	0.90	74	5.88	1.39	24	19.05	19.93	105
16	20	0.95	0.40	42	5.66	1.34	24	20.96	22.07	105
18	19	0.95	0.31	33	5.17	2.19	42	28.84	23.20	80
19	21	1.17	0.39	33	6.05	2.24	37	18.00	19.49	108
20	17	0.91	0.33	36	5.19	1.23	24	21.00	22.79	109
21	19	1.17	0.67	57	4.77	2.15	45	11.81	17.55	149
22	12	1.14	0.54	48	3.49	2.21	64	11.08	17.39	157
23	17	1.17	0.35	30	5.62	2.36	42	17.32	19.99	115
24	21	1.05	0.38	36	5.46	2.41	44	30.94	25.17	81
25	17	1.17	0.49	42	3.83	2.54	66	21.78	16.71	77
27	18	0.91	0.66	73	4.87	1.72	35	29.92	22.17	74
28	21	0.86	0.46	53	5.95	2.55	43	17.56	16.40	93
31	20	1.10	0.40	37	4.22	3.34	79	18.45	17.76	96
32	21	1.11	0.36	33	6.10	2.64	43	14.87	19.15	129
40	15	1.00	0.36	36	4.395	1.85	42	18.10	23.40	129
41	11	0.85	0.44	51	3.97	2.12	53	19.05	23.05	121
42	15	0.84	0.43	51	4.50	2.27	50	16.41	18.18	111
44	13	1.21	0.53	44	6.11	4.50	74	11.75	15.09	128
49	18	0.94	0.44	46	5.84	2.66	46	10.58	12.06	114
50	13	1.05	0.47	45	6.21	2.39	38	19.60	22.02	112
51	8	1.64	0.67	41	6.03	1.86	31	14.57	15.59	107
All	470	1.03	0.47	46	5.00	2.32	48	18.45	19.42	110

Appendix 2: Gas chromatograms of silylated ethanol extracts from heartwood (blue), woundwood (red) and sapwood (green) of *E. bosistoana* with retention times.

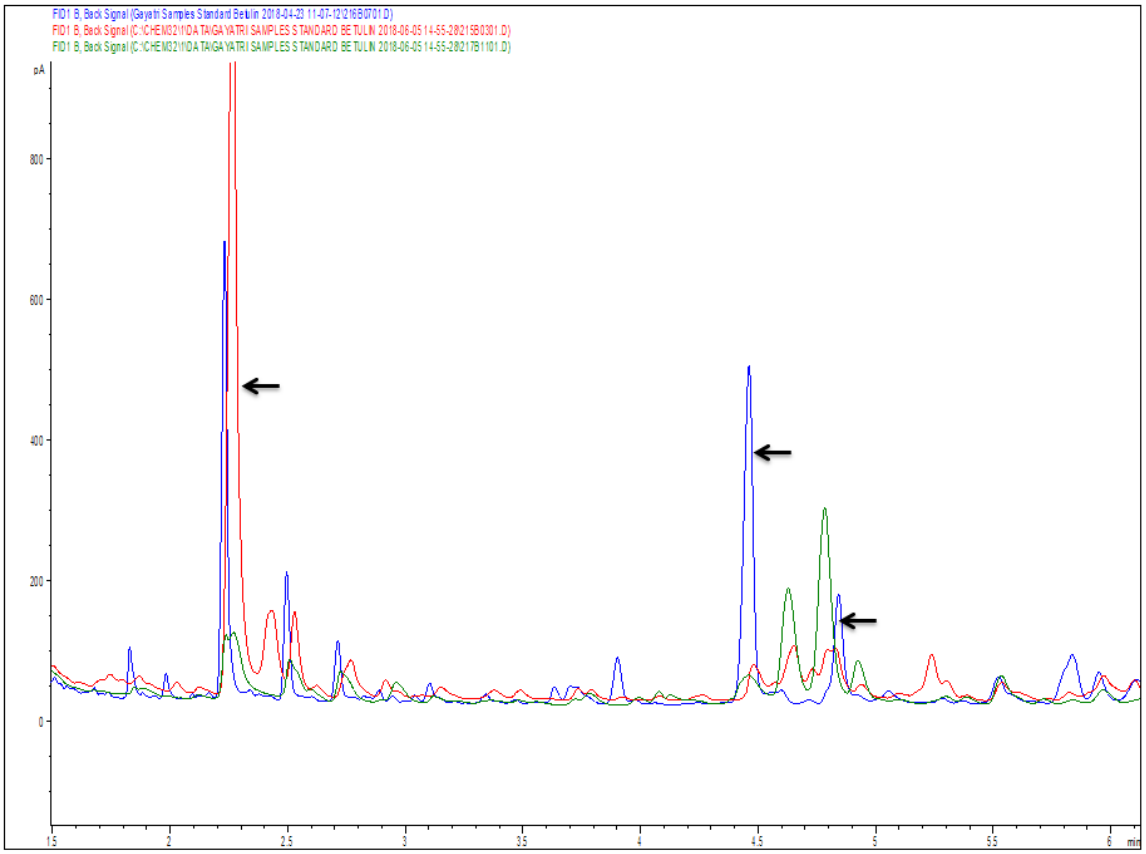

Figure 1: Gas chromatograms of silylated ethanol extracts from heartwood (blue), woundwood (red) and sapwood (green) of *E. bosistoana* between 1.5 and 6 min retention time. Indicated peaks (arrows) at the retention times 2.2, 4.5, and 4.8 min were selected for further analysis.

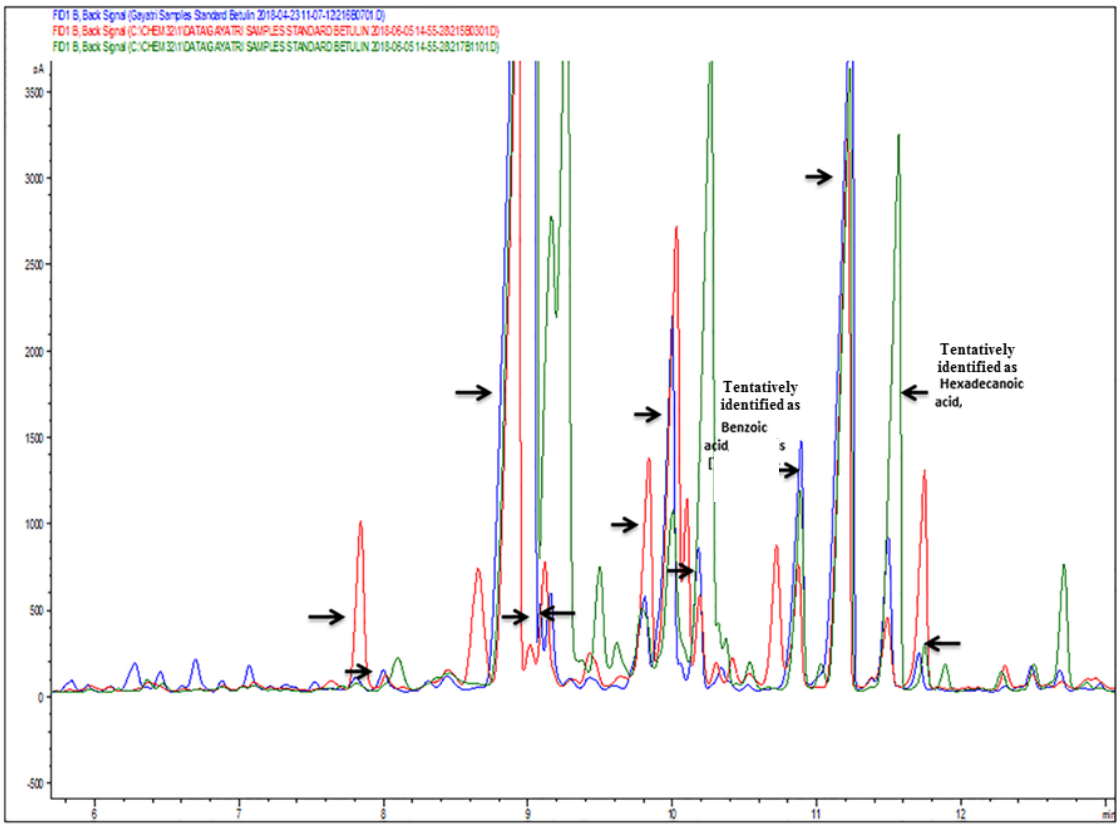

Figure 2: Gas chromatograms of silylated ethanol extracts from heartwood (blue), woundwood (red) and sapwood (green) of *E. bosistoana* between 6 and 12 min retention time. Indicated peaks (arrows) at the retention times 7.8, 8.0, 9.0, 9.1, 9.2, 9.7, 9.9, 10.2, 10.9, 11.2, 11.5 and 11.7 min were selected for further analysis. Compound identified at the retention times 10.9 and 11.5 min by comparing the data with that of Schroettke (2018).

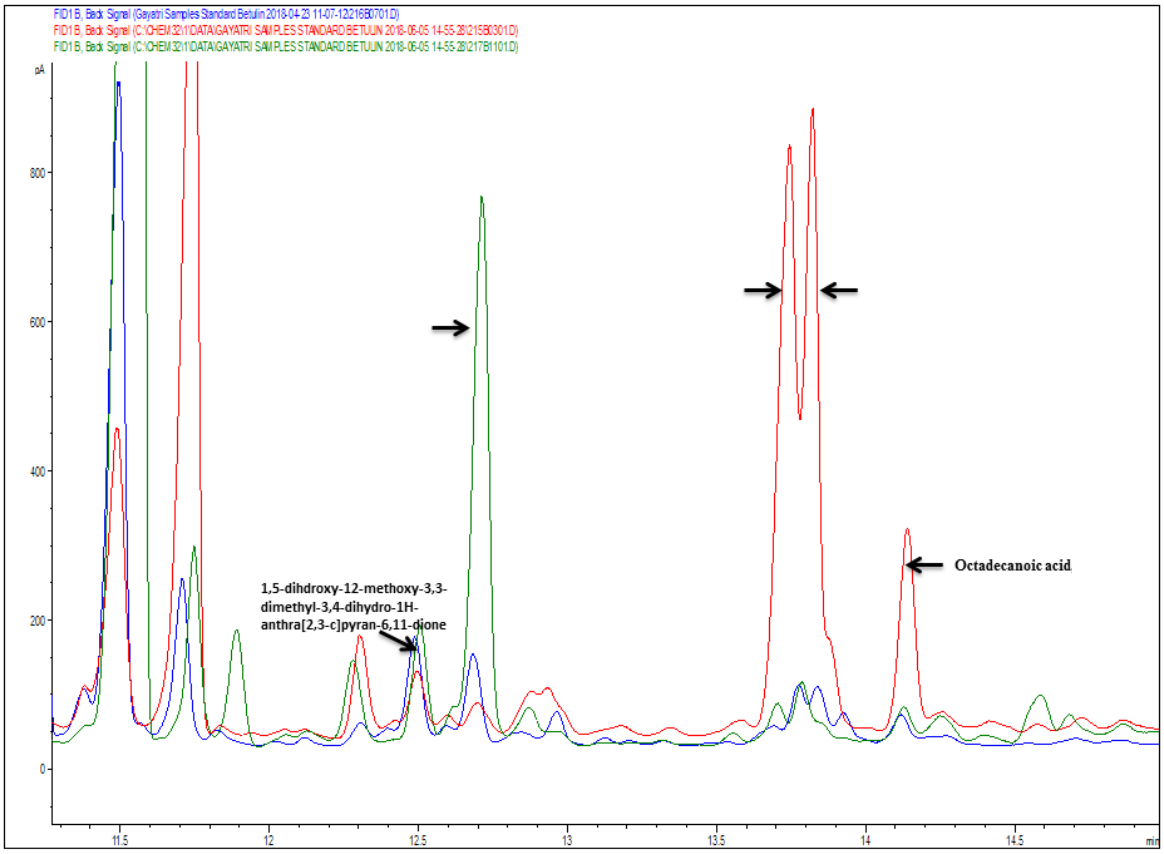

Figure 3: Gas chromatograms of silylated ethanol extracts from heartwood (blue), woundwood (red) and sapwood (green) of *E. bosistoana* between 11.5 and 14.5 min retention time. Indicated peaks (arrows) at the retention times 12.5, 12.7, 13.7, 13.8 and 14.1 were selected from both the families for further analysis**.** Compound identified at the retention times 12.5 and 14.1 min by comparing the chromatograms of *E. bosistoana* heartwood extracts with *E. globoidea* Schroettke (2018).

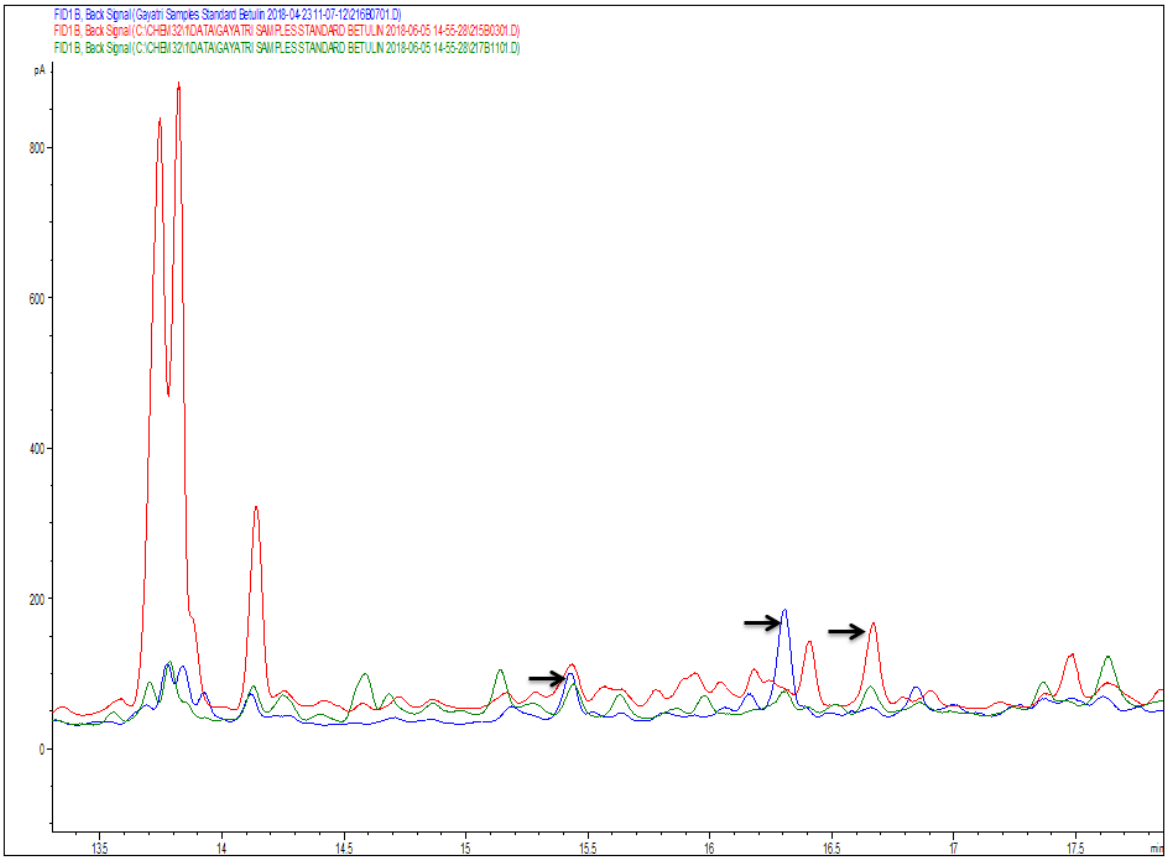

Figure 4: Gas chromatograms of silylated ethanol extracts from heartwood (blue), woundwood (red) and sapwood (green) of *E. bosistoana* between 13.5 and 17.5 min retention time. Indicated peaks (arrows) at the retention times 15.5, 16.3 and 16.7 min were selected from both the families for further analysis**.**

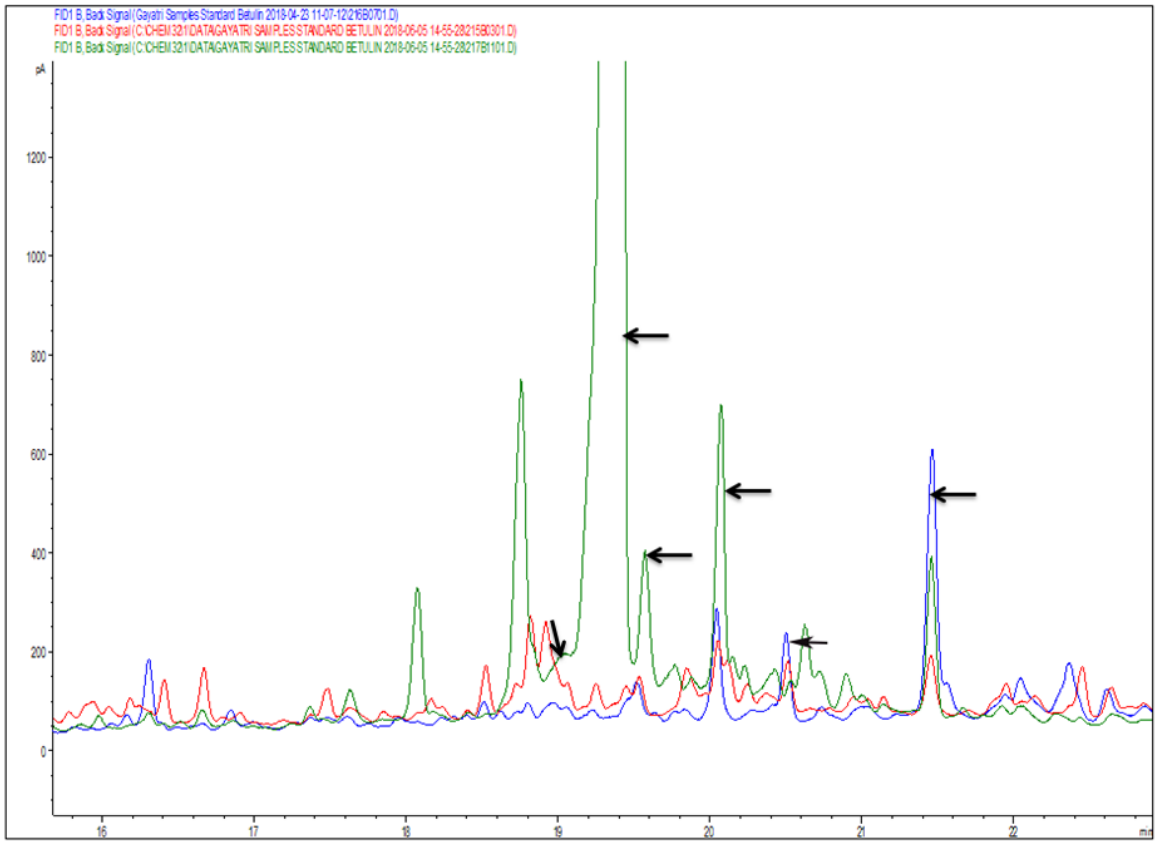

Figure 5: Gas chromatograms of silylated ethanol extracts from heartwood (blue), woundwood (red) and sapwood (green) of *E. bosistoana* between 16 and 22 min retention time. Indicated peaks (arrow) at the retention times 19.0, 19.2, 19.5, 20.0, 20.5 and 21.5 min were selected from both the families for further analysis.

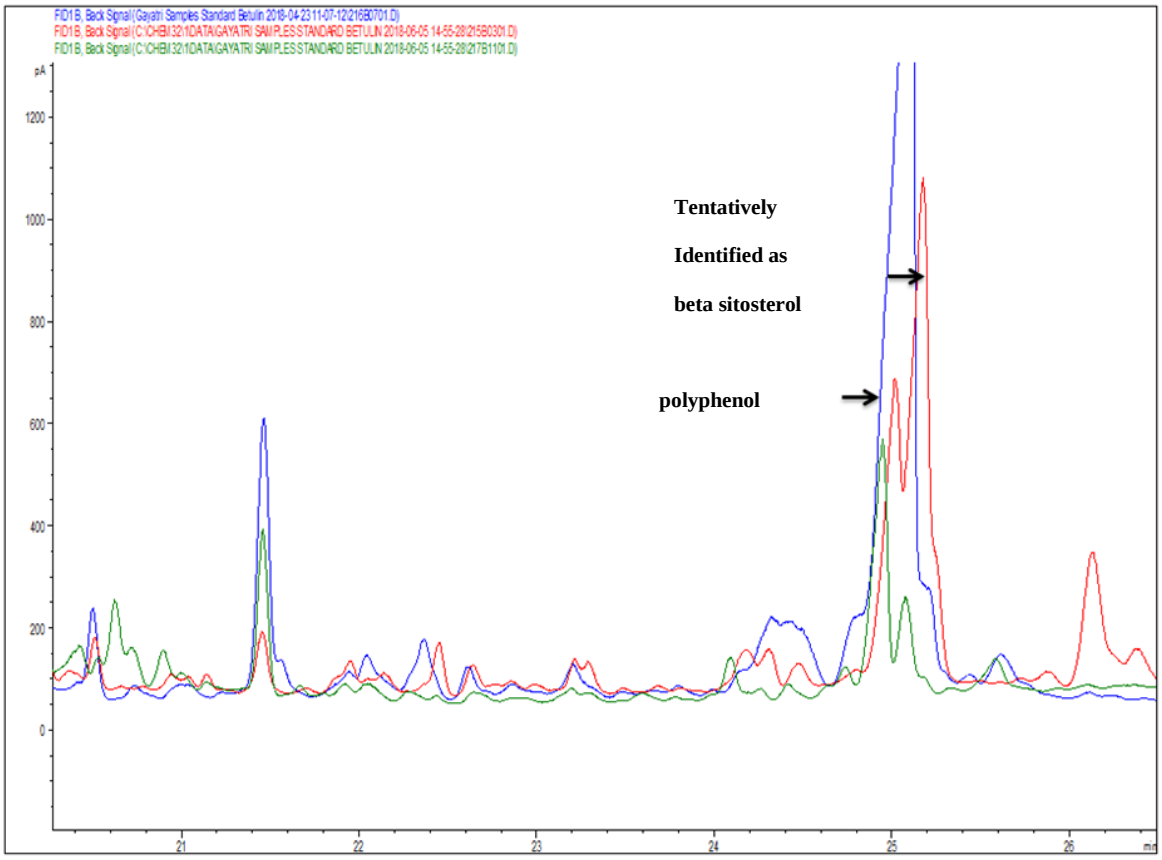

Figure 6: Gas chromatograms of silylated ethanol extracts from heartwood (blue), woundwood (red) and sapwood (green) of *E. bosistoana* between 21 and 26 min retention time. Indicated peaks (arrow) at the retention times 25.1 and 25.2 min were selected from both the families for further analysis. Compound identified at the retention times 25.1 and 25.2 min by comparing the chromatograms of *E. bosistoana* heartwood extracts with *E. globoidea* Schroettke (2018).

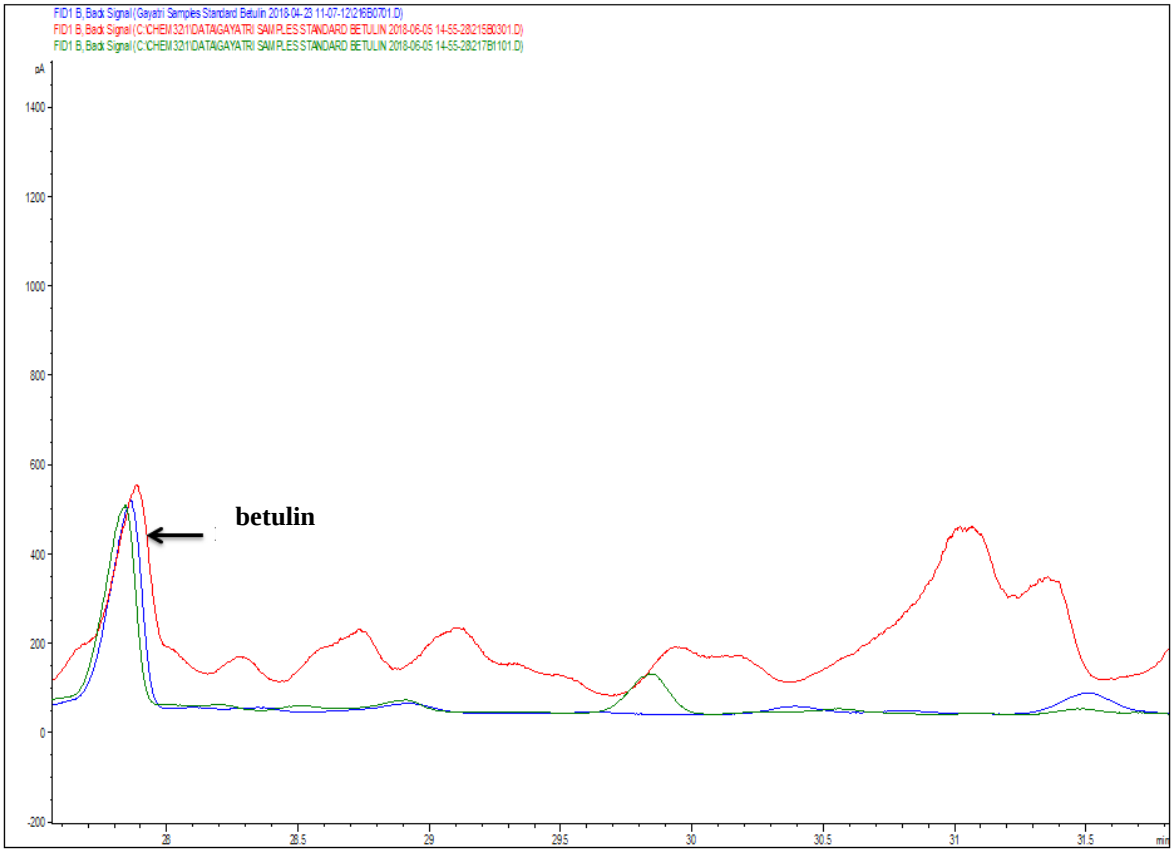

Figure 7: Gas chromatograms of silylated ethanol extracts from heartwood (blue), woundwood (red) and sapwood (green) of *E. bosistoana* between 27 and 31.5 min retention time. Standard (betulin) at 27.9 min (arrow).

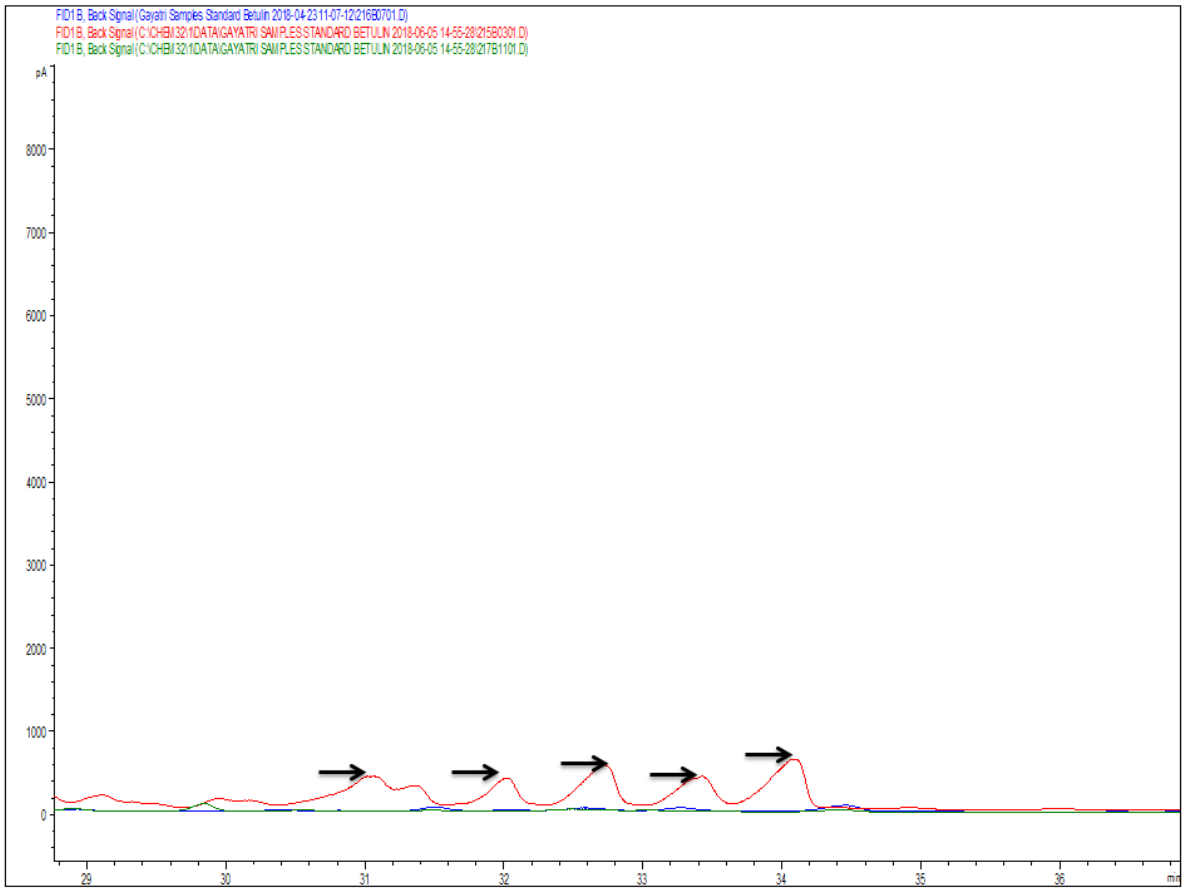

Figure 8: Gas chromatograms of silylated ethanol extracts from heartwood (blue), woundwood (red) and sapwood (green) of *E. bosistoana* between 29 and 36 min retention time. Indicated peaks (arrow) at the retention times 31.0, 32.0, 32.5, 33.2 and 34.0 min were selected from both the families for further analysis.

Appendix 3: Gas chromatograms of silylated ethanol extracts from sapwood of *E. bosistoana* (red) and *E. globoidea* (blue) with retention times.

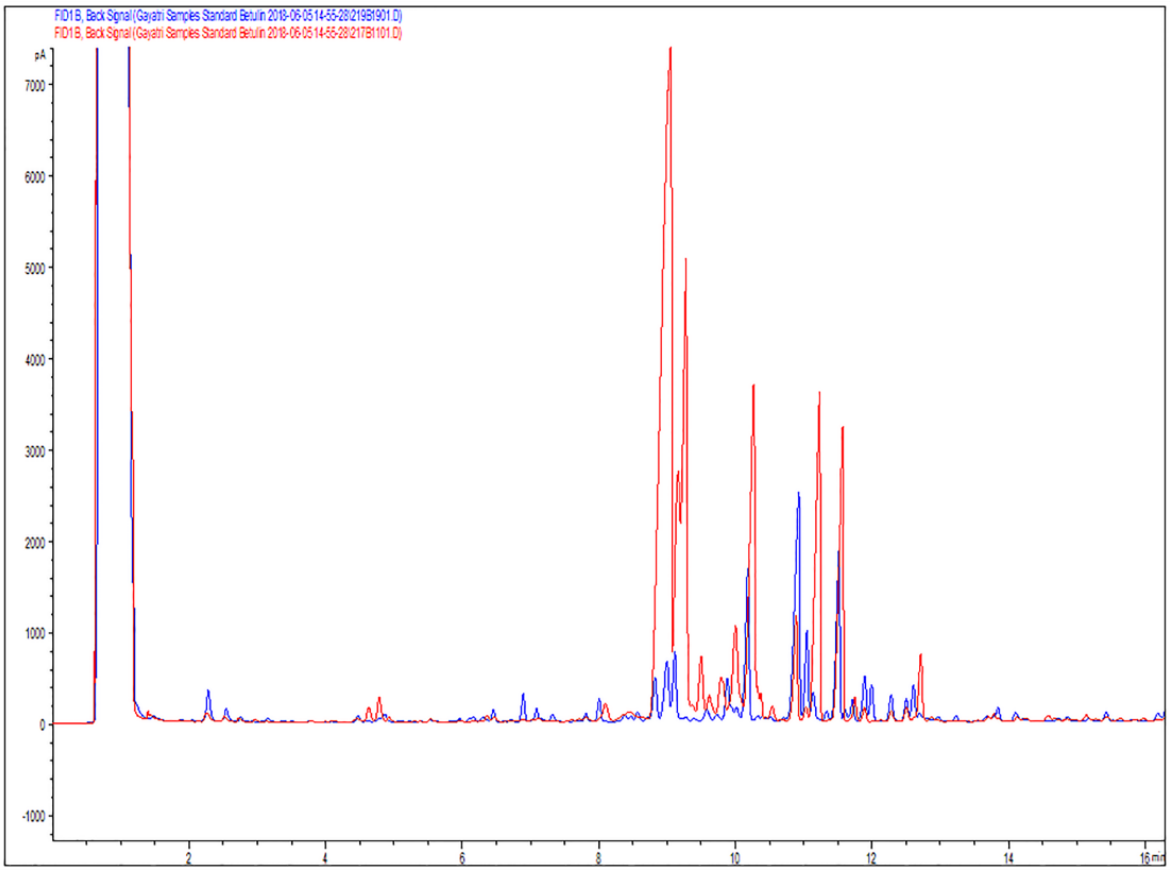

Figure 1: Gas chromatograms of silylated ethanol extracts from sapwood of *E. bosistoana* (red) and *E. globoidea* (blue) from 2 to 14 min.

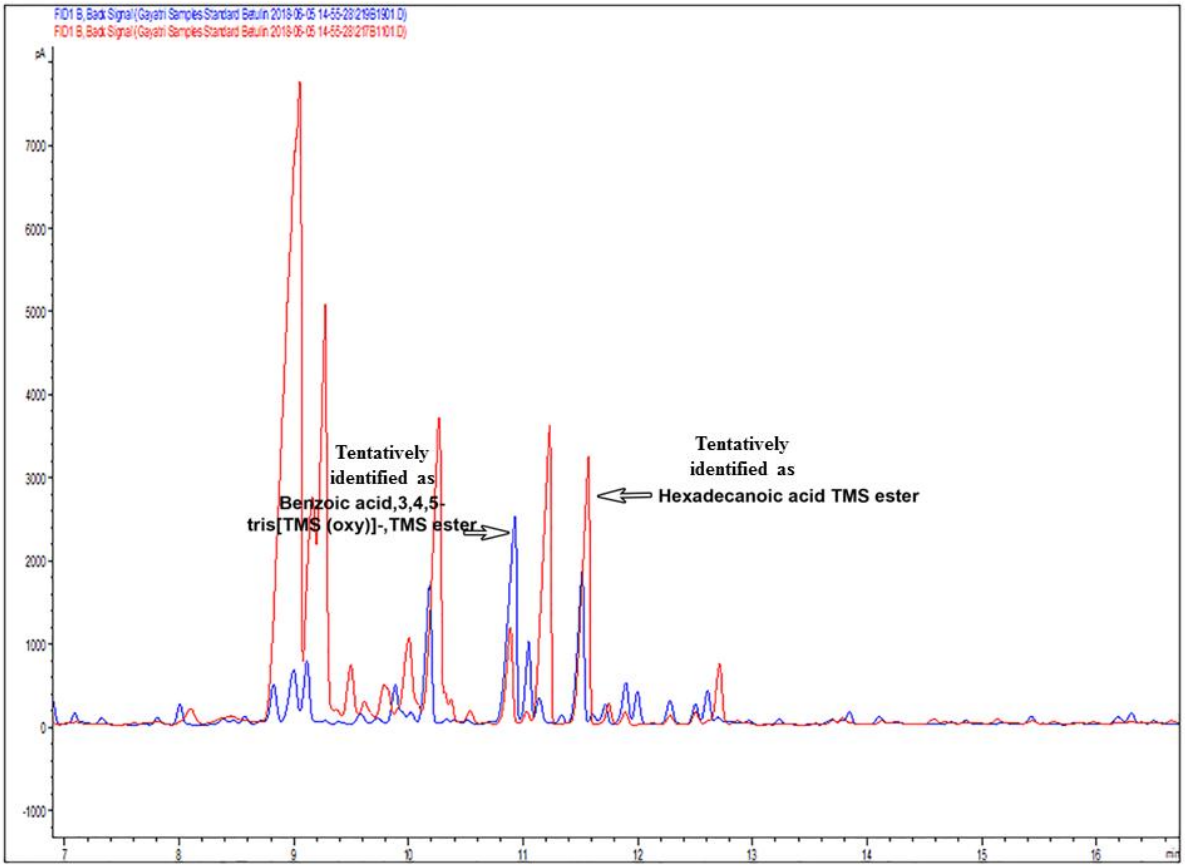

Figure 2: Gas chromatograms of silylated ethanol extracts from sapwood of *E. bosistoana* (red) and *E. globoidea* (blue) from 7 to 16 min. Compound identified at the retention time 10.9 and 11.7 min (arrow) by comparing the chromatograms of *E. bosistoana* sapwood extracts with *E. globoidea* Schroettke (2018).

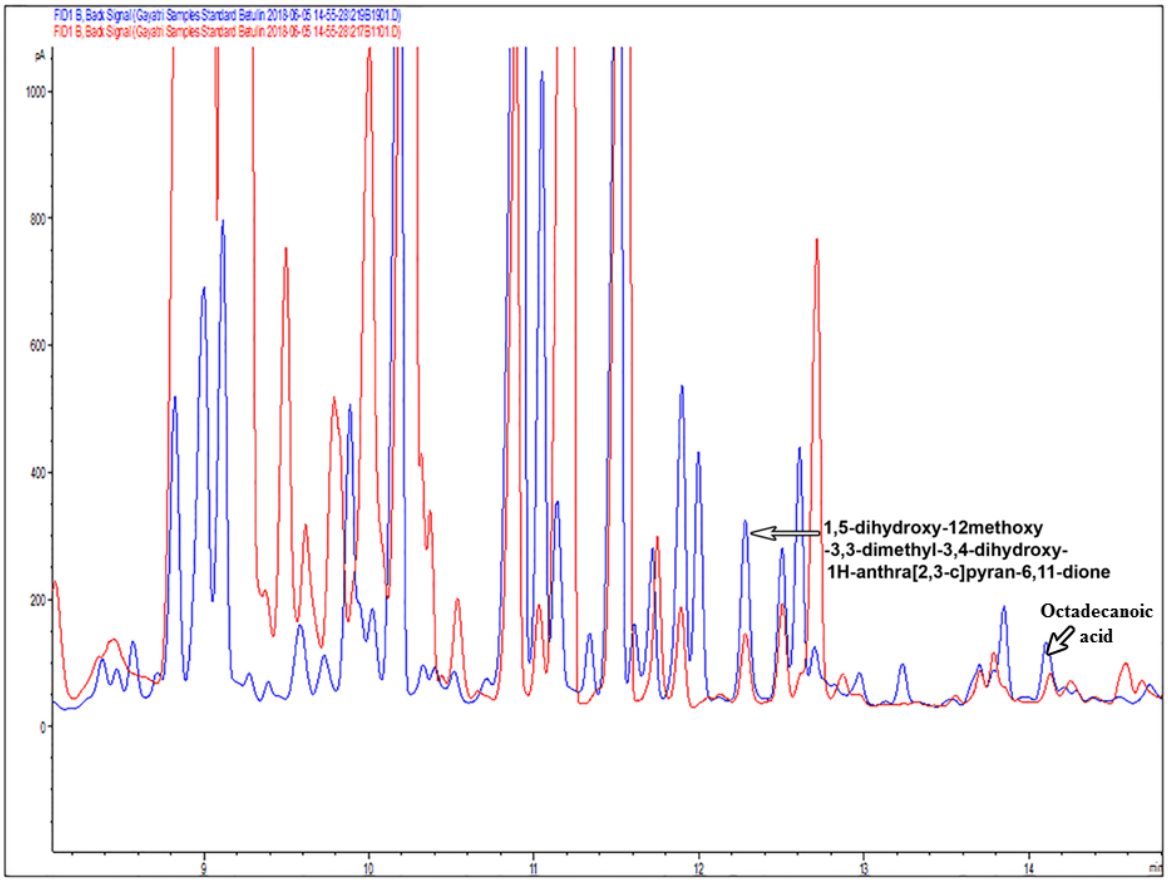

Figure 3: Gas chromatograms of silylated ethanol extracts from sapwood of *E. bosistoana* (red) and *E. globoidea* (blue) from 9 to 14 min. Compounds identified at the retention times 12.5 and 14.1 min (arrow) by comparing the chromatograms of *E. bosistoana* sapwood extracts with *E. globoidea* Schroettke (2018).

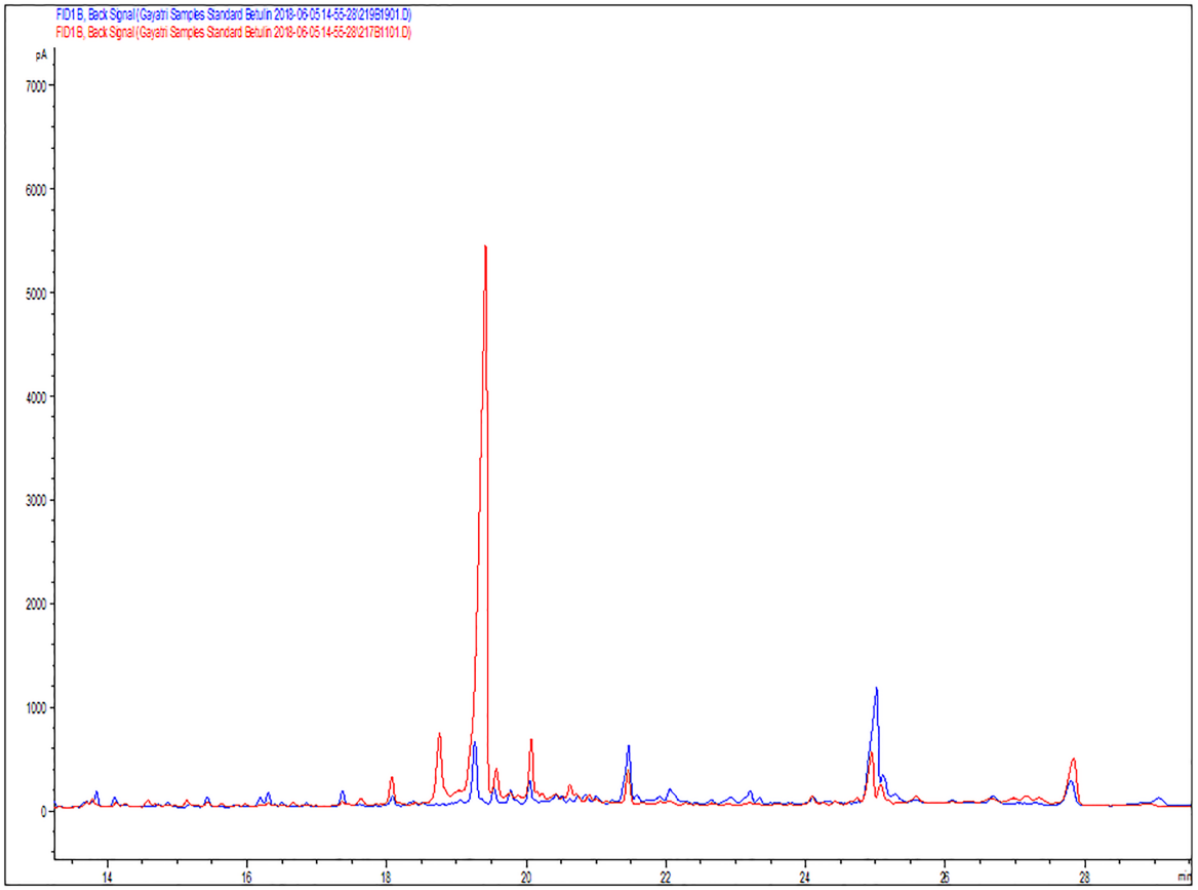

Figure 4: Gas chromatograms of silylated ethanol extracts from sapwood of *E. bosistoana* (red) and *E. globoidea* (blue) from 14 to 28 min.

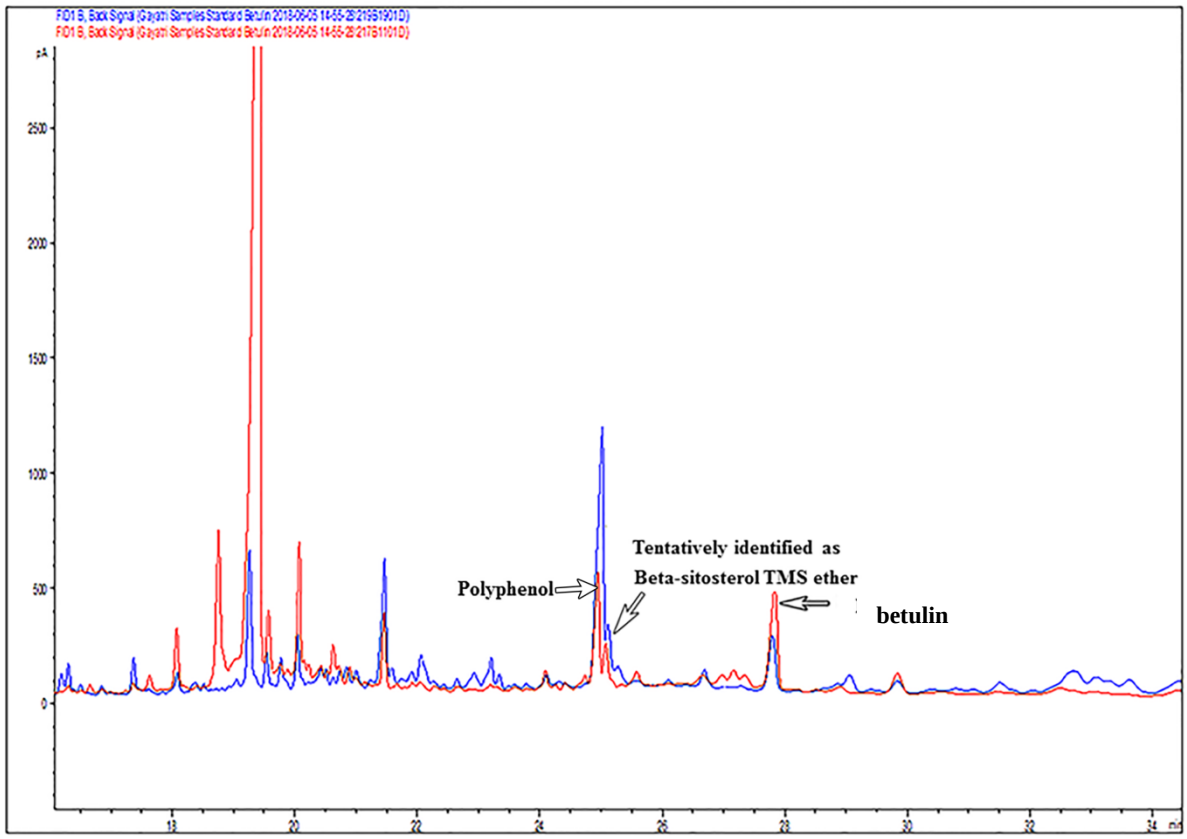

Figure 5: Gas chromatograms of silylated ethanol extracts from sapwood of *E. bosistoana* (red) and *E. globoidea* (blue) from 18 to 34 min. Compound identified at the retention times 25.1 and 25.2 min (arrow) by comparing the chromatograms of *E. bosistoana* sapwood extracts with *E. globoidea* Schroettke (2018). Standard (betulin) at 27.9 min (arrow).

Appendix 4: F-test (ANOVA) showing significant variation in the amount of compounds between *E. bosistoana* heartwood, woundwood and sapwood ethanol extracts.

Compounds (Retention times)	**P values**
2.2	< 0.001
4.5	< 0.001
4.8	< 0.001
7.8	< 0.001
8.0	< 0.001
9.0	< 0.001
9.1	< 0.001
9.2	< 0.001
9.7	< 0.001
9.9	< 0.001
10.2	< 0.001
10.9 (Tentatively identified as benzoic acid, 3,4,5-tris[TMS(oxy)]-,TMS ester)	< 0.001
11.2	< 0.001

Compounds (Retention times)	P values
11.5 (Tentatively identified as hexadecanoic acid, TMS ester)	< 0.001
11.7	< 0.001
12.5 (1,5-dihdroxy-12-methoxy-3,3-dimethyl-3,4-dihydro-1H-anthra[2,3-c]pyran-6,11-dione)	< 0.001
12.7	< 0.001
13.7	< 0.001
13.8	< 0.001
14.1 (Octadecanoic acid, TMS ester)	< 0.001
15.5	< 0.001
16.3	< 0.001
16.7	< 0.001
19.0	< 0.001
19.2	< 0.001
19.5	< 0.001
20.0	< 0.001
20.5	< 0.001
21.5	< 0.001
25.1 (Polyphenol)	< 0.001
25.2 (Tentatively identified as beta-sitosterol TMS ether)	< 0.001
31.0	< 0.001
32.0	< 0.001
32.5	< 0.001
33.2	< 0.001
34.0	< 0.001

Appendix 5: t-test showing significant variation in the amount of compounds between *E. bosistoana* woundwood and sapwood extracts. P values for the retention times shown in italics are not significant.

Compounds (Retention times)	P values
2.2	< 0.001
4.5	< 0.001
4.8	< 0.001
7.8	< 0.001
8.0	< 0.001
9.0	< 0.001
9.1	< 0.001
9.2	< 0.001
9.7	< 0.001
9.9	***0.765***
10.2	< 0.001
10.9 (Tentatively identified as benzoic acid, 3,4,5-tris[TMS(oxy)]-,TMS ester)	< 0.001
11.2	***0.536***

Compounds (Retention times)	P values
11.5 (Tentatively identified as hexadecanoic acid, TMS ester)	< 0.001
11.7	< 0.001
12.5 (1,5-dihdroxy-12-methoxy-3,3-dimethyl-3,4-dihydro-1H-anthra[2,3-c]pyran-6,11-dione)	< 0.001
12.7	< 0.001
13.7	< 0.001
13.8	< 0.001
14.1 (Octadecanoic acid, TMS ester)	< 0.001
15.5	< 0.001
16.3	< 0.001
16.7	< 0.001
19.0	< 0.001
19.2	< 0.001
19.5	< 0.001
20.0	< 0.001
20.5	***0.666***
21.5	< 0.001
25.1 (polyphenol)	< 0.001
25.2 (Tentatively identified as beta-sitosterol TMS ether)	< 0.001

Appendix 6: t-test showing significant variation in the amount of compounds between *E. bosistoana* woundwood and heartwood extracts. P values for the retention times shown in italics are not significant.

Compounds (Retention times)	P values
2.2	< 0.001
4.5	< 0.001
4.8	< 0.001
7.8	< 0.001
8.0	< 0.001
9.0	< 0.001
9.1	< 0.001
9.2	< 0.001
9.7	< 0.001
9.9	< 0.001
10.2	< 0.001
10.9 (Tentatively identified as benzoic acid, 3,4,5-tris[TMS(oxy)]-,TMS ester)	< 0.001
11.2	< 0.001
11.5 (Tentatively identified as hexadecanoic acid, TMS ester)	< 0.001

Compounds (Retention times)	P values
11.7	< 0.001
12.5 (1,5-dihdroxy-12-methoxy-3,3-dimethyl-3,4-dihydro-1H-anthra[2,3-c]pyran-6,11-dione)	< 0.001
12.7	< 0.001
13.7	< 0.001
13.8	< 0.001
14.1 (Octadecanoic acid, TMS ester)	< 0.001
15.5	< 0.001
16.3	< 0.001
16.7	< 0.001
19.0	< 0.001
19.2	***0.110***
19.5	< 0.001
20.0	< 0.001
20.5	< 0.001
21.5	< 0.001
25.1 (Polyphenol)	< 0.001
25.2 (Tentatively identified as beta-sitosterol TMS ether)	< 0.001
31.0	< 0.001
32.0	< 0.001
32.5	< 0.001
33.2	< 0.001
34.0	< 0.001

Appendix 7: t-test showing significant variation in the compounds between *E. bosistoana* heartwood and sapwood extracts. P values for the retention times shown in italics are not significant.

Compounds (Retention times)	P values
2.2	< 0.001
4.5	< 0.001
4.8	< 0.001
7.8	< 0.001
8.0	< 0.001
9.0	< 0.001
9.1	< 0.001
9.2	< 0.001
9.7	***0.186***
9.9	< 0.001
10.2	< 0.001
10.9 (Tentatively identified as benzoic acid, 3,4,5-tris[TMS(oxy)]-,TMS ester)	< 0.001
11.2	< 0.001

Compounds (Retention times)	P values
11.5 (Tentatively identified as hexadecanoic acid, TMS ester)	< 0.001
11.7	***0.115***
12.5 (1,5-dihdroxy-12-methoxy-3,3-dimethyl-3,4-dihydro-1H-anthra[2,3-c]pyran-6,11-dione)	***0.138***
12.7	< 0.001
13.7	< 0.001
13.8	< 0.001
14.1	***0.370***
15.5	< 0.001
16.3	< 0.001
16.7	< 0.001
19.0	< 0.001
19.2	< 0.001
19.5	< 0.001
20.0	< 0.001
20.5	< 0.001
21.5	< 0.001
25.1 (Polyphenol)	< 0.001
25.2 (Tentatively identified as beta-sitosterol TMS ether)	< 0.001

Appendix 8: t-test showing significant variation in amount of woundwood, heartwood and sapwood compounds in *E. bosistoana* extracts between two different families (F2 and F24). P values for the retention times shown in italics are not significant.

Compounds (Retention times)	Woundwood	Heartwood	Sapwood
2.2	0.024	***0.567***	***0.317***
4.5	***0.664***	***0.345***	0.016
4.8	0.001	< 0.001	***0.344***
7.8	0.008	< 0.001	*0.936*
8.0	***0.139***	***0.130***	***0.645***
9.0	0.001	0.003	***0.568***
9.1	***0.109***	< 0.001	***0.175***
9.2	< 0.001	0.001	***0.071***
9.7	0.025	***0.480***	***0.501***
9.9	***0.119***	**< 0.001**	***0.738***
10.2	< 0.001	*0.123*	***0.278***

Compounds (Retention times)	Woundwood	Heartwood	Sapwood
10.9 (Tentatively identified as benzoic acid, 3,4,5-tris[TMS(oxy)]-,TMS ester)	0.001	0.001	***0.755***
11.2	0.003	< 0.001	0.020
11.5 (Tentatively identified as hexadecanoic acid, TMS ester)	< 0.001	***0.735***	***0.222***
11.7	0.001	0.007	0.049
12.5 (1,5-dihdroxy-12-methoxy-3,3-dimethyl-3,4-dihydro-1H-anthra[2,3-c]pyran-6,11-dione)	< 0.001	< 0.001	0.033
12.7	0.001	< 0.001	0.020
13.7	0.002	< 0.001	0.007
13.8	0.001	0.009	0.046
14.1 (Octadecanoic acid, TMS ester)	0.002	***0.122***	0.008
15.5	***0.631***	***0.165***	0.039
16.3	0.002	***0.221***	0.004
16.7	< 0.001	*0.072*	0.004
19.0	< 0.001	0.009	***0.242***
19.2	< 0.001	0.005	0.003
19.5	0.009	***0.457***	0.024
20.0	< 0.001	**< 0.001**	0.001
20.5	0.001	0.002	***0.066***
21.5	< 0.001	0.004	***0.102***
25.1 (Polyphenol)	0.004	0.002	***0.203***
25.2 (Tentatively identified as beta-sitosterol TMS ether)	< 0.001	0.021	0.021
31.0	< 0.001	***0.940***	Not present in sapwood
32.0	0.002	< 0.001	Not present in sapwood
32.5	0.001	0.018	Not present in sapwood
33.2	0.029	< 0.001	Not present in sapwood
34.0	0.011	< 0.001	Not present in sapwood